![University of Glasgow]

Larronde-Larretche, Mathieu (2018) Development of a novel membrane bioreactor for cost-effective wastewater treatment and microalgae harvesting. PhD thesis.

Development of a Novel Membrane Bioreactor for Cost-Effective Wastewater Treatment and Microalgae Harvesting

Mathieu Larronde-Larretche

Submitted in fulfilment of the requirements for the degree of

Doctor of Philosophy

School of Engineering

College of Science and Engineering

University of Glasgow

September 2018

Abstract

The rapid depletion of fossil fuels has raised increasing attention worldwide, and initiated intensive research for sustainable alternatives for energy production. Among these, biodiesel from microalgae has appeared as one of the most promising candidate due to their ability to accumulate large amount of lipids. Indeed, microalgae can achieve a productivity up to 25 higher than other crop sources without need of cultivatable soil, therefore without competing with food production. In the meantime, microalgae have also shown promising results for the treatment of various kind of wastewaters. However, the cultivation of microalgae for energy production suffers from the large costs of harvesting and dewatering of biomass, prior to lipid extraction and biofuel production, which accounts for up to 50% of operating costs. Therefore, the search for cost-effective methods of harvesting and dewatering of microalgae biomass has become necessary to optimize their usage. This study investigates forward osmosis (FO) for the dewatering of microalgae biomass and its implementation within a photobioreactor used for wastewater treatment. FO is a cost-effective filtration process based on the differences of osmotic pressure across a semi-permeable membrane. The use of FO for microalgae dewatering is of high interest, given the high fouling ability of microalgae biomass and the low fouling promises of FO.

First, the feasibility of using FO for microalgae dewatering was assessed, focusing on better understanding the fouling mechanisms involved. The filtration performances have been investigated under various operating parameters. It has been found that when Ca^{2+}-containing draw solutions were used, microalgae responded to the back diffusion of calcium ions by an extensive excretion of carbohydrates, accelerating the formation of algal flocs, thus enhancing the rate and extent of flux decline and reducing the algae dewatering efficiency. However, most of the fouling was reversible by simple hydraulic flushing. In addition, substantial adsorption of algal biomass was observed on the feed spacer. Also, *Scenedesmus obliquus* and *Chlamydomonas reinhardtii*, with fructose and abundant glucose and mannose in its cell wall, showed strong response to the back diffusion of calcium ions which encouraged *S. obliquus* to produce more extracellular carbohydrates and formed a stable gel network between algal biomass and extracellular carbohydrates, leading to algae aggregation and severe loss in both water flux and algae biomass during FO dewatering

with Ca^{2+}-containing draw solution. Among the species investigated, *Chlorella vulgaris* without fructose was the most suitable microalgae species to be dewatered by FO with a high algae recovery and negligible flux decline regardless of which draw solution was applied. These findings improve mechanical understanding of FO membrane fouling by microalgae; have significant implications for the algae species selection; and are critical for the development and optimization of FO dewatering processes.

Finally, the implementation of FO dewatering with continuous microalgae biomass production and synthetic wastewater treatment was investigated. Two systems (External FO ; Immersed FO) have been studied and compared in order to provide insights on the advantages and disadvantages of each system. Constant parameters have been set identical for both systems: operation time; photobioreactor; hydraulic retention time; biomass production; FO permeate volume. The results reveals that the wastewater treatment efficiency (nutrients removal), as well as the production of biomass were greater with the immersed system due to a greater microalgae growth. However, these may not be sustainable in a long term operation of the immersed system. The external FO system was found better in terms of salinity build-up and FO dewatering performances. Overall, an external FO dewatering is recommended due to its better flexibility and sustainability.

Table of Contents

2. Microalgae (*Scenedesmus obliquus*) Dewatering using Forward Osmosis Membrane: Influence of Draw Solution Chemistry

List of Tables

List of Figures

Acknowledgement

I would first like to acknowledge and thank my supervisor, Xue Jin, for giving me this great opportunity, and for her guidance and support throughout my PhD. Thanks also to Ian Watson for his endless enthusiasm.

I offer my sincere thanks to Julie, Anne, and Tim, for the essential help they provided me every day in the laboratory. Thank you also to and all the Bill, Caroline, Umer, Manousos, Ameet, Cindy, and all the PIs in our group. You can all be proud of the work you have accomplished to form a strong group with a wonderful cohesion and enthusiasm.

I would like to give special thanks to Kevin, Fabien, Szymon, Alex, Melina, Maria, Davide, Ioannis, Jill, Big Steph, Wee Steph, Gu, Sahra, Melanie, and all the PhD students and postdocs who spent time with me in the lab. It was really great working with you guys. Don't worry, I'm not forgetting all the fun we had going out and partying.

Thank you also to Maxine for your cheerfulness every morning and for teaching me all those hilarious Scottish expressions. I will be sad to not see you every morning when I will leave.

Grazie a la Coffee Mafia (Eugenio, Manuel, Sissy, Ricardo, Francesco, Marta, Emanuele, Mike, Manlio, and everyone I forgot) for all those espressos and laughs in our tiny kitchen. I think I became one of the best barista now.

A big thank to my very best friends back in France (Alex and Lena, Romain and Coralie, Anthony and Elodie, Florent and Clémence, Jérémy and Priscillia, Jordan, Benjamin, and Xavier) who were always happy to see me coming back for holydays, and who have been here for me in the best and the worst. I'm really glad I have all of you guys. Thanks also to DAD (Dr Awesome Dong) for all the laugh. Even though we lost a bit contact, I know I can always count on you.

I would like to thank all my family, my mom, my dad, my sisters and brothers in law and my niece. Even though we had to go through very difficult times, we were always here to support each other. I feel extremely lucky to have such a great family.

Finally, I would like to thank Giulia for coming to Glasgow to find me, and for supporting me in all those stressful moments. You really changed my life for the best.

Author's Declaration

I declare that no portion of the work in this thesis has been submitted in support of any application for any other degree or qualification from this or any other university or institute of learning. I also declare that the work presented in this thesis is entirely my own contribution unless otherwise stated.

Mathieu Larronde-Larretche

Glasgow, February 2018.

List of Abbreviations and Symbols

A	Pure water permeability (m/s/Pa)
B	Solute permeability
C	Concentration (mol/m^3)
C_{De}	Solute concentration in the bulk of the draw solution (mol/m^3)
C_{Dm}	Solute concentration in the membrane surface of the draw side (mol/m^3)
C_{Fe}	Solute concentration in the bulk of the feed solution (mol/m^3)
C_{Fm}	Solute concentration in the membrane surface of the feed side (mol/m^3)
C_i	Solute concentration at the interface active and support layer (mol/m^3)
D	Solute diffusion coefficient (m^2/s)
D_{eff}	Effective diffusion coefficient (m^2/s)
J_w	Water flux (m^3/m^2/s)
$J_{w,0}$	Initial water flux (m^3/m^2/s)
$J_{w,a}$	Water flux during algae dewatering experiment (m^3/m^2/s)
$J_{w,b}$	Water flux during baseline test (m^3/m^2/s)
$J_{w,c}$	Water flux after cleaning (m^3/m^2/s)
k	Mass transfer coefficient (m/s)
K	Resistance to solute diffusion (s/m)
l	Length (m)
l_{eff}	Effective length (m)
m_{total}	Total mass of biomass produced throughout the experiment (g)
R	Recovery rate
R_s	Solute rejection
R_g	Ideal gas constant (8.3145 J/K/mol)
S	Structural parameter (m^{-1})
t_s	Membrane thickness (m)
T	Temperature (K)
V	Volume (m^3)
$V_{Harvest}$	Volume of biomass harvested every day (L)

$V_{Reactor}$	Volume of biomass in the reactor after last FO dewatering experiment (L)
V_{Sample}	Volume of sample taken in PBR every day before each experiment (L)
X_{1-7f}	Biomass concentration harvested after FO dewatering each day (g)
X_i	Initial algae biomass concentration in the feed solution (g/L)
X_f	Final algae biomass concentration in the feed solution (g/L)

Greek letters:

β	Van't Hoff coefficient
ΔC_{eff}	Effective concentration difference (mol/m^3)
$\Delta \pi$	Osmotic pressure difference across the membrane (Pa)
$\Delta \pi_{bulk}$	Bulk osmotic pressure difference (Pa)
$\Delta \pi_{eff}$	Effective osmotic pressure difference (Pa)
ΔJ_w	Normalized water flux loss
ΔP	Hydraulic pressure difference across the membrane (Pa)
ε	Porosity
π	Osmotic pressure (Pa)
π_D	Osmotic pressure of the draw solution (Pa)
π_F	Osmotic pressure of the feed solution (Pa)
σ	Reflection coefficient
τ	Tortuosity

Abbreviations:

AFO	Assisted forward osmosis
AL-DS	Active layer facing the draw solution
AL-FS	Active layer facing the feed solution
AOM	Alogenic organic matter
ATP	Adenosine triphosphate
CA	Cellulose acetate
CCAP	Culture Collection of Algae and Protozoa
CCM	Carbon concentrating mechanism
CDA	Cellulose diacetate

CFV	Crossflow velocity
CP	Concentration polarization
CTA	Cellulose triacetate
CECP	Cake enhanced concentration polarization
CEOP	Cake enhanced osmotic pressure
DHA	Decosa hexaenoic acid
DI	Deionized
DLVO	Derjaguin-Landau-Verwey-Overbeek theory
DNA	Deoxyribonucleic acid
ECP	External concentration polarization
EDL	Electrical double layer theory
EPA	Eicosa pentanoic acid
EPS	Extracellular polymeric substance
ES	Embedded support
FO	Forward osmosis
HRT	Hydraulic retention time
HTI	Hydration Technology Innovation
ICP	Internal concentration polarization
LMH	$L/m^2/h$
MBR	Membrane bioreactor
MD	Membrane distillation
MF	Microfiltration
MNP	Magnetic nanoparticle
MPBR	Membrane photobioreactor
NADPH	Dihydronicotinamide-adenine dinucleotide phosphate
NASA	National Aeronautics and Space Administration
NF	Nanofiltration
NOM	Natural organic matter
OMBR	Osmotic membrane bioreactor
OMEGA	Offshore Membrane Encolsures for Growing Algae
PBR	Photobioreactor

PEG   Polyethylene glycol

PES   Polyethylene sulfone

PMMA Polymethyl methacrylate

PRO   Pressure retarded osmosis

PS   Photosystem

PSf   Polysulfone

PVP   Polyvinylpyrrolidone

RNA   Ribonucleic acid

RO   Reverse osmosis

SEM   Scanned electron microscopy

SMP   Soluble microbial product

SRT   Solid retention time

SWRO   Seawater reverse osmosis

TDS   Total dissolved solids

TEP   Transparent exopolymeric particles

TFC   Thin film composite

UF   Ultrafiltration

UV   Ultraviolet

VDW   Van der Waals forces.

Introduction

The development of sustainable bio-energies has become a major concern since the early 20th century, and increasing attention is given towards novel methods and technologies able to cope with these problematics. In the meantime, the amount of wastewater produced by both municipalities and industries constantly increases, raising new issues in terms of treatment and disposal of these waters. Recently, microalgae processes emerged as a potential methods capable of assisting the resolution of these challenges. Microalgae are photosynthetic microorganisms living in both freshwaters and seawaters. Briefly, nutrients and inorganic carbon are captured by the cells and transformed into biomass from the energy generated by the absorption of photons. The recent interest of researchers and industries on microalgae mostly emerged from the dwindling petroleum resources and the need for alternative sustainable energies. Microalgae cells accumulates a significant amount of lipids which can be extracted and transformed for the production of biodiesel. The biodiesel surface productivity has been estimated from 10 to 25 times greater with microalgae than with palm oil, depending on the lipid concentration, reaching more than 70% of the dry biomass for certain species [1]. Microalgae have also shown a great potential for the production of other bioenergies such as biogas, biohydrogen, and bioethanol [2].

Along with their potential as energy source, microalgae have been intensively studied as an efficient treatment for various types of municipal, agricultural, and industrial wastewaters [3]. Indeed, phosphorus and nitrogen sources can be totally removed for initial concentrations of respectively few dozen and few hundred milligrams per litre [4]. Heavy metals, greatly contributing to the pollution of ecosystems and the emergence of many diseases, are also removable by the microalgae through bio-fixation phenomena [5]. The adsorption capacity (mg/g of dried biomass) of microalgae varies from few dozen (Cu^{2+}, Ni^{2+}) to hundreds (Cd^{2+}, Pb^{2+}, Zn^{2+}) with moderately low pH values, required for an efficient biosorption of heavy metals. A substantial inhibition of coliforms development has been observed in algal ponds, due to unfavourable environmental factors during the growth of microalgae, and a reduction of over 60% of both chemical and biological oxygen demand in the treatment of domestic wastewaters has been reported [3]. However, most of the research on wastewater treatment by microalgae is conducted at laboratory scale, thus lacking of

large scale plants investigations. Industrial applications may also face several issues due to the variation of water composition, the contamination by other microorganisms, and the sunshine variations in the case of a natural light supply.

Due to their photosynthetic metabolism, microalgae have also shown an interesting potential for the reduction of carbon dioxide emissions. However, it has been estimated that 40% of the energy consumption needed for the algae cultivation is attributed to CO_2 supply [6]. Therefore, research has been focused on the use of industrial flue gas as an alternative for inorganic carbon source. In this case, potential hurdles might come from the potential toxicity and the tolerance of microalgae in presence of NO_x and SO_x, and the high temperature of flue gas [7]. Even in the most optimistic simulations, the CO_2 bio-fixation rate of microalgae remains lower than its emissions during the transformation of the biomass into biodiesel, mostly due to the energy consumption for the harvesting and concentration of biomass [8].

The economic viability of microalgae for energy production mostly suffers from the high cost of biomass harvesting and dewatering. Operating cost of microalgae harvesting has been estimated up to 50% of the total operating costs [9], and the cost of the equipment dedicated to harvesting estimated to 90% in open systems [10]. Various harvesting techniques have been studied. Among these, centrifugation remains the most efficient and rapid technique, thus being widely used in industry. However, this method is extremely energy intensive, principally suiting for the production of high value compounds [11]. Sedimentation methods are very interesting as an efficient low-cost microalgae harvesting method, suitable for biofuel production as a preliminary concentration step [12]. Microalgae sedimentation can also be improved by flocculation methods by addition of chitosan, magnesium and calcium, bacteria and fungi, or magnetic particles [13]. Flotation, has been found to be faster than sedimentation for the harvesting of small unicellular microalgae. However, due to its high operational and investment costs, flotation is not economically and technically interesting for biofuel production from microalgae [14]. Membrane filtration methods, mostly micro and nano-filtration, are also used and studied but suffers from fouling issues and high maintenance costs [12].

In parallel, forward osmosis (FO) also gained a significant interest in both research and industry. This recent membrane filtration process is based on the driving

force obtained from the difference of osmotic pressure across a semi-permeable asymmetric membrane. In this process, pure water from the lower concentrated side (feed), crosses the membrane to dilute the more concentrated draw solution in order to reach an equilibrium state. FO membranes are usually composed of a dense active layer allowing solute rejection, and a support layer providing mechanical strength. Osmotic processes have been first studied for power generation [15]. The separation of freshwater (feed) and saltwater (draw) by an FO membrane can generate electricity from the subsequent increase of hydraulic pressure in the draw side [16]. In the last decade, FO process has been widely studied for seawater desalination and wastewater reclamation. In most cases, a highly concentrated draw solution, with high osmotic potential solute, is used to withdraw pure water from seawater, the draw solution being generally easily recoverable by other techniques such as column and membrane distillations [17]. Several applications introduces forward osmosis for wastewater treatment in membrane bioreactors (MBRs) [18]. Recently, FO process has been proposed as a combined system for both wastewater treatment and costs reduction in seawater desalination. The purpose is to dilute seawater with pure water withdrawn from wastewater, prior to a desalination step by reverse osmosis (RO). In this case, the energy cost of the RO step, related to the high hydraulic pressure applied, is reduced from the dilution of the seawater [19]. Other applications of forward osmosis includes liquid food concentration and controlled release of drugs in pharmaceutical industry.

In all membrane process, fouling remains one on the greatest cause of the decrease of performances over time, its impact generally increasing with the applied pressure. The forward osmosis process has the advantage to operate without additional hydraulic pressure, thus reducing the impact of membrane fouling. However, different materials are notwithstanding involved in FO membrane fouling deposition at different stages and with different impacts. Organic fouling, associated to inter-molecular adhesion and hydrodynamic conditions, can increase the negative charge property and hydrophilicity of the membrane, and increases the absorption capacity for hydrophilic compounds organic fouling [20]. It also has important effects on the removal of inorganic contaminants [21]. A high concentration of organic material also induces a more severe concentration polarization (CP) and cake enhanced osmotic pressure (CEOP) effects on the active layer [22]. However, the cake layer formed on the active layer by organic material is almost fully reversible by physical cleaning [23]. Colloidal

fouling is accentuated by the foulant concentration and the reverse solute diffusion, which also influence its reversibility [24, 25]. Scaling is one of the most dominant inorganic fouling. It has been found to be strongly influenced by the temperature [26], and could induce a stronger organic fouling [27]. Humic acid [28], natural organic matter (NOM) and transparent exopolymeric particles (TEP) [29] have also been identified as foulant materials in FO processes.

FO has been recently proposed as a new cost-effective method for the dewatering of microalgal biomass. The National Aeronautics and Space Administration (NASA) first proposed an FO process, called Offshore Membrane Enclosure for Growing Algae (OMEGA), for dewatering miroalgal biomass, grown in wastewater inside photobioreactors immersed into the ocean, as an alternative for the production of aviation fuels [30]. FO membranes immersed into the ocean has also been studied for a partial dewatering of microalgae, reaching an average water flux of 2 $l.m^{-2}.h^{-1}$ (LMH) and obtaining a final biomass concentrated by 6.5. A significant biofouling was observed, without affecting the flux [31]. Physical and chemical parameters affecting membrane fouling have been investigated. Fouling, found much more severe when the membrane support layer was facing the microalgae solution, was accentuated in presence of $MgCl_2$ due to interactions between divalent ions and the algal biomass [32]. It has been demonstrated that a critical flux phenomenon, beyond which the water flux is kept stable and above which the water flux decrease dramatically because of the fouling deposition, appears in the filtration of microalgae strains by FO [33]. However, the fouling is mostly reversible for both membrane orientation with a cross flow flushing step, mostly if the concentration of Mg^{2+} ions is low.

The investigation of FO process for microalgal biomass concentration with seawater has only started recently and a consequent gap of knowledge on fouling mechanisms related to the ionic composition of seawater and influence of microalgae specie remains. In the meantime, research still lack of combined systems for an optimal use of microalgae potential and the production of concentrated valuable biomass. Membrane photobioreactors (MPBRs) have been investigated as coupled systems for the production of pre-concentrated microalgal biomass. The treatment of wastewater in MPBRs was reported as efficient but suffered from the accumulation of metal ions, negatively affecting the microalgae cells and the long term efficiency [34]. The significance of solid retention time (SRT) and hydraulic retention time (HRT) has been

highlighted as a major parameter in the development of MPBRs for sewage treatment and carbon dioxide capture [35]. MPBRs have also been studied as a method for feed recycling, allowing an increase of microalgae growth rate and a reduction of nutrient supply [36]. Overall, further research is needed for the combination of wastewater treatment and bioenergy production from microalgae to reach its full potential.

Objectives

The general aim of this project is to develop a novel membrane bioreactor incorporating microalgae for wastewater treatment and the production of concentrated microalgae biomass through the utilization of forward osmosis (FO) technique. The use of forward osmosis for microalgae dewatering is very recent and lots remain unknown concerning the different phenomena taking place during the filtration. Therefore, the first aim of this project is to proves the feasibility and assess the performances of FO for pre-concentration of microalgal biomass. To achieve this, gaining a deeper understanding of fouling mechanisms involved is key to select the various operating parameters and achieve the best filtration performances.

The first objective of this project is the determination of the best available commercial FO membrane for the dewatering of microalgae biomass. The determination of membranes characteristics is essential to better understand the phenomena happening during the filtration of microalgal biomass. This investigation will lead to the choice of a FO membrane to be used further in this study.

Then, experiments will be conducted to determine the combination of operating parameters that better optimize the use of FO for microalgae dewatering. This study will investigate the effect of membrane type and orientation, draw solution chemistry, and microalgae species, in order to gain a deeper understanding of fouling mechanisms during the dewatering of microalgae biomass by forward osmosis.

Finally, the FO membrane process will be integrated with the photobioreactor for the continuous wastewater treatment and production of concentrated algal biomass (Figure 1.1). Two integrated systems, external and immersed, will be investigated and compared to demonstrate the most efficient method of FO integration with a photobioreactor. This work will greatly contribute to the extension of knowledge in both forward osmosis, and microalgae dewatering fields.
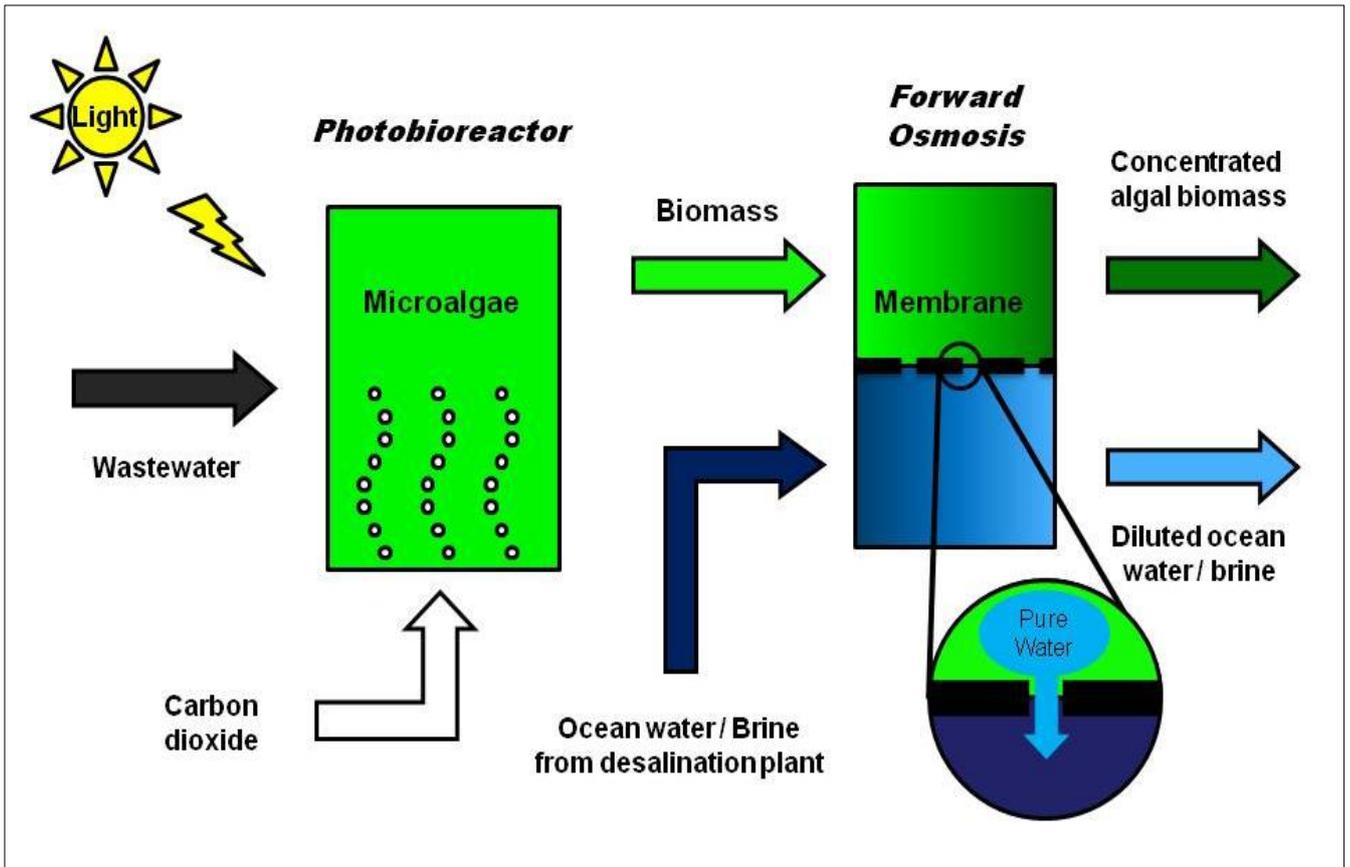
Figure 1.1 – Schematics of a combined membrane bioreactor used for wastewater treatment, carbon dioxide capture, and concentrated biomass production through forward osmosis filtration used with ocean water or brine from desalination plant.

1. Literature Review

1.1. Microalgae

1.1.1. Overview

Microalgae are unicellular microorganism, with a size varying from a few to a hundred of micrometres (Figure 1.2). From a taxonomic point of view, microalgae belong to different families, with their own characteristics, but have common features within their ultrastructure and their metabolism. Photosynthetic microorganisms are divided into three categories: photosynthetic bacteria, algae, and terrestrial plants. The term algae gathers chlorophyllic species living essentially in water and that are not embryophytes, such as *Rhodobiontes* (red algae), *Chlorobiontes*, *Stramenopiles* (brown algae), and *Haptophytes*. A microalgae is a unicellular photosynthetic microorganism containing a plasma membrane containing within its cytoplasm various organelles necessary for its metabolism: chloroplasts, amyloplasts, oleoplasts, mitochondria, and an envelope containing the nucleus. These microorganisms belong to two groups: eukaryotes and prokaryotes. Eukaryotes microalgae have a conventional plant cell structure compartmentalized, with or without cellulosic wall, and photosynthetic pigments contained within the plasts. Prokaryotes microalgae, also known as cyanobacteria, have a classical bacterial structure without compartments, the photosynthetic pigments being contained aithin the lamellar membrane. Microalgae colonizes the medium by dividing through mitosis, fast and actively if the physicochemical and nutritive conditions are favourable. Microalgae are present in all existing earth ecosystems, not just aquatic but also terrestrial, representing a big variety of species living in a wide range of environmental conditions. It is estimated that more than 50,000 species exist, but only a limited number, of around 30,000, have been studied and analysed [16].
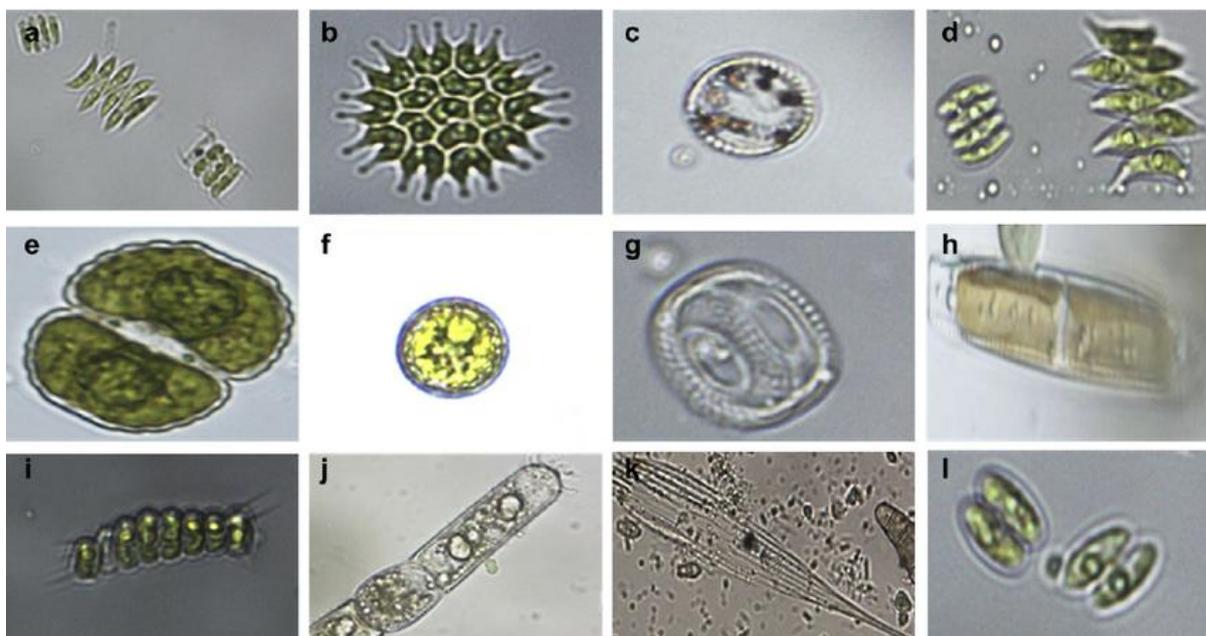
Figure 1.2 - *Diversity of microalgae species: a) Scenedesmus quadricauda ; b) Pedisatrum boryanum ; c) Cyclotella bodanica ; d) Scenedesmus dimorphus , e) Cosmarium quadrifarium , f) Chlorella vulgaris ; g) Centric diatom ; h) Pinnate diatom ; i) Scenedesmus obliquus ; j) Oedogonium ; k) Nageliella , l) Cosmarium depressum [37].*

1.1.2. Photosynthesis

The light constitutes the initial energy supply, allowing the assimilation of carbon and other essential elements by chlorophyllians livings through photosynthesis, synthesizing organic matter from light (Figure 1.3). Photosynthesis takes place within the chloroplasts of chlorophyllian tissues such as the mesophylle. It starts with a photochemical phase in which a strong reducer (NADPH) and ATP (adenosine triphosphate) are elaborated. The light energy, absorbed by the photosystems (PSI and PSII), ensure the transfer of electrons supplied by water. Then, the chemical part includes a carboxylation, catalysed by the RuBisCO, consisting in the reduction of the CO_2 using the ATP and NADPH previously produced. Microalgae contain various essential pigments such as chlorophyll, consisting in a metalloprotein with a long hydrophobic chain allowing a great solubility within the nonpolar medium of the membrane. The role of the chlorophyll is to absorb the energy from the light and convert it into chemical energy (ATP, NADPH, H^+). Microalgae also contain high concentration of lutein (carotenoid pigment). Photochemical reactions and photosynthesis allows the reduction of CO_2 and the formation of carbohydrates through the Calvin-Benson cycle.
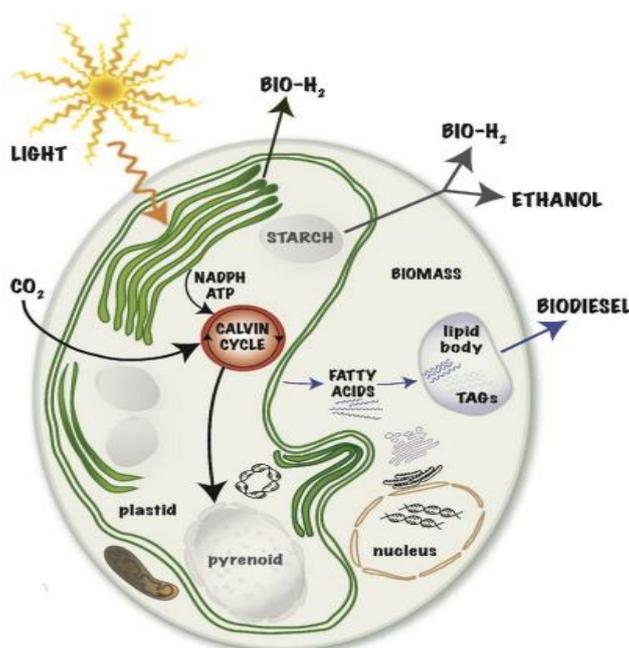
Figure 1.3 - *Metabolic pathways in microalgae related to biofuel production. The integration of metabolic pathways is coordinated through complex mechanisms that regulate photosynthetic output for the synthesis of proteins, nucleic acids, carbohydrates, lipids, and H2 [38].*

1.1.3. Growth Parameters

1.1.3.1. Nitrogen

Nitrogen is, after carbon, the major element composing biological cells. Its quantity varies depending on the species and the composition of the surrounding medium, but correspond in average to 7% of the cells dry matter [39, 40]. Lourenço *et al.* (2004), showed that nitrogen is principally used for the synthesis of proteins in *Chlorella minutissima* [41]. However, it is also found under inorganic form (NH_4^+, NO_2^-, NO_3^-) within nucleic acids (DNA and RNA), and in lower amount in chlorophyll. Several studies have investigated the effect of nitrogen concentration in the growth medium. An increase of nitrogen have been found to induces an increase of biomass content, and proteins and chlorophyll within the cells for *Chlorella vulgaris* [42-45], and *Chlorella ellipsoidea* [46]. However, when the nitrogen concentration becomes higher than 0.5 g/L (NO_3), the adverse effect is observed [42-44]. Also, for *C. sorokiniana*, *Oocystis polymorpha, and C. ellipsoidea*, it has been demonstrated that a nitrogen limitation stimulates the lipid production [47, 48]. However, the decrease of nitrogen in the growth medium leads to a decrease of the cells photosynthetic metabolism [47, 49, 50]. This effect is due to (1) a decrease of the concentration of

RuBisCO proteins [51, 52], and (2) a reduction of chlorophyll content within each cell [47]. This decrease of photosynthetic activity reduces the cells ability to transform the energy from the photons into carbonated products, which subsequently makes the microalgae more subject to photo inhibition phenomenon [53, 54]. Indeed, 50% of intracellular carbon is coupled with nitrogen metabolism, which highlights the close link between nitrogen and photosynthesis [55]. The assimilation of nitrogen is also associated with glutamate synthesis during the production of proteins. Using a radioactive tracker ($_{14}$C), it has been demonstrated that this reaction mobilizes intermediaries of the Krebs cycle. Therefore, the cell needs pyruvate to drive the Krebs cycle, which is synthesized from glucose, produced by photosynthetic activity [56]. If the cells are deprived of nitrogen, they accumulate more glucids which is preferentially directed to the synthesis of starch, instead of providing carbonated precursors necessaries for the synthesis of amino acids, basic element of proteins. These glucids stocks will therefore be used to synthesize amino acids [56].

1.1.3.2.   Phosphorus

Phosphorus is involved in the synthesis of nucleic acids and phospholipids (components of the cell walls), and in the constitution of ATP and NADPH, involved in the energetic metabolism [57-59]. Therefore, it is involved in numerous metabolic processes within the cells [48]. For example, it is involved in metabolic pathways regulating the cells division, which will have a direct impact on biomass production. It is also necessary within the cells to satisfy the energetic needs and organelles biosynthesis [57]. A phosphorus limitation leads to a reduction of biomass, chlorophyll content, polysaccharides and proteins aithin the cells [60-62]. It also decreases the fixation of carbon [63], by decreasing the synthesis of RuBisCO [64], or by affecting the intermediaries of the pentose phosphate pathways [57]. A phosphorus limitation will also affect the photosynthetic apparatus by reducing the transport of electrons at the PSII site [60, 65], and denature the polypeptides of the photosynthetic apparatus, regulating the absorption of light [57]. It has been demonstrated that in some microalgae, a limitation of phosphorus in the medium induces the synthesis of phosphatase, an extracellular enzyme capable of splitting phosphorylated molecules on organic compounds present in the medium, allowing the cell to compensate this lack of

phosphorus [57, 66, 67]. It has been demonstrated, with *Chlorella vulgaris*, that the cells lacking of phosphorus increased the production of glycolate through photorespiration mechanism, allowing the dissipation of the excess of energy, thus preventing damages of the cells [63]. However, these regulation mechanisms in case of phosphorus shortage remain poorly known [57]. Several studies, within photoplanktonic communities, have demonstrated the existence of a co-limitation on growth by phosphorus and nitrogen. Davey *et al.* (2008) have shown that in tropical and subtropical waters of northern Atlantic, an increase of chlorophyll intervenes after addition of both phosphorus and nitrogen [58]. Same pattern is observed with *Skeletonema costatum*, for which the fixation of carbon was stable after addition of nitrogen, but increased after coupled addition of phosphorus and nitrogen [68]. Nevertheless, the mechanisms linking nitrogen and phosphorus remain unclear [59].

1.1.3.3. Microelements

Microelements designates to elements presents in the medium in very small amount, and their concentration varies greatly in the environment. In laboratory, microelements limitation is rarely encountered because growth mediums are adapted to prevent the lack of these elements. Changes in microelements concentration can have impacts on the microalgae cells. With *Isochrysis galbana*, an iron deprivation leads to a decrease of cells density, size, chlorophyll content, intracellular proteins and polysaccharides, a decrease of anhydrase carbonic activity, and a decrease of other nutrients assimilation such as nitrogen, phosphorus, and carbon [69]. The anhydrase carbonic is a metalloenzyme containing zinc. Therefore, a decrease of its activity generated by a zinc deprivation can affect the whole carbon metabolism of the cell and then, the production of intracellular metabolites. Microelements limitations often affect the functioning of the photosynthetic apparatus. For example, an insufficient concentration of sulphur reduces the electron flux in the photosynthetic apparatus [70], and a decrease of iron concentration induces a reduction of the constituents of the photosynthetic apparatus (PSI, PSII, cytochromes) because these contain numerous iron-based co-factors [71]. Copper is also present in various enzymes of the photosynthetic apparatus. Therefore, its limitation also affects the photosynthetic

metabolism [70, 72]. Other intracellular processes can be affected, such as nitrogen metabolism which is diminished in case of molybdenum deprivation [73]. An increase of these elements will generally have a positive impact on the cells, which is the case for magnesium and iron inducing an increase of cells concentration when these are already at high concentration in the medium [39, 44, 71]. However, this positive impact occurs up to a certain level, after which these compounds become toxic for the cell. For example, an excessive concentration of iron can damage the biological membranes, the proteins, or the DNA [74]. Also, an excess of zinc block the growth of microalgae [62, 69]. To face these variations of concentration in the medium, microalgae have demonstrated various physiological adaptive ways. For example, *Chlorella vulgaris* produces a hormone, the brassinolide, which helps the cells to counter the cytotoxic effects of high concentration of heavy metals ($>10^{-6}$ mol/L) [75]. The photosynthetic apparatus can also adapt in response of microelements deprivation. An example is iron deprivation, for which the photosynthetic antenna reorganize to adapt to physiological changes an limit cells damages due to the light, while optimizing the photosynthetic activity [76, 77].

1.1.3.4.   Light

In the vegetable kingdom, light controls the carbon fluxes and the production of energy within the cells, through photosynthetic process. It determines the yield of nutrients consumption for photoautotrophic organisms [78]. Therefore, light is a key parameter to consider for the growth of microalgae and the design of photobioreactors [79, 80]. Both limitation and excess of light will have consequences on the cells metabolism and growth. When the cell receives more light than it can absorbs through the synthesis of ATP and carbon assimilation, the photosynthesis is inhibited and the growth greatly declines [81, 82]. This phenomenon is called photo-inhibition, during which the photosystem II (PSII) is excessively excited and is inactivated. An accumulation of electrons occurs between the two photosystems (PSI and PSII), leading to irreversible damages within the cell [83]. In order to counter balance these photo-inhibition phenomena, the cell activates photo-protection mechanisms which will relieve the PSII and allows the photosynthetic apparatus to recover its optimal functioning. The first of these mechanism is the elimination of excess energy as heat

through specific pigments called carotenoids [83-85]. Inactivation of the PSII car also be a photo-protection mechanism, which will results in photo-acclimation of the cell. The cell will enhance its photosynthetic activity through the increase of RuBisCO and ATPase activity. In some cases, photo-inhibition will also lead to synthesis of other intracellular compounds such as astaxanthin (*Haematococcus pluvialis*), a highly sought compound in food industry [86]. All these responses allows the cells to enhance its metabolic yield and prevent further damages. Other environmental parameters can also influence the photo-inhibition phenomenon. When the diatom *Phaeodactylum tricornutum* is subject to a CO2 concentration of 0.1%, its growth, inorganic carbon fixation, and photosynthetic production are enhanced, however it also becomes more prone to photo-inhibition, which does not occur when cultivated with 0.038% CO_2 [87]. However, an increase of light intensity can stimulate the metabolism, if remaining within the acceptance range of the microalgae. Therefore, a high light intensity will increase the biomass, carbon consumption, and ratio of intracellular elements C:N, C:P, and N:P [78, 81, 88-90]. However, the cells response to these phenomena will depend on the physiological condition of the cells [83]. For example, no increase of specific growth rate was observed when increasing the light intensity from 122 to 336 $\mu mol.m^{-2}.s^{-1}$ with *Prymnesium parvum* [91]. Similarly, another limiting nutrient in the growth medium can affect the adaptability of the microalgae. With *Ulva rotundata*, a nitrogen shortage will reduce the photo-acclimation at high light intensities and leads to intracellular damages [92]. Yun and Park (1997) demonstrated that the increase of light intensity allowed an enhancement of the growth specific rate, photosynthetic activity, carbon fixation, but the cells concentration was not modified and depended on the amount of nitrates in the medium [93]. Modifications within the metabolism can also be an adaptive response in case of light deprivation. For example, such stress will lead to a modification of the photosynthetic apparatus in order to optimally use the available light through an increase of chlorophyll and PSII/PSI ratio [78, 83, 94, 95]. The cell will also increase the synthesis of polysaturated lipids in the thylakoids membrane and the concentration of intracellular antioxidants, however the cells concentration and the specific growth rate will decrease [78, 94]. The light intensity is not the only parameter affecting the microalgae. Indeed, the illumination time also impacts the biomass production. Studies on day/night cycles showed that the photosynthetic activity and CO_2 fixation were more important when the day duration was greater [96, 97]. It is also possible to enhance the photosynthetic activity by using specific wavelengths of the

light spectrum. Vesk and Jeffrey (1977) showed that an addition of blue light increased the concentration of chlorophyll a of some diatoms species but not on the dinoflagellates considered [98]. In comparison with white light, no modification of growth parameters was observed when *Skeletonema costatum* was cultivated under blue light [99]. On the other side, when *Spirulina platensis* is exposed to red light, the specific growth rate and biomass production are enhanced [100]. Therefore, the efficiency of a photobioreactor is directly linked to the light penetration in the culture. Indeed, an optimal light intensity exists for each concentration of biomass, and an increase of the ratio illuminated surface/volume is necessary to enhance the productivity of a photobioreactor [79, 97, 101, 102]. Qiang *et al.* (1998) increase the growth rate of *Spirulina platensis* by 20% when decreasing the culture thickness from 200 mm to 7.5 mm [101].

1.1.3.5. Carbon Dioxide

As explained previously, two different mechanisms allows the microalgae to absorb and metabolize inorganic carbon, through CO_2 and through HCO_3^-. Therefore the addition of CO_2 during the growth will have a different impact depending on the preferential inorganic carbon metabolism of the microalgae, and depending on the presence or the absence of a CCM within the cell [103]. Indeed, a specie for which the inorganic carbon assimilation is mostly or essentially done by the diffusion of CO_2 through its cell wall will be promoted by an increase of dissolved CO_2. On the other hand, a specie that favours assimilation of inorganic carbon through the CCM and therefore HCO_3^-, will be affected by the addition of CO_2 due to the decrease of pH which will also decrease the quantity of HCO_3^-. For example, the expression of the genes controlling the CCM with *Chlamydomonas reinhardtii* is deleted when grown at high CO_2 concentrations [103]. On the other hand, when these species are transposed from high to low CO_2 concentration in their environment, the activity of the CCM therefore the photosynthetic activity, increases [104, 105]. This activity can increase by a factor of 10 with *Chlamydomonas reinhardtii* [105]. Although most of the microalgae and cyanobacteria are able to grow at high CO_2 concentrations, it has long time been believed that they couldn't grow at concentrations over 30% [105]. When a high concentration of CO_2 is dissolved in the medium, the pH of this medium and the

intracellular pH decrease. However, a decrease of the pH in the stroma of the chloroplasts leads to an inactivation of the RuBisCO and therefore affects the CO_2 fixation. However, studies highlighted the existence of species resisting to high CO_2 concentrations. *Chlorella sp.* and *Scenedesmus obliquus* have been cultivated at CO_2 concentrations from 30 to 50% [106-109], and *Chlorecoccum littorale* resisted to 40% of CO_2 [110, 111]. Also, the species *Cyanidium caldarium*, *Cyanidioschyzon merollae* and *Galdieria partite* are able to live at 100% of CO_2 [105]. Investigations have been realized to better understand this extreme resistance of the cells to high CO_2 concentrations. When *C. littorale* is transposed from low to very high CO_2 concentration, at first its photosynthetic activity is reduced which results in a reduction of the CO_2 fixation, a drop of O_2 production, and a reduction of the PSII efficiency [111-113]. Meanwhile, the cyclic transfer of electrons of the PSI is greatly increased. This leads to the synthesis of supplementary ATP. These ATP molecules will drive the implementation of ATP-dependent proton pumps which will help maintaining a neutral pH within the cell, more precisely at the RuBisCO compartment which will keep its CO_2 fixation activity [114]. CO_2 is provided to the culture through gaseous injection, usually a mixture of air and CO_2. The dissolution and transfer of CO_2 determines its availability in the culture. This method can also provide an efficient mixing of the culture, substituting mechanical mixing and allowing the homogenization of the concentration of cells and nutrients, and limiting the photo-inhibition and shadowing effects. However, an excessive mixing can also lead to a damaging of the cells [115, 116]. The transfer gas-liquid depends on several parameters: k_La, hydraulic retention time, gas retention time, gas holdup [115]. The holdup represents the bubbles volume which depends on the shape and size of the reactor, the temperature, the gas pressure, and the way the gas is introduced in the reactor [117]. Therefore, controlling the gas transfer is the reactor is a key factor for microalgae cultivation. Several studies have been done to assess the role of gas transfer on the microalgae biomass production. Contreras *et al.* (1998) highlighted the interaction of the CO_2 transfer and the cells density in a culture of *Phaeodactylum tricornutum* [116]. For a low cells density, the CO_2 consumption was inferior to the CO_2 transfer. The authors concluded that the CO_2 concentration was not the limiting factor but the CO_2 gradient inside the reactor was affecting its consumption by the microalgae. On the contrary, when the cells density was increasing, the CO_2 consumption was higher than the CO_2 transfer, thus becoming the limiting factor. Also, the optimal growth rate in this study was reached for a gas

speed of 0.055 m/s. However, beyond this speed, the growth was dramatically decreasing due to an excessive holdup. Soletto *et al.* (2008) also highlighted the relationship between gas flow rate and the growth of *Spirulina platensis* [89]. When the CO_2 flow rate was increased from 0.74 to 1.03 g/L/d, the microalgae growth and CO_2 fixation were reduced. The authors explain these results by both an excess of CO_2 and an increase of salinity due to the high amount of NaOH added to compensate the decrease of pH.

1.1.3.6. pH

pH is a key parameter during the growth of microalgae. An optimal pH exist for each microalgae specie, which will react in different ways to changes of pH depending on its physiology [118-120]. An equilibrium exists between intracellular and extracellular pH and numerous metabolic processes depends on the pH, such as the enzymatic activity [121]. Indeed, these protonation and deprotonation mechanisms activates the fixation sites for their substrate. The modification of internal pH will then lead to a modification of enzymatic activities. When the extracellular pH is modified, le pH gradient between the cell and the medium will chance and a new equilibrium will lead to the modification of the intracellular pH. The ability of the cell to follow these variations will depends on its ability to modify its physiology. For example, when the extracellular pH decreases, the quantity of extracellular H^+ ions increases and the cells will adapt their ATP production [120]. Also, pH variations also affects the cells through its impact on the assimilation of inorganic carbon [122]. Bartual and Galvez (2002) demonstrated that the association of a basic pH (from 7.9 to 9.5) and a light limitation (saturation with 150 $\mu mol.m^{-2}.s^{-1}$, and limitation with 30 $\mu mol.m^{-2}.s^{-1}$) generates a stress with *Phaeodactylum tricornutum* [121]. In light saturation conditions and a very basic pH, the specific growth rate was not modified. However, a pH higher than 8.5 associated with a light limitation greatly reduced the specific growth rate, which was also associated with an increase of the intracellular ratio C:N, and a decrease of intracellular nitrogen. The authors supposed that these results reflected an energy competition between carbon and nitrogen metabolisms. Indeed, with this specie, nitrates and HCO_3^- transport is activated, and when the cell is subject to a light limitation the quantity of ATP and NADPH available for these mechanisms greatly

decreases. In case of a high pH and a light limitation, assimilation of organic carbon was maintained at the expense of nitrates transport.

1.1.3.7. Temperature

The cells response to different temperatures varies among the microalgae species [96]. For example, the specific growth rate of *Nannochloropsis oculata* is optimal at 20°C, whereas the optimal temperature for *Scenedesmus almeriensis* is 35°C [123, 124]. The cells content can also vary with the temperature. Indeed, the quantity of unsaturated fatty acids increases when the temperature decreases for *Botryococcus braunii*, *Phaeodactylum tricornutum*, *Chlorella vulgaris*, and *Spirulina platensis* [125, 126]. With *Scenedesmus almeriensis*, the quantity of lutein increases with the temperature [124]. At temperatures lower than 5°C, *Dunaliella salina and Chlorella vulgaris* shows a reduction of CO_2 assimilation, photosynthetic capacity, synthesis of chlorophyll, and increase of xanthophylles [127]. With *Spirulina platensis*, the temperature affects the ultrastructure, the morphology, and the photosynthetic activity of the cells. A correlation between light radiations and temperature has also been found [128]. Indeed, UV-Rs damage the double helix of the DNA, which effect is enhanced at 15°C temperatures. DNA repairing mechanisms seems to be more efficient at 30°C, through metabolism modifications similar to those observed to counterbalance photo-inhibition. In addition, temperature variations affects the assimilation of inorganic carbon, in both direct and indirect ways. In an indirect way due to the lower CO_2 dissolution in water at high temperature, and in a direct way because an increase of temperature reduces the affinity of the RuBisCO with CO_2 [129].

1.1.4. Microalgae Culture

Microalgae are grown in biological reactors referred as photobioreactors (PBRs) (Figure 1.4). Two different production modes exists for microalgae cultivation in PBRs. First, the production of microalgae biomass in large scale is conducted in raceways operated in batch mode [130]. These are constituted of closed ponds of a few dozens of centimetres deep, circulars and forming successive loops. Raceways are equipped with paddle wheels used to prevent a settling of the microalgae and to reduce shading effects

by providing a mixing of the culture [14, 131]. Raceways requires a low investment and workforce, therefore this method is widely used for high volumes production [132]. Even though raceways are widely used worldwide, these also have disadvantages. Indeed, growth parameters such as temperature or light weather dependent, and therefore very difficult to control [133-135]. Also, these system are prone to contamination by local species such as bacteria which will grow at the expense of the cultivated microalgae. Carbon dioxide is usually provided to the culture directly from the air, however CO_2 adsorption can be improved through the addition of aerators or bubbling systems [14]. Improving the mixing may also improve the CO_2 and light transfer, therefore enhancing the productivity of raceways [14]. Using raceway ponds seems to be the more viable for microalgae production due to a very low energy ratio in comparison with closed cultivation systems [136]. However, considering the application of biofuel production, it appears that cultivation should be carried in continuous mode [137]. Continuous growth is more easily carried out using closed systems, more expensive but allowing a greater control of microalgae growth conditions and therefore able to achieve much higher productivities [14, 138]. Therefore, these are usually operated for the production of high value compounds. Common design of photobioreactor includes column, tubular, vertical, annular, or flat panel configurations, which optimizes the light supply through the culture [14, 134, 138]. Photobioreactors are usually mixed either mechanically or by airlift, combining simultaneous stirring and aeration [138]. Tubular reactors have large surface area, and are widely used in outdoor culturing for the production of high value compounds such as astaxanthin [131]. Flat panels have an even greater surface area and therefore can achieve a higher productivity than tubular or air lift reactors, however these require higher operation and installation costs [14, 131]. Closed photobioreactors allows the cultivation of a wide range of microalgae species and can sustain very high biomass concentrations [139, 140]. Despite the great advantages of closed systems, these shows limitations such as operating costs or the difficulty to scale up.

Figure 1.4 *– Examples of industrial microalgae cultivation systems [141, 142].*

1.1.5. Applications

1.1.5.1. Wastewater Treatment

Microalgae can be used for the tertiary and quaternary treatment of wastewater, consisting in the removal of all organic ions (ammonia, nitrate and phosphate) [43, 143], heavy metals [144], and various toxic organic compounds [145]. Microalgae also produces oxygen and therefore can serve as disinfectant for the removal of coliform bacteria due to the elevation of pH in the medium through photosynthesis [146]. A growing interest on microalgae use for wastewater treatment is observed worldwide due to a better comprehension of the biology of the microalgae and improvements in the design of cultivation systems [147-149]. Based on numerous studies, microalgae, diatoms, and flagellates have been listed depending on their tolerance to organic pollutants, highlighting the eight most interesting species (*Chlamydomonas*, *Scenedesmus*, *Chlorella*, *Euglena*, *Oscillatoria*, *Nitzschia*, *Stigeoclonium*, and *Navicula*) [150]. Concentrated microalgae cultures have been investigated to reduce the land-space requirements, with a great reported efficiency in the fast removal of nitrogen and phosphorus [151]. A wide range of wastewaters such as piggery effluent, industrial wastes, agricultural wastes, or human sewage, have also been treated efficiently by microalgae cultures [152-155]. Microalgae have been proved to adequately fit the requirements of tertiary and quaternary treatment processes, but have also been proposed for secondary treatment [156].

1.1.5.2. Biofuel Production

First and second generation of biofuel refers to bioenergies recovered from biological feedstocks such as wheat, corn, palm, sunflower, or soybean, transformed into biodiesel, bioethanol, or biomethanol [157-159]. However, these feedstocks requires large cultivation areas, therefore competing with agricultural lands used for food production [160, 161]. Microalgae are considered as the third generation of biofuel source, which efficiency outperforms first and second biofuel generation in terms of land requirements and productivity [162, 163]. Microalgae can be used in two different ways for the production of biofuel. The biomass can be transformed either through biochemical (transestherificaton, fermentation) or thermal processes (pyrolysis, liquefaction, gasification, and hydrogenation). Biodiesel production has been widely investigated by many research groups [164-166]. Transestherification is used for the production of biodiesel from the lipids accumulated by the microalgae cells. Indeed, various microalgae species produces and store large amount of lipids, reaching over 60% of their dry weight for species such as *B. braunii*, C. emersonii, *D. tertiolecta*, *Nannochloropsis sp.*, *N. oleoabundans*, or *P. cruentum* [133, 167-172]. In this process, blended methanol and catalysts reacts with the triglycerides from the lipids. The conversion yield of into biodiesel production can reach over 90% under strict temperature conditions [1, 173]. The fermentation of starch, sugar, and cellulose from the microalgae biomass can be applied for the production of bioethanol. Indeed, the carbohydrate content of microalgae can reach up to 70% of the dry mass, with a starch content reaching up to 60% [174]. The starch content can be increased by a strict control of nitrogen and iron supply to the culture [44, 175]. The biomass can also be transformed into bio oil or methane through pyrolysis at temperatures ranging from 200 to 750 °C. Pyrolysis rate of over 85% have been achieved at temperatures between 300 to 600 °C [176]. Bio oil can also be produced by liquefaction, in which the biomass is subjected to high temperature (over 200 °C) and high pressure (over 20 bar) in presence of a catalyst. Conversion yields range from 9 to 72% with the liquefaction process [177-179]. Finally, microalgae biomass can be converted into combustible gas (H_2, CH_4) through gasification. During the gasification, carbonated compounds of the biomass react with oxygen-containing gas at high temperature (200-700 °C).

1.1.5.3. Carbon Dioxide Capture

As the release of carbon dioxide in the environment due to human activities became one of the major causes of climate change, researchers have focused their attention towards solutions for its sequestration. Ecological development and artificial capture methods have helped reducing, capture, and store the carbon and release the oxygen. Various physicochemical techniques CO_2 capture techniques have been developed and are now widely employed for CO_2 mitigation [180, 181]. However, these techniques are usually expensive and requires a high amount of energy [182, 183]. Alternative mitigation methods have been investigated and microalgae have gained increasing attention for CO_2 capture due to their high carbon reduction capacity and fast growth [110, 184-187]. Most of the research on the ability of microalgae for CO2 capture has focused on cultivation in artificial mediums [110, 188-190]. However the literature strongly lacks of real-case studies using natural growth environments. Various microalgae strains such as *Chlorella kessleri*, *Chlorocuccum littorale*, or *Chlorella vulgaris*, have been investigated for carbon dioxide mitigation [191-193]. *Scenedesmus sp*. also appeared to be one of the most promising microalgae specie for the mitigation of large amounts of carbon dioxide [8]. Recently, improvements in the design of photobioreactors have allowed high efficiency in the carbon dioxide capture and biomass productivity [115, 194-196]. Media containing high concentration of nitrogen and phosphorus, as well as gas supplies containing elevated CO_2 partial pressures have been widely investigated [197-199]. However the increase of energy requirements necessary for the production of high-nutrient containing media and the supply of high CO_2 concentrations may ultimately reduce the interest of microalgae for this application. The reduction of these costs can be achieved using pre-treated sewage, easily available in urban areas as nutrient source, combining it with carbon dioxide capture [197-199]. Flue gases from power plants can contain up to 15% of carbon dioxide, which can therefore make them a suitable source of CO_2 for microalgae culture, reducing in the meantime CO2 emissions [200, 201]. Feeding microalgae cultures with artificial flue gases has been successfully investigated with the green alga *Monoruphidium minutum*, demonstrating the ability of the microalgae to sustain high levels of nitrogen and sulfur oxides [202]. Microalgae also shown ability to sustain high concentration of CO_2 (up to 40%) and high temperatures (up to 42°C) [106, 111]. It therefore microalgae appears

to have high potential for CO2 capture when used for the combined treatment of wastewaters and flue gases.

1.1.5.4.   Heavy Metals Biosorption

The contamination of waters sources and freshwater reserves by heavy metals represent a severe pollution issue which can ultimately affect both aquatic and human beings. Indeed, the effect of heavy metals can be dramatic when these are introduced within the food chain through any agricultural activity. Due to the high toxicity of heavy metals, wastewater effluents have to be treated accordingly [203, 204]. Metal ions removal is usually achieved with technics such as activated carbon adsorption, precipitation, resin ionic exchange, or reverse osmosis [205, 206]. In this context, microalgae have shown a great potential alternative to these methods, through their ability to accumulate heavy metals in high proportion [205, 207, 208]. Indeed, previous studies reported the bioaccumulation of various metal ions (Ag, Au, Zn, Hg, Cd, Mn, Cr, Ni, Fe, Cu, Cs) by different microalgae species, and valuable metals such as gold or silver can furthermore be recovered from the biomass [209-216]. Two different mechanisms are responsible for heavy metal removal by microalgae [214, 217, 218]. Metal ions can be absorbed into the microalgae metabolism for the synthesis of enzymes, vitamins, and proteins. They can also be involved in the cells enzymatic metabolism. The second metabolism may involve the binding of metal ions with extra- or intracellular carbohydrates.

1.1.5.5.   Production of High Value Compounds

Microalgae can produce various types of high value compounds which can be of interest in food, pharmaceutical, or cosmetic industries. Indeed, microalgae contains high amounts of biochemical compounds such as proteins or carbohydrates highly appropriates as food supplements [219].The microalgae biomass also contains vitamins (A, B, C, E, folic acid, nicotinate, biotin), and pigments (phycobiliproteins, chlorophyll, carotenoids), which can be used in many applications [220]. Many examples of the use of these compounds are found in the literature. Chlorophyll can indeed been used in ulcer and liver recovery treatments, but also to enhance the human cells growth and

increases the haemoglobin amount within the blood. The high amount of phycobiliproteins, a natural antioxidant and anti-inflammatory compound, found in cyanobacteria also makes them very interesting for leukemia and tumor treatments [221, 222]. Phycobiliproteins such as phycoerythrin and phycocyanin can also be used as fluorescent pigments for labelling of antibodies [223]. In addition, microalgae contains high nutritional value fatty acids such as decosa hexaenoic acid (DHA) and eicosa pentanoic acid (EPA), from which can be extracted omega-3 [224]. Fish oil still remains the main source of omega-3-rich fatty acids, however instability and unsustainability of fish oil production shifted the attraction towards alternative sources [225]. Indeed, the extraction of omega-3 from microalgae has been proven to be more cost-effective than fish oil. Eicosa pentanoic acid, found in microalgae, can serve various purpose within medical applications, such as for inflammatory and heart diseases or asthma treatments [226].

1.1.6. Harvesting and Concentration

With the recent interest in the development of techniques conciliating efficiency and sustainability, microalgae have become one of the most attractive research field. Indeed, microalgae offer many possibilities with direct applications in industry. There is basically two different ways to avail microalgae. First for the growth metabolism and its impact on the culture environment. The need for nutrients the growth phase, and the ability of microalgae to set fix heavy metals and toxic organic compounds, creates a direct interest in the treatment of several types of wastewater. The capture of carbon dioxide, necessary for the photosynthetic metabolism of microalgae, is one of its most studied research area since the ratification of the Kyoto Protocol by most of the developed countries. Microalgae are also grown for the production of biomass. The main application is the production of bioenergy but due to their high concentration of high added value compounds such as pigments and antioxidants, they are also very interesting for food-processing and pharmacology. However, in order to be used, the biomass needs to be harvested and concentrated. Different techniques are applicable, such as centrifugation, filtration, or flocculation. The main issue of the biomass concentration is its energy costs, which if not reduced, can jeopardize the global interest in these microorganisms for industry.

1.1.6.1. Centrifugation

One of the fastest and most efficient way to concentrate diluted microalgae biomass is by using centrifugal force. Indeed, centrifugation can achieve very high harvest efficiency without chemical or bacterial contamination, which is greatly suitable for the harvesting of high value compounds [1]. However, the high amount of energy needed for the centrifugation of microalgae biomass reduces its interest for lower value applications such as biofuel production [227, 228]. The designs of centrifuges used for the harvesting of microalgae biomass for biofuel production has evolved recently. However, these centrifuges still require a high investment and operating costs in comparison with other alternatives. Consequently, research has shifted towards the investigation of pre-concentration methods prior to centrifugation to decrease these costs. Flocculation has been investigated with four different flocculating microalgae strains (*Tetraselmis suecica*, *Ankistrodesmus falcatus*, *Ettlia texensis*, and *Neochloris oleoabundans*), for the harvesting of two non-flocculating strains (*Chlorella vulgaris* and *Scenedesmus obliquus*), prior to centrifugation [229]. The authors managed to reduce the operating costs of the concentration from 13.8 to 1.83 MJ/kgDW. Bilad et al. (2012), investigated the use of a submerged microfiltration system for the pre-concentration of *C. vulgaris* and *P. tricornutum* biomass, successfully decreasing the operating costs from 8 kWh/m3 to respectively 0.84 and 0.91 kWh/m3.Indeed, only 6.7% of the medium was left after the pre-concentration step [230].
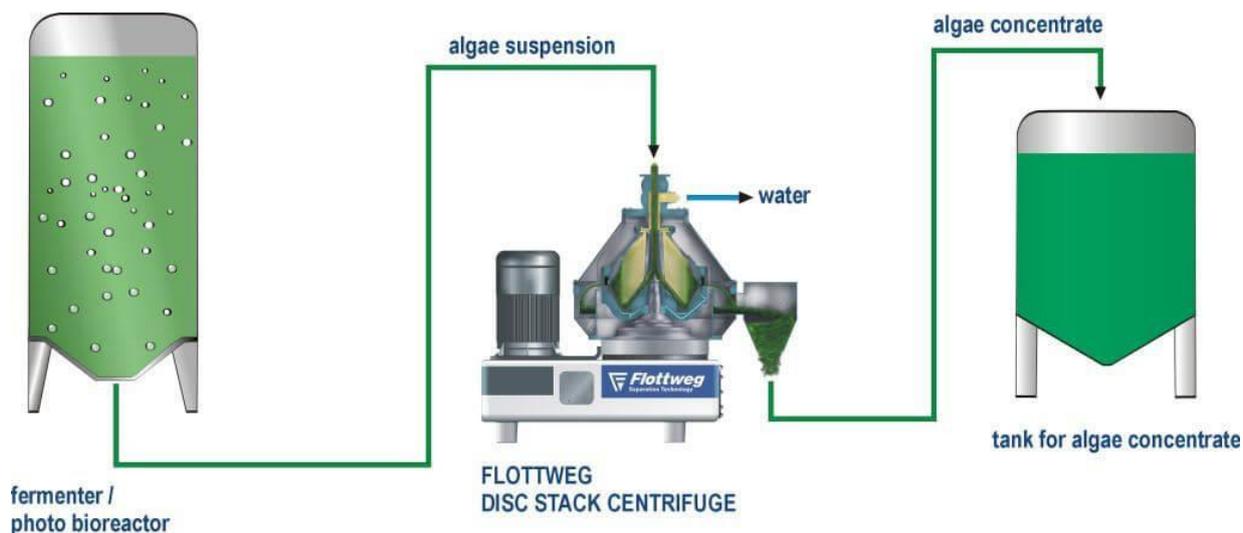
Figure 1.5 *– Industrial centrifugation process for the concentration of microalgae biomass (Flottweg SE) [231].*

1.1.6.2.   Flocculation

Different methods have been investigated for the aggregation of microalgae cells and the creation of flocs, more easy to separate from the medium. Flocculation process has been employed alone or as pre-concentration method in complement with other methods, for the harvesting and concentration of microalgae biomass. The surface of the microalgae cells is negatively charged which can be destabilized by a positively charged coagulant. These coagulants can be cationic polymers or polyvalent cations, such as aluminium- and iron-based metal salts. However, the efficient use of metal salts in the flocculation process requires high amount of costly flocculants and a low pH [232]. Also, the addition of aluminium salts induce a lysis of the microalgae cells [233]. Also, metal salts residues can alter the quality of the products and the recycled medium [74, 234, 235]. Organic polymers such as grafted starch or chitosan can also be used as flocculating agents. These polymers help achieving a good recovery of microalgae at low dosage, thus reducing the environmental impact of the process [227, 236]. More recently, another alternative to these flocculants has emerged. Cationic metal-bound aminoclays have been successfully used for the harvesting of microalgae [237, 238]. In these studies, Al- and Mg-bound aminoclays have been used for harvesting, and Fe-bound aminoclays was used for the coating of a filtration membrane. The results obtained were satisfactory, nevertheless the cost of these methods needs to be reduced

in order to compete with other technics. The choice of microalgae is also to be considered, as the efficiency of the flocculation decreases when marine algae are harvested due to the ionic strength of their surface [239, 240]. Extracellular polymeric substances (EPSs), such as polysaccharides or proteins synthetized by microorganisms, can also be used as an environmental friendly bioflocculant [241]. Kim et al (2011) investigated the use of a bioflocculant from *Paenibacillus polymyxa* AM49 combined with cationic chemicals for the harvesting of *Scenedesmus sp* [242]. They managed to harvest over 95% of the biomass while enhancing the growth rate with a recycled medium. It has also been demonstrated that mixtures of EPS-producing microbes, such as *Bacillus cereus* and *Pseudomonas stutzeri*, grown could effectively improve the harvesting of *Pleurochrysis carterae* [243]. However, the production of EPSs is not mandatory to induce the flocculation of microalgae [229]. Recently, auto-flocculating microalgae was employed for the harvesting of *C. vulgaris* and *S. obliquus*, thus reducing the final energy required for centrifugation. The auto-flocculation process describes the flocculation of microalgae cells due to the presence of multivalent cations such as calcium and magnesium ions at elevated pH [244]. A flocculating activity comparison has been conducted for *Botryococcus brauniiwith* using three different methods: inorganic flocculation, polymer flocculation, and auto-flocculation, the last one showing the greatest efficiency [245]. More generally, for an efficient auto-flocculation, the presence of multivalent cations in the culture medium should be sufficient. Therefore, ion-rich waters such as wastewater or seawater seems optimal for the auto-flocculation of microalgae. However, iron has to be preferred in comparison with magnesium hydroxide for the microalgae auto-flocculation, due to its ability to enhance the biomass productivity using recycled medium [242]. Ultimately, the effects of the flocculant and acid used for the pH adjustment also has to be considered in terms of both economic and environmental point of view [246].

1.1.6.3.   Flotation

The flotation process has also been investigated for microalgae harvesting. With this method, gas bubbles are sparged in a tank containing the microalgae leading to the creation of an easily collectable vacuole layer on top of the suspension. In this application, the size of the microalgae cells is determinant, and a diameter from 10 to

500 μm is found to be more suitable. However, aggregation of microalgae cells has been proven to be effective in creating flocs attaining the requiring mass for an effective flotation [247, 248]. Also, flotation efficiency greatly depends on the size of the bubbles sparged. The bubbles size is generally sorted into three different categories: nanobubbles (<1 μm), microbubbles (1–999 μm), and fine bubbles (1–2 mm), each category having a different impact during the flotation process. Indeed, nanobubbles shows a longer longevity, as well as a greater carrying capacity, due to the optimized ratio between surface area and volume [249]. In comparison with large bubbles, the slow rising of small bubbles also allows a more efficient attachment and transport of the microalgae cells [247]. Also, the surface characteristics of the microalgae cells such as the charge and hydrophilicity are determinants in the interaction with the bubbles. Indeed, although the surface of both microalgae cells and air bubbles are negatively charged, the cells exhibits a hydrophilicity whereas the air bubbles are hydrophobic. However, these can be modified to ensure a better interaction. Ozone flotation has been proven efficient to enhance the interaction between air bubbles and two microalgae strains (*C. vulgaris* and *S. obliquus* FSP-3), even with the greater electronegativity of the cells surface after this process [250, 251]. The ozonation partially breaks the cells which release protein-like substances, believed to be biopolymers, making the air bubbles more hydrophilic, thus enhancing the interaction with microalgae cells. Similar findings have been reported by another research group [248]. Another interaction between ozone and microalgae can potentially reduce the efficiency of the process. Ozone tends to sweep humic-like substances reducing the efficiency of the ozonation. Therefore, the selection of species producing low amount of humic-like substances has to be privileged. Garg et al. (2012) reported an enhancement of the flotation performance of *Tetraselmis sp*. M8 with the enhanced cells hydrophobicity by addition of C14TAB, a cationic surfactant [252]. The authors concluded that the hydrophobicity of the microalgae cells was primordial for the process efficiency, in comparison with the cells ionic strength.

1.1.6.4.   Filtration

Membrane filtration technology has been widely used in many applications due to its high separation ability, easy operation, and unnecessary of using chemicals for its processing. When applied for the harvesting and concentration of microalgae biomass, filtration can also help recycling the culture medium, therefore optimizing the nutrients consumption and retain viruses and protozoa [253]. It can also simplify further processes such as extraction, refining, or biomass conversion and [254]. However, it is widely accepted that fouling is the main issue in every membrane process. It is caused by the deposition of alogenic organic matter (AOM) and the creation of an algal cake layer on the membrane surface [253, 254]. To reduce the detrimental impact of fouling, cross-flow filtration is preferred in opposition with dead-end filtration due to the backwashing and ventilation provided with this method [255]. Ultrafiltration has been successfully investigated in cross-flow mode for the concentration of microalgae culture from 1 to over 150 g/l with the addition of pulsated air scouring and backwashing [254]. A submerged microfiltration module has also been studied as a first step biomass concentration stage with promising results due to the reduction of fouling due to the shearing caused by air scouring [230]. Bhave et al. (2012) achieved a medium recovery of 99% and a concentration of microalgae biomass from 1 to over 150 g/l using hollow fiber membranes combined with a ceramic tubular membrane [256]. In order to prevent fouling issues, dynamic filtration has been investigated due to the high shear stress and turbulences induced, resulting in plateau fluxes 2 to 3 times higher than a conventional cross-flow microfiltration system [257, 258]. Dynamic filtration can also reduce the energy costs of the filtration in comparison with cross-flow filtration [259]. The principle of forward osmosis has been recently studied for the dewatering of microalgal biomass by the National Aeronautics and Space Administration (NASA) [30]. This project, called Offshore Membrane Enclosures for Growing Algae (OMEGA), aimed to use FO bags immersed into the ocean to grow microalgae using wastewater, and concentrate the biomass at the same time (Figure 1.6). The final goal of this project was to study microalgae as an alternative for the production of aviation fuels. FO membranes immersed into the ocean have also been studied for a partial dewatering of microalgae, reaching an average water flux of 2 $l.m^{-2}.h^{-1}$ (LMH) and obtaining a final biomass concentrated by 6.5. A significant biofouling was observed, without affecting the flux [31]. Despites the research conducted for the application of

membrane filtration for microalgae dewatering, improvements of membrane properties and characteristics, focusing on microalgae dewatering, have to be studied in order to further optimize these methods. The development of integrated systems combining the different steps of biomass cultivation, concentration, and extraction has to be investigated in a larger scale.
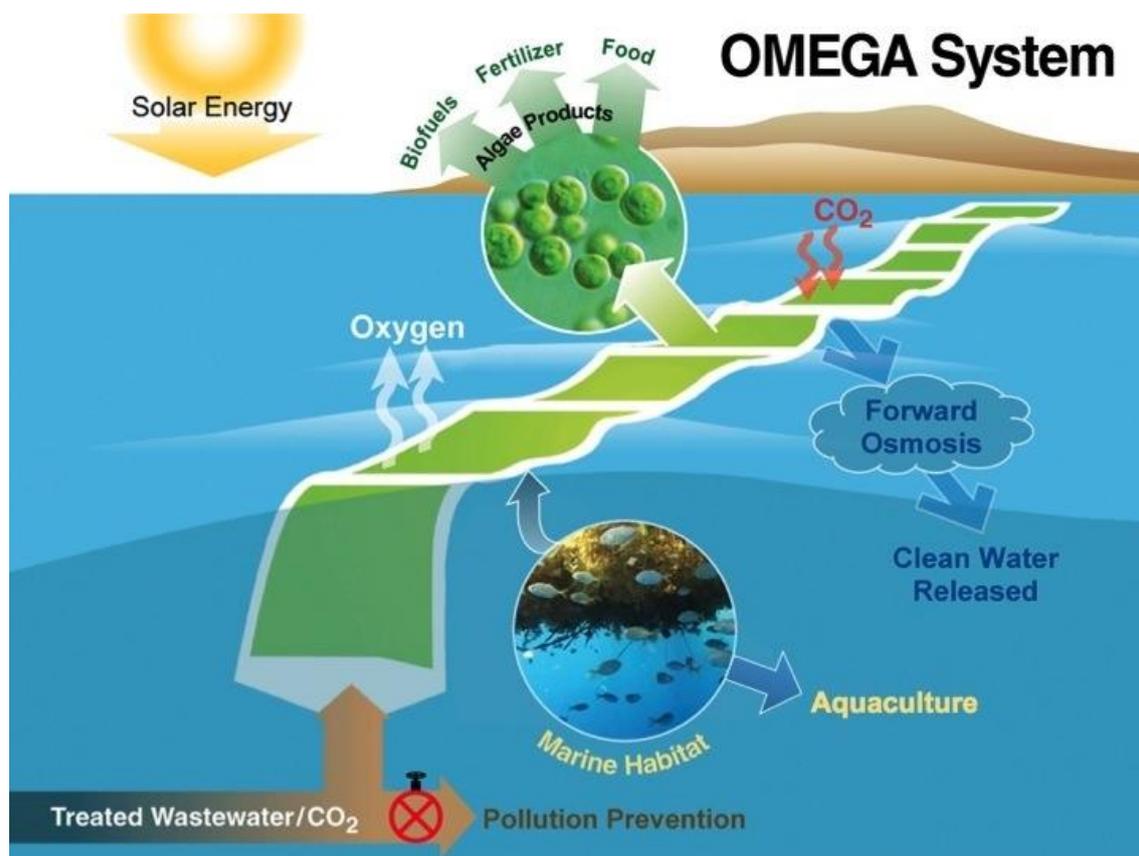
Figure 1.6 – Schematic of the OMEGA System (NASA) [260].

1.1.6.5.   Comparison of Harvesting and Concentration Methods

Many methods have been applied and investigated for the harvesting and concentration of microalgae biomass, and each of them present advantages and disadvantages (Table 1.1). Some methods, such as coagulation, flocculation, sedimentation, or flotation are inexpensive. However, these may require the addition of potentially harmful chemicals and issues of contamination also appears. Other methods, such as filtration or electrical-based processes are more expansive, but can achieve greater recovery rates. More generally, each method will be best applied for the

harvesting and concentration of a specific microalgae strain, a specific growth medium and mostly for a specific application. For example, the cultivation of microalgae for biofuel production will require cost-efficient harvesting and concentration methods such as flotation [1]. Usually, a combination of two harvesting processes will be used, such as bio-flocculation followed by gravity sedimentation. On the other hand, the production of high value compounds will require the use of highly effective concentration methods, even if this means increasing the harvesting costs. Also, the addition of other chemicals will be avoided. Therefore, techniques such as filtration or electrical-based processes will be preferred [261].

Table 1.1 – *Comparison of advantages and disadvantages of different microalgae biomass harvesting and concentration methods. Table taken from [262].*

Harvesting Method	Advantages	Disadvantages
Chemical coagulation / flocculation	- Simple and fast method - No energy requirement	- Chemical flocculation may be expensive and toxic to microalgae biomass - Recycling of culture medium is limited
Auto and bio-flocculation	- Inexpensive method - Allows culture medium recycling - Non-toxic to microalgae biomass	- Changes in cellular composition - Possibility of microbiological contamination
Gravity sedimentation	- Simple and inexpensive method	- Time-consuming - Possibility of biomass deterioration - Low concentration of the algae cake
Flotation	- Feasible for large scale application - Low cost method - Low space requirement - Short operation time	- Generally requires the use of chemical flocculants - Unfeasible for marine microalgae harvesting
Electrical-based processes	- Applicable to a wide variety of microalgae species - Do not require the addition of chemical flocculants	- Poorly disseminated - High energetic and equipment cost
Filtration (other)	- High recovery efficiencies - Allows the separation of shear sensitive species	- The possibility of fouling/clogging increases operational costs - Membrane should be regularly cleaned - Membrane replacement and pumping represents the major associated costs

1.2. Forward Osmosis

The physical phenomenon of osmosis has been exploited from the beginning of mankind when it was discovered that salt could be used for food desiccation. Indeed, salt preserves food from most of bacteria, fungi, and other potentially pathogens microorganisms by killing or inactivating them from dehydration [263]. The osmosis phenomenon was first described in 1748 by Jean-Antoine Nollet, after he immersed a bottle of water closed with an animal bladder into water and discovered that water was permeating through the bladder into the bottle, but the alcohol was not permeating on the opposite way. However, this phenomenon first got named in 1827, when René Dutrochet proposed the terms "endosmosis" and "exosmosis" while conducting experiments with aqueous solutions. Osmosis has then been studied during the 19th century by Thomas Graham who discovered that colloid substances are retained by animal membranes, by M. Traube who first conceived an artificial membrane made of copper ferrocyanide, and W.F.P. Pfeffer who continued Traube's work by precipitating copper ferrocyanide in a porous material to give mechanical strength to the membrane. In 1886, Van't Hoff made an analogy between thermodynamics and osmosis, and established a law similar to the Gay-Lussac law. He received the Nobel Prize in 1901 for his contribution in the field of chemistry. In 1899, A. Crum Brown noticed a phenomenon of osmosis while using three liquid phase: water saturated with phenol, pure phenol, and calcium nitrate saturated with phenol, and observed the water passing from the first phase to the third one, the pure phenol layer acting as a semipermeable membrane. From 1901, H.N. Morse and J.C.W. Frazer carried on the work by investigating the permeability of gelatinous precipitates such as ferrocyanides and phosphates of uranyl, iron, zinc, manganese, and cadmium. Nowadays, membrane filtration widely used for various industrial applications. Among these processes, forward osmosis has gained increasing attention in the past few decades and is now employed for in a wide range of applications such as power generation, seawater desalination, wastewater treatment, or food processing [264].

1.2.1. Principle

Forward osmosis is an osmotically-driven membrane process based on the difference of solute concentration between two solutions separated by a semi-permeable membrane. The presence of solute within a solution induces the existence of an osmotic pressure. The relationship between solute concentration and osmotic pressure is given by the Morse equation, derived from the Van't Hoff equation [265]:

$$\pi = \beta \cdot C \cdot R \cdot T \qquad\qquad 1.1$$

where, π is the osmotic pressure of the solution (Pa), β is the Van't Hoff coefficient, C is the concentration of solute (mol/L), R is the ideal gas constant (8.3145 J/K/mol), and T is the temperature (K). The forward osmosis principle can be described as the separation of a highly concentrated salt solution called "Draw solution" from a low concentrated salt solution called "Feed solution" by a semi-permeable membrane. An osmotic pressure difference arises between both sides of the membrane, and creates a driving force leading to the permeation of pure water from the feed side through the membrane. The pure water therefore dilutes the draw solution and the system eventually reaches an equilibrium state. Therefore, this process does not require the application of hydrostatic pressure, while maintaining a retention rate of contaminants very high and a very low fouling compared to other pressurized membrane processes. The water flux crossing the membrane is classically calculated with the following equation:

$$J_W = A \cdot (\Delta\pi + \Delta P) \qquad\qquad 1.2$$

where Jw is the water flux ($m^3.m^{-2}.s^{-1}$), A the pure water permeability of the membrane ($m.s^{-1}.Pa^{-1}$), $\Delta\pi$ is the osmotic pressure difference (Pa), and ΔP is the hydrostatic pressure difference (Pa). However, for simplicity reasons, the water flux is usually displayed in LMH (L. $m^{-2}.h^{-1}$).
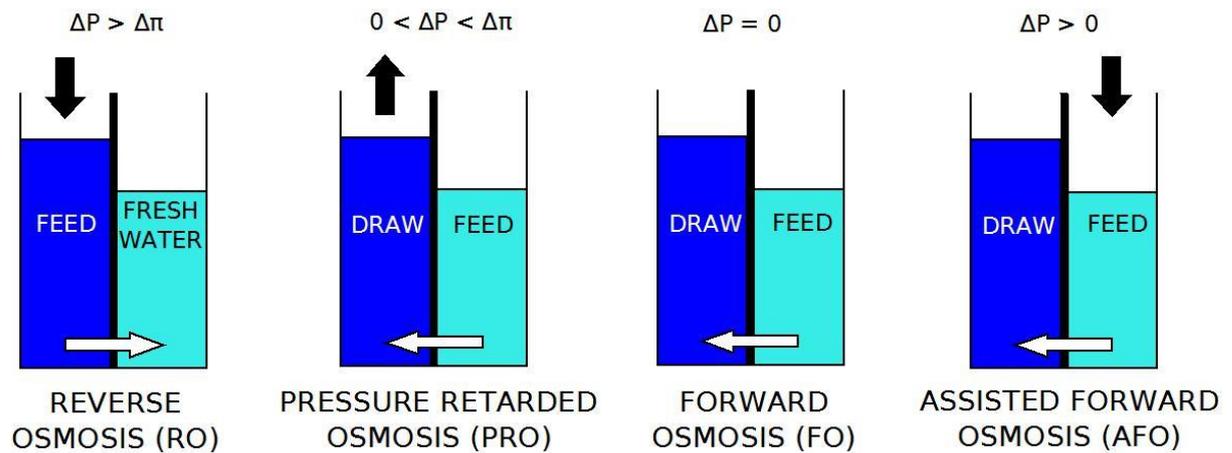
Figure 1.7 - Description of the principle of osmotic processes.

Various osmotic process can be found, as described in Figure 1.7. All of these processes involves the filtration of solutions with different osmotic pressures using semi-permeable membranes. Reverse osmosis (RO) is one of the main osmotic process. During RO, a high hydraulic pressure is applied on a solution of high osmotic pressure to force fresh water to pass through the membrane. For this process to work, the hydraulic pressure difference (ΔP) needs to remain higher than the osmotic pressure difference ($\Delta\pi$). Pressure retarded osmosis (PRO) describes an osmotic process using the difference of osmotic pressure between the draw and the feed to produce energy. The feed solution permeating through the membrane increases the pressure on the draw side, which energy is recovered using turbines. As mentioned, FO describes the concentration of a feed solution using a draw solution. Assisted forward osmosis (AFO) is a variation of FO in which an additional hydraulic pressure is applied on the feed side to increase the permeate flux.

1.2.2.   Industrial Applications
1.2.2.1.   Seawater Desalination

FO has been proposed for removing salt from saline water since the 1970s [266-269]. FO can be used for seawater desalination in two ways. The first one use seawater as feed solution and a draw solution with a higher osmotic pressure. This requires the development of draw solutions with an osmotic pressure much higher than that of water. The only problem is the need to separate the diluted draw solution afterward. Various

separation processes such as distillation or membrane separation can be implemented depending on the products used to produce the concentrated solution. The osmotic pressures generated by the presence of different products depends on the concentration but also on the type of compound used. Two compounds (CaCl2 and MgCl2) can be very interesting to get a significant osmotic pressure because of their number of ionic species in solute [15]. The use of these compounds, however, depend on their price and the feasibility of their subsequent separation. As shown on a pilot [270], salt retention is above 95% for a permeate flux of 25 LMH. The major drawback of the direct osmosis is the need to obtain a concentrated solution easily separated in the second part of the process. Indeed, if the reverse osmosis process is used to desalinate the draw solution, whose osmotic pressure is very high, the amount of energy needed became very important. Draw solution component must provide a huge osmotic pressure and be easy to separate. Because of that, many studies have been made in order to improve and optimize draw solutions. One method of FO desalination employs thermolytic draw solutions which can be decomposed into volatile gases (e.g. CO_2 or SO_2) by heating after osmotic dilution. McCutcheon et al. proposed another novel method using a mixture of CO_2 and NH_3 as the draw solute for desalination [269-271]. The resultant highly soluble and thermolytic ammonium bicarbonate (NH_4HCO_3) draw solution can yield high water fluxes and result in high feed water recovery. The other type of FO desalination uses water-soluble salts or particles as the draw solutes, and fresh water is generated from diluted draw solution by other methods. Khaydarov and Khaydarov [272] proposed utilizing solar power to produce fresh water from the diluted draw solution after osmotic dilution. An et Ng investigated seven draw solutes (i.e. NaCl, KCl, $CaCl_2$, $MgCl_2$, $MgSO_4$, Na_2SO_4 and $C_6H_{12}O_6$) for seawater desalination using hybrid FO-NF system [273].Ling and Chung used hydrophilic nanoparticles as the draw solutes for desalination and the nanoparticles could be regenerated by UF [274]. Zhao et al. proposed using divalent salts (e.g. Na_2SO_4) as the draw solutes for brackish water desalination because the diluted solution could be recovered via NF [26, 275]. Another way to use forward osmosis in water desalination purpose is as pre-treatment for reverse osmosis in term of reducing operating costs. This hybrid process has been tested and it has been concluded that this process had the ability to reduce fouling power of very poor water quality and reduce production costs [276]. Indeed, this process can be used for diluting the seawater decreasing the osmotic pressure, and then decreasing the amount of energy needed in the reverse osmosis process and the fouling on the RO

membrane. For this application, the best way is disposing a source of water with a low salts concentration. Then this water is user as feed solution and the seawater can be used as draw solution. Cath et al. employed FO as an osmotic dilution process using seawater as the draw solution for impaired water purification in a hybrid FO-RO process [19]. Similar FO-RO desalination system were proposed to generate both potable water [277, 278] and the osmotic power of RO brine [276]. In these combined FO-NF or FO-RO processes, FO offers several major benefits, including high quality of drinking water due to the multi-barrier protection, reduced RO fouling because of the pre-treatment by FO, recovery of osmotic energy of RO brine, low energy input and no need for chemical pre-treatment. In fact, the FO process acts as a pre-treatment process (i.e. osmotic dilution) in a second type of FO desalination. To get fresh water, further water recovery methods must be used to desalinate the diluted draw solution.
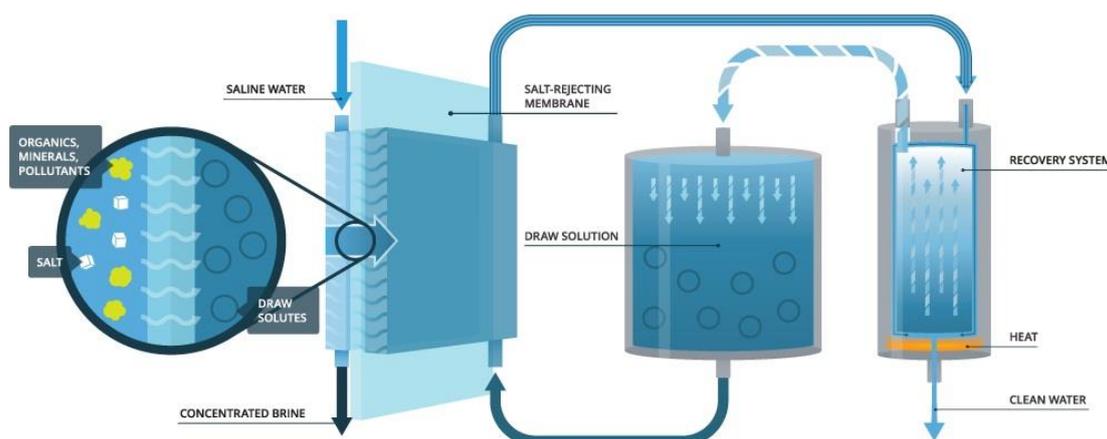
Figure 1.8 – *Seawater desalination system using forward osmosis for the production of purified water (Source: Oasys Water) [279].*

1.2.2.2.   Water Treatment

Forward osmosis has been studied for its potential in the treatment of wastewaters, which interest grows due to the increase of population combines with the depletion of fresh water sources and the growth of water use in industry. Indeed, many advantages exists when using FO to treat wastewater. In comparison with other membrane processes, FO does not require the application of hydraulic pressure, which lowers the

energy requirements and the process global costs [280, 281]. This lack of hydraulic pressure also reduces the impact of fouling and the costs of cleaning, and therefore enhances the membranes lifetime [282, 283]. FO membranes efficiently removes total dissolved solids (TDS), rejects pathogenic microorganisms, and can also reject emerging contaminant [281, 284, 285]. Cath et al. obtained promising results while studying the production of drinking water using impaired water as feed solution and saline water as draw solution [19]. FO has also been investigated for the concentration of activated sludge [18], and centrate from anaerobic digestion [286]. FO has been recently proposed in hybrid systems called osmotic membrane bioreactors (OMBRs) [18, 287-289]. In these systems, forward osmosis is combined with the aerobic or anaerobic digestion in order to treat diluted wastewaters. The wastewater is concentrated by FO and the freshwater is produced afterwards, by the recovery of the diluted draw solution, usually by reverse osmosis of membrane distillation. Indeed, FO is perfect in combination with anaerobic treatment, which is generally insufficient for the treatment of municipal wastewaters due to their low concentration of organic matter [290-292]. The different possible configurations of OMBRs are shown on Figure 1.9. Two main configurations arise, depending on the FO integration methodology. Indeed, the FO concentration can occur prior to feeding the bioreactor or directly inside the bioreactor. In case of pre-concentration of the feed solution, a high fouling propensity has been reported [33, 293], and the increase of crossflow velocity in order to prevent this fouling may endanger the structure of the activated sludge flocs [294]. In immersed configurations, the accumulation of salt diffusing from the draw solution into the bioreactor may potentially become an issue. The impact of this accumulation on FO performances has been investigated using a model including different membrane parameters and operating conditions of the OMBR [289]. The authors found that the membrane selectivity (B/A), and the ration between hydraulic and sludge retention time (HRT/SRT), were the main parameters to take into account. Indeed, the lower these parameters are, the lower the permeate flux decline is and the better the performances of the system are. Finally, OMBRs can be combined with micro or ultra-filtration processes (Figure 1.9e) in order to reduce the salinity within the bioreactor, and achieve high fluxes and low fouling propensity [295-298]. Overall, the use of forward osmosis in wastewater treatment will mostly focus on the pre-treatment in order to reduce the overall costs by reducing membrane fouling [264].
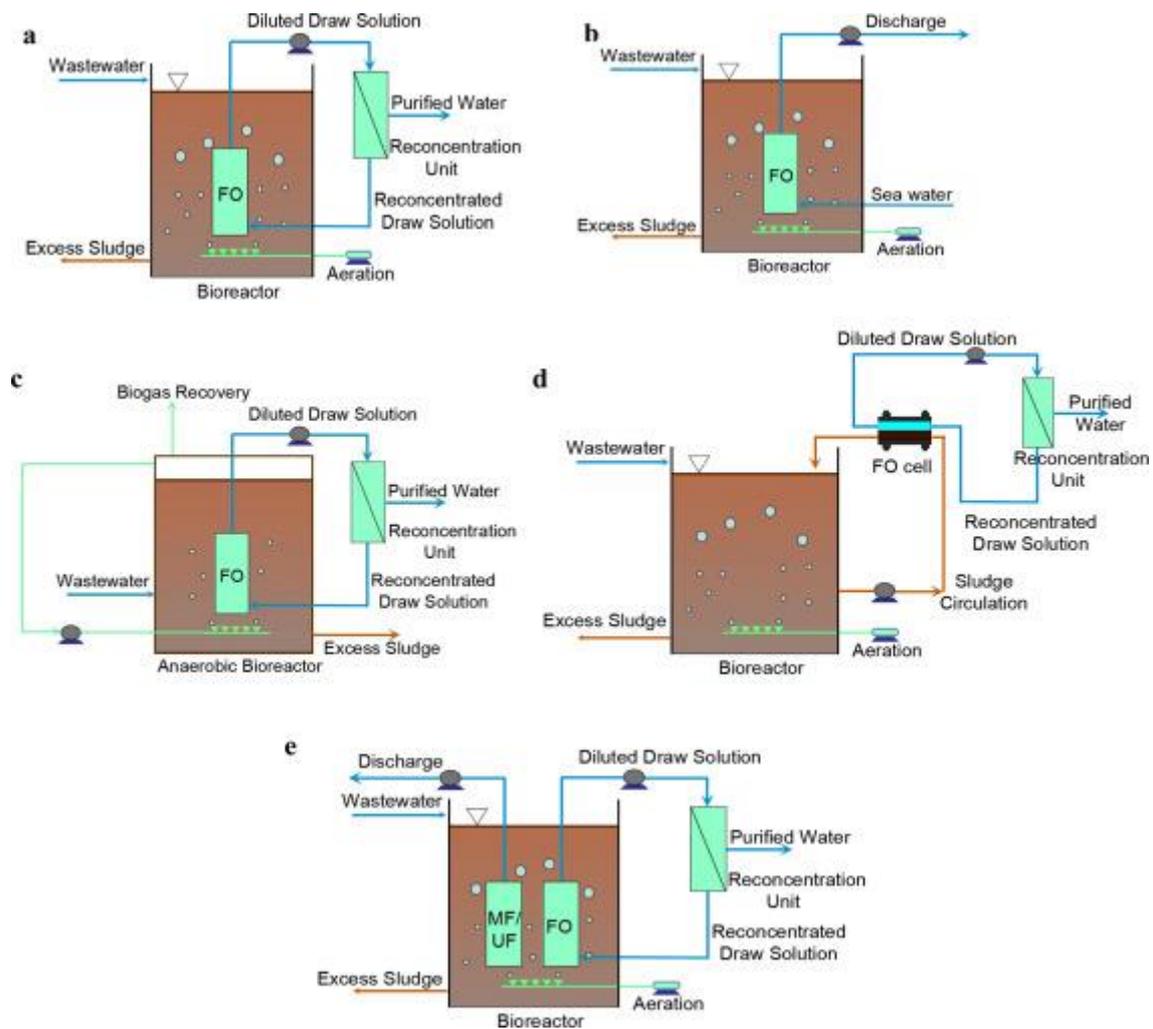
Figure 1.9 *- Schematic diagram of OMBR systems. (a) Submerged OMBR for wastewater reclamation, aerobic condition; (b) Submerged OMBR for wastewater treatment, aerobic condition; (c) Submerged OMBR for biogas recovery, anaerobic condition; (d) Side-stream OMBR, aerobic condition; (e) Combined OMBR, aerobic condition [299].*

1.2.2.3.   Food Industry

The concentration of liquid food, such as juices or purees, is one a major process in the food industry because it affects the stability and product quality, but also in transport costs, handling and storage [300]. Currently, different processes are employed mainly using thermal evaporation procedures or freeze concentration. These processes are energy intensive, and can also alter the organoleptic profile of concentrated products such as flavour, colour or texture and even induce a sensory loss and nutritional value

with the deterioration of vitamins or other heat sensitive compounds [301]. Several filtration processes have been investigated such as reverse osmosis, osmotic distillation, and membrane distillation. Reverse osmosis has been widely used in the industry for the concentration liquid food products, however the high hydraulic pressure, the high concentration polarization, and high organic fouling could be detrimental for its use in food industry [302]. Among the osmotic-based technologies, forward osmosis has shown promising results, since FO membranes are much cheaper and have a longer lifetime of than other membrane processes [300]. Forward osmosis, has been greatly employed for the concentration of various products, including many juices [303, 304], fruits (pears, apricots, strawberries, etc…) [305-307], vegetables and tubers (carrots, peppers, potatoes, etc…) [308-310]. In these applications, forward osmosis is employed for the removal of water by dehydration. Indeed, this process provides numerous advantages such as low working temperatures and pressures, and the feasibility of treating products containing substantial amount of suspended solids. The choice of draw solution is essential, since it impact not only the performances of the process but also the quality of the final product. Indeed, a small amount of solute from the draw diffuses through the FO membrane into the feed solution. Therefore, the draw solute used must be compatible with the food product dewatered, which means that it should not alter its organoleptic properties and nutritional value. The most common draw solution used for food concentration is NaCl which is inexpensive, gives good performances, and is easily recovered by reverse osmosis [281]. NaCl solutions from 2 to 6M have been studied for the concentration of Juices [311, 312], milk whey [313], or orange liquors [314]. The effectiveness of using these draw solution was proven but high reverse solute diffusion was observed. Simple carbohydrates such as glucose, fructose, or corn syrup have also been used for the concentration of juices [304, 315], natural colour extracts [316], or coffee [317]. These draw solutions presents a lower water flux than NaCl and their higher viscosity also enhances the concentration polarization and the power consumption through the use of pumps. Therefore, draw solutions combining NaCl and sucrose have been successfully investigated for the concentration of pineapple juice, achieving high performances and reducing the reverse diffusion of NaCl [311]. No optimal draw solution has been found yet for the application of FO in food industry, which presents one of the major impediment for further commercial applications.

1.2.2.4.   Pharmaceutical Industry

In pharmaceutical industry, FO process has mostly been used for the controlled release of drugs, acting as a pump driven by osmosis phenomenon [318, 319]. Most pharmaceutical products are sensitive to heat and are large enough to be rejected by FO membranes. In comparison to conventional chemical and physical dewatering treatments, FO is simpler and more environmental friendly, and should therefore be of a high interest in pharmaceutical industry. However, this process is not very common in this industrial field, but a few application applications have still been investigated. Under special circumstances, an accurate release of drug is more adequate than the usual oral route of medication, which is where the use of osmotic pumps becomes relevant. It also achieves a regular drug concentration in the bloodstream and can help reducing side effects [320]. Few companies have already developed drug delivery systems for human therapy, and osmotic systems such as OROS$^{®}$ Push-Pull^{TM}, EnSoTrol$^{®}$, or L-OROS^{TM} have been developed [321]. Also, FO membranes with MgCl$_2$ as draw solution have been successfully used for the enrichment of a lysozyme solution without denaturation [322]. In addition, the proteins fouling is minimized due to the hydrophilicity of the layer facing the proteins feed.

1.2.2.5.   Power Generation

Pressure retarded osmosis (PRO) has been first proposed and investigated by Sidney Loeb in 1976 [323, 324]. Since then, this process has raised a great interest for its ability to generate power from the abundant resources that are seawater and freshwater. This process is used to produce energy from the pressure difference arising when two solutions of different osmotic pressure are separated by a semi-permeable membrane. Theoretically, 1.7 to 2.5 MJ of energy can be generated when 1 m^3 river water is mixed with 1 m^3 seawater or with a large surplus of seawater [325]. It is estimated that the gross power potential of this unconventional energy source reaches up to 2.4 − 2.6 TW [326, 327]. PRO membranes specifically designed for power generation reported the highest power density (up to 10.00 W/m^2) [328]. McGinnis et al. proposed a closed cycle PRO process (i.e. osmotic heat engine) to exploit the osmotic power generated using a concentrated ammonia-carbon dioxide draw solution [329]. The main advantage of this osmotic heat engine include allowing the use of low-

grade heat sources (e.g. waste heat or geothermal heat) to generate power and the achievement of high energy conversion efficiency [269]. The first power generation plan has been started by Statkraft on November 2009 in Tofte, Norway (Figure 1.10). This plant is using the pressure differential between seawater and river water to produce about 4 kW which is very little compared to the installation and operating costs. However, several improvements on membranes and turbines efficiency can be made to enhance the performances and profitability of the power generation.
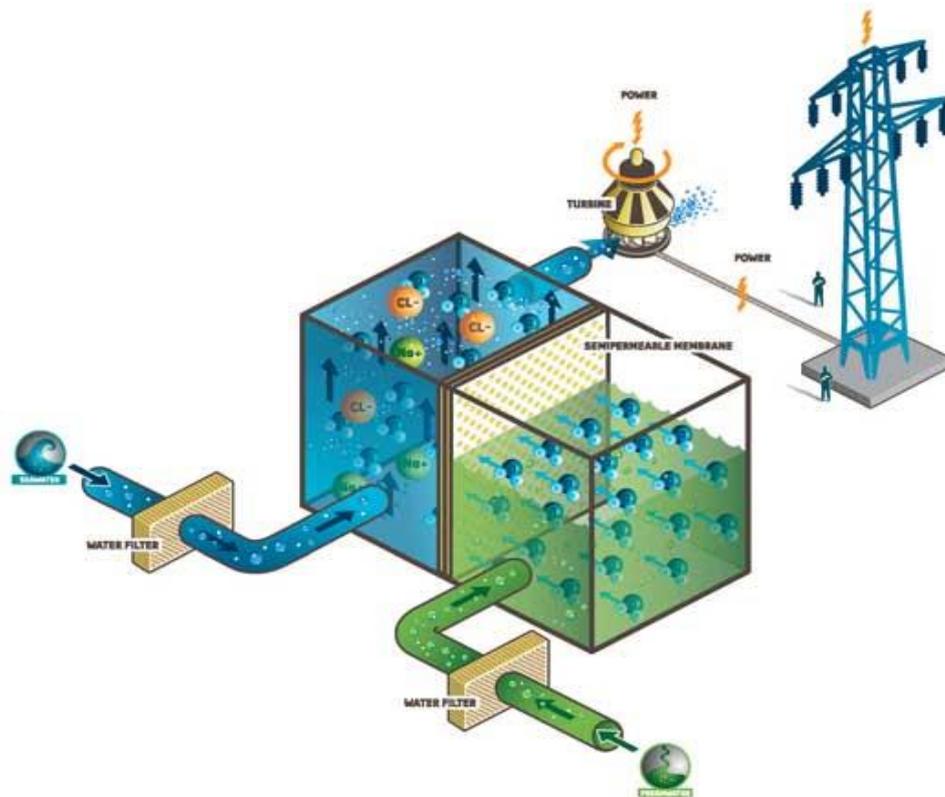
Figure 1.10 -*Schematic of a PRO power plant as used by Statkraft in Tofte, Norway [330].*

1.2.3. FO Membranes

1.2.3.1. Asymmetric Membranes

Asymmetric membranes are commonly manufactured by phase inversion [331]. The composition of most of asymmetric membranes is based on cellulose acetate, either diacetate (CDA), or triacetate (CTA), due to its low fabrication cost [332, 333]. Cellulose acetate can exhibit high water fluxes and can prevents fouling due to its

hydrophilic properties. In addition, cellulose acetate have good resistance to common oxidative species which prevents its alteration during cleaning processes [333]. Cellulose acetate membranes are typically prepared by coating the polymer solution onto a woven fabric [334, 335]. The porosity of the membranes is ensured by the presence of compounds such as lactic acid, zinc chloride, or maleic acid in the dope solution used. More recently, cellulose acetate membranes composed of a porous layer coated on both sides with active dense layer were proposed [332, 334, 336, 337]. It was reported that, during the fabrication, the structure of the bottom layer was affected by the substrate used to cast the membrane [332, 338]. Glass substrate resulted in a dense layer at the bottom of the membrane, whereas when Teflon was used the bottom layer was more porous, the top layer not being affected by the substrate. The main limitations of cellulose acetate membranes remains its narrow pH range of operation (4-8) and temperature limits (0-35℃).
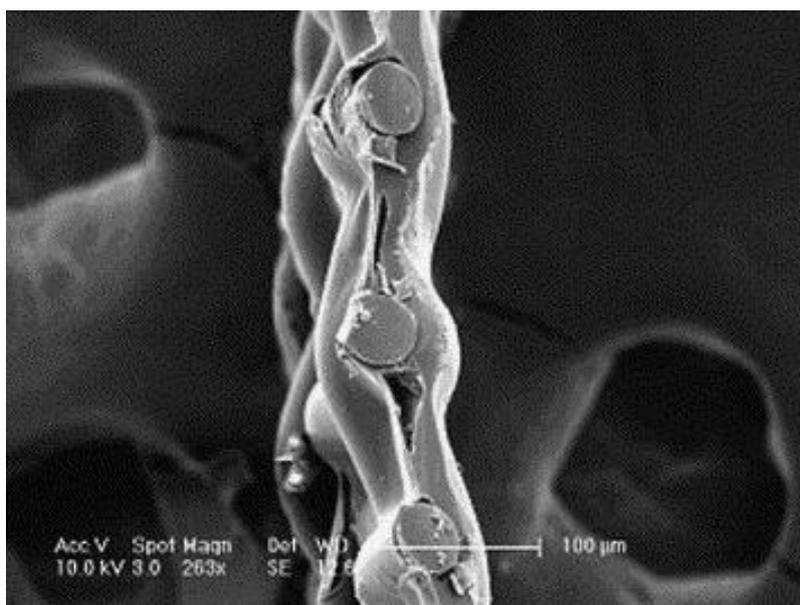
Figure 1.11 - *A cross-sectional SEM image of HTI's FO membrane. A polyester mesh is embedded within the polymer material for mechanical support [269].*

1.2.3.2. Thin Film Composite Membranes

As an alternative to celluloside membranes, thin-film composite membranes have been developed for a better control of the membranes properties. Various strategies have been employed for the improvement of the separate properties of both active layer

and support layer. The desired properties of the support layer are a high porosity, low tortuosity, and a good mechanical resistance. Indeed, a high porosity and low tortuosity will lower the resistance to the water passage, therefore increasing the permeate flux. It will also reduce the internal concentration polarization effect, discussed in the next section. The good mechanical resistance will allow the membrane to sustain moderate pressure differences and prevent structural damages. The most common material used as support layer is polysulfone (PSf) which has been largely studied [339-342]. The dense layer is usually formed by interfacial polymerization on top of the before mentioned support layer. Yip et al. (2010) fabricated a thin-film composite membrane with a polysulfone support layer, achieving very high water fluxes (18 LMH) and high sodium chloride rejection (over 97%) [340]. The membrane was also investigated with ammonium bicarbonate as draw solution and high pH, proving its resistance to such operating conditions. Water flux can also be enhanced by increasing the hydrophilicity of the membrane, which can be achieved by the addition of polyethylene glycol (PEG) or polyvinylpyrrolidone (PVP) to the PSf substrate, however the results obtained did not prove its efficiency [343, 344]. Electro-spun PES fibers and nanofiber supports have also been investigated, showing promising results in membrane properties enhancement [345-347].

1.2.4. Concentration Polarization

Concentration polarization (CP) is a phenomenon appearing in every pressure driven and osmotically-driven process [15, 348-352]. This phenomenon is due to the variation of salt concentration inside and outside the membrane. It reduces the osmotic pressure differential and then decreases the permeate flux. Concentration polarization can be divided into two different phenomenon: External Concentration Polarization (ECP) which appears on each surfaces of the membrane, and Internal Concentration Polarization (ICP) which appears inside the membrane, between the active layer and the support layer. The effect of both ECP and ICP is the reduction of osmotic potential, therefore of the water flux permeating through the membrane.
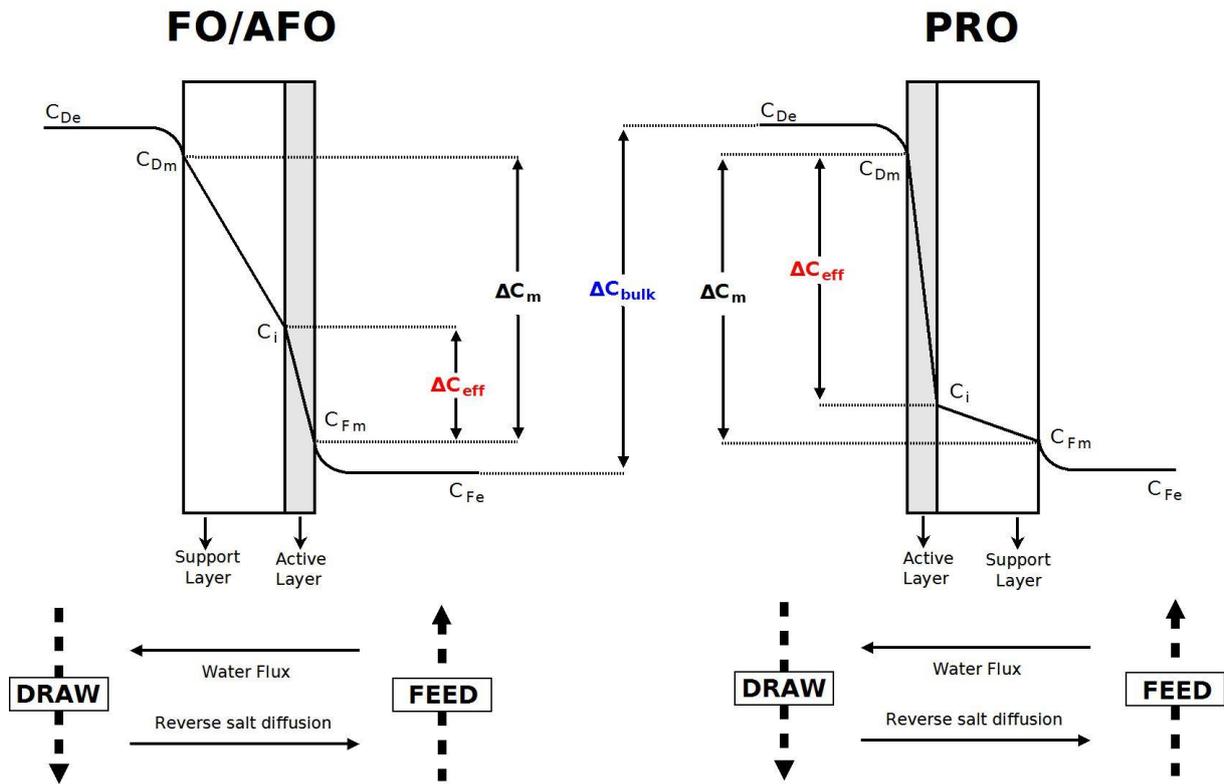
Figure 1.12 *- Schematic of the concentration <u>polarization</u> phenomenon with both orientation of FO membranes.*

Figure 1.12 explains CP phenomenon for FO membranes. C_{De} and C_{Fe} are respectively the salt concentrations of the draw and feed solutions, C_{Dm} and C_{Fm} are respectively the salt concentrations on the surface of the membrane on the draw and feed sides, and C_i represent the salt concentration inside the membrane, between the support layer and the active layer. Two different membrane orientations, representing FO/AFO mode and PRO mode are presented. On this figure, ECP appears between C_{De} and C_{Dm} for the draw side, and C_{Fe} and C_{Fm} for the feed side. ICP appears inside the membrane between C_{Dm} and C_i.

1.2.4.1.   External Concentration Polarization

As in pressure-driven membrane processes, ECP in FO occurs at both sides of the surface of the membrane. Indeed, the pure water cross the membrane from the feed side to the draw side while a reverse salt diffusion, due to the salt concentration differential, appears on the opposite direction. Consequently, it is possible to differentiate two types of ECP. The first one, called concentrative ECP, correspond to the increase of salt

concentration between the feed and the membrane surface due to the imperfect salt rejection of the membrane and the two fluxes mentioned previously [350, 353, 354]. The second one, called dilutive ECP, correspond to the decrease of salt concentration between the draw solution and the membrane surface. Only concentrative ECP can take place in a pressure-driven membrane process, while both concentrative ECP and dilutive ECP may occur in an osmotically driven membrane process depending on the membrane orientation. Concentrative ECP occurs when the membrane support layer is facing the feed solution. ECP reduces the net driving force due to increased osmotic pressure at the membrane active layer interface on the feed side of the membrane, or decreased osmotic pressure at the membrane active layer surface on the draw solution side. However, the adverse effect of ECP on the permeate flux can be reduced by increasing the flow turbulence or velocity, or optimizing the water flux [15, 355]. McClutcheron and Elimelech have modelled ECP in FO using boundary layer film theory [348]. The general equation for concentration polarization modulus in pressure-driven membrane process can be expressed as [355].

$$J_w = k \cdot \ln\left(\frac{\pi_D}{\pi_F}\right)$$

1.3

where k is the mass transfer coefficient (m.s^{-1}), π_D the osmotic pressure of the draw solution (bar), π_F the osmotic pressure of the feed solution (bar). Even if the ECP reduce the water flux crossing the membrane and then the efficiency of the process, the global role of ECP is minor in FO configuration and is not able to jeopardize it [270].

1.2.4.2.   Internal Concentration Polarization

ICP is the most important phenomenon in osmotically driven membrane processes. Indeed, the flux decline is principally caused by ICP [348, 356-358]. It only occurs in asymmetric membrane systems, correspond to the loss of driving force because of the decrease of salt concentration into the support layer. AS shown on Figure 1.12, two types of ICP can appear depending on the membrane orientation. The concentrative ICP appears when the active layer faces the draw solution as in PRO mode. In this case, because of the high salt rejection of the active layer, salt

concentration inside the membrane C_i is low and the driving force $\Delta\pi_{eff}$ related to ΔC_{eff} in high. Then, the effect of concentrative ICP is small and the water flux can remain high. The dilutive ICP appears when the active layer faces the feed solution as in FO mode. In this case, the difference between the osmotic pressure differential across the membrane ($\Delta\pi_m$) and the effective osmotic pressure differential ($\Delta\pi_{eff}$) is very high compared to concentrative ICP. In order to understand and reduce the internal CP, several models have been developed to describe the phenomenon. Adopting the models developed by Lee et al [359] as a simplified equation to describe the water flux during FO without consideration of the membrane orientation have been introduced.

$$J_W = \frac{1}{K} \cdot \ln\left(\frac{\pi_D}{\pi_F}\right) \qquad\qquad 1.4$$

where K is the resistance to solute diffusion within the membrane porous layer ($m^{-1}.s$) defined as:

$$K = \frac{t_s \cdot \tau}{D \cdot \varepsilon} \qquad\qquad 1.5$$

where t_s is the membrane thickness (m), τ the tortuosity, ε the porosity and D the diffusion coefficient of the solute ($m^2.s^{-1}$). The effect of ICP has also been modelled by adopting the classical solution-diffusion theory [348, 359, 360]. When the draw solution is placed against the membrane support layer (i.e. FO mode), dilutive ICP dominate the water flux (J_w), and it can be expressed as [360] :

$$J_W = \frac{1}{K} \cdot \ln\left(\frac{A \cdot \pi_{draw} + B - J_W}{A \cdot \pi_{feed} + B}\right)$$

$$1.6$$

where B is the solute permeability ($m.s^{-1}$). Both ICP and ECP greatly reduces the membrane performances, and research has focused on the improvement of membrane characteristics through the reduction of concentration polarization effects.

1.2.5. Draw solutions

1.2.5.1. Inorganic Salts

A large variety of water soluble inorganic salts have been investigated as potential draw solutes, due to the high resulting fluxes and the ease of draw solute recovery through reverse osmosis [287, 361-363]. Inorganic solutes represents most of the draw solutes investigated in forward osmosis studies (Figure 1.13). Examples of inorganic salts includes magnesium, calcium, sodium, potassium, barium, or caesium, which have been studied from the early 1970s [303]. Inorganic salts can be sorted into three groups depending on the recycling method used for their recovery. The first group is composed by inorganic salts thermally recoverable such as ammonium bicarbonate which has been investigated for seawater desalination for the past decade [269, 270, 348, 358]. Ammonium bicarbonate generates high water fluxes and can be recovered through heating (around 60 °C). At this temperature, ammonium bicarbonate is decomposed into carbon dioxide gas and ammonia, which can be further re-dissolved in order to regenerate the draw solution. This process only requiring relatively low energy consumption, its utilization has been reported to save up to 85 % of energy in comparison to other methods during seawater desalination [271]. However, the high reverse solute diffusion appears to be an issue when using ammonium bicarbonate due to the reduction of osmotic power and the contamination of the feed solution [361]. The second group of inorganic salts is composed by those possibly usable as fertilizers, which have been investigated only recently [364]. After dilution through the FO process, the draw solution can be directly used for irrigation without any treatment, also reducing the overall amount of energy needed which is reported to be the most energy-intensive process in seawater desalination [263, 264, 271]. The utilization of these still suffers from limitations due to the acidic nature of these, not suitable for all FO membranes such as these made of cellulose acetate and cellulose triacetate [365]. Also, the partial dissolution of most of these salts leads to a reduction of efficient osmotic pressure and therefore low observable water fluxes [366]. The third category of inorganic salts is composed by those recovered through the use of pressure driven processes [361, 367, 368]. These salts have been investigated in various FO applications and methods for the selection of an appropriate draw solute depending on the applications have been developed [361, 369]. Over the 500 salts investigated, 14 were selected based on the

high permeate fluxes obtained as well as the low reverse diffusion and the ease of further draw solution recovery.
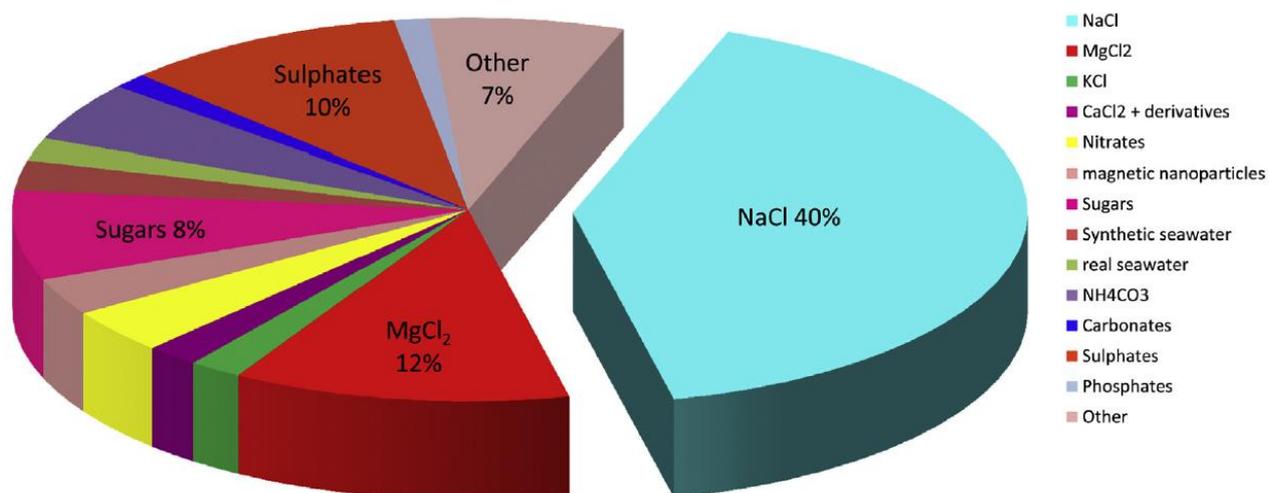
Figure 1.13 *- Draw solutions used in FO based on approximately 50% of FO publications. Results are expected to increase in similar ratios when considering all published works. [370]*

1.2.5.2. Organic Salts

Organic salts have proposed recently by Bowden et al. (2012) in an osmotic membrane bioreactor for wastewater treatment due to their biodegradability [371]. After a selection process, sodium acetate, sodium propionate, sodium formate, and magnesium acetate were chosen for further investigation. Organic salts outperform inorganic salts in terms of salt rejection during the re-concentration step by reverse osmosis and the biodegradability. However, organic salts exhibits low permeate fluxes in comparison with inorganic salts. Indeed, organic sodium salts at an osmotic pressure of 28 atm generates permeate fluxes from 8.7 to 9.4 LMH, whereas around 14 LMH are produced using similar osmotic pressure of sodium chloride [372]. The lower diffusion coefficient of these salts enhances the negative effects of concentration polarization, which also increases the energy needs for its recovery through reverse osmosis [23].

1.2.5.3. Volatile Compounds

Volatile compounds have been first proposed by Neff (1964) as draw solute for desalination by forward osmosis [373]. He investigated the potential, regeneration, and applications of mixtures of carbon dioxide and ammonia gases (NH_4CO_3) with forward osmosis (Figure 1.14). The osmotic pressure resulting being very low due to the low solubility of the mixture used, the addition of ammonium hydroxide in various proportions has been studied for the increase of solubility in water, therefore enhancing the performances of the process [269, 270]. Mixtures of sulphur dioxide (SO_2) and seawater or freshwater have also been suggested as draw solution [374]. The recovery of SO_2 was realized by heating or air stripping. Mixtures of SO_2 and aliphatic alcohols were also studied in order to decrease water activity and therefore increase the resulting osmotic pressure [375]. More recently, saturated potassium nitrate (KNO_3) was proposed as draw solution for seawater desalination, which recovery was achieved by a second FO unit using SO_2 as draw solution [376]. The SO_2 of the second FO unit was then recovered through heating. Despites the promising results obtained, the risks inherent to the use of volatile SO_2 reduces its attractiveness for seawater desalination by forward osmosis. The number of studies on volatile compounds as draw solution is still limited and the results obtained cannot compete yet with other draw solutions.
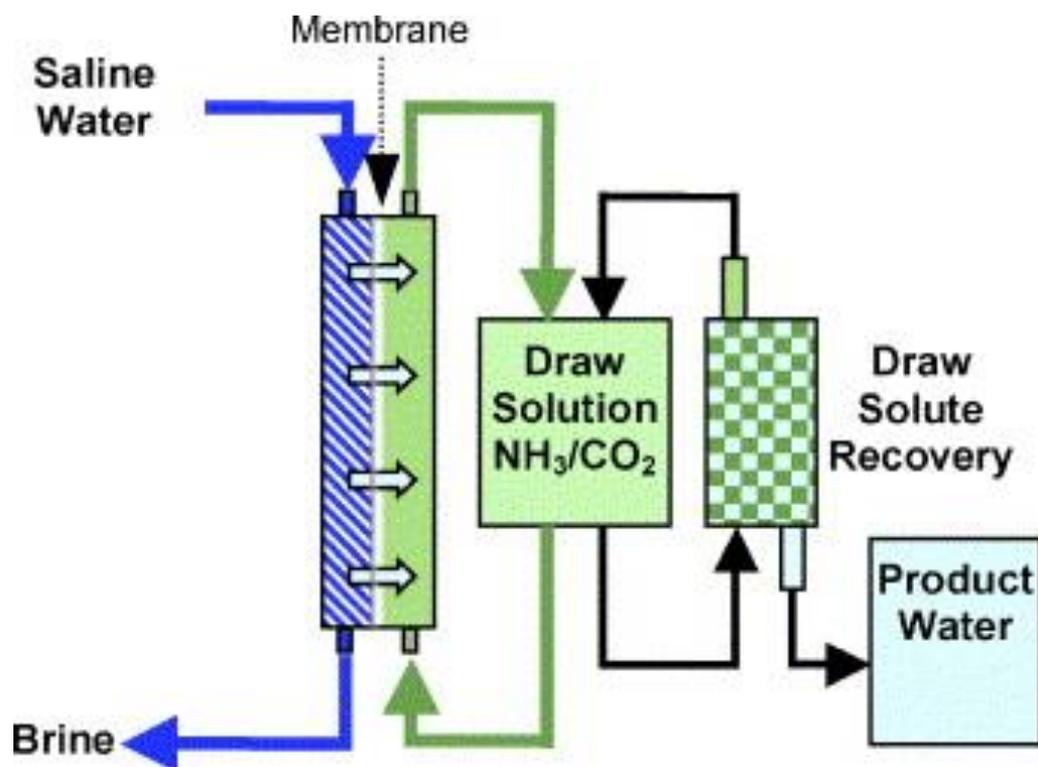
Figure 1.14 - *Schematic drawing of the novel ammonia–carbon dioxide FO process [269].*

1.2.5.4.   Synthetic Materials

Several synthetic materials have been recently proposed as draw solutions for forward osmosis. Among these, hydrophilic magnetic nanoparticles (MNPs) have shown promising results and have therefore raised a great interest [367, 372, 377-380]. Solutions of MNPs coated with polyacrylic acid or polyethylene glycol diacid have exhibited water fluxes around 18 LMH [372, 379]. An external magnetic field was used for the recovery of the draw solutions. Studies revealed that the hydrophilicity and the size of the nanoparticles was highly related to the osmotic pressure exhibited due to the effect of surface ligands. As no reverse solute diffusion was observed, MNPs draw solutions possess a great advantage over inorganic salts, in FO applications where feed contamination has to be avoided [377]. Despites the great potential of nanoparticles for FO applications, their performances still remain below these of inorganic draw solutions due to a lower osmotic pressure and much higher concentration polarization effects. Therefore, the use of highly soluble synthetic materials has been explored [381, 382]. Solutions of charged and neutral 2-methylimidazole have been investigated for seawater desalination using an FO-MD process for draw recovery, however the reverse

diffusion into the feed solution still remains an issue. Additionally, the elevated cost of 2-methylimidazole synthesis also alter its potential for FO processes. Finally, solutions of polyelectrolytes such as polyacrylic acid sodium, easily recoverable by ultrafiltration, have been investigated and have shown great performances in comparison with usual inorganic salts [358, 381, 383]. The relatively high viscosity of concentrated polyelectrolytes solutions may decrease their potential, but this issue can be solved by increasing the temperature of the draw solution. More work has to be carried on the use of synthetic material, these showing a great potential for FO draw solution.

1.2.6. Membrane Fouling

Fouling is recognized as the major issue in every membrane processes. It is due to the attachment of matter composing the flux onto the membrane surface and result in an additional resistance to the permeate flux and eventually a decrease of the process performances (Figure 1.15). It also has a direct impact on the life duration of the membrane, and the membrane cleaning/replacement frequency [384]. FO fouling suffers, at different levels, from the same mechanisms described with pressure-driven membrane filtration processes, which are principally due to the coupled effect of chemical and hydrodynamic interactions [385]. Other fouling mechanisms, due to the reverse solute diffusion, are only described in osmotically-driven processes [386]. More generally, fouling can be decomposed into different mechanisms described in this section.

Figure 1.15 – Examples of fouled industrial membrane modules [387, 388].

1.1.1.1.   Colloidal Fouling

Colloids can be defined as small particles of a diameter ranging from 1 to 1000 nm [389]. The deposition of these particles onto the membrane surface causes the formation of a cake layer which effect is an increase of resistance and the reduction of permeate flux. The deposition and development of fouling is governed by foulant-foulant and foulant membrane interactions [390, 391]. In the case of colloidal particles, the classical Derjaguin-Landau-Verwey-Overbeek (DLVO) theory, based on the van der Waals forces (VDW) and electrical double layer theory (EDL), is used to describe these interactions [390, 392, 393]. The DLVO theory can also be used in case of colloidal-sized microorganisms to explain biofouling [394, 395] , 113). In order for the colloids to aggregate, they must overcome the energy barrier which is represented by the addition of VDW and EDL forces [393, 396]. Colloidal fouling can affect the FO filtration performances by two related mechanisms: cake layer formation, and cake-enhanced osmotic pressure (CEOP). The cake layer formation induces the appearance of an additional resistance to the initial membrane resistance, thus reducing the water flux permeating through the membrane. The CEOP describes the reduction of driving force by enhancement of concentration polarization effects, due to the formation of the cake layer aforementioned [25, 397]. In this case, the salt diffusing through the membrane accumulates at the interface of the membrane and the cake layer or within the cake layer, thus reducing the difference of osmotic pressure across the active layer of the membrane. The increase of salt concentration within the cake layer also results in stronger interactions between the colloids [24]. The distinct effect of these two mechanisms has been studied. It appears that cake layer formation plays a major role in colloidal fouling in early stages of filtration, whereas CEOP dominates in later stages, as the thickness of the cake layer increases [24, 25]. Several studies have been conducted to assess the effect of different parameters, such as salinity, crossflow velocity, and foulant concentration, on filtration performances. A high salinity combined with a high colloids size has been demonstrated to accelerate the deposition of these onto the membrane surface, by creating a dense foulant layer on the membrane surface through the enhancement of Van der Waals forces [398]. The pH of the feed solution also affects fouling by acting on the repulsive electrostatic forces between the membrane and the colloids [24]. Chong et al. (2008) observed an increase of CEOP effects with high permeate flux and low crossflow velocities, mostly due to the thicker

cake layer [399]. The structure of the cake layer also plays a key role on the effects of colloidal fouling, according to Lee et al. (2011) [397]. The reversibility of colloidal fouling in FO has been investigated in few studies. It appears that a physical cleaning, conducted by increasing the crossflow velocity, is efficient to recover most of the performances in absence of colloids aggregation [24].

1.2.6.1.   Organic Fouling

Organic fouling describes the fouling due to the presence of organic substances such as humic acid, proteins, or carbohydrates. In this case, membrane fouling starts with the initial adhesion of these substances onto the membrane by interfacial interactions. Once organic macromolecules completely adsorbed and covered the membrane surface, the deposition of organic compounds is governed by interactions between this initial layer and newly deposited organic substances [400]. These mechanisms are described as membrane-foulant-foulant interactions, in which chemistry and hydrodynamics plays a key role [23]. Among the different factors affecting organic fouling, the membrane materials (composition, surface charge, hydrophobicity, roughness), the properties of the organic compounds (size, surface charge and composition), and the hydrodynamics conditions (fluid dynamics) are predominant. Mi and Elimelech studied alginates fouling and cleaning on FO membranes. They concluded that the fouling layer formed is less compact than in RO because of the lower hydraulic pressure which avoids the use of chemicals [23]. Fouling with mixtures of oppositely charges lysosome and alginate has also been studied, demonstrating a more severe flux reduction and foulant layer deposition in presence of these two foulant in comparison with single foulant feed solutions [401]. This finding was explained by the strong electrostatic interaction between the negatively charges alginates and the positively charged lysosomes. The role of membrane characteristics and orientation has also been widely studied. Valladares Linares et al. observed that organic foulants on the membrane surface (active layer) could enhance the negative charge property and hydrophilicity of the surface, and also increase absorption capacity for hydrophilic compounds [20]. Indeed, hydrophobic membranes are more prone to organic fouling through adsorption [402]. The active layer of FO membranes, smoother than the rough and porous support layer has also been identified as less subject to organic fouling deposition and pore blocking [401, 403]. Jin et al. found that organic

fouling could also have important effects on the removal of inorganic contaminants (e.g. boron and arsenic). The influence were dependent on the membrane orientation: in FO mode organic fouling on the membrane active layer could enhance the sieving effect and thus improve the rejection for arsenic; in PRO mode organic fouling in the membrane support structure could decrease the rejection for boron [21]. Hydrodynamic conditions are also crucial concerning the deposition and development of organic fouling. A high initial flux, resulting in a high permeation drag force, combined with a low crossflow velocity, resulting in a low turbulence level, have been described as the main factors affecting fouling with specific organic compounds [23]. Organic fouling can be prevented by membrane surface modifications [404], pre-treatment of the feed solution [405], or improvement of hydrodynamic conditions. Cleaning of organic fouling has also been investigated to assess the recovery of FO membrane performances. It has been shown that physical methods are efficient enough to remove most of organic fouling, thus avoiding the use of additional chemical cleaning agents [385, 406]. Indeed the fouling layer is generally loosely attached to the membrane surface and less compact, due to the lack of hydraulic pressure applied in FO processes. As an example, it has been shown with seawater as feed solution that a crossflow velocity of 16.7 cm.s^{-1} is enough to prevent organic fouling on the active layer for at least 30 days [67].

1.2.6.2.   Scaling

Scaling can be described as fouling caused by salts which are concentrated beyond their solubility limit and precipitate onto the membrane surface [407]. Scaling has been widely discussed in RO systems [408], and most of the findings are also applicable in osmotically driven membrane processes. Scaling usually limits the capital cost of the circulating pumps and the pipes, and increases the energy required for the circulation of the draw solution. The emergence and severity of scaling mostly depends on the concentration and the solubility of the compounds causing it, and scaling only occurs if the concentration of scalant locally exceeds the saturation value. Indeed, using calcium sulphate under the saturation concentration, Zhang et al. noted the appearance of gypsum scaling inside the membrane support layer, due to the local exceeding of saturation concentration. The saturation index reached 4.0 at the interface between the active layer and the support layer, although the saturation index of the bulk solution

was 0.8 [409]. Li et al. also investigated silica scaling during seawater desalination by FO, reporting the polymerization of dissolved silica as the dominant fouling mechanism occurring [27]. When the crossflow velocity (CFV) decreased from 16.7 to 4.2 cm.s-1, a fouling layer principally due to the polymerization of dissolved silica appear and the flux decrease for about 20%. It has also been reported that silica fouling layer facilitate the deposition of NOMs onto the membrane surface [132]. It has to be noted that most of the studies on scaling uses gypsum as a model, which is independent of the pH of the solution, and also has a high solubility [26, 410-412]. Actually, scaling can also be caused by other alkaline species (calcium carbonate, calcium phosphate), or silica-based species [413, 414]. The scaling caused by these last species are also dependent on the pH, which can change locally due to the diffusion of H^+ or OH^-. Therefore, more studies on scaling in osmotically driven membrane processes are necessary.

1.2.6.3.   Biofouling

In membrane processes, biofouling describes the deposition and the development of microbial communities onto the membrane surface, which is enhanced by the presence of nutrients in the feed solution [415, 416]. These colonies form a biofilm composed of dead and living cells producing and releasing extracellular polymeric substances (EPSs) enhancing the detrimental impact of the biofilm and reducing the filtration performances [417]. Biofouling is usually considered as the most recalcitrant among the different types of fouling mechanisms [418]. Indeed, as soon as a biofilm develops on the membrane, physical and chemical cleaning strategies fail to efficiently recover the initial membrane performances because of the strong adhesion of the layer of EPSs [419]. Several studies have been conducted, with pressure-driven membrane processes, to assess the impact of biofouling on permeate flux, membrane rejection, and fouling control [415, 418, 420, 421]. However, biofouling occurring during FO processes mostly focused on the characterization of the biofilm and the comparison with pressure-driven membrane processes. Important differences have been found between FO and RO concerning the biofilm size and composition. Indeed, FO biofilms are less compact than with RO, which moderately reduces the permeate flux [422, 423]. FO biofouling is also more reversible than with RO, although physical cleaning strategies, used to remover other fouling types, still remain inefficient. Physical and

chemical cleaning strategies have been studied by Yoon et al. (2013) [423]. Their results shows that chlorine was effective for the control of biofouling in FO. In the meantime, a further chemical cleaning associated with a physical cleaning (high cross flow velocity) further improve its efficiency. Biofouling mitigation has also been investigated. It appears that the use of thick mesh spacers [424], or the reduction of phosphate in the feed solution [425], can efficiently reduce the impact of biofouling in FO. More generally, a pre-treatment of the feed solution and the modification of membrane properties seems to be the optimal strategies for biofouling mitigation [426-428].

2. Microalgae (*Scenedesmus obliquus*) Dewatering using Forward Osmosis Membrane: Influence of Draw Solution Chemistry

2.1. Introduction

Microalgae have attracted increasing attention due to their promising application in sustainable biofuel generation, wastewater remediation, carbon dioxide sequestration and pharmaceuticals production [429]. Despite the promise, one technical challenge remaining to be overcome is the high energy cost of algae harvesting and dewatering that accounts for 20-30 % of the total operating cost [430]. Conventional methods for microalgae dewatering include centrifugation, flocculation, sedimentation and any combination of these. But they are either prohibitively energy intensive, damaging algal cells, or negatively affecting biomass quality [431]. Pressure-driven membrane filtration processes such as ultrafiltration are alternative techniques for microalgae harvesting due to their higher separation efficiency, easy operation and no or little need of chemicals addition. Petrusevski et al. [432] reported to harvest microalgae with an overall intact biomass recovery between 70 % and 89 % by using tangential crossflow 0.45 µm membrane filtration. However, these pressure-driven membrane processes are highly susceptible to fouling with much of them irreversible [433].

The forward osmosis (FO) membrane filtration process is an emerging and promising alternative for microalgae primary harvesting prior to further thickening and drying. It is a passive process that uses an osmotic pressure difference as the driving force. In the FO process, water moves across a semipermeable membrane from a feed solution of lower osmotic pressure (e.g., algal suspension) to a draw solution of higher osmotic pressure (e.g., desalination brine) [15]. In comparison with pressure-driven microfiltration and ultrafiltration, FO demonstrates unparalleled advantages of lower energy consumption, superior separation efficiency, potentially lower fouling tendency and more recovery of intact algal cells due to the lack of hydraulic pressure [434]. With the development of more efficient membranes, FO has been considered for various dewatering applications, such as pre-concentration of wastewater to facilitate the subsequent anaerobic digestion [435], landfill leachate dewatering [15] and concentration of fruit juice [436].

In 2009, the National Aeronautics and Space Administration (NASA) proposed an elegant concept – a coastal floating system integrating photobioreactor and FO [437]. In brief, the system is designed to grow microalgae in sewage inside a plastic bag that floats offshore. The bag is made of FO membranes that allow fresh water to flow out into the ocean while concentrating the algal biomass. As long as the draw solution has higher osmotic pressure than the algal suspension in the feed side, the process can be carried out indefinitely with no other inputs. This technology is still in an early stage of development and significant processes of optimizations are required. Some critical issues remain unsolved. For example, high biomass concentration is expected in the concentrated feed water. This will cause potential fouling problem, which can reduce algae dewatering efficiency and increase the overall operating costs and membrane degradation. Understanding the fundamental mechanisms and consequences of membrane fouling is critical to develop efficient and cost-effective fouling control strategies and, thus, enabling more sustainable application of FO membrane technology for microalgae dewatering.

A variety of draw solutions have been explored for FO applications, such as naturally available ocean water [438], brine from desalination plants [439], thermolytic salt ammonium bicarbonate and various simple electrolytes (e.g., NaCl and $MgCl_2$) [361]. Amongst these, the use of desalination brine for algae dewatering is most promising because (1) it is usually viewed as an unwanted residue and thus cheap; (2) it contains a significant amount of osmotic energy due to its very high salinity; (3) disposal of large quantities of brine can be very costly and there is an increasing concern over the adverse environmental and ecological impacts of brine disposal. When brine is used to draw clean water out of algae suspension in the FO process, the high quality permeate water mixes with the brine and substantially reduces its concentration. Thus the algae dewatering process also allows cost effective and environmentally friendly brine disposal.

The back diffusion of salts from draw solution to feed solution may induce complicated interactions with algal biomass and thus the draw solution chemistry may play an important role in the FO performance for algae dewatering. Zou et al. [32] highlighted the adverse impact of Mg^{2+} ions, that bind with carboxylic acid functional groups during the concentration of *Chlorella sorokiniana* and thus cause a severe flux

decline. Given the diversity of draw solutions and complexity of algal biomass, further research efforts are necessary to better understand the FO process applied for algal dewatering. For example, the intricate relationship between draw solution types, algal species, membrane fouling behaviour, and algal dewatering efficiency is still poorly understood. In addition, more study is needed to determine the maximum achievable algae concentration level, which depends on membrane type and orientation [358], module configuration and hydrodynamic conditions (e.g., spacer design) [440], and feed/draw solution composition and concentration [17]. These factors influence mass transfer, internal concentration polarization (ICP) and membrane fouling and thus govern the FO performance.

As a first step towards filling these knowledge gaps, we conducted a study of green algae *Scenedesmus obliquus* dewatering by commercially available FO membranes. *S. obliquus* was selected as model microalgae because it is often applied for biofuels production and wastewater treatment [441]. The objectives of this study were to (1) systematically investigate the effect of draw solution chemistry on flux behavior and algal dewatering efficiency; and (2) develop a fundamental understanding of the membrane fouling mechanisms involved during algal dewatering process with FO, by combining the data derived from filtration experiments and microalgae suspension/membrane characterization. The effect of orientation, membrane type and feed spacer were also investigated. The findings of this study provide comprehensive insights into the FO process design in terms of draw solution selection, membrane module design and fouling control.

2.2. Materials and Methods

2.2.1. Microalgae Cultivation and Characterization

Freshwater green algae *Scenedesmus obliquus* was obtained from Culture Collection of Algae and Protozoa (CCAP, UK). The alga has an ellipsoidal shape and is around 5 µm in width and 10 µm in length based on microscopic observation (Olympus IX71, Olympus Corporation, Tokyo, Japan). *S. obliquus* was cultivated in modified BG-11 medium (Appendix 1) following the recommendations of CCAP. Suspensions were continuously stirred and lit with fluorescent lights at 100 µmol photons/m^2·s. Air (75 L/h), naturally containing a small portion of CO_2, was also

sparged into the photobioreactor, using an aquarium pump, to maintain optimal algal growth. The pH of the culture ranged from 6.5 to 7.5 depending on the growth phase. The growth of *S. obliquus* was periodically monitored by measuring its optical density with a spectrophotometer (Helios Zeta, Thermo Scientific, UK) at 435 nm wavelength [442]. The optical density was correlated to the algae concentration using a calibration curve (Appendix 2). The microalgae suspension was harvested at the end of exponential phase when its concentration reached 2-3 g dry weight/L. This stock solution of microalgal biomass was diluted in BG-11 medium for the preparation of the feed solution (containing 0.2 g/L algal biomass) used in all FO experiments, to mimic the algae concentration obtained in raceway ponds [443]. In the BG-11 medium, the algal cells exhibited negatively zeta potential of 15.45 ± 1.87 mV (Zetasizer nano, Malvern Instruments Ltd, UK).

2.2.2. Draw Solution Chemistry

Draw solution chemistries investigated for FO experiments included simple electrolytes (NaCl, $MgCl_2$ and $CaCl_2$) and a commercial sea salt. All salts were ACS reagent grade (Sigma-Aldrich, UK). The draw solution was made by dissolving each type of solute to achieve the desired concentrations. The concentration of sea salt was 70 g/L to mimic the salinity of brine from typical reverse osmosis (RO) desalination plant [444]. The ionic composition of 70 g/L sea salt is provided in Table 2.1 (calculated from manufacturer's data). The osmotic pressure of feed solution and all draw solutions was determined from:

$$\pi = \beta CRT \qquad\qquad 2.1$$

where π is the osmotic pressure (Pa), β is the dimensionless Van't Hoff factor, C is the molar concentration of solute, R is the gas constant (8.314 $m^3 \cdot Pa/K \cdot mol$) and T is the absolute temperature (K). The feed solution had a much lower osmotic pressure (0.9 bar) than the draw solutions. Thus FO driving force that causes the movement of water through membrane from algal biomass side (feed solution) to draw solution is dominated by the draw solution composition. In order to conduct a meaningful comparison of filtration performance between different draw solutions, 68.96 g/L NaCl

(55.1 bar), 86.55 g/L $MgCl_2$ (87.7 bar) and 114.31 g/L $CaCl_2$ (80.8 bar) were used to achieve the same initial permeate flux (~ 7 $L/m^2/h$) with 70 g/L (55.3 bar) sea salt. These solute concentrations were determined experimentally using the setup used for all dewatering experiments.

Table 2.1 - Ionic composition of 70 g/l sea salt solution.

Major Ion	Symbol	Concentration (g/L)	Mass Ratio (%)
Chloride	Cl^-	39.55	56.50
Sodium	Na^+	22.10	31.57
Sulfate	SO_4^{2-}	3.40	4.86
Magnesium	Mg^{2+}	2.71	3.87
Potassium	K^+	0.86	1.23
Calcium	Ca^{2+}	0.82	1.17
Bicarbonate	HCO_3^-	0.41	0.59
Bromide	Br^-	0.155	0.16
Strontium	Sr^{2+}	$1.8 \cdot 10^{-2}$	0.03
Boron	$B(OH)_3$	$1.1 \cdot 10^{-2}$	0.02

2.2.3. FO Membranes

Two commercial FO membranes (CTA and TFC) were used in this study. Both membranes were provided by Hydration Technologies, Inc. (Albany, OR, USA). CTA has a dense selective layer (active layer) made of cellulose triacetate and TFC has an active layer made of polyamide. Both membranes have asymmetric structure with the active layer supported by embedded polyester screen mesh to enhance their mechanical strength. Both membrane orientations, active layer facing feed solution (AL-FS) and active layer facing draw solution (AL-DS), were tested.

The pure water permeability (*A*) and solute permeability (*B*) of the FO membranes were determined at 25 ± 1 °C in a pressurized dead-end filtration test unit (Millipore, UK) with a stirring speed of 6 x g to minimize external concentration polarization on the membrane surface. The effective membrane area was 40 cm^2. The pure water permeability was determined by measuring the permeate water flux over a range of

applied pressures (1 – 5 bar). An example of the determination of the pure water permeability is given in Appendix 3. Using a feed solution containing 10 mM of individual simple electrolyte or commercial sea salt, the rejection of the corresponding solutes was calculated from feed and permeate conductivity measurements (Ultrameter II, Myron L Company, CA, USA). The solute permeability was calculated based on the solution-diffusion theory [445]:

$$B = A \cdot \left(\Delta P - \Delta \pi \right) \cdot \left(\frac{1}{R_s} - 1 \right)$$
$$2.2$$

where ΔP and $\Delta \pi$ are the hydraulic pressure difference and osmotic pressure difference across the membrane, respectively; R_s is the rejection of specific solutes.

2.2.4. FO Experimental Setup

All FO experiments were conducted using a custom fabricated bench-scale crossflow FO system (Figure 2.1), which is similar to that described in previous studies [21, 446, 447]. Conceptual illustration of microalgae dewatering by FO is depicted in Appendix 4. Briefly, a membrane coupon with an effective area of 200 cm^2 was housed in a cross-flow membrane cell. Diamond-patterned spacers were obtained from a commercial FO spiral wound module (HTI, OsMem™) and placed on both sides of the membrane to promote mass transfer [348]. Counter-current flow was used to circulate both feed and draw solutions on both sides of membrane using a variable-speed peristaltic pump (Cole-Parmer, Vernon Hills, IL, USA). The cross-flow velocities were maintained at 9.6 cm/s during all experiments on both side of the membrane. The feed solution was well mixed by a magnetic stirrer to prevent microalgae sedimentation. The draw solution tank was placed on a digital scale (Denver Instrument, Denver, USA) and weight changes as a function of time were used to determine permeate water flux. The solution temperature was maintained at 25 ± 1 °C using a recirculating water chiller/heater (Fisher Scientific, Loughborough, UK). Samples from the feed tank and draw solution tank were taken at specified time intervals for conductivity measurement.
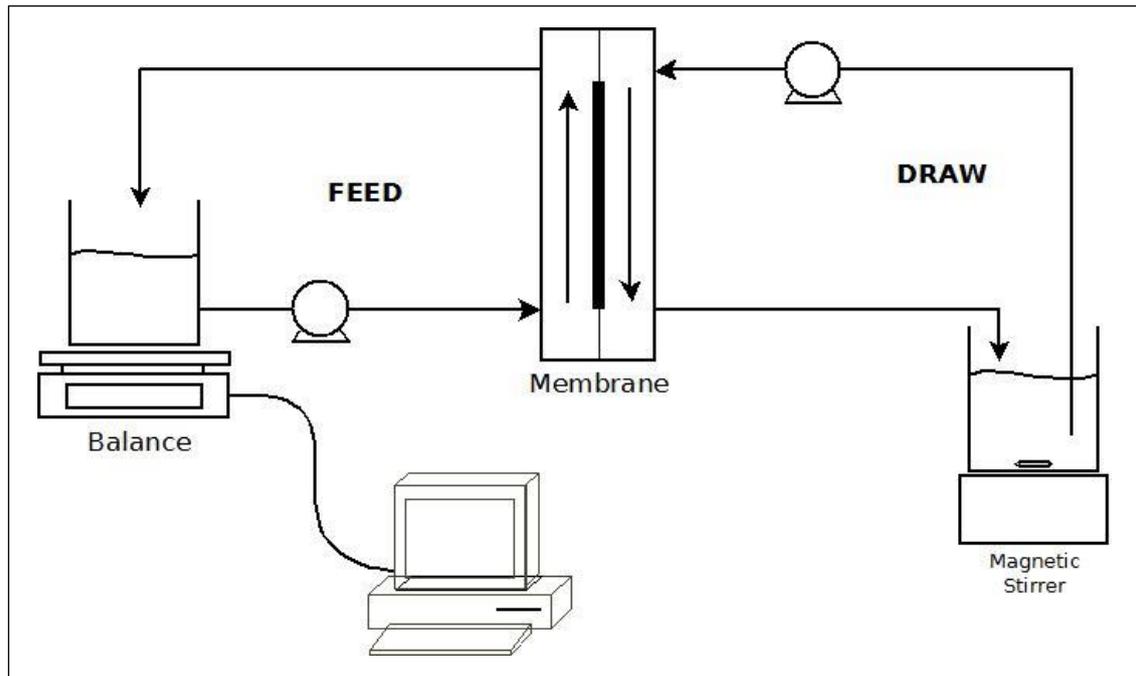
Figure 2.1 *- Schematic of laboratory forward osmosis system*

2.2.5. Protocols of Algae Dewatering by FO Membrane Filtration

FO algae dewatering experiments comprised three steps: (1) equilibration, (2) algae dewatering, and (3) cleaning. First, membrane coupon was equilibrated with BG-11 medium as feed solution and desired draw solution for at least 30 min until a stable water flux was achieved. This flux was recorded as initial flux. Second, algae dewatering was initiated with 1 L of algae suspension (0.2 g/L) in feed tank and 6 L of draw solution. The FO filtrations were considered complete when the concentration factor reached 4 (750 mL of permeate was extracted from the original algal suspension), which took 4.5-6.5 hours depending on membrane type, orientation and draw solution chemistry. To minimize the impact of draw solution dilution on FO performance, draw solution concentration was monitored by conductivity measurement and maintained constant by manually dosing from a concentrated stock solution every 15 min [448]. To quantify the permeate flux loss caused by algae fouling, baseline experiments were also conducted under identical conditions to the corresponding algae FO experiments, except no algae biomass was added into the feed solution. The flux loss caused by algae fouling was determined by:

$$\Delta J_w = 1 - \frac{J_{w,a}}{J_{w,b}}$$

2.3

where ΔJ_w is normalized water flux loss, $J_{w,a}$ and $J_{w,b}$ are water flux in algae dewatering test and baseline test at specific concentration factor, respectively.

At the end of algae dewatering experiments, both feed and draw solution tanks were emptied and the membrane system was rinsed with deionized water at a crossflow velocity of 19.2 cm/s for 30 min. After rinsing, permeate water flux was measured to determine flux recovery (cleaning efficiency). Conditions for this flux test were identical to those for initial water flux test of the virgin membrane (as mentioned above). To further clean the fouled membrane, osmotic backwashing with deionized water as draw solution and salt water as feed solution was performed for 30 min. The permeate flux was then measured again to determine flux recovery with the conditions identical to those for initial water flux test. Flux recover was determined from:

$$\text{Flux recovery} = \frac{J_{w,c}}{J_{w,0}}$$

2.4

where $J_{w,0}$ and $J_{w,c}$ are initial water flux and water flux after cleaning, respectively.

2.2.6. Extracellular Proteins and Carbohydrates Analysis

At specified time intervals, feed samples (15 ml) were taken and centrifuged at 6 x g for 20 min. Protein concentration in the supernatant was determined using the modified Lowry method with bovine serum albumin as a standard [449]. Carbohydrate concentration was determined using phenol-sulfuric acid method with glucose as a standard [450]. Total extracellular protein/carbohydrate contents (mg) in the feed solution were then calculated from the product of protein/carbohydrate concentrations (mg/L) and feed volume at the time when the samples were taken.

2.3. Results and Discussion

2.3.1. Membranes Performance Parameters

Table 2.2 shows the pure water permeability (A), solute permeability (B), and selectivity (B/A) of the FO membranes used. The A value of CTA membrane was about half that of the TFC membrane. This is consistent with the finding by Ren and McCutcheon [451]. The lower B/A ratios of CTA membrane indicate its better salt rejection compared to TFC membrane. For both membranes, the B values followed the same order of decline: NaCl > sea salts > $MgCl_2$ > $CaCl_2$. The higher B value of NaCl is attributed to the smaller hydrated radius and lower electrical charge of Na^+ compared to Mg^{2+} and Ca^{2+} [452, 453].

Table 2.2 - Membrane performance parameters.

Membrane		CTA	TFC
Water permeability (m/s.Pa)	A	1.51×10^{-12}	2.78×10^{-12}
Solute permeability (m/s)	$B_{seasalts}$	5.08×10^{-8}	1.54×10^{-7}
	B_{NaCl}	9.07×10^{-7}	4.34×10^{-7}
	B_{MgCl2}	4.69×10^{-8}	1.18×10^{-7}
	B_{CaCl2}	3.57×10^{-8}	0.98×10^{-7}
Selectivity (KPa)	$B_{seasalts}/A$	34	55
	B_{NaCl}/A	60	156
	B_{MgCl2}/A	31	42
	B_{CaCl2}/A	24	35

2.3.2. Flux Decline during Dewatering of *S. obliquus* by FO membranes

This section shows the water flux behaviour during the filtration of *Scenedesmus obliquus* with sea salts as draw solution. The filtration flux as a function of volumetric concentration factor for both baseline and algae dewatering experiments are summarized in Figure 2.2a. The method and calculations necessary for the realization of Figure 2.2 is described in Appendix 5, for the CTA membrane with the AL-FS orientation. In all cases, water flux declined with the increase of concentration factor. The flux decline is attributed to (1) membrane fouling and (2) a loss of osmotic driving force across the FO membrane due to an enhanced salinity in the feed solution. To better understand membrane fouling during algae dewatering, it is necessary to separate the effect from feed salinity increment. In this regards, the baseline flux was discussed first.
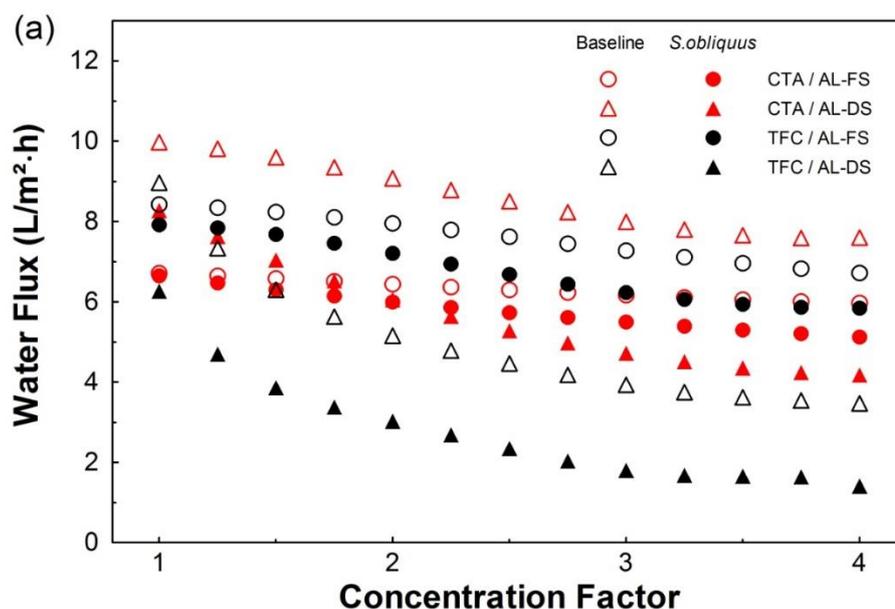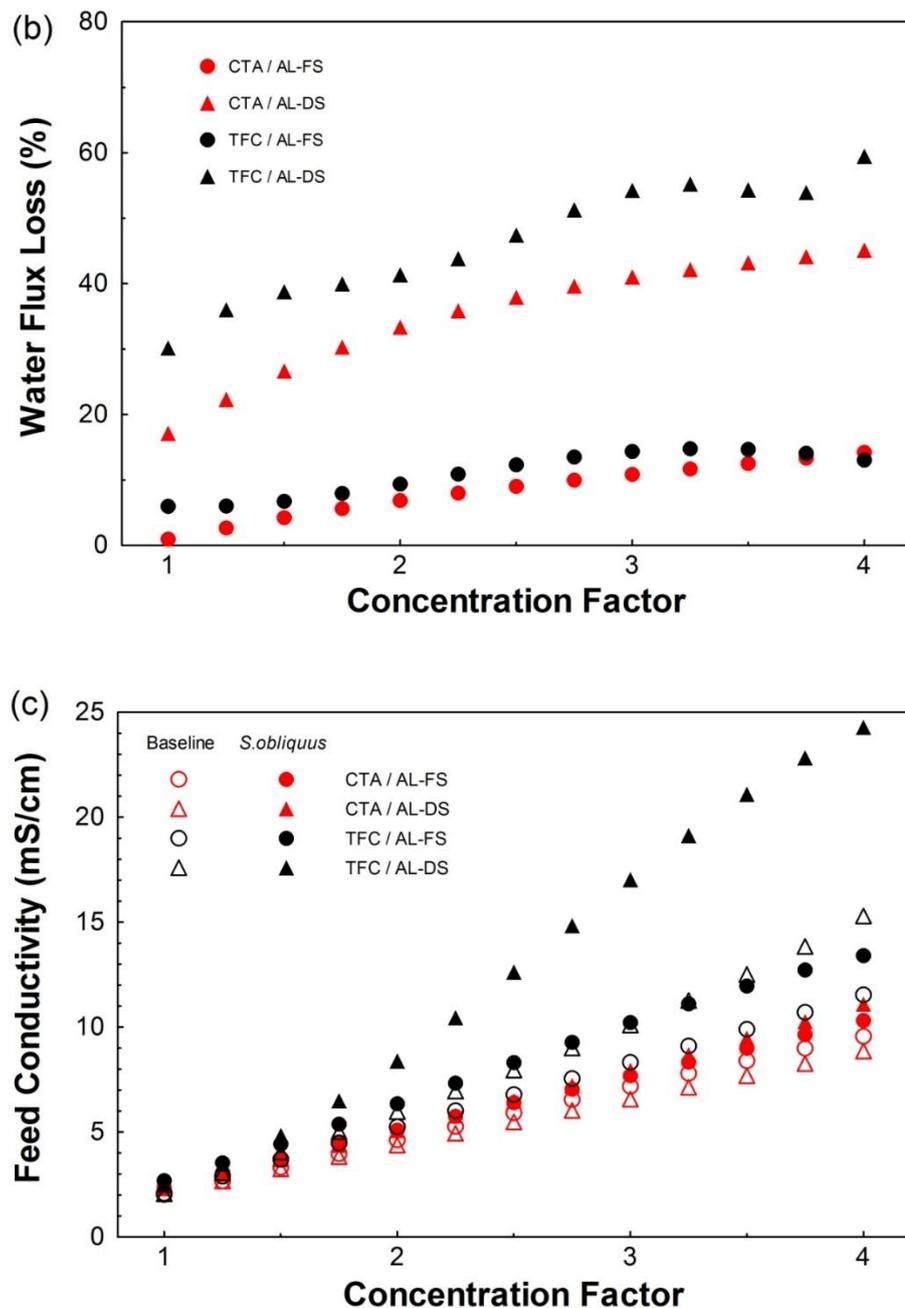
Figure 2.2 - *Changes of water flux and feed conductivity as a function of volumetric concentration factor for CTA and TFC membranes: (a) water flux in baseline and algae dewatering experiments; (b) normalized flux loss; and (c) conductivity in the feed solution. The draw solution contained 70 g/L sea salt.*

For both CTA and TFC membranes, the initial baseline flux in the AL-FS orientation was lower than that in the AL-DS orientation. This observation is consistent with previous studies and is due to the fact that the dilutive internal concentration polarization (ICP) in the AL-FS orientation has greater effect on water flux compared

to the concentrative ICP effect in the AL-DS orientation [348, 358, 445]. In all the baseline tests, water flux declined with the increase of concentration factor. This decline is caused by a reduction of the osmotic driving force across the membrane active layer, due to (1) an increase in feed solution concentration as pure water was "pumped" from feed to draw solution; and (2) the back diffusion of draw solutes into the feed solution. As the water flux is plotted as a function of concentration factor in Figure 2.2a, a greater flux decline rate indicates a more severe effect of draw solutes reverse diffusion. When active layer was facing the feed solution, the TFC membrane achieved a higher initial water flux (8.42 L/m^{2}h) than CTA membrane (6.71 L/m^{2}h). The higher initial flux of TFC membrane is consistent with its higher A value (Table 2.2). However, the TFC membrane exhibited a more noticeable flux decline. At the end of baseline tests, TFC membrane showed a greater flux reduction (20.3 %) than CTA membrane (11 %). The greater flux decline of TFC is due to its lower salt rejection (indicated by a higher B/A value) which leads to more back diffusion of draw solutes (Figure 2.2c). In the AL-DS orientation, TFC exhibited a lower initial flux (8.97 L/m^{2}h) than CTA membrane (9.98 L/m^{2}h). Considering its higher A value, this phenomenon indicates that an immediate back diffusion of draw solutes took place during the equilibration step. Draw solutes diffused through the membrane active layer accumulate in the porous support layer to exacerbate ICP effect which causes a reduction in the effective osmotic driving force and thus a lower water flux. At the end of baseline tests, TFC membrane exhibited a much greater flux reduction (61.3 %) compared to CTA membrane (23.8 %). This can be explained by its more severe draw solutes back diffusion (Figure 2.2c). For both membranes, flux decline rate was more significant in the AL-DS orientation (particularly for TFC membrane), indicating that the effect of draw solute back diffusion on water flux reduction is more severe (due to the reverse solute diffusion induced ICP) when active layer is facing the draw solution.

The degree of membrane fouling was assessed by comparing the water flux of algae dewatering experiments to its corresponding baseline flux. Figure 2.2b presents the normalized flux loss due to algae fouling. Generally, flux loss in the AL-DS orientation increased more drastically with the increase of concentration factor than that in the other orientation. This demonstrates that more severe algae fouling occurred when active layer was facing the draw solution. In the AL-DS orientation, the flux loss increased instantaneously after algae was added into the feed solution, and then slowed

down. At the end of tests, the water flux was significantly declined by 59.5 % for TFC membrane and 45.1 % for CTA membrane. Such severe membrane fouling can be caused by a combination of (1) internal adsorption of algal biomass inside the porous support layer of membrane which results in an increase of hydraulic resistance; and (2) pore clogging enhanced concentrative ICP due to the reduction of mass transfer coefficient in the membrane support layer [21, 445]. In contrast, the AL-FS orientation exhibited a superior fouling resistance. At the end of test, water flux loss was less than 15 % for both membranes. The marginal membrane fouling is attributed to the deposition of algal biomass onto the active layer surface which can change the effective pore size of the membrane through sealing the molecular-scale defects and introducing an additional barrier to restrict the transport of water molecules [21].

Membrane cleaning experiments were performed immediately after algae dewatering in order to test the fouling reversibility. Figure 2.3 presents the flux recovery after cleaning with deionized water flushing and by osmotic backwash. In the AL-FS orientation, water flux could be recovered up to 90 % of the initial flux by deionized water flushing and could be further recovered by osmotic backwashing. This suggests that algal biomass is loosely attached onto membrane surface, most of the membrane fouling is reversible by simple hydrodynamic cleaning steps. In this regard, algal dewatering by FO may offer a great benefit in eliminating the need for harsh chemical cleaning and air scouring, both of which are widely used for microfiltration and ultrafiltration fouling control but increase membrane degradation, energy consumption, and operating cost. Thus, FO has the promise for low-chemical and energy efficient microalgae dewatering. In the AL-DS orientation, the flux loss could not be recovered by deionized water flushing. The osmotic backwash was not very effective with the AL-DS orientation, with flux recovery of only 76% and 72% for CTA and TFC membrane, respectively. This observation indicates that algal biomass binds strongly to the internal structure of membrane support layer and this internal adsorption/clogging is the dominating fouling mechanism. Based on the above discussion, AL-FS outperformed AL-DS in the application of algae dewatering.
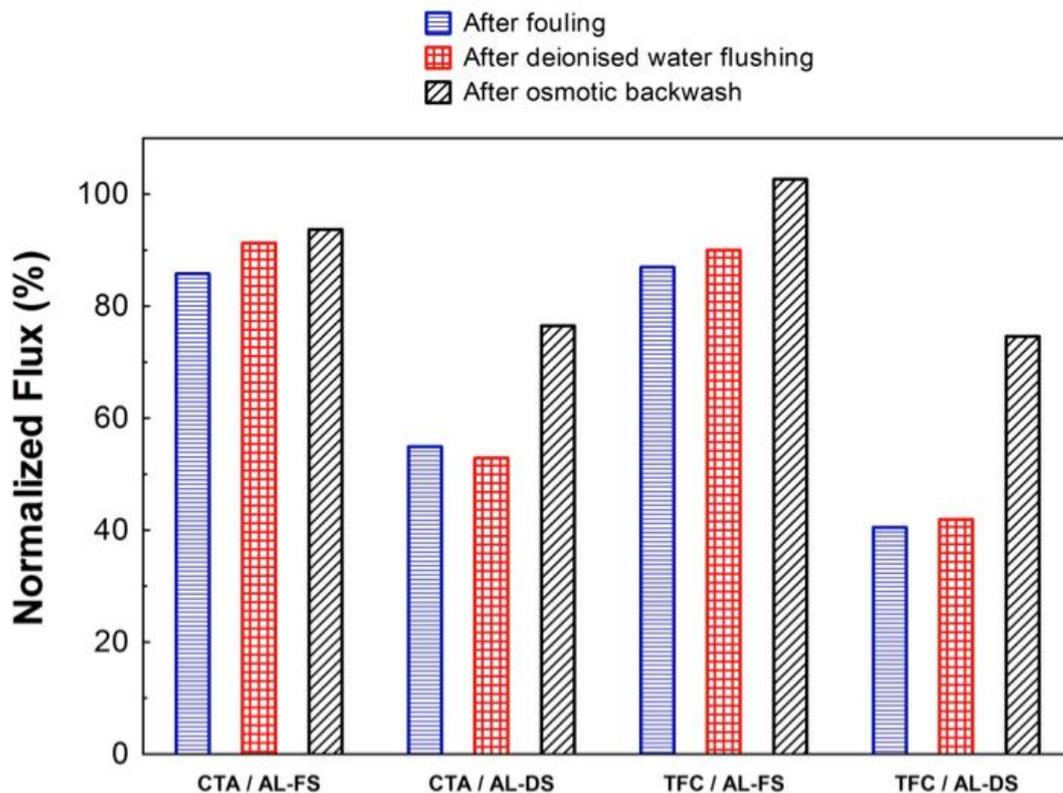
Figure 2.3 *- Flux recovery after cleaning. Note that the flux after fouling is normalized by the flux at the end of baseline test, while the recovered flux after cleaning is normalized by the pure water flux of a clean membrane. Results are presented in percentages.*

To support above discussion that the back diffusion of draw solutes plays a key role in the flux loss during FO process, conductivity in the feed solution was measured along all the tests. The changes of feed conductivity against concentration factor are illustrated in Figure 2.2c. In all cases, feed conductivity increased with the increase of concentration factor. The enhanced conductivity is caused by (1) the extraction of pure water from feed to draw solution and (2) the reverse diffusion of draw solutes into the feed solution. As the conductivity is plotted as function of concentration factor, a greater increment rate indicates a more severe effect of draw solutes reverse diffusion. TFC membrane always exhibited a more remarkable enhancement in the feed conductivity than CTA membrane, indicating a greater draw solutes back diffusion. This is attributed to its lower salt rejection (indicated by a higher *B/A* value). It was also observed that the addition of *S. obliquus* in the feed solution increased the conductivity increment rate. For example, at the end of the test with TFC membrane in the AL-DS

87

orientation, the feed conductivity sharply increased to 24.3 mS/cm with the addition of algae in comparison with 15.3 mS/cm in the baseline test. This phenomenon indicates a greater draw solutes back diffusion during the algae dewatering process and offers an additional explanation for the flux loss caused by algae fouling which may cause the membrane to have less salt rejection. As these experiments were only carried out once, more work should be done to confirm these findings.

To better understand the FO performance on algae dewatering and gain more insight into the adverse role of draw solutes back diffusion, the effect of draw solution chemistry on flux behavior and algal dewatering efficiency using CTA membrane in the AL-FS orientation was systematically investigated in next section. The selection of CTA membrane is due to its superior separation efficiency.

2.3.3. Effect of Draw Solution Type on Algae Dewatering

Figure 2.4a presents the water flux loss due to membrane fouling with different types of draw solution. Algae biomass did not cause much membrane fouling for NaCl and $MgCl_2$ draw solutions during the whole filtration process (water flux loss was below 8 %). However, when Ca^{2+} ions were present in the draw solution, flux declined to a greater extent. At the end of experiments, the overall extent of flux loss followed the order of $CaCl_2$ >> sea salts (containing 0.82 g/L of Ca^{2+}) > NaCl ≈ $MgCl_2$. This finding indicates severe fouling will occur when $CaCl_2$ is used as draw solution although CTA membrane was proven to have a better fouling resistance in the AL-FS orientation [454]. Thus, selection of a proper draw solution should be an important consideration for the FO application in algae dewatering.
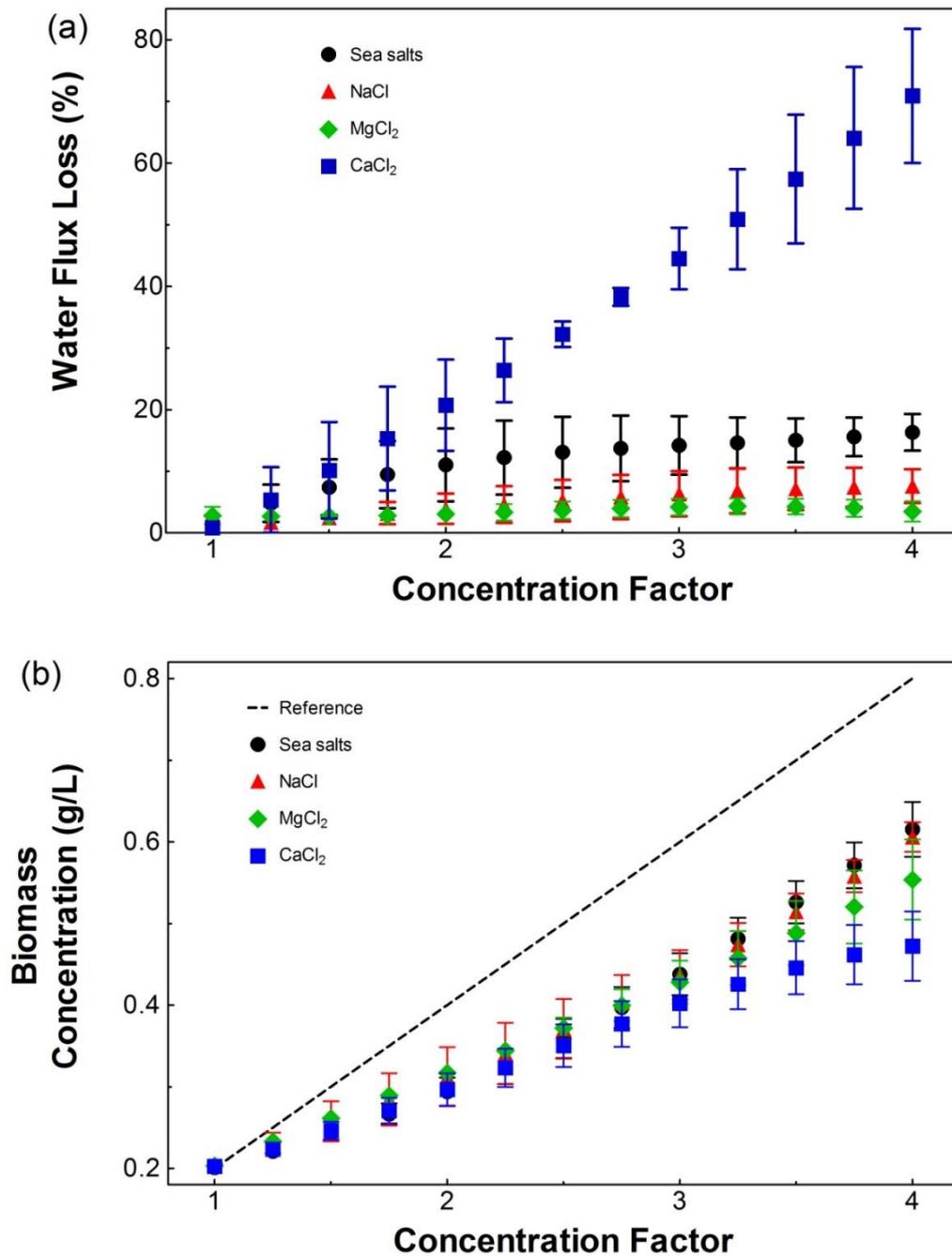
Figure 2.4 - *Influence of draw solution type on (a) water flux loss and (b) algal biomass concentration in the feed tank during S. obliquus dewatering by CTA membrane in the FS orientation. Error bars represent the standard deviations of the average values determined from two independent experiments.*

Figure 2.4b shows the algal biomass concentration in feed tank over the filtration process. The black dash line demonstrates the expected algae concentration as a

function of concentration factor, which should reach 0.8 g/L at the end of experiments if all the algae biomass can be harvested effectively. However, experimental results were always lower than the prediction. Because feed water was re-circulated back to the feed tank throughout the filtration test, the observed biomass loss is most probably attributed to algae deposition onto membrane and/or feed spacer. A greater loss indicates a more severe deposition. The overall algae harvesting efficiency followed the order of sea salts $\approx$ NaCl > MgCl$_2$ > CaCl$_2$. When CaCl$_2$ was used as draw solution, the greatest loss in both water flux (70.9 %) and algal biomass (47.2 %) can be explained by the back diffusion of Ca^{2+} ions from draw solution into feed solution. However the lowest B value for CaCl$_2$ (Table 2.2) indicates there is specific interactions between Ca^{2+} and algal biomass. Once diffused through the membrane, Ca^{2+} ions bind preferentially to oxygen atoms of carboxylate groups in a highly organized manner and form bridges between adjacent algal cells as well as their extracellular polysaccharides (EPSs) and soluble microbial products (SMPs), leading to the egg-box-shaped gel network [32, 455-457]. As a result, large microalgae flocs were formed in the feed tank (Figure 2.5c). The larger size of microalgae flocs may increase the compressibility of the fouling layers, leading to a greater overall hydraulic resistance [458]. Therefore, the use of CaCl$_2$ as draw solution led to a severe loss in both algal biomass and water flux. When NaCl and MgCl$_2$ were used as draw solution, water flux decline was found lower than 8 %. However, more than 25 % of algal biomass was lost at the end of experiment. This phenomenon suggests (1) most of the algae deposition takes place onto the mesh spacer in the feed channel rather than onto membrane and (2) the biomass deposited on feed spacer may not augment the hydraulic resistance significantly. The finding in this study disagree with a previous work by Zou et al. [32]. They showed a significant flux decline during *Chlorella sorokiniana* dewatering with MgCl$_2$ as draw solution. These conflicting findings can be attributed to the different surface chemistry (such as charge, functional groups and free energy) between *Scenedesmus obliquus* and *Chlorella sorokiniana* used in the two studies. *Scenedesmus obliquus* differs from *Chlorella sorokiniana* in their cell wall chemical composition by the presence of a great concentration of mannose and fructose, which can bind/interact specifically with Ca^{2+} [459, 460]. Clearly, an optimal dewatering method depends on the species of microalgae. As presented in Table 2.1, sea salt contained 0.8 g/L of Ca^{2+} and 18 mg/L of Sr^{2+}. The back diffusion of these divalent cations led to the formation of algal flocs

which could readily deposit onto membrane and feed spacer, resulting in 23.1 % of algal biomass lost from the feed and 16.3 % of water flux reduction when sea salt was used as draw solution. The higher flux loss with sea salt as draw solution compared to that with NaCl and $MgCl_2$ is due to the strong gel formation ability of Ca^{2+} (and Sr^{2+}), which promotes membrane fouling [461]. As confirmed via microscopic observation (Figure 2.5), the size of algal flocs formed at the end of FO test followed the order: $CaCl_2 \gg$ sea salt $> MgCl_2 \approx NaCl$.
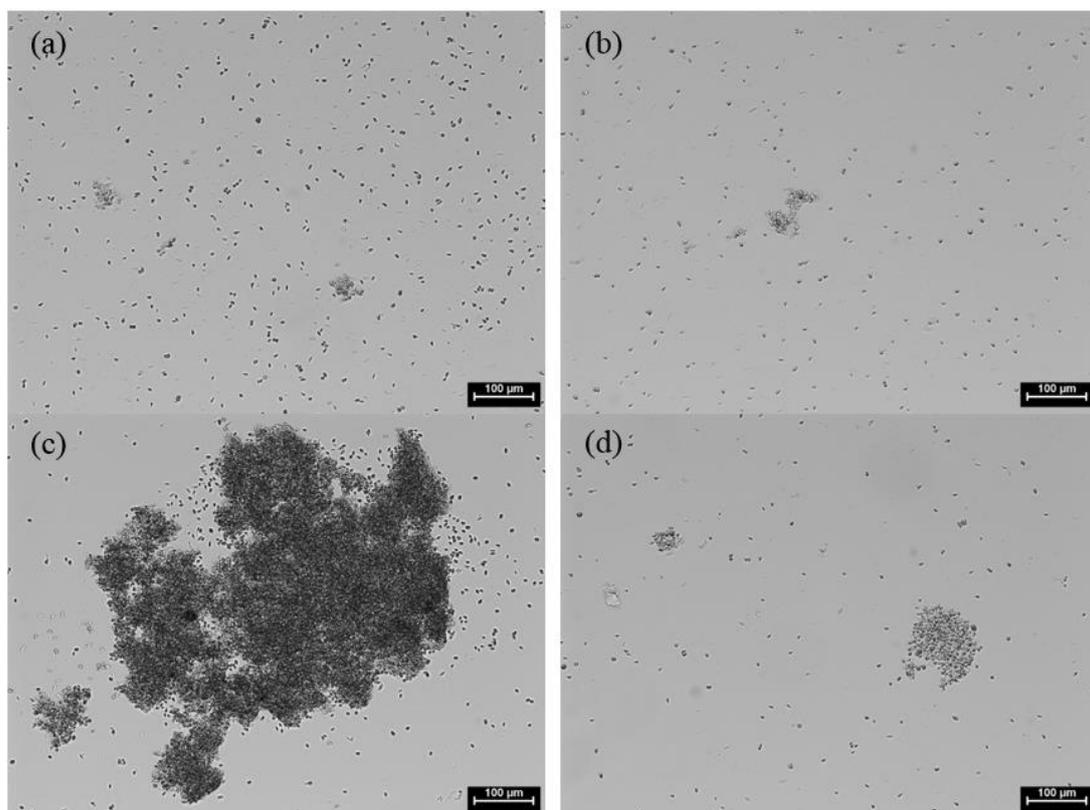
Figure 2.5 - Microscope image of feed solution after algal dewatering test with different draw solutions: (a) NaCl; (b) MgCl₂; (c) CaCl₂; and (d) sea salt.

To further understand the mechanisms underneath the significant fouling with $CaCl_2$ as draw solution, the amount of dissolved extracellular carbohydrates and proteins was determined in the feed solution, filtrated from microalgae (Figure 2.6). In all cases, protein level (below 3 mg) was more than two orders of magnitude lower than carbohydrate level. Furthermore, no obvious patterns of change were seen in the protein amount. Hence, the discussion below will focus on the changes in carbohydrate amount

throughout the algae dewatering experiments. When NaCl and $MgCl_2$ were used as draw solution, carbohydrates amount showed a decline after FO filtration, followed by an increase to its initial level after deionized water flushing (Figure 2.6a). This trend indicates that the extracellular carbohydrates deposit onto membrane and/or feed spacer during the FO processes and the deposited compounds can be easily removed by simple flushing. In contrast, more carbohydrates were detected after filtration with Ca^{2+}-containing draw solutions. Particularly, the carbohydrates amount was up to 3 times higher than its initial value after filtration with $CaCl_2$ as draw solution. The authors speculate that algal cells "leak" more carbohydrates after interacting with the Ca^{2+} ions back diffused from the draw solution. Indeed, a high local concentration of Ca^{2+} could cause disturbance in a complex mechanism involved in photosynthesis known as "Ca^{2+} signal", which is also a response to stress conditions in the nutrition process [462, 463]. These carbohydrates, in turn, specifically bind with Ca^{2+} ions and further enhance the formation of gel network containing algal cells, Ca^{2+} ions, EPS and SMP [385, 445, 454]. Further investigation needs to support this hypothesis.
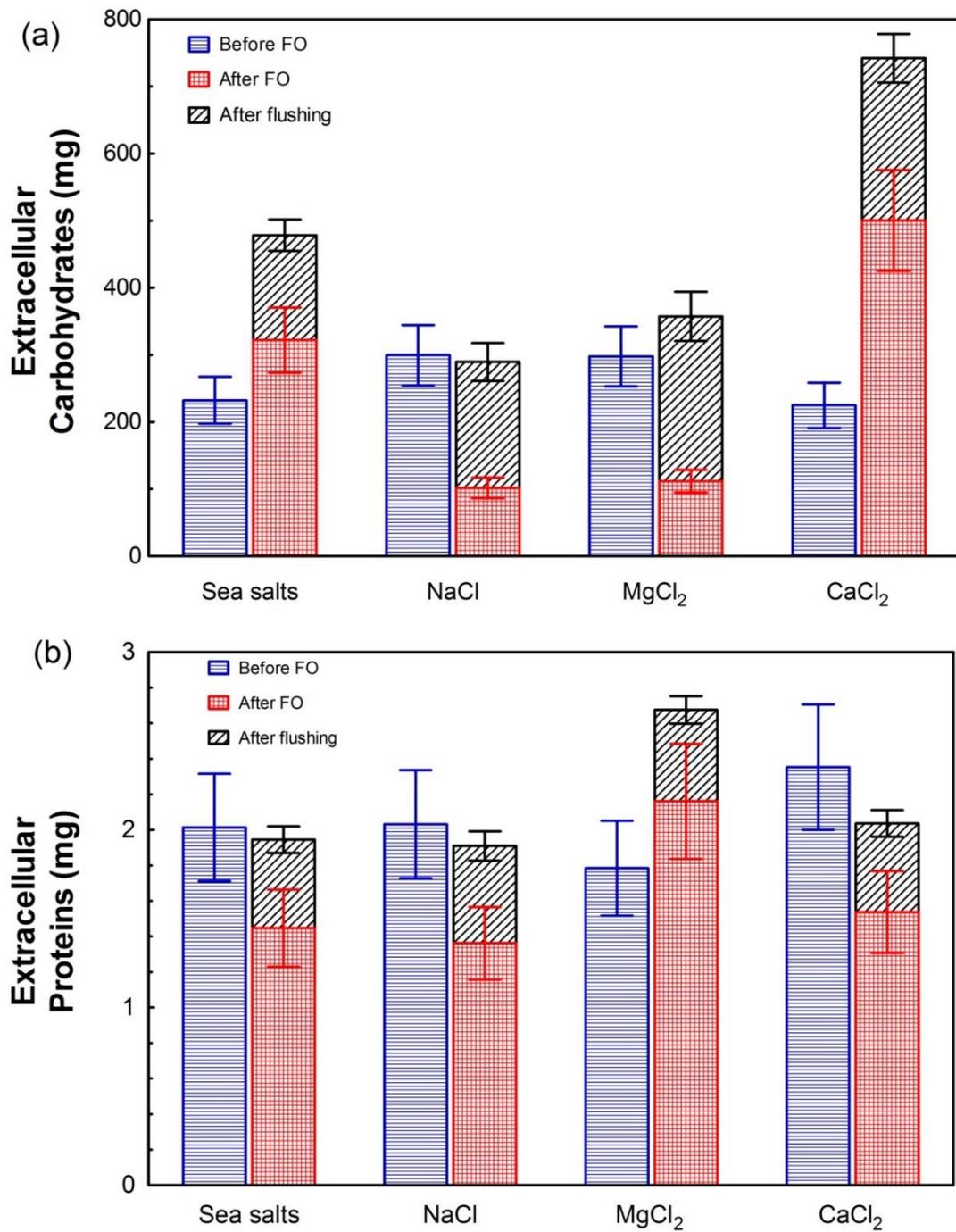
*Figure 2.6 - Extracellular (a) carbohydrate and (b) protein content in feed solution.
Error bars shows standard deviation from triplicates analysis of the experiment
samples.*

2.3.4. Effect of Feed Spacer on Algae Dewatering

To test our hypothesis that most algal biomass deposits onto and/or traps inside the feed spacer, FO experiments with sea salt as draw solution were performed without a spacer in the feed channel. Figure 2.7 shows the effect of feed spacer on algal biomass concentration. Without using a feed spacer, the experimentally measured biomass concentration was very close to the predicated values. At the end of test, over 95% of the algal biomass was harvested in the feed tank, significantly higher than that achieved with a feed spacer (around 75 %). These findings revealed a negative effect of using feed spacer on algae dewatering efficacy due to the easy accumulation of algal cells inside spacer. However, the beneficial effect of feed spacer is well known for both pressure-driven and osmotically driven membrane filtration thanks to the improved mass transfer (and thus the reduced external concentration polarization effect) over the membrane surface [33]. Hence, in the application FO for algae dewatering, feed spacer needs to be further optimized in terms of material and geometry to reduce the risk of cell accumulation into the spacer and enhance mass transfer over the membrane surface in the feed channel.
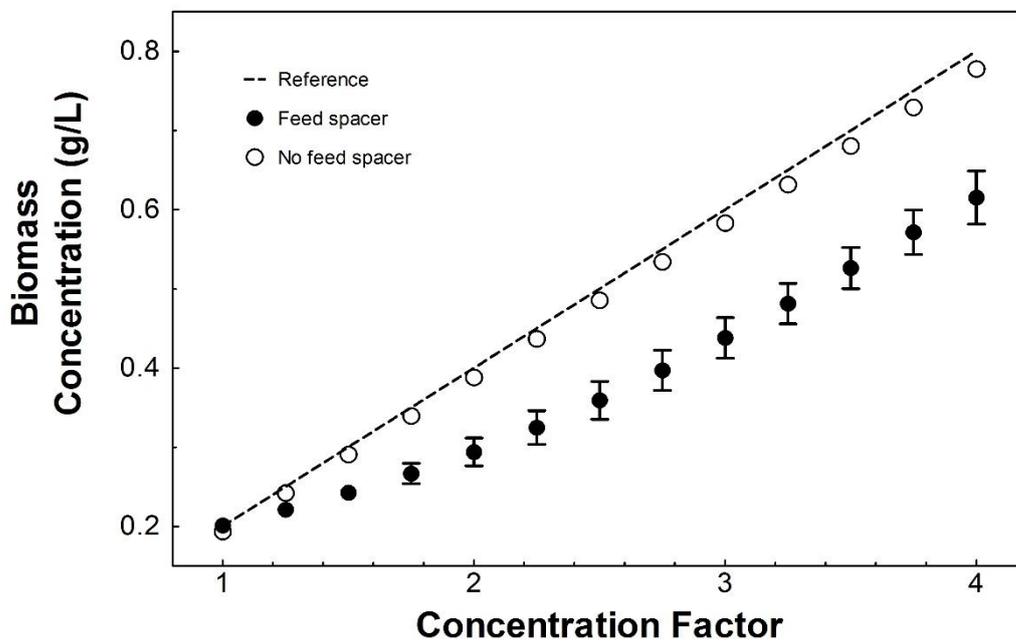
Figure 2.7 - *Effect of feed channel spacer on algal biomass concentration in the feed tank during S. obliquus dewatering by CTA membrane in the AL-FS orientation. The draw solution contained 70 g/L sea salt. Experiment took respectively 315min and 480min, with and without feed spacer, highlighting the permeate flux difference due to the presence of feed spacer.*

2.4. Conclusions

This study explored the potential of utilizing FO as a low-energy and low-chemical consuming process for microalgae dewatering. Effects of membrane orientation, draw solution chemistry and feed spacer were investigated. AL-FS orientation outperformed AL-DS orientation due to its much lower membrane fouling and greater cleaning efficiency. Algae dewatering by FO in the AL-FS orientation may eliminate the need for harsh chemical cleaning which not only shortens membrane life but also increases operating cost. When using reverse osmosis (RO) desalination brine as draw solution, the diluted brine offers additional benefits including reduced environmental impact of brine discharge together with reduced energy consumption/cost in RO desalination. In the AL-FS orientation, the efficiency and productivity of the dewatering process depended on draw solution chemistry. Among the four types of draw solution tested, NaCl exhibited best results. In contrast, for Ca^{2+}-containing draw solutions, back diffusion of Ca^{2+} ions into the feed solution encouraged *Scenedesmus obliquus* to excrete more carbohydrates, accelerated the formation of algal flocs, enhanced the rate and extent of flux decline and reduced the algae dewatering efficiency. In addition, a large amount of microalgae adhered onto feed spacer which negatively affects the whole process yield. Further studies on feed spacer optimization and FO dewatering of other algae species are necessary. The next chapter will investigate the fouling mechanisms observed with different microalgae species and the role of their cell wall composition. As NaCl did not induce a severe fouling, due to the absence of divalent cations, it will be excluded of the next study.

3. Microalgal Biomass Dewatering using Forward Osmosis Membrane: Influence of Microalgae Species and Carbohydrates Composition

3.1. Introduction

Microalgae are recently considered as an excellent renewable energy feedstock due to their high-yield production without impinging on food crops [166]. In addition, microalgae are able to serve the roles of carbon dioxide sequestration and wastewater remediation by nutrients fixation [429]. Algae biomass can be also used to produce a variety of high-value products such as cosmetics, antioxidants and food supplements [261]. Despite such promises, due to their similar density to water [256], and usually very diluted cultures [4], separating and concentrating algae cells from the culture medium (algae dewatering) is one of the technical and economical bottlenecks to large-scale microalgae production. Microalgae can be dewatered by conventional methods (such as centrifugation, flotation, chemical flocculation and sedimentation) and advanced pressure-driven membrane processes (such as microfiltration and ultrafiltration). The conventional methods are either highly energy intensive or require harmful chemical addition. Compared to conventional methods, membrane filtration requires lower energy but is prone to fouling which greatly reduces the algae dewatering efficiency and overall process sustainability. Thus, there is an innovation demand for more energy efficient and environmentally sustainable algae dewatering alternatives to overcome the many drawbacks of existing technologies.

Forward osmosis (FO), an emerging membrane separation process, has recently been considered as a promising and sustainable dewatering technology [464, 465]. FO is based on the natural tendency of water to flow through a semi-permeable membrane from a feed solution of lower osmotic pressure (higher water chemical potential) to a draw solution of higher osmotic pressure (lower water chemical potential). The driving force for water movement is the osmotic pressure difference across membrane. The absence of external hydraulic pressure allows FO to offer many advantages including (1) low energy consumption if an appropriate draw solution is applied [435], (2) lower fouling propensity and higher cleaning efficiency and (3) greater recovery of unbroken algae cells.

Previously [464], we proposed to integrate FO and seawater reverse osmosis (SWRO) processes to significantly improve the energy efficiency and environmental sustainability of algae dewatering and existing desalination. Briefly, highly concentrated SWRO brine (osmotic pressure ~ 5.4 MPa) is used as draw solution to pull clean water through the FO membrane from algae culture in the feed side while the FO membrane with superior separation efficiency retains all algal biomass and thus enhances the algae concentration. During the FO dewatering process, most of membrane fouling is reversible by simple hydraulic flushing without any chemical addition. Meanwhile, the high quality FO permeate water mixes with the brine and substantially reduces its concentration. The diluted brine can be disposed back to the sea with minimal environmental impact or sent to the SWRO desalination process to further recover clean water. The dilution of brine significantly reduces the required hydraulic pressure and thus overall energy consumption during SWRO desalination process.

Despite the low fouling tendency of FO, FO dewatering performance may still be adversely impacted by membrane fouling, resulting in lower water flux and algae recovery efficiency, shorter membrane life and greater operating cost [464]. FO fouling is reported to be governed by membrane characteristics and orientation, draw solution concentration and chemistry, feed water composition, and hydrodynamic conditions [407]. Compare to pressure-driven membrane process, FO has a unique mass transfer phenomenon called draw solute back diffusion that may play an important role in membrane fouling. Previously, FO was applied for *Scenedesmus obliquus* dewatering with various types of draw solution [464]. We found that the back diffusion of Ca^{2+} ions into the algae suspension on the feed side of membrane encouraged algae to release more carbohydrates and induced more severe fouling in comparison with Mg^{2+} and Na^+. For example, significant water flux decline and algae biomass loss were observed due to membrane fouling when $CaCl_2$ was used as draw solution. In contrast, Zou et al. reported a great membrane fouling when $MgCl_2$ was used as draw solution to concentrate microalgae *Chlorella sorokiniana* [33]. These different observations can be attributed to the different characteristics (such as surface chemistry, cell size and morphology) of different algae species.

During the FO dewatering process, membrane fouling is caused by the deposition of algae cells and their released extracellular polysaccharides (EPS) on the membrane surface. Such fouling layer can be further fortified by the back diffusion of certain draw solutes. For example, Ca^{2+} ions bind specifically with the carboxylate functional groups at the interface of algae cells/EPS, and form egg-box-shaped gel network [32, 455, 466, 467]. Clearly, algae surface chemistry (such as charge, functional group and free energy) determined by cell wall composition can impact the interfacial forces between algae cell and membrane in the aqueous media [468]. Cell shape and size may further influence the cake layer structure and compactness [469-471]. In addition, during the FO process, the cross-flow velocity in feed channel lifts algae particles away from membrane and thus reduces the cake layer formation [472]. However the shear force caused by feed pump may induce cell rupture and EPS production, both of which can enhance membrane fouling. Different algae species may have different sensitivity and response to this hydraulic stress and the salt stress caused by draw solute back diffusion, and thus are expected to exhibit different impacts on membrane fouling and overall algae dewatering efficiency. To realize a feasible FO dewatering process, selection of optimal microalgae species is essential. However, to date, very little is known about the role of algae species-dependant characteristics (such as cell wall composition and stress sensitivity/response) on FO membrane performance.

The objective of this work is to compare the FO dewatering performance in terms of water flux behaviour and algae dewatering efficiency between three freshwater microalgae species (*Scenedesmus obliquus*, *Chlamydomonas reinhardtii*, and *Chlorella vulgaris*). Specific aims were to (1) examine the role of cell wall carbohydrate composition and demonstrate that it is a key factor affecting FO performance; (2) investigate the effect of hydraulic stress on the EPS production from the three algae species; and (3) identify the most suitable algae species for FO dewatering. Based on the results, important mechanisms and factors that govern FO fouling are discussed and elucidated. The findings of this study will provide important insights into the efficient operation of FO for algae dewatering in terms of optimal algae species selection, fouling control and FO system design, assisting the future development of FO technology for more effective microalgae dewatering.

3.2. Materials and methods

3.2.1. Microalgae species, cultivation and characterization

Three freshwater microalgae species (*Scenedesmus obliquus*, *Chlamydomonas reinhardtii*, and *Chlorella vulgaris*) were investigated in this study. They were selected due to their high lipid content, reaching over 50 % of the dry weight [138, 473], as well as excellent potential for wastewater treatment [474, 475], and CO_2 capture [476, 477]. Pure cultures of them were obtained from the Culture Collection of Algae and Protozoa (CCAP, UK). Each species was individually cultivated in modified BG-11 medium with compositions described previously [464]. Algae suspensions were continuously stirred with air injected (75 L/h) at room temperature (25 ± 1 °C). Illumination was provided by fluorescent lamps (100 μmol photons/m^2·s). The algae growth was periodically monitored by optical density measurement with a spectrophotometer (Helios Zeta, Thermo Scientific, UK) at 435 nm wavelength [442]. The pH of each algae suspension was maintained at 7±0.5 for the optimum algae growth. After 14 days of cultivation, 2-3 g dry weight/L of each algae species was obtained. This stock suspension was diluted with BG-11 medium to prepare the feed water for FO dewatering experiments and hydraulic stress tests.

Based on microscopic observation (Olympus IX71, Olympus Corporation, Tokyo, Japan), *S. obliquus* has an ellipsoidal shape and is around 5 µm in width and 10 µm in length; *C. reinhardtii* has a circular shape with a diameter of around 10 µm and possesses two flagella; and *C. vulgaris* has a circular shape with a diameter of around 5 µm. In the BG-11 medium, *S. obliquus*, *C. reinhardtii* and *C. vulgaris* exhibited negatively zeta potential of 15.45 ± 1.87 mV, 19.07 ± 0.75 mV, and 16.8 ± 1.15 mV, respectively (Zetasizer nano, Malvern Instruments Ltd., UK).

3.2.2. FO membrane

In all FO experiments, a new flat sheet cellulose triacetate (CTA) membrane (Hydration Technologies Innovation, Albany, OR, USA) was used. The membrane has an active layer made of CTA supported by an embedded woven mesh to enhance its mechanical strength [263]. Total membrane thickness is around 50 µm [478]. The membrane active layer exhibited a slightly negative zeta potential of approximately – 10 mV in 10 mM KCl at pH of 7±0.5 [479].

3.2.3. Experimental setup and protocols for algae dewatering

All algae dewatering experiments were conducted using a bench-scale FO membrane setup (Figure 2.1) that has been described previously [464]. A flat sheet membrane coupon was housed in a plate-and-frame membrane cell with two identical channels on both sides of the membrane. Diamond-patterned spacers were placed on either side of the membrane for additional support. Counter-current flow was applied with cross-flow rate on each side of the membrane controlled by a variable-speed peristaltic pump (Cole-Parmer, Vernon Hills, IL, USA). To prevent microalgae sedimentation, a magnetic stirrer was used to provide mixing in feed tank. Draw solution tank was placed on a digital scale (Denver Instrument, USA) which was interfaced with an automatic data acquisition system to determine permeate water flux. The temperature of both feed and draw solutions was kept constant using a re-circulating water chiller (Fisher Scientific, Loughborough, UK). Samples from feed tank were taken periodically to measure pH, conductivity and algae biomass concentration.

ACS reagent grade sea salts, $MgCl_2$, and $CaCl_2$ (Sigma-Aldrich, UK) were used to make the draw solutions. The sea salts concentration was 70 g/L to mimic the salinity of desalination brine [444], and its composition has been reported previously [464]. In order to have a meaningful comparison of FO performance, 86.5 g/L $MgCl_2$ and 114.3 g/L $CaCl_2$ were used to achieve a same initial permeate flux of 7 L/m^2·h with 70 g/L sea salts.

At the start of each algae dewatering experiment, a fresh membrane coupon was placed in the membrane cell with membrane active layer facing the feed solution. The FO membrane was first stabilized with BG-11 medium as feed solution and desired draw solution for 30 min to achieve a stable water flux. Algae dewatering was then initiated with 1 L of algae suspension (0.2 g/L of algae biomass) in the feed tank and 6 L of draw solution. Each FO experiment was continued until the initial algae suspension was concentrated by 4 times (permeate volume of 750 mL was attained). Other experimental conditions included temperature of 25 ± 1 °C and cross-flow velocity of 9.6 cm/s for both feed and draw solution sides. The extent of algae fouling was represented by the flux decline curves obtained during algae dewatering tests corrected by the water flux obtained from the baseline tests conducted with each solutes

investigated, and where no algae biomass was added into the feed solution. Permeate flux loss caused by algae fouling was calculated by:

$$\Delta J_w = 1 - \frac{J_{w,a}}{J_{w,b}}$$

3.1

where ΔJ_w is normalized water flux loss, $J_{w,a}$ and $J_{w,b}$ are water flux in algae dewatering test and baseline test at specific concentration factor, respectively.

To determine the algae dewatering efficiency of FO, algae biomass concentration in the feed tank was measured at specified time intervals. The algae dewatering efficiency was calculated by:

$$R = \frac{X_f}{X_i \cdot CF}$$

3.2

where R is the algae dewatering efficiency (or recovery rate), X_i and X_f are algae biomass concentration in the initial suspension before FO dewatering experiments and in the final feed tank (which is the algae suspension available for downstream processing), respectively. CF is the concentration factor. The FO dewatering experiments were very reproducible, as shown in Appendix 3. Therefore, not all the experiments were replicated and no error bars were provided for the flux loss and biomass recovery data.

3.2.4. Hydraulic stress test

To examine the impact of hydraulic stress on the production of extracellular carbohydrate by microalgae, simple tests were conducted. For each algae species, three conical flasks containing 200 mL of algae suspension (0.2 g/L) were prepared from the same stock suspension. Flask-1 was placed on a benchtop shaker with rotating speed of 150 rpm. Flask-2 was placed on a magnetic stir plate so that the algae suspension could be continuously mixed. Flask-3 was also placed on a magnetic stir plate with same stirring speed as Flask-2. In addition, the algae suspension in Flask-3 was continuously recirculated at a flowrate of 0.576 L/min (identical to that used in FO experiments) by a peristaltic pump. Other experimental conditions kept same for the three flasks. After

6 hours, 20 mL samples were collected from each flask and the concentration of extracellular carbohydrate was then determined as described in Section 2.5.

3.2.5. Extracellular carbohydrate analysis

In order to elucidate the response of microalgae to (1) various hydraulic stress conditions and (2) back diffusion of draw solutes during FO filtration, the amount of extracellular carbohydrate was examined. Briefly, algae suspensions were centrifuged at 6 x g for 20 min to pellet the cells. 2 ml of the supernatant was then filtered through a 0.2 μm hydrophilic nylon filter (Millipore, UK). Carbohydrates concentration in the filtrate was analysed by phenol-sulphuric acid assay with glucose as a standard [450]. For the feed samples during algae dewatering experiments, total extracellular carbohydrate contents (mg) were then calculated from the product of the carbohydrate concentrations (mg/L) and feed volume at the time when the samples were taken. All samples were prepared in triplicates. Data were analysed by one-way ANOVA. The carbohydrate values obtained in different conditions were compared using a Tukey's multiple comparison test (Prism 4, GraphPad Software, San Diego, CA). Differences at the < 5% level were considered significant and discussed.

3.3. Results and discussion

3.3.1. Algae species affect FO dewatering performance

During FO dewatering experiments, clean water permeates from the algae suspension on the feed side to the draw solution side due to the osmotic pressure difference across the membrane. Microalgae cells and their EPS are retained by the membrane active layer due to the high retention nature of membrane, resulting in the accumulation of algae biomass onto the membrane surface. Such algae accumulation leads to (1) cake layer formation and pore blocking, both of which enhance membrane resistance to the water permeation, and (2) an enhanced salt concentration in the cake layer by hindering the back diffusion of salts from the membrane surface to bulk feed solution, a phenomenon called cake enhanced concentration polarization (CECP), which increases the osmotic pressure on the membrane surface and thus reduces the net osmotic driving force across membrane active layer for permeate water flux [480]. As a result, water flux loss was observed over the course of all FO dewatering experiments (Figure 3.1). For example, the FO membrane experienced a drastic flux loss (up to

70.9 %) when *S. obliquus* suspension was concentrated with CaCl$_2$ draw solute. In
addition to algae deposition onto membrane surface, algae biomass may trap inside the
feed spacer [464]. Such algae deposition and trapping reduce the amount of biomass
that can be recovered for downstream processes and thus reduce the overall dewatering
efficiency. Thus, the FO membrane performances were evaluated by (1) water flux loss
and (2) algae dewatering efficiency in the algae dewatering experiments.
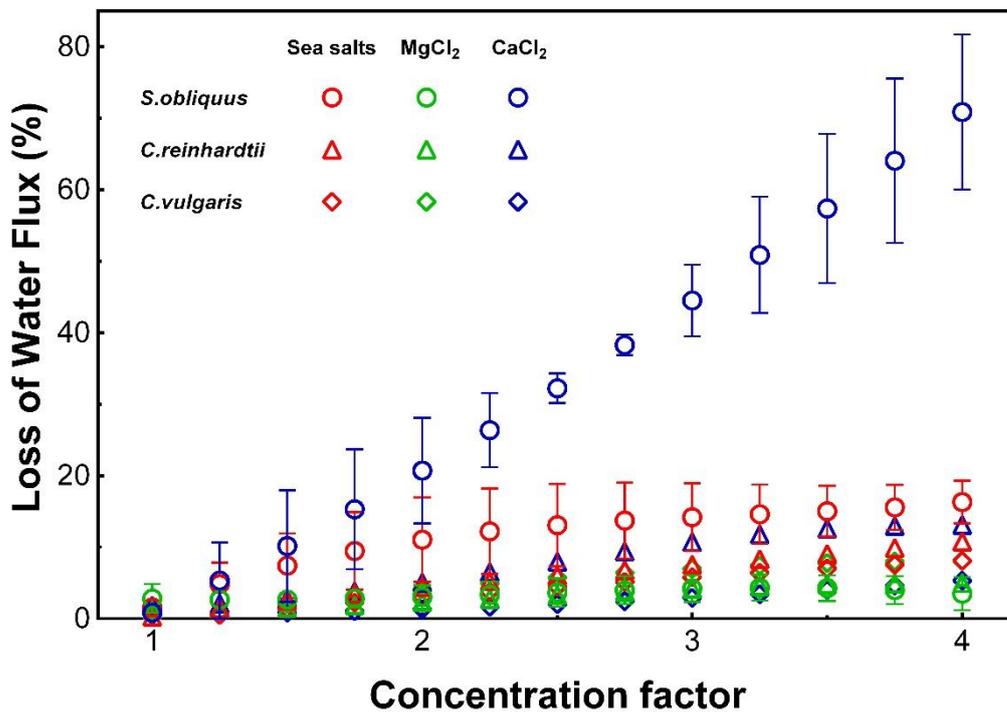
Figure 3.1 *– Evolution of the loss of water flux (%), calculated from Equation 3.1,
during all experiments conducted.*

Figure 3.1 presents the permeate water flux loss due to membrane fouling at the
end of microalgae dewatering tests when concentration factor reached 4. With same
experimental conditions, the tests were carried out with different algae species. For
Ca^{2+}-containing draw solutions, the overall extent of water flux loss followed the order
of *S. obliquus > C. reinhardtii > C. vulgaris*. For example, with CaCl$_2$ as draw solution,
flux loss was 70.9 %, 13.1 % and 5.3 % for *S. obliquus*, *C. reinhardtii*, and *C. vulgaris*,
respectively. With sea salts (containing 0.82 g/L Ca^{2+}) as draw solution, flux loss was
16.3 %, 10.8 % and 8.1 % for *S. obliquus*, *C. reinhardtii*, and *C. vulgaris*, respectively.
Previous studies attributed the severe water flux loss with Ca^{2+}-containing draw

solutions to the back diffusion of Ca^{2+} and subsequent Ca^{2+} complexation mechanism [481]. Once diffused through the membrane into the feed water, divalent calcium ions formed bridges between the carboxylate functionality on algae cells and their EPS interfaces producing much stronger attraction [466, 481]. As a result, a stable and dense cross-linked gel network was developed on the membrane active layer surface. This tightly bound fouling layer accelerated the CECP phenomenon and enhanced overall resistance to water permeation, leading to a significant water flux loss. The results in Figure 3.1 indicate that *S. obliquus* is most sensitive to the back diffusion of Ca^{2+}, followed by *C. reinhardtii*. For *S. obliquus*, the final water flux loss followed the order of $CaCl_2 \gg$ sea salts $> MgCl_2$. *C. reinhardtii* exhibited a similar trend but to a lower extend. In contrast, *C. vulgaris* did not cause obvious membrane fouling for all draw solutions (water flux loss was below 8.1 %) without remarkable response to the back diffusion of Ca^{2+}. We propose the difference in calcium complexation and fouling potential specific for each algae species to their different cell wall composition which will be further explored in Section 4.3.4.

When $MgCl_2$ was used as draw solution, all three algae species did not cause much membrane fouling. The extent of final flux loss followed the order of *C. vulgaris* > *C. reinhardtii* > *S. obliquus*. The extremely low fouling behaviour of *S. obliquus* with $MgCl_2$ draw solution can be attributed to its ellipsoidal shape, which prevented the tight packing of cells on the membrane surface and thus reduced the blocking of water passage [482]. However, this low fouling propensity may more likely be due to magnesium binding behaviour with carboxylate functional groups, as further explained in the next sections.
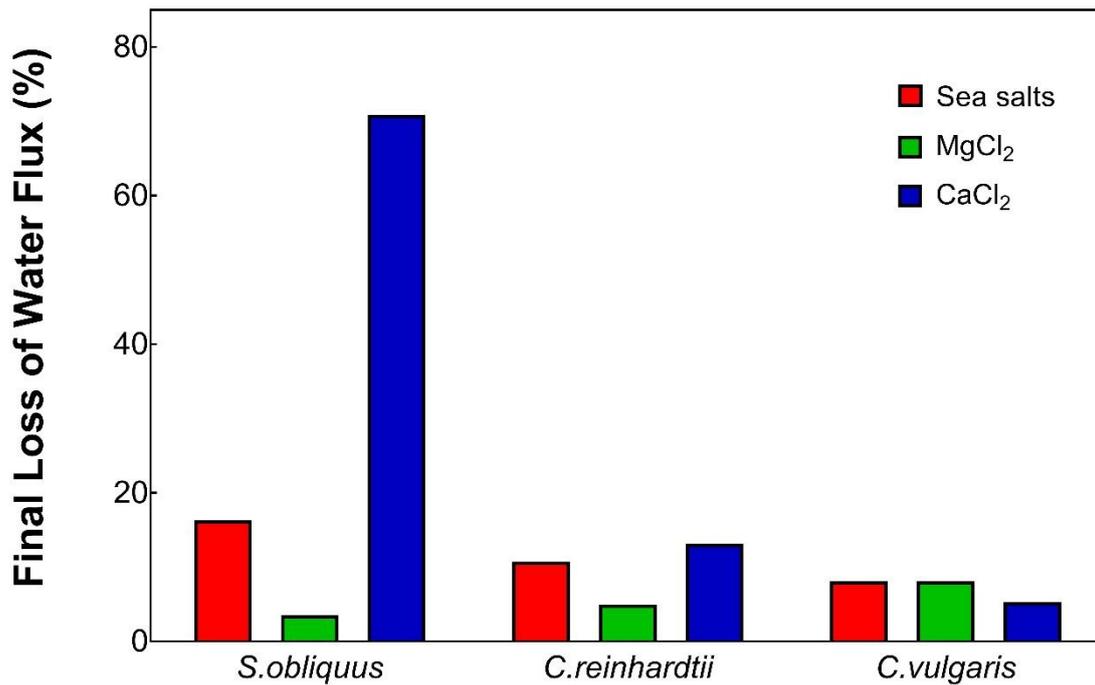
Figure 3.2 - *Water flux loss, calculated from Equation 3.1, at the end of single microalgae dewatering experiments when concentration factor reached four.*

Figure 3.2 presents the microalgae dewatering efficiency when *S. obliquus*, *C. reinhardtii*, and *C. vulgaris* suspensions were harvested by FO process with various draw solutions. A lower value indicates more algal biomass lost during the dewatering process due to deposition onto membrane surface or trapping inside the feed spacer. For *S. obliquus* and *C. reinhardtii*, much greater algal biomass loss was observed with 0.91 mol/L $MgCl_2$ or 1.03 mol/L $CaCl_2$ draw solution, compared with sea salts draw solution (containing 0.11 mol/L Mg^{2+} and 0.02 mol/L Ca^{2+}). Given the faster back diffusion of Mg^{2+}/Ca^{2+} into feed water when $MgCl_2$ or $CaCl_2$ was used as draw solution (due to their much higher concentration) compared with sea salts draw solution, the greater biomass loss with $MgCl_2/CaCl_2$ draw solutions indicates that *S. obliquus* and *C. reinhardtii* are sensitive to the back diffusion of divalent cations. As discussed above, once diffused through the membrane, calcium-carboxylate complex formation exacerbates the deposition of algal cells onto membrane and/or feed spacer. This leads to the algal biomass loss (41.0% for *S. obliquus* and 34.3% for *C. reinhardtii*) and water flux decline (70.9% for *S. obliquus* and 13.1% for *C. reinhardtii*) governed by enhanced membrane resistance and CECP with $CaCl_2$ draw solution.

When $MgCl_2$ was used as draw solution, 30.8% of *S. obliquus* and 36% of *C. reinhardtii* were lost during the FO dewatering process however no obvious water flux decline (below 5%) was observed. Possible explanations are proposed below. Mg^{2+} has almost same rate of back diffusion with Ca^{2+} [386], and can form complexes with algal cells and their EPS matrix via specific ion interaction and charge neutralization [466, 483]. This complexation of magnesium ions to algal biomass results in the flocculation of algae cells (Figures 3.4a and 3.4b), accumulation of biomass onto membrane surface and/or trapping inside feed mesh spacer, and thus a reduced algae dewatering efficiency. However, magnesium ions are much less effective in terms of binding with carboxylate functional groups [484], and form smaller algae flocs in comparison with calcium ions (Figure 3.3a and 3.3b). As a result, the deposited algal biomass introduces a looser and less compact cake layer that has lower cake resistance and less effect of CECP [469, 470], leading to a negligible water flux loss for $MgCl_2$ draw solution during the whole FO dewatering process.

In contrast, the dewatering efficiency (recovery rate) of *C. vulgaris* is practically similar for the three types of draw solution with all recovery rates above 80% which is comparable to the algae recovery rate achieved by pressure-driven membrane processes [482, 485]. This indicates (1) the FO process can efficiently recover *C. vulgaris* from water regardless of draw solution chemistry; and (2) the functionality at the interface of *C. vulgaris* cells and/or their EPS matrix has little affinity to divalent cations and *C. vulgaris* biomass has less fouling propensity. Clearly the FO dewatering method to be used greatly depends on the species of microalgae considered. The promising dewatering performance with *C. vulgaris* in terms of prominent dewatering efficiency and insignificant flux loss reveals that *C. vulgaris* is more suitable to be harvested by FO membrane process compared to the other two species. In the following sections, we explore the potential causes behind the different FO membrane fouling behaviour of the 3 algae species.
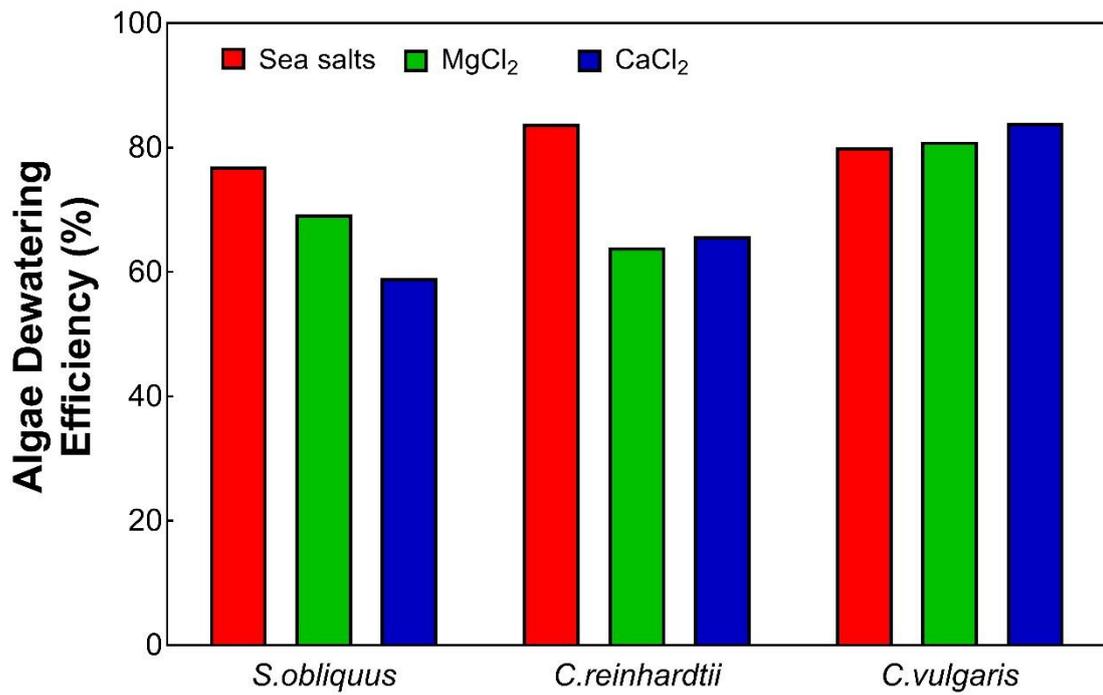
Figure 3.3 *- Microalgae dewatering efficiency, calculated from Equation 3.2, at the end of single FO experiments when concentration factor reached four.*
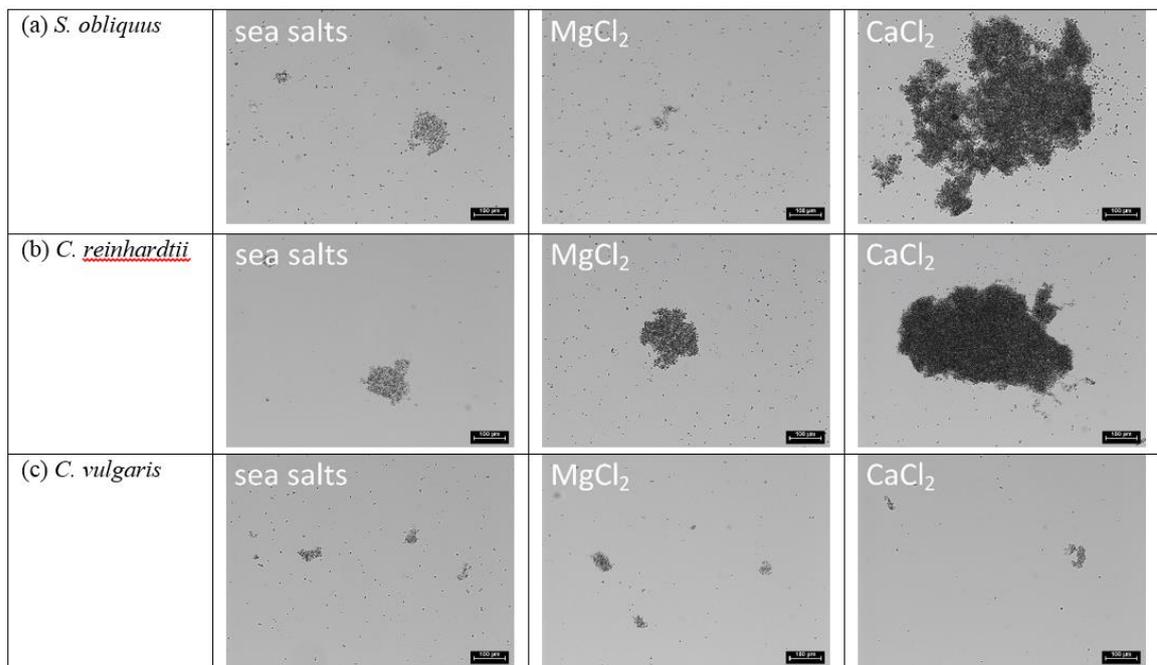
Figure 3.4 *- Microscope images of feed solution after FO dewatering experiments for (a) S. obliquus; (b) C. reinhardtii; and (c) C. vulgaris.*

3.3.2. Extracellular carbohydrate production under hydraulic stress

As discussed above, *S. obliquus* exhibited strong sensitivity to the back diffusion of divalent cations which however had little impact on the behaviour of *C. vulgaris* during FO dewatering process. Divalent cations (especially Ca^{2+}) promote algae biomass aggregation near the membrane surface and deposition onto membrane by (1) forming crosslink gel network between polysaccharide chains at the interface of algae cells and their EPS [416, 486], and (2) stimulating algae to secret more EPS into the culture medium due to salt stress, which in turn further enhances the formation of gel network [464]. Thus we propose that the different algae fouling behaviour may be explained by their different (1) cell wall carbohydrate composition and (2) amount of EPS excreted during the FO dewatering process. As described previously, during all FO experiments, magnetic stirrer was used to provide better mixing to the algae suspension and prevent algae sedimentation to the bottom of feed tank. In addition, the algae suspension was circulated by a peristaltic pump. The shear effects caused by the stirrer and pump may induce algae cells damage and releasing more EPS [487]. First, we examined the response and sensitivity of each algae species to the shear effects. Figure 3.5 shows the production of extracellular carbohydrate by the three algae species under different hydraulic stress conditions. For all algae species, the extracellular carbohydrate production followed the order of simple shaking (Flask 1) < magnetic stirring (Flask 2) < magnetic stirring + peristaltic pumping (Flask 3). This proves that all three algae species produced more carbohydrate in response to the shear effects induced by magnetic stirring and/or peristaltic pumping. In flask 3 which mimicked the hydraulic condition in the feed tank during FO experiment, *C. reinhardtii* excreted the highest total amount of carbohydrate, followed by *C. vulgaris* and *S. obliquus*. There seems to be no clear relationship between the algae dewatering performance (Figures 3.2 and 3.3) and the amounts of carbohydrate released under the hydraulic stress condition during FO tests (Figure 3.5). However, the lower release of carbohydrates by *S. obliquus* may be linked with the low fouling observed when using $MgCl_2$ as draw solution (Figure 3.2). Indeed, as mentioned previously, the binding of magnesium with extracellular carbohydrates is relatively weak. Therefore, the low release of carbohydrates observed reduces the binding of these with magnesium ions, which prevent the formation of large flocs and also reduces the impact of fouling.
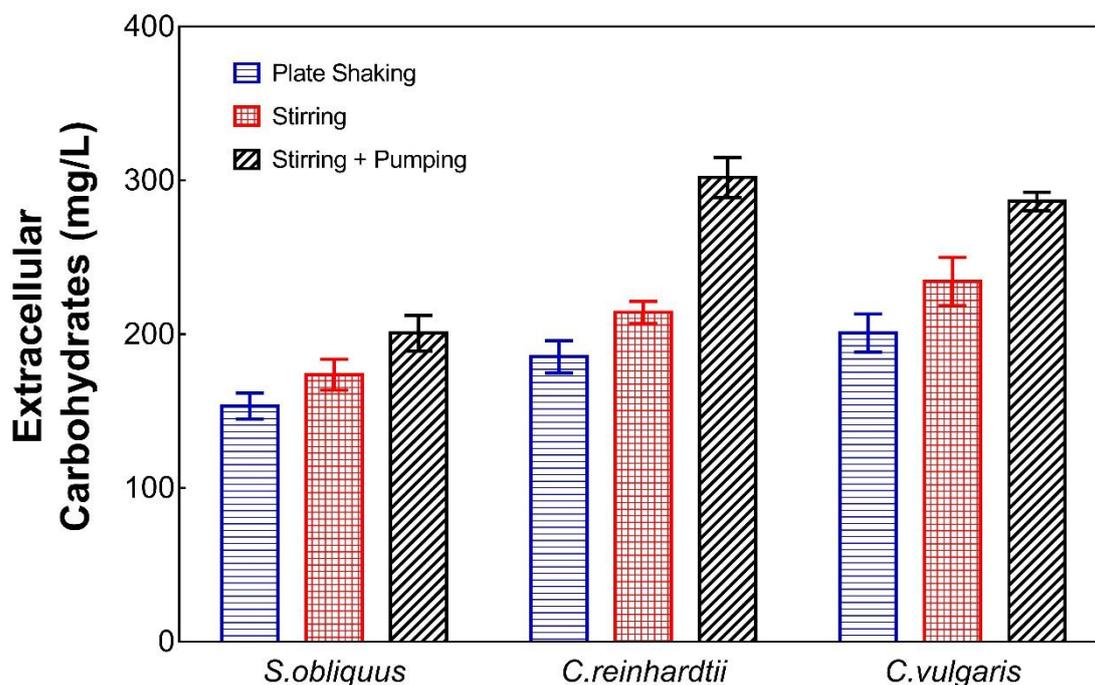
Figure 3.5 *- Extracellular carbohydrate produced by S. obliquus, C. reinhardtii and
C. vulgaris suspensions subjected to different hydraulic stress conditions. Error bars
represent the standard deviations of the average values determined from three
measurements.*

3.3.3. Extracellular carbohydrate content in feed tank

In addition to hydraulic stress, salinity stress can also stimulate algae to produce
more EPS [44]. During FO dewatering process, the permeation of pure water from feed
to draw solution and the back diffusion of draw solutes into the feed side of membrane
result in an enhanced salinity in the feed tank [464]. Next we examined the amount of
extracellular carbohydrate excreted by each algae species before and at the end of each
dewatering experiment. For the three conditions (*S. obliquus* with sea salts draw
solution, *S. obliquus* with $CaCl_2$ draw solution, and *C. reinhardtii* with $CaCl_2$ draw
solution) highlighted in Figure 3.6, it is interesting to find that carbohydrate amount in
the feed tank was increased after FO filtration. This observation suggests that the back
diffusion of calcium ions greatly promoted the production of extracellular carbohydrate
by *S. obliquus*. A complex mechanism has been proposed for the enhanced EPS
subjected to high local concentration of calcium, which could lead to disturbance in the
photosynthetic metabolism of algae [488, 489]. *C. reinhardtii* exhibited similar
response to the back diffusion of calcium but only in the case with $CaCl_2$ draw solution

where calcium back diffusion rate was much faster compared to the case with sea salts draw solution. Recall microalgae caused the most severe flux decline in the above three conditions (16.3% for *S. obliquus* with sea salts draw solution, 70.9% for *S. obliquus* with CaCl$_2$ draw solution, and 13.1% for *C. reinhardtii* with CaCl$_2$ draw solution). This further supports our hypothesis that calcium-promoted carbohydrate contributes to the algae biomass depositions onto membrane surface and water flux loss.

It is worth noting here that *S. obliquus* caused a much more dramatic flux decline (70.9%) than *C. reinhardtii* (13.1%) when CaCl$_2$ was used as draw solution although the two algae species exhibited similar amount of calcium-promoted carbohydrate. This indicates that in addition to the amount of carbohydrate, the type and chemistry of the carbohydrates excreted by algae which may relate to algae cell wall composition plays an important role in the formation of cross-linked gel network and membrane fouling.
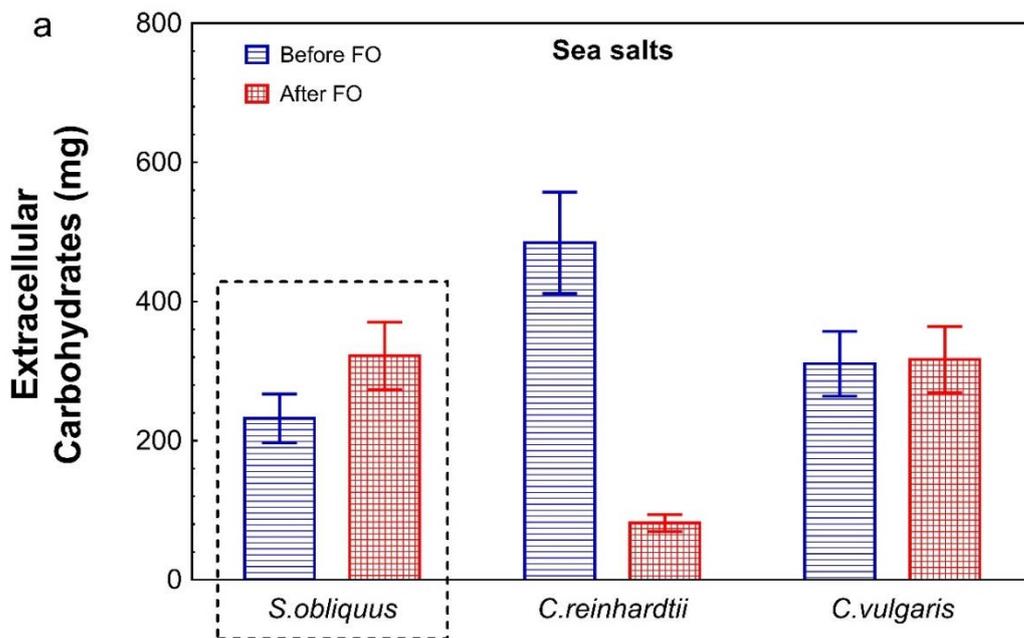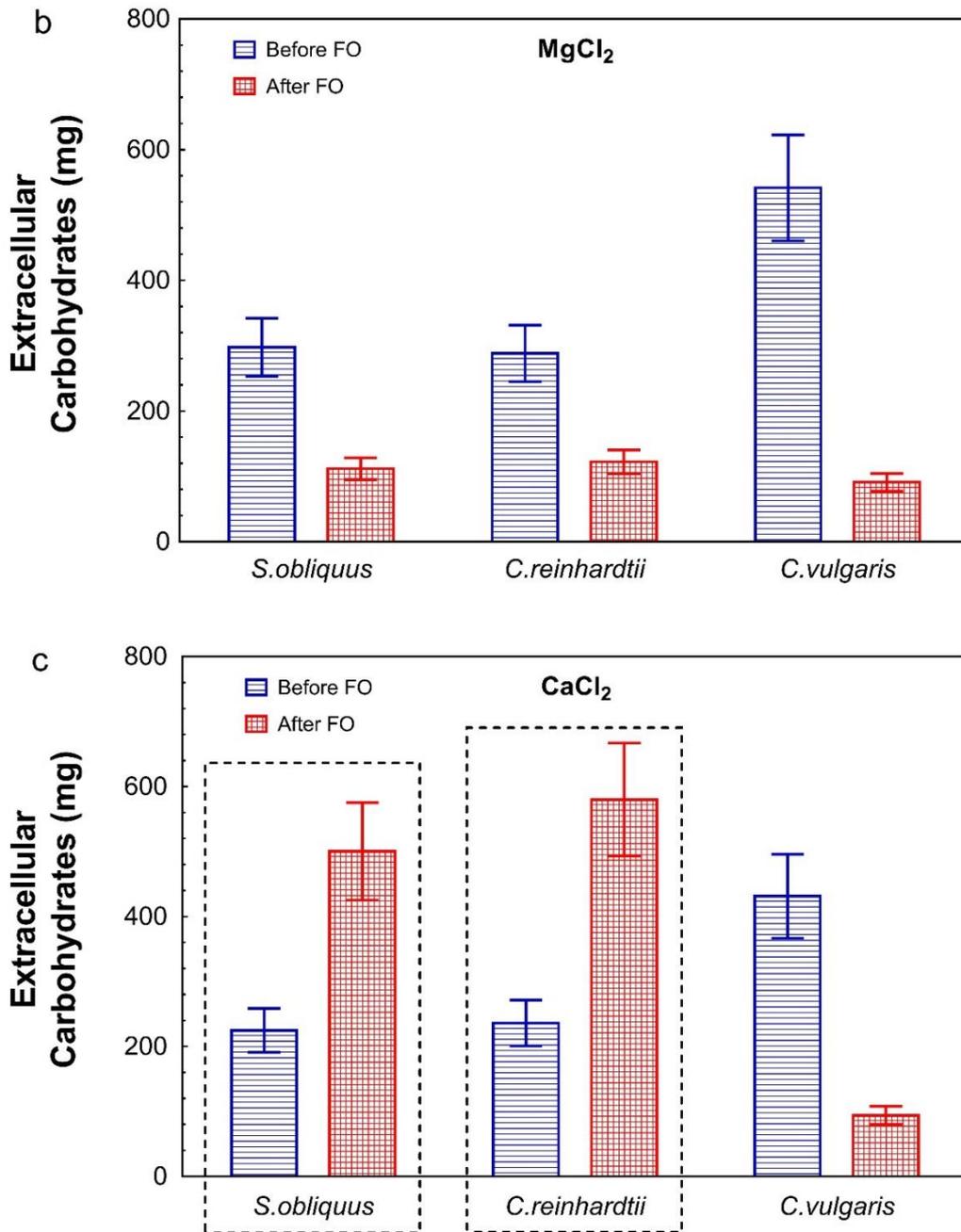
Figure 3.6 *- Extracellular carbohydrate content in feed tank before and after algal dewatering tests with different draw solutions: (a) sea salt, (b) $MgCl_2$ and (c) $CaCl_2$. Error bars represent the standard deviations of the average values determined from three measurements.*

3.3.4. Algae cell wall carbohydrate composition controls membrane fouling

As discussed above, the carbohydrate part of microalgae cell wall composition is expected to influence their interaction with divalent cations, algae aggregation, biomass deposition onto membrane surface and overall dewatering efficiency. Table 3.1

summarizes the cell wall carbohydrate compositions of the three algae species investigated in this study. Although these carbohydrates are presented as neutral sugars, they will be most likely to exist as polysaccharides [490].

The main carbohydrate chains from *S. obliquus* consisted mainly of glucose (42%), mannose (26%), galactose (16%), rhamnose (11%) and fructose (5%). The most abundant glucose and mannose are likely to be found as glucomannan, a polysaccharide formed by two glucoses and two mannoses [491]. Divalent cations (especially calcium) can bind preferentially to the carboxylate groups of glucomannans and form bridges between adjacent algae cells and their EPS, leading to a highly interconnected gel network. Furthermore, among the three algae species, *S. obliquus* is the only one containing fructose. The non-vicinal hydroxyl groups of fructose bind specifically with calcium to form a strong extensive hydrogen-bond network [492]. For example, β-D-fructose can bind with calcium chloride, forming $Ca(\beta\text{-D-fructose})Cl_2 \cdot 2H_2O$ and $Ca(\beta\text{-D-fructose})2Cl_2 \cdot 3H_2O$ [460]. We therefore attribute the most severe loss in both water flux and biomass during FO dewatering of *S. obliquus* with Ca^{2+}-containing DS to the presence of fructose and great amount of glucose and mannose on its cell wall.

The cell wall carbohydrate of *C. reinhardtii* was mainly composed of galactose, glucose and arabinose, in which galactose was the most abundant. Furthermore, it is worth noting that *C. reinhardtii* contained higher percentages of galactose in its neutral sugar matrix compared to the other two algae species. Galactose was reported to be able to form strong bonds with divalent cations, the binding affinity with galactose following a trend of $Ca^{2+} > Mg^{2+}$ [493]. In addition, galactose was found to form acidic polysaccharides which have a high propensity to form calcium-stabilized gels [494]. Thus the abundant amount of galactose in *C. reinhardtii*'s cell wall is proposed to cause the formation of algae flocs (Figure 3.5b) and great algae biomass loss (Figure 3.3) with $MgCl_2$ and $CaCl_2$ draw solutions as well as moderate flux decline (Figure 3.2) with Ca^{2+}-containing draw solution.

The carbohydrate part of *C. vulgaris*'s cell wall was complex, with rhamnose as the most abundant (45-54%). Galactose and xylose were present in smaller amounts while arabinose, mannose and glucose were identified amongst the trace monosaccharides. The lack of fructose, insufficient glucose, mannose and galactose may explain the low fouling propensity of *C. vulgaris*. Further research efforts need to

112

understand the role of abundant rhamnose in the promising dewatering performance with *C. vulgaris*.

Table 3.1 *- Cell wall carbohydrate compositions of S. obliquus, C. reinhardtii and C. vulgaris. Data obtained from various sources.*

Neutral sugars	*S.obliquus* [495]	*C.reinhardtii* [496]	*C.vulgaris* [497]
Arabinose		17-43 %	2-9 %
Fructose	5 %		
Galactose	16 %	26-62 %	14-26 %
Glucose	42 %	0-50 %	1-4 %
Mannose	26 %	0-5 %	2-7 %
Rhamnose	11 %		45-54 %
Xylose		0-7 %	7-19 %

3.4. Conclusions

In this study, well-controlled laboratory experiments were conducted to compare the FO dewatering performance between three freshwater microalgae species with divalent cation-containing draw solutions. Membrane fouling extent and algae dewatering efficiency were found to correlate with the algae cell wall carbohydrate composition. *S. obliquus* having fructose and abundant glucose and mannose in its cell wall demonstrated strong response to the back diffusion of calcium. During the FO filtration with Ca^{2+}-containing draw solution, *S. obliquus* excreted more extracellular carbohydrate, formed large flocs and dense gel network, leading to dramatic water flux loss and algae biomass loss. *C. reinhardtii* without fructose but great galactose showed a similar response to the calcium back diffusion but to a lower extent compared with *S. obliquus*. *C. vulgaris* without fructose and containing lower amounts of glucose, mannose and galactose, demonstrated best dewatering performance regardless of draw solution chemistry, with negligible water flux decline and over 81% of algae recovery rate. FO dewatering performance is clearly dependent on microalgae species. More attention should be paid to the selection of a proper algae species in order to minimize membrane fouling and maximize biomass recovery. The shape of each species may also play a role, as it affects the surface available for binding with various compounds, including divalent cations and carbohydrates. Overall, our results suggest *C. vulgaris* rather than *S. obliquus* and *C. reinhardtii* is the optimal microalgae species to be dewatered by FO process due to its unique cell wall carbohydrate composition. Further studies are necessary to identify which components in the cell wall of *C. vulgaris* contribute to the best FO dewater performance. Given the promising results obtained with *C. vulgaris*, as well as its demonstrated ability for wastewater treatment, this specie has been chosen for further investigation and integration within a combined system for wastewater treatment and concentrated biomass harvesting.

4. Selection of a New Forward Osmosis Membrane for Microalgae Biomass Dewatering through Determination of Main Characteristics

4.1. Introduction

At the early stages of this study, Hydration Technologies, Inc. provided the best commercially available FO membranes. Most of the research on FO processes using commercial membranes was conducted using the CTA-ES membrane provided by this company and many data were available with this membrane. Therefore, after proceeding to a characterization of the membrane, the experimental work was conducted using this membrane. However, Hydration Technologies, Inc. closed business during this study and a research of a new commercially available membrane was necessary to find a replacement for the CTA-ES membrane previously used. The following section provides details of the experimental methods and results of the characterisation of the FO membranes investigated. Membrane characteristics such as the water flux, solute diffusion, or chemical resistance, are crucial to decide their application in an industrial process. These characteristics differs for every FO membrane and these parameters have to be taken into account for the design of any process. Understanding the differences between each membranes allows to better understand the different results obtained with each one. It is also crucial for the selection of membrane to be used for a specific application. In this study, several membranes were characterized in order to select the most suitable membrane commercially available for the dewatering of microalgal biomass. Therefore, a high permeate flux, low solute diffusion, and low fouling propensity, are desired characteristics for this application. The methods for the characterization of FO membranes are well defined. An example of the steps involved is displayed on Figure 4.1.
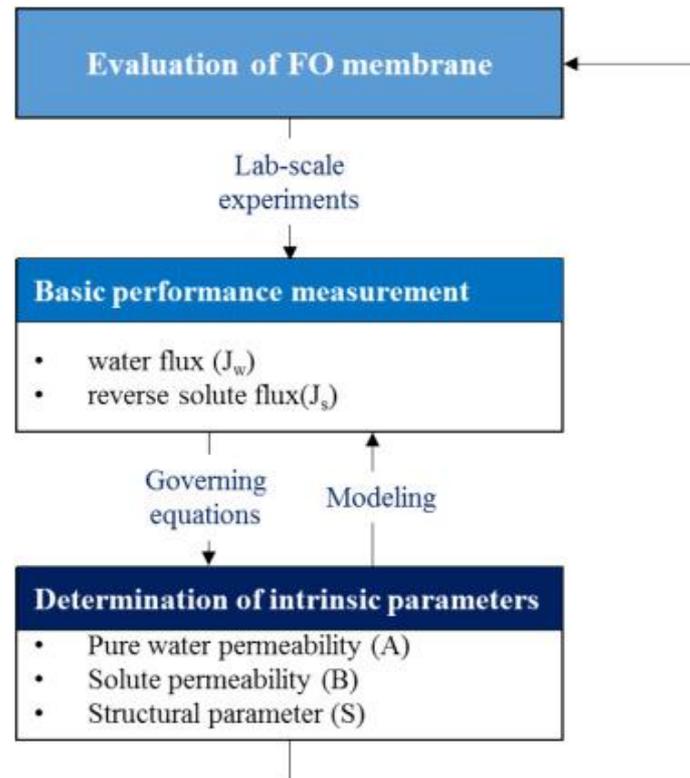
Figure 4.1 – *Guidelines for obtaining the values of the performance parameters A, B, and S [498].*

4.2. FO Membranes

In this preliminary study, three forward osmosis membranes were tested and their characteristics compared for the selection of the most suitable membrane for microalgae dewatering. The membranes used were (1) a cellulose triacetate membrane supported by an embedded polyester mesh (CTA-ES) provided by Hydration Technologies, Inc. (Albany, OR, USA), (2) a thin-film composite FO membrane provided by Porifera, Inc. (Hayward, CA, USA), and (3) a biomimetic membrane using aquaporin proteins as functional building blocks and provided by Aquaporin (Kongens Lyngby, Denmark).

4.3. Experimental Setup and Operating Conditions

All FO experiments were conducted using a custom fabricated bench-scale crossflow FO system (Figure 2.1). Briefly, a membrane coupon with an effective area of 41 cm^2 was housed in a cross-flow membrane cell. Diamond-patterned spacers were placed on both sides of the membrane to improve support of the membrane as well as

promote mass transfer [499, 500]. Counter-current flow was used with cross-flow rate on both sides of membrane controlled by a variable-speed peristaltic pump (Cole-Parmer, Vernon Hills, IL). The cross-flow velocities for both feed and draw solutions were maintained at 15.5 cm/s during all experiments. The draw water tank was well mixed by a magnetic stirrer. The feed solution tank was placed on a digital scale (Denver Instrument, add place and country) and weight changes as a function of time were utilized to determine permeate water flux. The solution temperature was maintained at 25 ± 1 °C.

Both membrane orientations, AL-FS and AL-DS, were tested. In all FO experiments, the feed solution was deionised water. The draw solutions included simple electrolytes and a commercial sea salt at a various concentrations ranging from (15 – 230 g/L). All salts were ACS reagent grade (Sigma-Aldrich, UK). The volume of both feed and draw solutions was 2.5 litre at the beginning of each experiment. The duration of each FO membrane test was 1 h. Samples from feed tank were taken at specified time intervals for conductivity and temperature measurements. From the conductivity and water flux measurements, the amount of solute in the feed solution was calculated. Then, the reverse solute flux was obtained from the slope of the linear trend line of the determined amount of solute in the feed side over time.

4.4. Determination of Pure Water and Solute Permeability

Pure water permeability (A) describes the ability of water to pass through the membrane. It is generally determined by measuring the water flux (Jw) during a simple experiment using feed and draw solutions of known concentrations, and therefore osmotic pressures (π). The osmotic pressure of a solution is usually calculated from the solute concentration C, the temperature T, the ideal gas constant R_g, and the Van't Hoff factor β, using Equation 2.1. β is generally associated to the ideal number of dissociated ionic species of the solute, generating the osmotic pressure (e.g. 2 for NaCl, dissociating into Na$^+$ and Cl$^-$). The water flux Jw is then determined using Equation 2.1, from the osmotic pressure difference across the active layer $\Delta\pi_{eff}$, and the membrane pure water permeability A. Equation 2.1 can be modified using the bulk osmotic pressure difference $\Delta\pi_{bulk}$ and the reflection coefficient σ defined by Staverman in 1951 [501].

$$\pi = \beta \cdot C \cdot R_g \cdot T \qquad\qquad 4.1$$

$$Jw = A \cdot \Delta\pi_{eff} = A \cdot \sigma \cdot \Delta\pi_{bulk} \qquad\qquad 4.2$$

The pure water permeability coefficient, A, and solute permeability coefficient, B, of the FO membranes were evaluated in a dead-end filtration test unit (Millipore, UK). A schematic of the dead-end experimental setup used is presented on Figure 4.2. The effective membrane area was 36 cm^2. The cell was filled with 400 ml of pure water and a controlled pressure was applied using compressed air. The experiments were conducted at room temperature which was measured at around 20°C. The A value was determined by measuring the water flux over a range of applied pressures (1 - 5 bar). The water flux is then plotted as function of the hydraulic pressure difference across the membrane. The resulting slopes gives the pure water permeability A for each membrane. An example of the determination of the pure water permeability is given in Appendix 3.
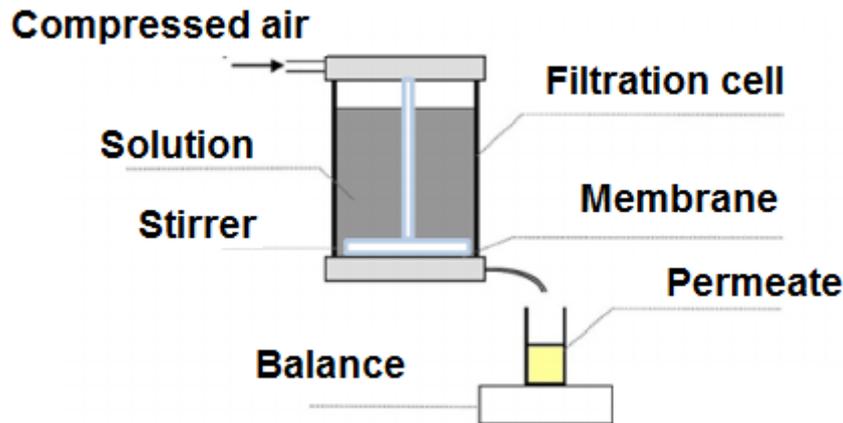
Figure 4.2 - Schematic diagramm of the dead-end system used for the determination of the pure water permeability of the FO membranes used.

Using a feed solution containing 10 mM of individual simple electrolyte or commercial sea salt (Sigma Aldrich, UK), the rejection of NaCl, MgCl2, CaCl2, and sea salts was determined based on feed and permeate conductivity measurements (Ultrameter II, Myron L Company, Carlsbad, CA). B value was determined based on the solute rejection in a range of applied pressures (1 – 5 bar) using Equation 2.3 [502]:

$$B = A \cdot (\Delta P - \Delta \pi) \cdot \left(\frac{1}{R} - 1 \right)$$

4.3

where ΔP and $\Delta \pi$ are the hydraulic pressure difference and osmotic pressure difference across the membrane, respectively. R is the rejection of specific solutes.

Table 4.1 - Characteristics of the CTA-ES, Porifera, and Aquaporin membranes.

Membrane	A (m.s^{-1}.Pa^{-1})	B (m.s^{-1})				B/A (Pa^{-1})			
		Sea salts	NaCl	MgCl$_2$	CaCl$_2$	Sea salts	NaCl	MgCl$_2$	CaCl$_2$
CTA-ES	$1.51 \cdot 10^{-12}$	$5.08 \cdot 10^{-8}$	$9.07 \cdot 10^{-8}$	$4.69 \cdot 10^{-8}$	$3.57 \cdot 10^{-8}$	$3.36 \cdot 10^{4}$	$6.00 \cdot 10^{4}$	$3.11 \cdot 10^{4}$	$2.36 \cdot 10^{4}$
Porifera	$5.65 \cdot 10^{-12}$	$5.00 \cdot 10^{-7}$	$1.45 \cdot 10^{-6}$	$3.29 \cdot 10^{-7}$	$6.51 \cdot 10^{-7}$	$5.82 \cdot 10^{4}$	$8.86 \cdot 10^{4}$	$2.57 \cdot 10^{5}$	$1.15 \cdot 10^{5}$
Aquaporin	$2.69 \cdot 10^{-12}$	$2.09 \cdot 10^{-6}$	$1.61 \cdot 10^{-5}$	$4.56 \cdot 10^{-7}$	$9.82 \cdot 10^{-7}$	$7.77 \cdot 10^{5}$	$5.99 \cdot 10^{6}$	$1.70 \cdot 10^{5}$	$3.65 \cdot 10^{5}$

The results presented in Table 4.1, the membrane provided by Porifera exhibits the highest pure water permeability and solutes permeability slightly higher than the CTA-ES membrane from HTI. *B/A* parameter of Porifera membrane is also slightly higher than the HTI membrane. The membrane provided by Aquaporin has a pure water permeability coefficient higher than the CTA-ES membrane, but also solute permeability coefficient much higher than the two other membranes, leading to higher selectivity for all solutes considered. From these results, the membrane provided by Porifera outperform the two other membranes.

4.5. Structural Parameter Determination

The structural parameter of FO membranes is used to quantify the mass transport length scale across the membrane support layer. Its determination is conducted using the following methodology. The water flux can be defined as:

$$Jw = \left(\frac{1}{K} \right) \cdot \ln \left(\frac{A \cdot \pi_D + B}{A \cdot \pi_F + B + Jw} \right)$$

4.4

where

$$K = \frac{l_{eff}}{D_{eff}} = \frac{\tau \cdot l / \varepsilon}{D} = \frac{S}{D}$$

4.5

where, K is the resistance to solute diffusion (s/m), l_{eff} is the effective length (m), D_{eff} is the effective diffusion coefficient (m²/s), τ is the tortuosity, l is the length (m), D is the diffusion coefficient (m²/s), ε is the porosity, and S is the structural parameter (m⁻¹). Arranging Equations 2.4 and 2.5 gives Equation 2.6 below:

$$D \cdot \ln\left(\frac{A \cdot \pi_D + B}{A \cdot \pi_F + B + Jw}\right) = S \cdot Jw$$

4.6

Plotting $D \cdot \ln\left(\dfrac{A \cdot \pi_D + B}{A \cdot \pi_F + B + Jw}\right)$ as a function of Jw allows the determination of the structural parameter, S, given as the regression coefficient of the linear fitting curve. An Example of determination of the structural parameter is given in Appendix 6.

Table 4.2 below presents the comparison of the structural parameter S, determined for the Porifera and Aquaporin membranes, with the previously used CTA-ES membrane. The average structural parameter is found lower with the Aquaporin and Porifera membranes, in comparison with the previously used CTA-ES membrane, with a lower value for the Aquaporin membrane. This gives additional information on the membranes behaviour. Indeed, a lower S parameter means a lower mass transport across the support layer and thus an enhancement of the CP effect. Concerning the Aquaporin membrane, the higher CP effect (lower S value) is compensated by the higher pure water permeability coefficient, A, leading to similar water flux than the CTA-ES membrane. In comparison with the CTA-ES membrane, the Porifera membrane also demonstrates a higher CP effect (higher S value), but the much higher A value leads to much better results in terms of permeating water flux, Jw.

Table 4.2 - *Determination of structural parameter S.*

Membrane	Structural parameter S (m^{-1})				
	Sea salts	NaCl	MgCl2	CaCl2	Average
CTA-ES	8.79×10^{-4}	5.46×10^{-4}	4.46×10^{-4}	5.21×10^{-4}	5.98×10^{-4}
Porifera	4.83×10^{-4}	2.22×10^{-4}	4.03×10^{-4}	3.48×10^{-4}	3.98×10^{-4}
Aquaporin	2.33×10^{-4}	1.93×10^{-4}	1.92×10^{-4}	2.18×10^{-4}	2.09×10^{-4}

4.6. Zeta Potential

Analysis of the membranes zeta potential was conducted with the SurPASS™ Electrokinetic Analyzer (Anton Paar, Graz, Austria). Streaming potential measurements were performed with the SurPASS using the Adjustable Gap Cell shown in Figure 4.3. For each measurement a pair of membranes with same top layer was fixed on the sample holders (with a cross section of 20 x 10 mm^2) using double-sided adhesive tape. The sample holders were inserted in the Adjustable Gap Cell such that the membrane surfaces were exactly facing each other. A gap of approx. 100 µm was adjusted between the sample surfaces. Prior to the sample mounting, the membranes were soaked in deionized water for 24 hours. Before starting each measurement, the membrane samples were carefully rinsed with the measuring electrolyte. A 0.001 mol/l NaCl solution was used as the background electrolyte and the pH of this aqueous solution was adjusted with 0.05 mol/l HCl and 0.05 mol/l NaOH, respectively.
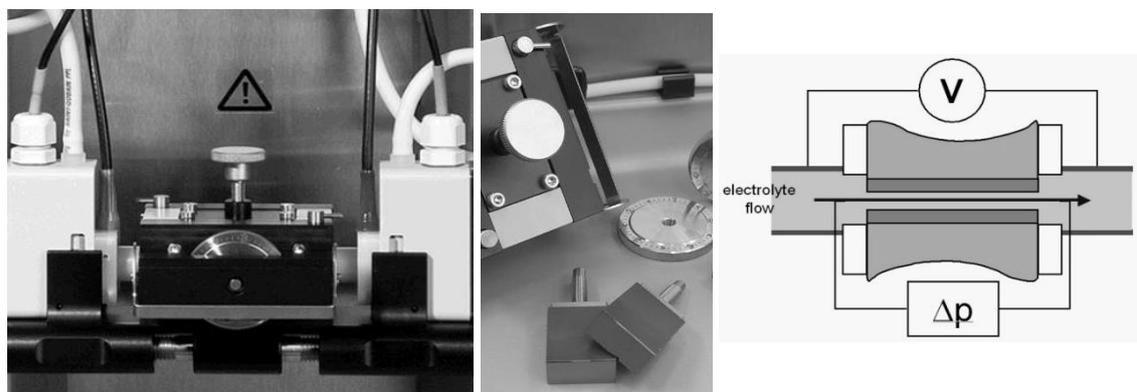
Figure 4.3 - Adjustable Gap Cell mounted between electrodes (left), sample holder with silicon wafer pieces as a representative sample (20 mm x 10 mm, center), and measuring principle (right).

Overall, almost no difference have been found between the active layer and the support layer for the three membranes. As observed on Figure 4.4, the isoelectric point of the membranes is respectively 4.5, 4.2, and 3.7, for HTI, Porifera, and Aquaporin membranes. The Aquaporin membrane is more fragile and couldn't be analysed at pH above 7. At pH around 7, all membranes shows a zeta potential around -35 mV, which proves the electronegativity of the membranes under the pH conditions used during the dewatering of microalgae biomass. These results, along with the zeta potential results of the microalgae cells, corroborates the hypothesis of the enhancement of fouling in presence of divalent cations, which are able to bind both with the membrane surface and microalgae cells or extracellular carbohydrates, thus enhancing membrane fouling.
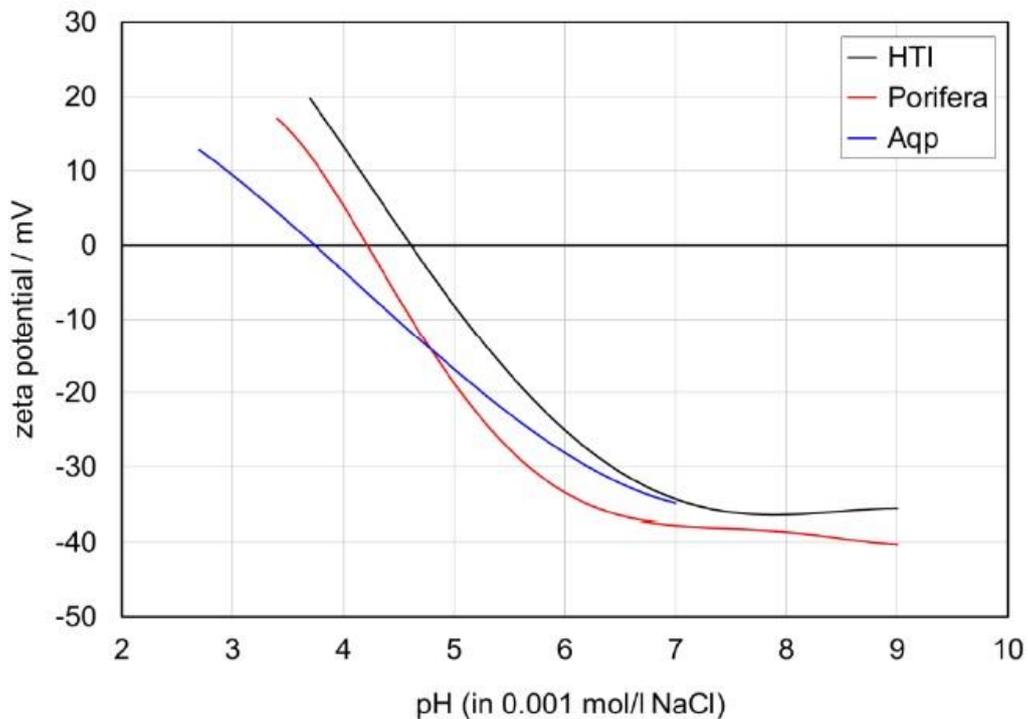
Figure 4.4 - *Average zeta potential vs. pH for active side of membranes HTI, Porifera, and Aquaporin.*

Table 4.3 - *Isoelectric points of active and support sides of membranes HTI CTA-ES, Porifera, and Aquaporin.*

Membrane	HTI CTA-ES		Porifera		Aquaporin	
Side	Active	Support	Active	Support	Active	Support
IEP	4.5	4.5	4.2	4.5	3.7	3.7

4.7. Contact Angle

Contact angle generally measures the hydrophilicity of a surface. In the context of membrane characterisation, is gives an indication of the interactions forces between water and the membrane surface and therefore the ease of the water to permeate through the membrane. The greater the contact angle, the less hydrophilic the membrane surface. Most foulants also exhibits a slight hydrophobicity, therefore hydrophilic membranes are usually preferred. Contact angle measurements were conducted using an optical tensiometer. The membrane sample is placed on a plane support. A small drop of deionized water is deposited onto the membrane surface and a picture is taken. From this picture, the angle between the support and each side of the drop can be measured and an average contact angle value is obtained. Contact angle has been measured for the two novel membranes and compared with the CTA-ES membrane provided by HTI. The results, presented in Table 4.4, shows a higher hydrophilicity of the Porifera membrane on both active and support layer, in comparison with the CTA-ES membrane. The Aquaporin membrane is found more hydrophilic than the two other membranes on both layer, with an active layer absorbing completely the water drop. On the other hand, the CTA-ES membrane exhibits a lower hydrophilicity than the two other membranes on both sides. The hydrophilicity of the Porifera membrane falls in between that of the CTA-ES and the Aquaporin membrane. These results shows that water will permeate more easily through the Aquaporin membrane

Table 4.4 - *Contact angle measurements of both sides of the membranes tested.*

Membrane	Contact angle	
	Active Layer	Support Layer
CTA-ES	65.4 ± 1.6	69.0 ± 2.3
Porifera	56.2 ± 3.7	55.9 ± 2.1
Aquaporin	Absorption	38.8 ± 3.8

4.8. Conclusion

Overall the Porifera membrane surpassed the two other membranes, and seemed then more suitable for replacing the CTA-ES membrane from HTI. Indeed, the membrane provided by Porifera exhibited a much higher pure water permeability than the two other membranes, indicating good performances in terms of permeating water flux. The Porifera membrane was also found efficient for retaining the salt from permeating through the membrane, as the diffusion of salt into the feed solution might impact the performances of the process through an enhancement of fouling on the feed side. In addition, the Aquaporin membrane was revealed more fragile than the other membranes and tearing appeared during few FO tests. Therefore, the membrane provided by Porifera Nano has been chosen for microalgae biomass dewatering experiments conducted with the integration of wastewater treatment within a photobioreactor.

5. Integration of Forward Osmosis in the Treatment of Sewage by *Chlorella vulgaris*: Comparison between External and Immersed Systems

5.1. Introduction

C. vulgaris has been highlighted for its potential in wastewater treatment and biofuel production [138, 474]. In an attempt to reduce the biomass dewatering costs, we previously investigated the utilization of FO for pre-concentration of microalgal biomass, and highlighted the low fouling propensity with *C. vulgaris* in comparison with two other species [503]. After the selection of *C. vulgaris*, the integration of FO dewatering process in a continuous microalgal wastewater treatment system needs to be studied in order to determine an appropriate system design and suitable operating parameters. Praveen and Loh (2016) investigated the integration of an immersed FO module within a photobioreactor (PBR) treating artificial tertiary wastewater with *C. vulgaris* [504]. The authors reported a removal of over 90% of ammonium, 50% of nitrates, and 85% of phosphates through microalgal assimilation and membrane rejection. However, despite the promising results, the very low water flux, the increase of salinity due to the reverse salt diffusion, and the relatively high EPS fouling (mostly polysaccharides), were highlighted as potential issues for the long term operation of the whole system. In an attempt to further develop the integration of FO dewatering with wastewater treatment by microalgae, we investigated the treatment of sewage wastewater with *C. vulgaris* comparing an immersed FO dewatering system and an external FO dewatering system. Indeed, the negative effects of the immersion of the FO module can be prevented by externalizing the FO module, as used in our previous investigations for microalgae biomass dewatering [464, 503]. The purpose of this study is to compare these two approaches by (1) evaluating the treatment efficiency of an artificial sewage wastewater by analyzing the removal of ammonium, nitrates, nitrites, and phosphates, (2) determining the production of biomass and its sustainability, and (3) assessing the forward osmosis efficiency through water flux and fouling analysis.

5.2. Materials and Methods

5.2.1. Microalgae Strain and Growth Conditions

Pure culture of *C. vulgaris* was obtained from the Culture Collection of Algae and Protozoa (CCAP, UK), and cultivated in modified BG-11 medium, which composition is given in Appendix 1. *C. vulgaris* suspensions were continuously stirred on a plate shaker and kept at room temperature (25 ± 1 °C). Illumination was provided by fluorescent lamps (100 μmol photons/m^2·s). The algae growth was periodically monitored by optical density measurement with a spectrophotometer (Helios Zeta, Thermo Scientific, UK) at 435 nm wavelength [442]. The pH was maintained at 7±0.5 for the optimum algae growth. These stock suspensions were further used as inoculum for experiments conducted in the FO-PBR

5.2.2. FO Membrane and Cells

A thin-film composite (TFC) FO membrane was provided by Porifera, Inc. (Hayward, CA, USA). The membrane is composed of a polyamide active layer, coated on top of a polysulfone support layer with an embedded woven mesh. The active layer of the membrane exhibits a negative surface charge due to the carboxyl groups of the polyamide [505]. Further membrane properties and morphological characteristics have been described in a previous study [506]. The membrane coupons were housed within two different membrane cells, depending on the microalgae dewatering method investigated. In the external FO cell, a 200 cm^2 membrane was separating the feed and the draw solution, flowing on each side in counter current mode, the active layer facing the feed solution. Mesh spacers were placed on both side of the membrane to increase turbulences and enhance the mass transfer. In the immersed FO cell, two 100 cm^2 membranes were placed in order to separate the draw solution flowing inside the cell. The active layer of both membrane was facing the outside of the cell, directly in contact with the microalgal biomass in which the cell was immersed. In this case, mesh spacer were only placed on the support layer in contact with the draw solution. Mesh spacers were not placed on the active layer in order to avoid the attachment of microalgae on the active layer

5.2.3. Artificial Wastewater and Draw Solution Chemistry

ACS reagent grade sea salts (Sigma-Aldrich, UK) was used as draw solution. The sea salts concentration was 70 g/L to mimic the salinity of desalination brine [444], and its composition has been reported in our previous study [464]. The removal of nitrogen and phosphorus sources by *Chlorella vulgaris* was investigated using SYNTHES artificial sewage wastewater [507]. The composition of the SYNTHES is detailed in Table 5.1. The SYNTHES was prepared from ACS reagent grade chemicals dissolved in tap water and sterilized by autoclaving prior to each experiment in order to avoid the contamination of the culture by other microorganisms.

Table 5.1 - *Composition of artificial wastewater (SYNTHES) [507].*

Component	Concentration (mg/L)
K2HPO4.3H2O	30
CaCl2.2H2O	7.5
$Cr(NO_3)_3.9H_2O$	1.125
$CuCl_2.2H_2O$	0.75
$MnSO_4.H_2O$	0.15
$NiSO_4.6H_2O$	0.375
$PbCl_2$	0.15
$ZnCl_2$	0.375
Urea	120
NH_4Cl	15
Na.acetate.$3H_2O$	168.75
Peptone	22.5
$MgHPO_4.3H_2O$	37.5
$FeSO_4.3H_2O$	7.5
Starch	157.5
Milk Powder	150
Dried Yeast	67.5
Soy oil	37.5

5.2.4. Experimental Setup

A flat panel photobioreactor was specially design for the continuous growth of microalgae under controlled environment (Figure 5.1). The PBR is made of transparent polymethyl methacrylate (PMMA). The dimensions of PBR are: 200 x 120 x 300 mm (length x width x height), for a total volume of 7.2 L. It comprises an inlet injection hole on one side,

an outlet hole on the opposite side, and a drain on the bottom. The bottom of the reactor also comprises 14 pin holes designed for the injection and bubbling of gas for both carbon dioxide supply and to optimize the mixing of the culture. A specially designed lid was placed on top on the reactor to ensure the sterility. Prior to the conduction of each experiment, the PBR was sterilized by filling it with peroxyacetic acid (1%) and rinsed 3 times with DI water filtered through 0.2 μm filters in order to avoid contamination by other microorganisms.
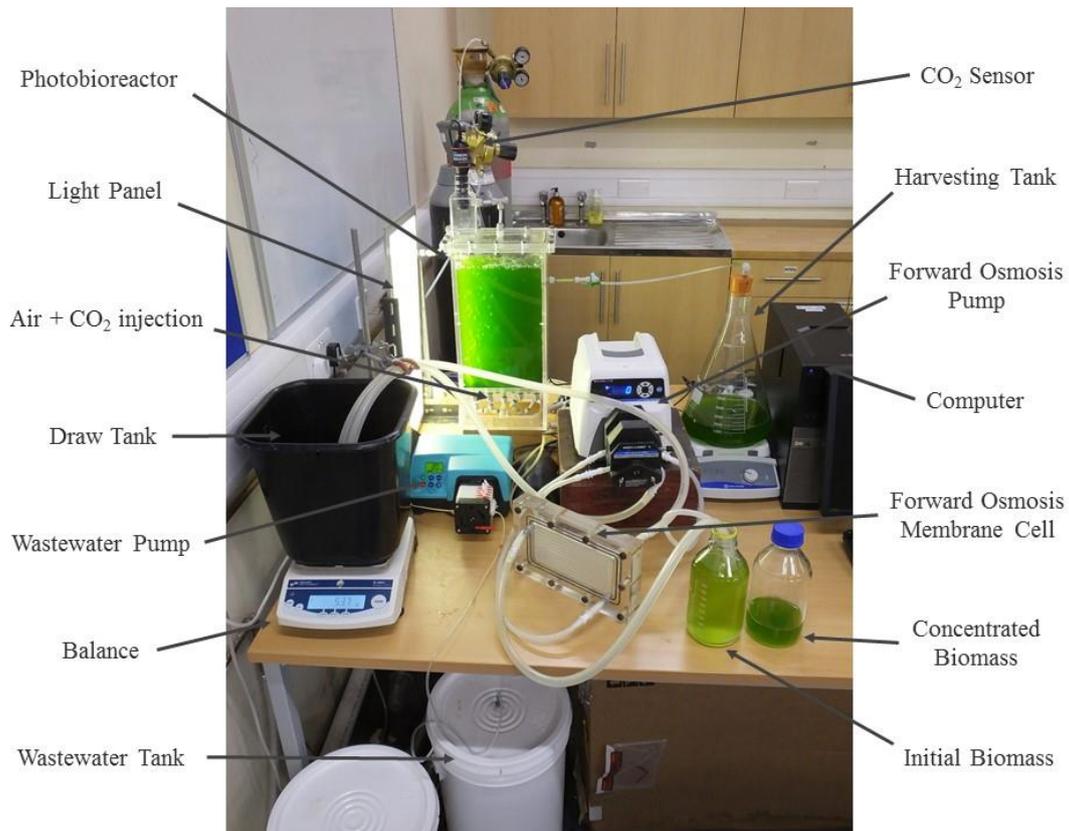
Figure 5.1 - *Design of the lab-scale experiment of the photobioreactor used for the growth of C. vulgaris in artificial wastewater.*

5.2.5. Experimental Procedure and Analytical Method

The experimental procedure aimed to compare the operation of the osmotic PBR with an external FO module and with an immersed FO module. As the two systems investigated cannot be operated identically, few operating parameters were selected as constant in both cases. Therefore, the effective FO membrane area of both module (200 cm^2), the working volume of the PBR (5 L), and the wastewater flow rate in continuous mode (1.1 L/day) were identical in

both cases. In addition, 750 ml of water was withdrawn by FO every day in both experiment. During each experiment conducted, *Chlorella vulgaris* was first grown in 5 L of artificial wastewater for 8 days in batch mode in order to reach a biomass concentration around 0.6 g/L. At the 8th day, the feed pump introducing artificial wastewater in the PBR was started. Considering the wastewater flow rate of 1.1 L/day, after 24 hours of continuous wastewater supply the volume of biomass in the PBR was 6.1 L. Before each FO concentration experiment, 100 ml of biomass was withdrawn from the reactor and samples were taken for further analysis. Finally, the conductivity within the reactor was measured with a conductivity meter (Ultrameter II, Myron L Company, Carlsbad, CA), and the corresponding salt concentration was calculated using a calibration curve realized beforehand. The following steps of the experiments for both systems are explained thereafter and detailed on Figure 2.
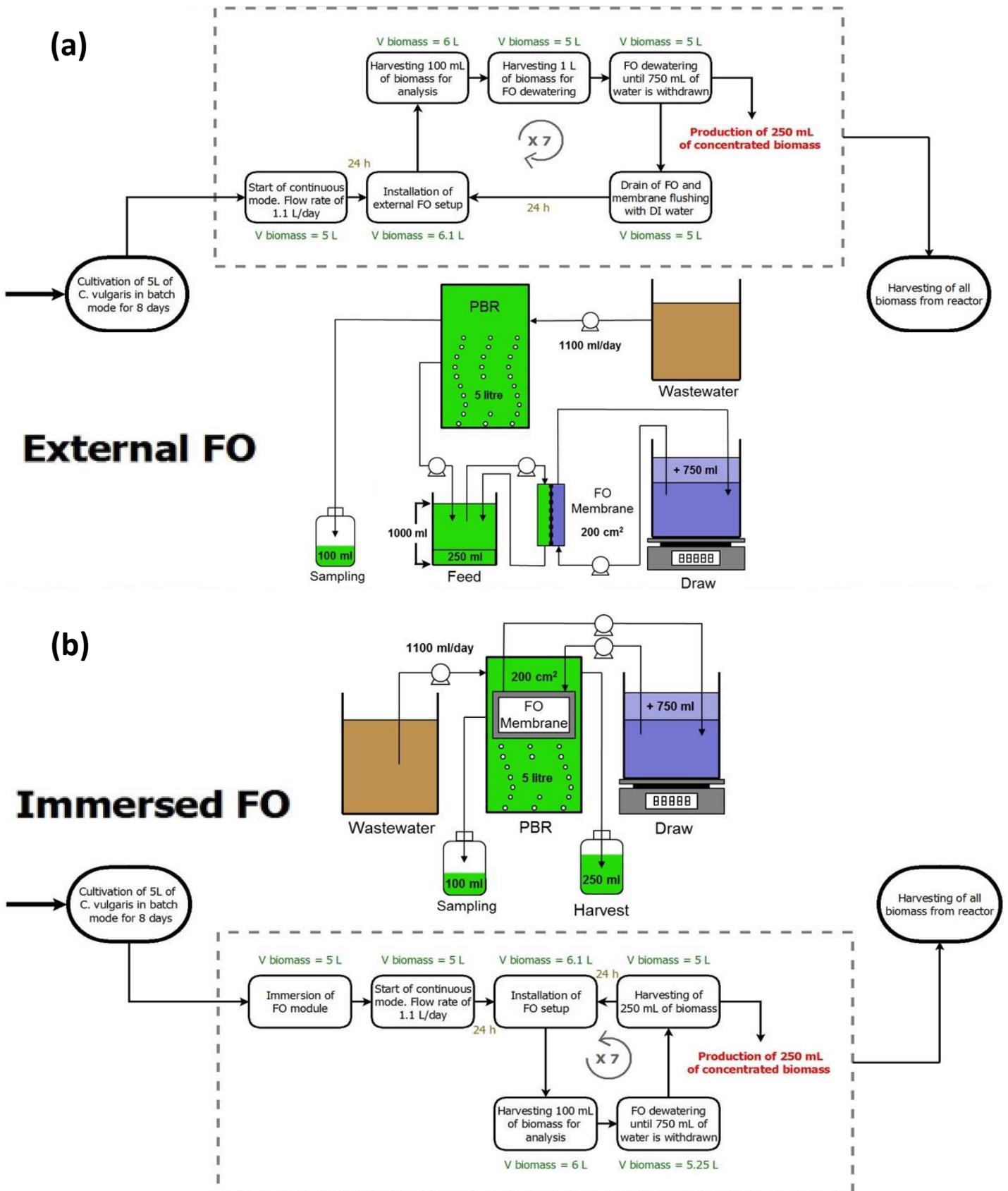
Figure 5.2 - *Details of the experimental protocol and lab-scale set-up used for the comparison of (a) External FO and (b) Immersed FO systems. Vbiomass represents the volume of biomass inside the reactor.*

5.2.5.1.   External FO System

In case of external FO concentration, 1000 ml of biomass was withdrawn from the reactor and concentrated by a factor of 4 (permeate volume of 750 ml) using sea salts as draw solution. The weight of the draw solution was monitored in order to measure the evolution of the permeate water flux. When the permeate volume reached 750 ml, the experiment was stopped and samples were taken from the concentrated biomass for further analysis. Then, both feed and draw sides were emptied and replaced with DI water, and the membrane was flushed at a velocity double than that used during the experiment for 30 min. Samples were taken from the flushing solution for further analysis. Then, the membrane cell was filled with DI water and left until the next day experiment. On the next day, the membrane cell was emptied, and the feed tank was filled with 1000 ml of microalgae biomass freshly harvested for FO dewatering. This procedure was repeated for 7 day at which point the PBR was emptied and washed. The biomass harvested at this step was stored for analysis.

5.2.5.2.   Immersed FO System

In case of immersed FO concentration, the FO module was introduced inside the reactor prior to the first dewatering experiment. After sampling of 100 ml, the volume of biomass in the reactor was 6 L. The draw pump was then operated until 750 ml of water had permeated through the membrane (concentration factor of 1.14), leaving 5.25 L of biomass inside the reactor. 250 ml of concentrated biomass was then withdrawn from the reactor in order to match with the volume of biomass harvested during the external FO concentration experiment. Samples were taken from these 250 ml for further analysis. DI water was then flushed inside the immersed cell in order to prevent further diffusion of salt inside the reactor and further dewatering of biomass. The membrane module was then left emptied inside the reactor until the next day experiment.

5.2.6. Samples Analysis

All samples were placed in a 2 ml tube centrifuged at 6 x g for 20 min. The supernatant was collected from the tube and replaced by DI water. This procedure was repeated a second time before the supernatant was collected and stored in a fridge for further analysis. Each

sample was then filtered and analyzed by ion chromatography (Metrohm AG, Ionenstrasse, Switzerland) in order to determine the concentrations of ammonium, nitrites, nitrates, and phosphates in the extracellular medium. The concentration of carbohydrates was analyzed using the phenol-sulfuric acid method [450]. Due to the high salinity of the draw solution samples, the ammonia, phosphate, nitrate, and nitrite content in the draw solution was measured using AQUAfast™ colorimeter AQ3700 (Thermo Fisher Scientific, Inchinnan, UK) and the corresponding nutrients test kits.

5.2.7. Biomass Production

In order to assess and compare the growth of microalgae and the associated biomass production, we calculated the total biomass produced during the whole experiment. This value corresponds to the amount of biomass sampled every day before FO dewatering added to the biomass harvested after FO dewatering, and added to the amount of biomass harvested from the reactor after the last FO dewatering. It can be calculated using Equation 5.1 below:

$$m_{total} = X_{7f} \cdot V_{Reactor} + \sum_{1}^{7} \left(X_f \cdot V_{Harvest} + X_i \cdot V_{Sample} \right) \qquad 5.1$$

were, m_{total} designates the total mass of biomass produced throughout the experiment (g), X_{1-7f} is the biomass concentration harvested after FO dewatering each day (g), $V_{Reactor}$ is the volume of biomass left in the reactor after the last FO dewatering experiment (L), $V_{Harvest}$ is the volume of biomass harvested every day (L), X_{1-7f} is the biomass concentration inside the reactor before each experiment, and V_{Sample} is the volume of sample taken from the PBR every day before each experiment (L).

5.3. Results and Discussion

5.3.1. FO Dewatering Efficiency

5.3.1.3. Water Flux Decline

The efficiency of the forward osmosis dewatering is assessed in order to determine and compare the sustainability of both FO systems investigated. Indeed, considering the high cost of FO membranes, the dewatering efficiency is of great importance to insure the membrane area is used during a long period of time and at its highest potential. Figure 6 presents a

comparison of the water flux decline during the dewatering of *C. vulgaris* biomass. The initial water flux (Jw) during the baseline experiments is much lower with the immersed system, despite the identical membrane area in both cases. Indeed, the initial baseline Jw with the external FO process is observed around 17.5 LMH, whereas it is around 12 LMH with the immersed system. This difference is due to (1) the enhancement of the mass transfer on the feed side of the membrane in the case of external FO dewatering, provided by the mesh space, and (2) the reduction of available membrane surface in case of immersed system, due the air scouring under the membrane cell and the passage or air bubbles on the membrane surface.
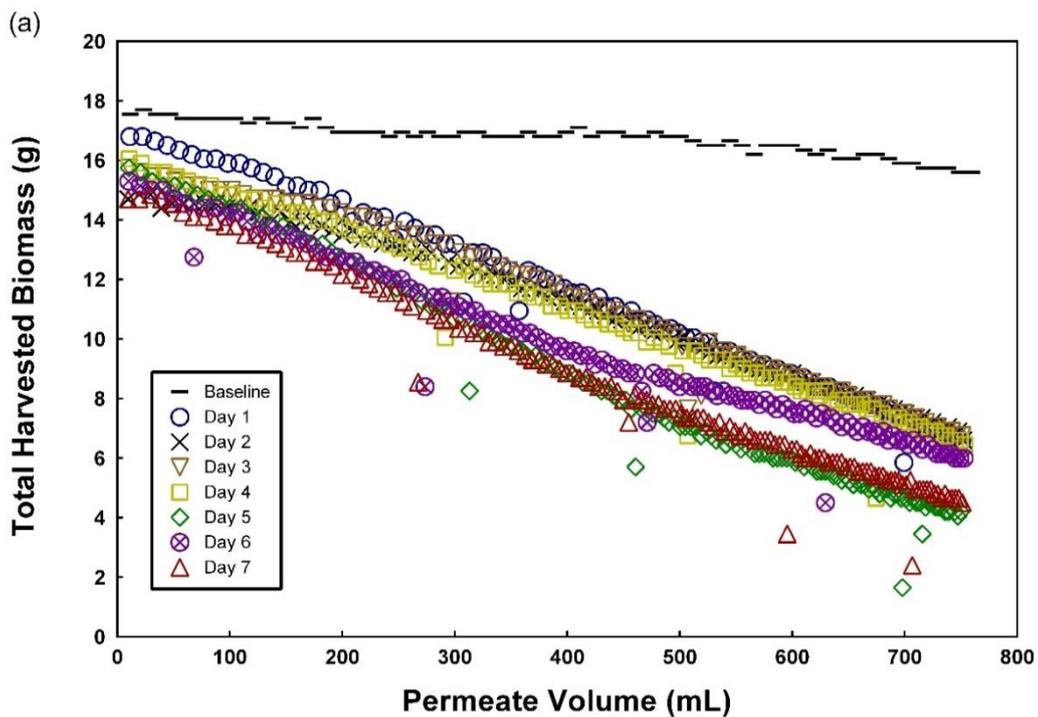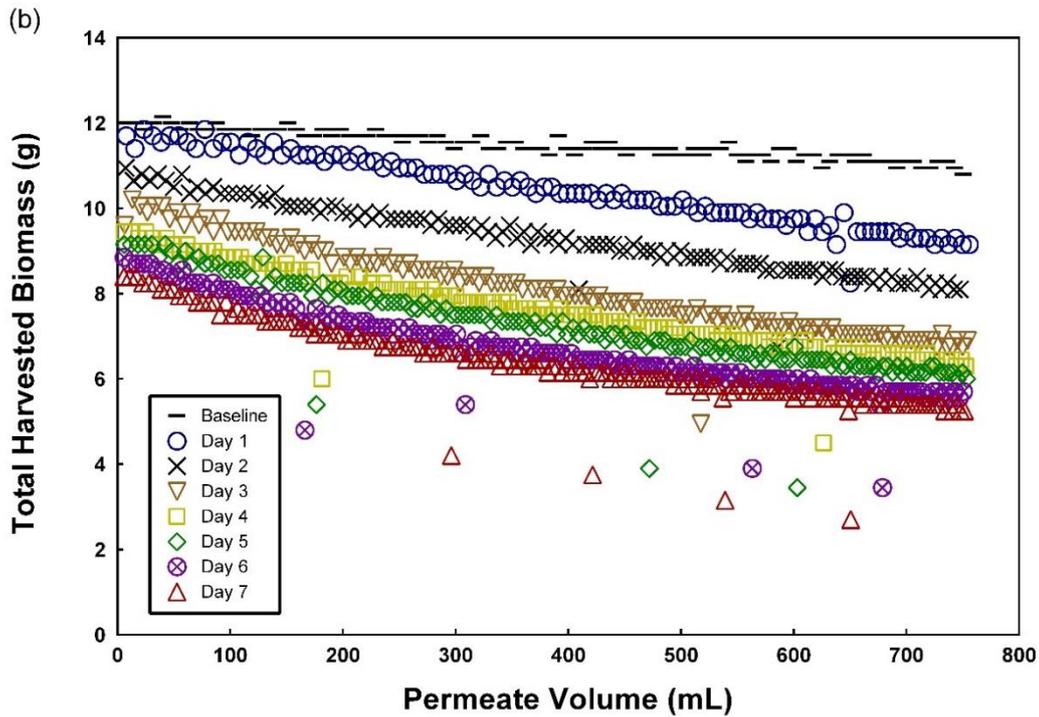
Figure 5.3 *- Water flux (LMH) decline during the dewatering of C. vulgaris biomass for 7 consecutive days with (a) External FO system, and (b) Immersed FO system.*

5.3.1.4. Water Flux Loss

The raw water flux gives insights about the dewatering performances, however it does not efficiently highlights membrane fouling, which reduces the water flux permeating through the membrane and may eventually jeopardize the whole filtration process has to be analyzed. Figure 4 presents the loss of water flux during the dewatering of microalgae biomass with both external and immersed FO systems. A very high loss of Jw was observed for each experiment conducted. In case of external system, the trend shows a relatively constant increase of water flux loss, indicating a constant fouling onto the membrane surface throughout the experiments. The final loss reaches around 60% during the first 5 days, but increases over 70% during the last 2 days. This high fouling is related to both the composition of the biomass, containing carbohydrates but also other fouling compounds found in the wastewater, and their increase of concentration throughout the experiment. Indeed, a highly concentrated biomass will have a higher fouling propensity than a low concentrated biomass. Despite the high fouling propensity and loss of water flux, the initial Jw loss was found relatively low (under 17%) for all dewatering experiments with this configuration. The flushing of the membrane after dewatering is proven to remove most of the cake layer fouling the membrane, which could be suitable for a long term usage. Concerning the immersed FO system, the increase of Jw loss is

moderated due to the lower permeate drag force and the lower increase of biomass concentration inside the reactor. Indeed, the final Jw loss reaches under 17% on the 1st day and less than 30% on the 2nd day of experiment. However, the final Jw loss keeps increasing, reaching over 50% during the last day of experiment, which follows a trend similar to the increase of initial Jw loss, reaching over 30% for the last day of experiment. No specific cleaning being conducted, the biomass remains onto the membrane surface and reduces its dewatering efficiency. This decrease of performances could be reduced by a physical cleaning of the membrane, however it would involve the removal of the membrane cell from the reactor after each experiment, which would eventually lead to the contamination of the microalgae culture.
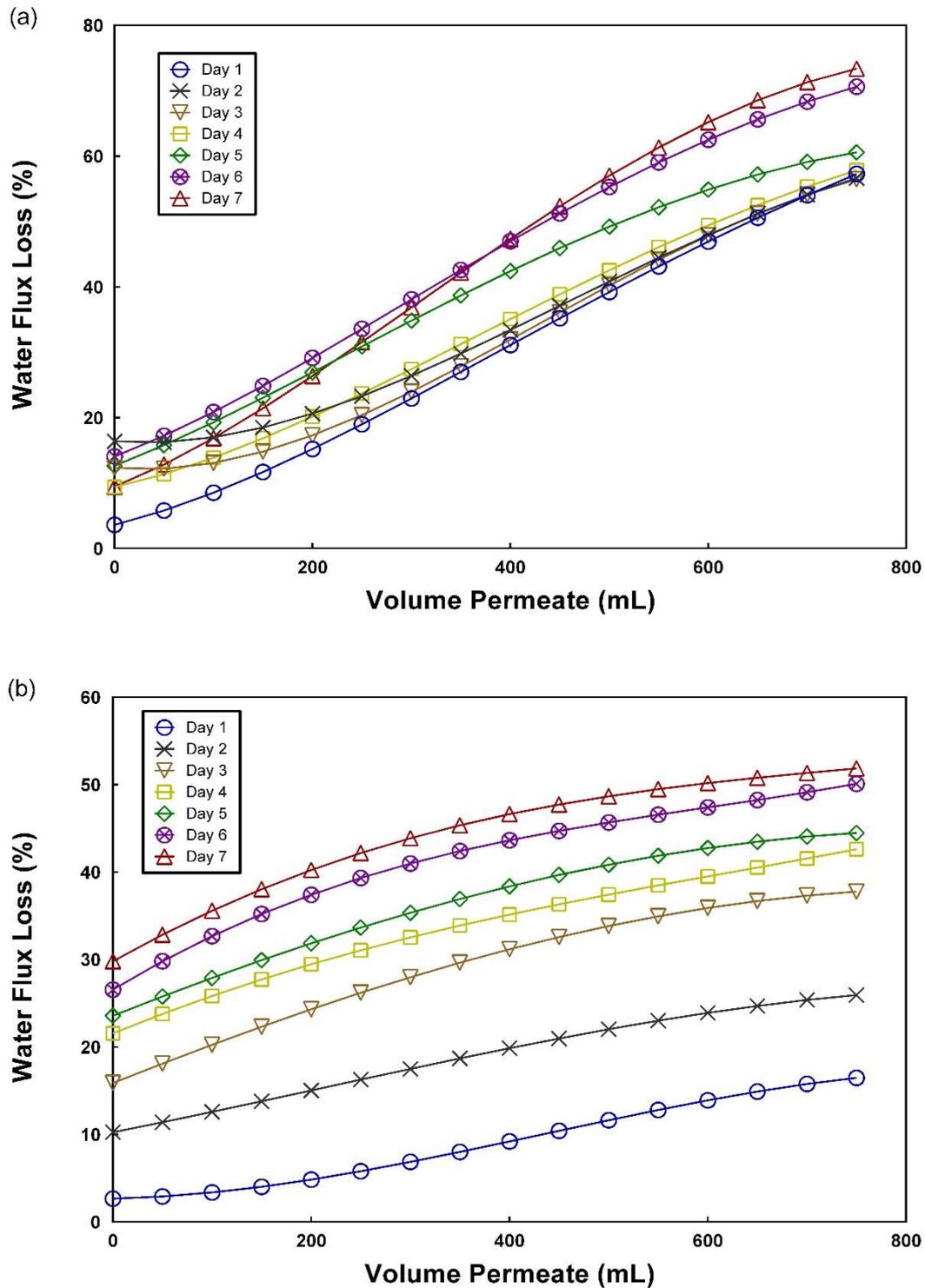
Figure 5.4 – Loss of water flux (LMH) during the dewatering of C. vulgaris biomass for 7 consecutive days with (a) External FO system, and (b) Immersed FO system.

5.3.2. Salinity Build-up

One of the concerns raised by the authors of the first study investigating the integration of FO with wastewater treatment by microalgae is the increase of salt concentration inside the photobioreactor [504]. Indeed, a high salinity can affect the microalgae growth through osmotic stress, salt stress (ions), and changes of ionic ratios within the cells [1]. Due to the differences between external and immersed FO systems, the salt concentration in the reactor has been measured throughout the whole duration of both experiment conducted. The variation of salt concentration inside the reactor shows an initial increase during the first 3-4 days for both experiments (Figure 5). This increase may be due to the nutrients decomposition by the microalgae cells, releasing ions in the extracellular medium. A slow decrease of salt concentration follows due to the nutrients consumption. On the 8th day, corresponding to the implementation of continuous wastewater supply, the trend differentiates between external and immersed systems. Indeed, with the external FO system, the salt concentration stabilizes below 200 mg/L due to the continuous wastewater supply and the continuous nutrients removal mechanisms which counterbalances each other. However, with the immersed system, the salt concentration regularly increases in the reactor, reaching over 600 mg/L on the last day, due to the reverse salt diffusion from the draw solution. Indeed, the higher permeate flux observed with the external system also leads to a greater solute diffusion through the membrane. Although the salt concentration does not reaches a very high level on the 15th day, the increase of salt concentration inside the PBR will ultimately affect FO performances due to the reduction of osmotic pressure difference across the FO membrane. It will also affect the growth of microalgae and potentially jeopardize the culture. In this regard, an external system seems more appropriate for a continuous and sustainable production of concentrated biomass
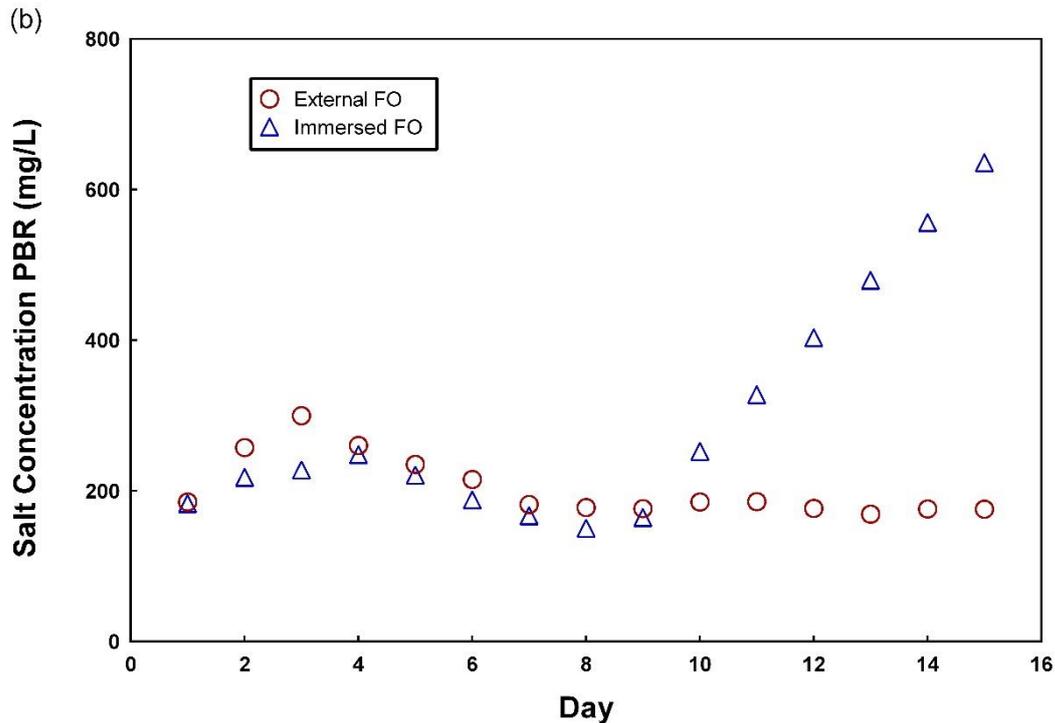
Figure 5.5 - *Evolution of salt concentration (mg/L in the photobioreactor throughout the duration of each experiment. The salt concentration was calculated through the measurement of conductivity and the use of previously made calibration curves (Appendix 7)*

5.3.3. Biomass Production

5.3.3.5. Biomass Production during FO Experiments

In addition to the nutrient removal from artificial sewage wastewater, the FO-PBR systems investigated produces concentrated biomass for potential used in biodiesel production. The evolution of biomass concentration inside the PBR is displayed on Figure 6a. During the experiment conducted with the external FO system, the biomass concentration is maintained stable around 0.6 g/l throughout the 7 days of FO dewatering. Indeed, the continuous supply of wastewater with an adequate flow rate allows the biomass to grow at a similar rate than it is removed every day for further dewatering. On the contrary, the concentration of biomass increases inside the PBR during the experiment with immersed FO system, reaching almost 1 g/L after 7 days of experiment. This increase of concentration is a direct effect of the in situ biomass dewatering, which further increases the concentration when added to the natural growth of microalgae. This constant increase of biomass concentration would further lead to a

drop of growth and a death of microalgae due to the reduction of accessible light. The increase of biomass concentration could be counter balanced by increasing the flow rate of wastewater, however this would lead to a reduction of the hydraulic retention time and therefore a decrease of wastewater treatment efficiency. The aim of this dewatering process being the production of concentrated microalgae biomass, the concentration of the harvested biomass, shown on Figure 6(b), is investigated. Due to the higher concentration factor reached (4 against 1.14), the biomass harvested with the external FO system is more concentrated than the biomass harvested with the immersed system. As mentioned in our previous studies, part of the biomass dewatered by FO is lost due to an entrapment inside the mesh spacer [464, 503]. Although no spacer was placed on the active layer of the membrane in the immersed FO system, biomass can also form a biofilm onto the membrane surface of settle down inside the reactor, therefore leading to a loss of biomass. Figure 6(c) presents a comparison of the total loss of biomass during external and immersed FO dewatering experiments. A high biomass loss (≈ 0.35 g) is observed the first during the first day of dewatering with external FO. However, this loss continuously decrease to reach below 0.2 g at the 7th day. It appears that the biomass easily attach to the clean membrane and entrap into the mesh spacer. However, the rate at which the biomass is being lost may be partially compensated by the rate at which entrapped biomass is being washed away throughout the FO dewatering. Concerning the immersed system, the lower increase of biomass concentration during the experiment, as well as the lower permeate drag force lead to a lower loss of biomass at the first day of experiment (≈ 0.2 g). This loss is stable until the 5th day, at which point it greatly increases, reaching almost 0.4 g after the 7th day. This sudden increase of biomass loss could be due to either a growth of microalgae biofilm onto the membrane, or a sedimentation and settlement of biomass on the bottom of the reactor, due to the increase of salt concentration inside the reactor and/or an effect of the excessive biomass concentration inside the reactor. Considering only the biomass, the external FO system seems to give better results in terms of both concentration of biomass harvested and also in terms of system sustainability.

(a)

(b)
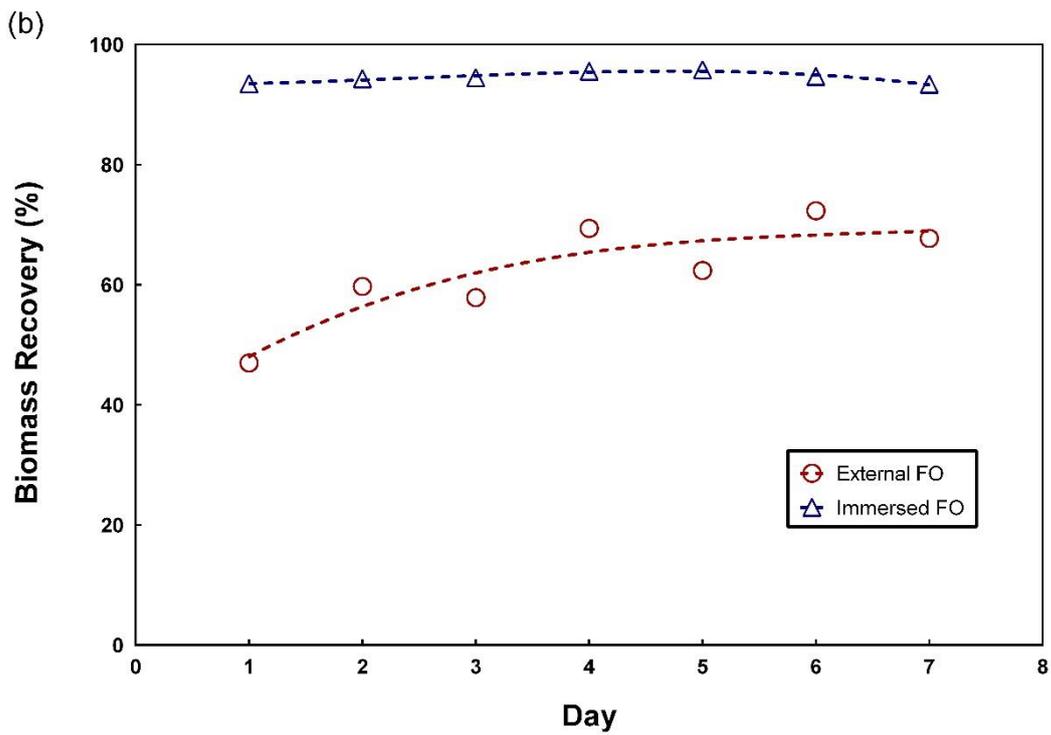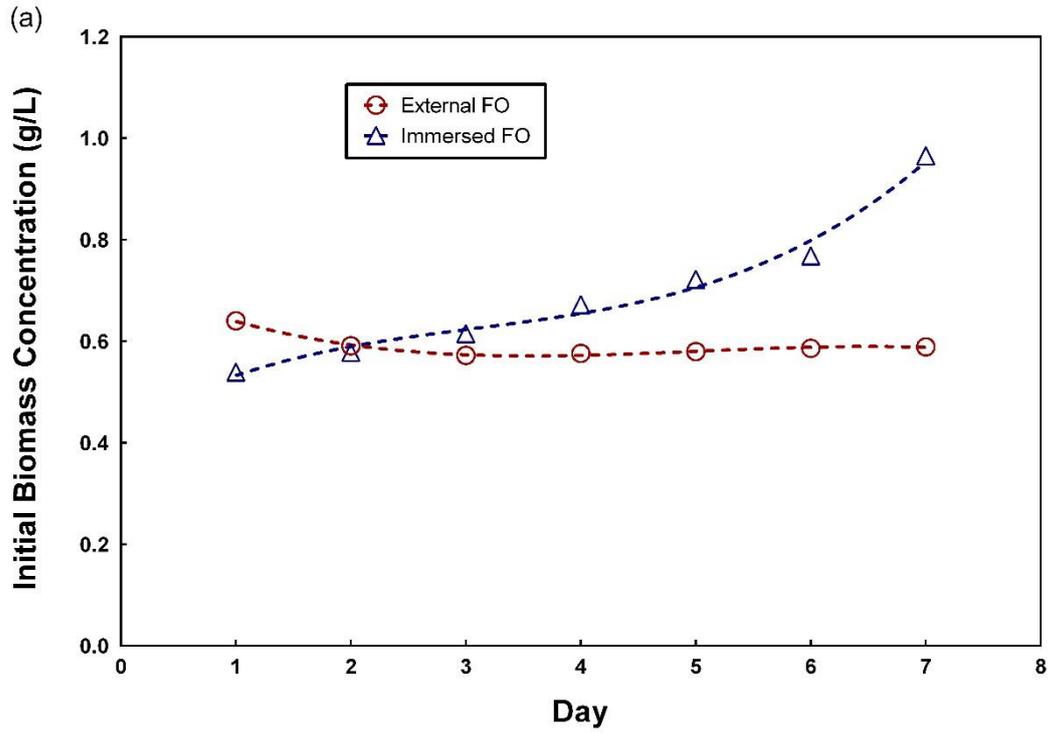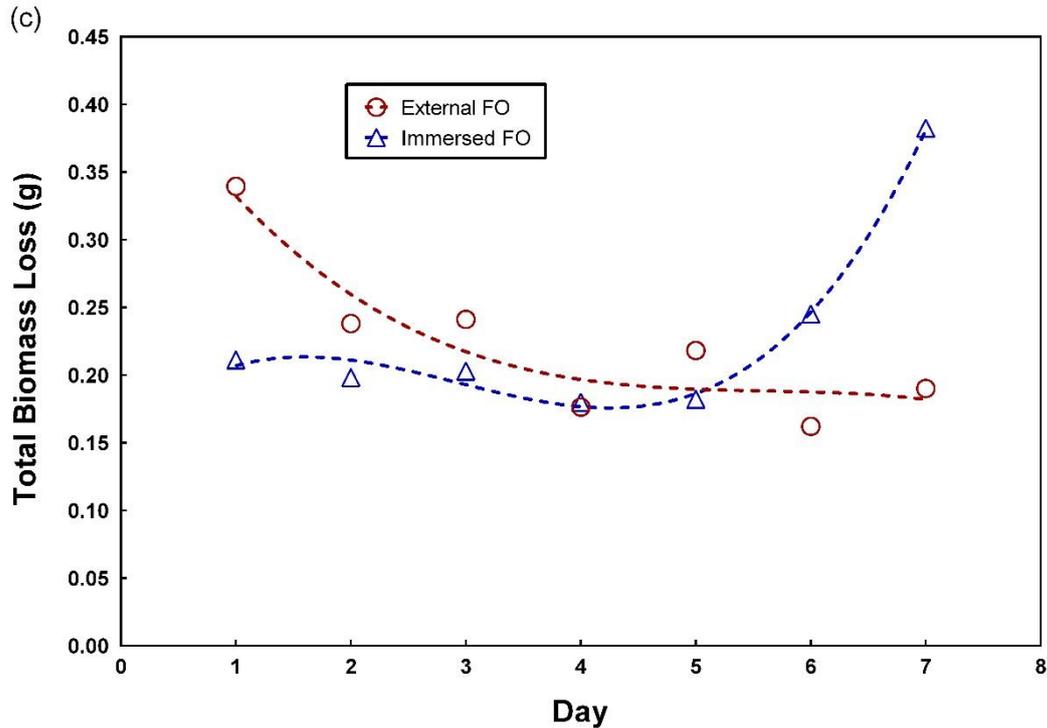
Figure 5.6 *– Evolution of (a) Initial biomass concentration and (b) Biomass recovery (%), and (c) Total loss of biomass (g) during FO concentration, throughout the 7 days of experiment.*

5.3.3.6. Total Biomass Production

The total amount of biomass has been calculated for both experiments conducted. As presented on Figure 7, the amount of biomass produced every day is greater with the external system due to the higher concentration factor reached during the dewatering process (4 against 1.14). Indeed, on the 7th day, over 3 g of biomass have been harvested with the external system, whereas less than 2 g were harvested with the immersed system. However, the final amount of biomass produced is greater with the immersed system due to the higher biomass concentration inside the PBR on the 8th day fof the FO dewatering experiment (6.56 g against 5.99 g). Despite the greater amount of biomass produced with the immersed system, the regular increase of biomass concentration in the reactor observed is not sustainable and will eventually result in a reduction of microalgae growth and a drop of biomass productivity. In case of external dewatering, the biomass concentration inside the PBR is maintained stable, which result in a more sustainable operation of the system.
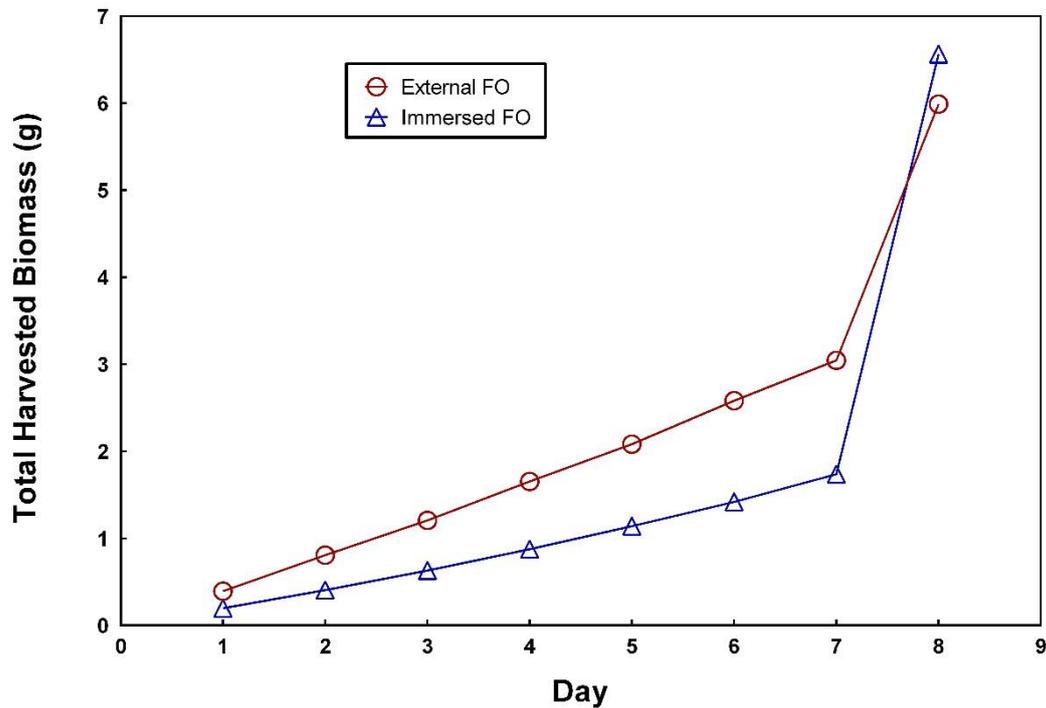
Figure 5.7 *- Evolution of the total amount of biomass produced throughout the experiment.*
The 8th day correspond to the harvest of all the biomass contained inside the reactor.

5.3.4. Carbohydrates Analysis

As investigated in our previous studies [464, 503], carbohydrates are released in the extracellular medium by the microalgae cells under stress conditions. These extracellular carbohydrates (EPS) are highly involved in membrane fouling, through simultaneous binding phenomenon with divalent cations and carboxylic functional groups at the interface of algae cells/EPS. Figure 8 presents the evolution of the carbohydrates content in extracellular medium inside the PBR. However, these data may not reflect the real amount of carbohydrates inside the reactor. Indeed, carbohydrates easily bind with microalgae cells and divalent cations which leads to the creation of flocs. Therefore, the analysis of the extracellular content do not display the carbohydrates that have bind with microalgae cells, or attached to the membrane surface in case of immersed FO system. Figure 8 shows the concentration of extracellular carbohydrates within the PBR for the whole duration of its operation. The values obtained are found quite dispersed for both systems, rendering complicated the identification of any trend. Nevertheless, it seems that the concentration of extracellular carbohydrates increases in both case, with a

greater increase observed with the external system. This observation is explained by the greater salt concentration observed within the PBR in case of immersed dewatering, leading to a greater flocculation and sedimentation of the microalgae, which also binds to the extracellular carbohydrates. These carbohydrates are then removed from the sample during centrifugation, which reduces the quantity of observable carbohydrates.
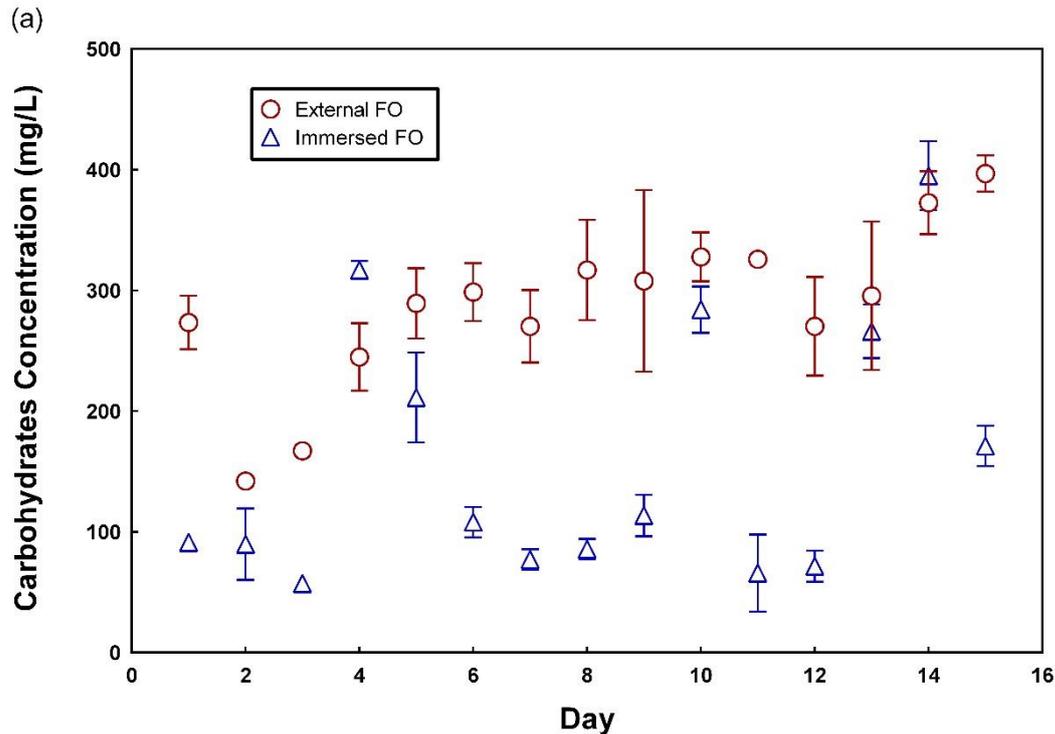
Figure 5.8 - *Evolution of carbohydrates concentration inside the PBR throughout the growth of C. vulgaris during the 8 days of batch growth and the 7 days of continuous growth during both experiment conducted (External FO and Immersed FO).*

5.3.5. Wastewater Treatment Efficiency

The first purpose of the osmotic membrane photobioreactor is the treatment of artificial sewage wastewater. Therefore, the removal of phosphate, ammonium, nitrate and nitrite by the microalgae was first investigated (Figure 9). The concentration of ammonium, nitrites, nitrates, and phosphates have been analyzed in the samples taken in the PBR during the whole duration of the experiment, including batch growth and continuous growth (15 days). The removal of nutrients was found relatively similar for both systems investigated. Concerning the phosphates, although the concentration increased during the first days with the external system,

the concentration rapidly drop for both systems to reach around 50 μM with the external FO system and 20 μM in case of immersed FO system. These values correspond to a removal of respectively 82 % and 93 %. Concerning the ammonium, the concentration dropped from the first day of growth in both cases, due to nitrification mechanisms induced by the microalgae. Furthermore, the concentration of ammonium stabilizes around 20 μM in both cases, corresponding to a removal of over 95 % of the initial ammonium. Ammonium is rapidly reduced into nitrites which are furthermore reduced into nitrates to be assimilated by the microalgae cells. Indeed, a sharp increase of nitrates is observed after the first day of experiment with the external system, dropping under 50 μM the next day. This sharp decline also correspond to an increase of nitrates concentration in the reactor. Although no pic of nitrites concentration is detected during the growth with the immersed system, it is likely that the reaction happened in between two samplings. The subsequent increase of nitrates is detected from the second day of growth in this case. Overall, the microalgae shows a great ability for treatment of phosphate and ammonium from sewage wastewater. Concerning the comparison between both external and immersed FO dewatering systems, nutrients are better removed with the immersed system due to the higher biomass concentration inside the reactor. However, this removal might not be sustainable due to the continuous increase of biomass concentration inside the reactor that will lead to a decline in growth due to light shortage.
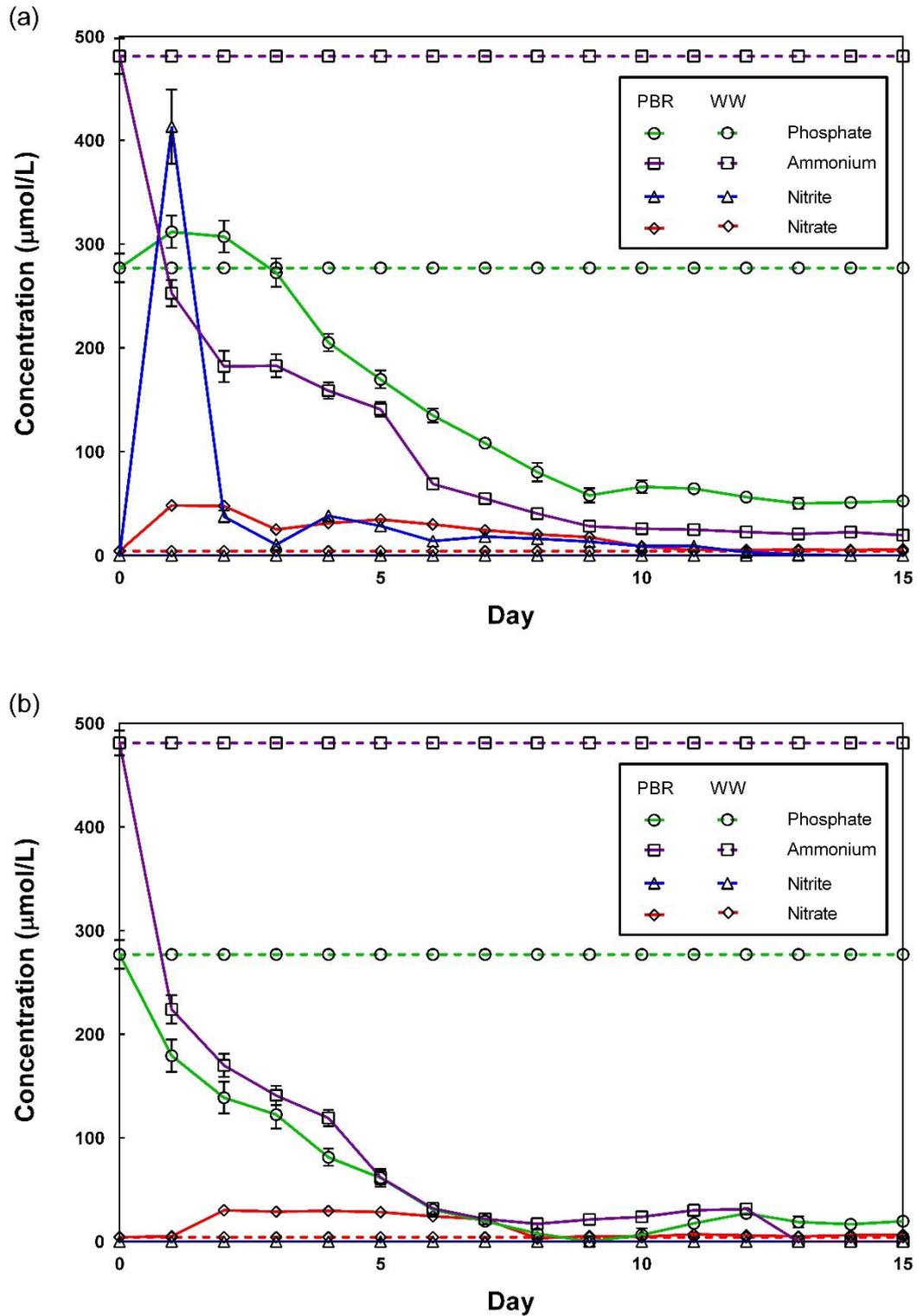
Figure 5.9 - *Concentration of ammonium, nitrites, nitrates, and phosphates in the samples
taken from the PBR, during the growth of C. vulgaris prior and during (a) External FO
dewatering, and (b) Immersed FO dewatering. For a comparison purpose, the concentration
of ammonium, nitrates, nitrites and phosphates in the artificial wastewater used is also
displayed (dash lines).*

5.3.6. Draw Solution Analysis

One of the main objective of the system studied is the possibility to produce drinkable water. The recovery of the draw solution was not studied in this work, however various recovery methods exists to re-concentrate (i.e. recycle) the draw solution and produce purified water [508]. Therefore, the quality of the diluted draw solution directly impacts the quality of the water produced. To assess the quality of the diluted draw solutions, we measured the concentration of the nutrients investigated during the wastewater treatment efficiency: phosphates; ammonia; nitrates; nitrites. Indeed, these compounds, possibly present in the feed solution during FO process, may permeate through the membrane and contaminate the draw solution.

First, no nitrites were found during the analysis of the draw solution samples. Therefore, nitrite concentrations do not appear in Table 5.2 below. Phosphates have been found in the draw solution at very low concentrations and only at the early stage of the experiment. This reveals a good rejection of phosphates, ammonium, and nitrates by the FO membrane. Concerning ammonium and nitrates, these were found in slightly higher concentration in the draw solution, possibly due to a slightly higher permeability of the FO membrane for these ions. Comparing the external system with the immersed system reveals a lower concentration of ammonium and nitrates in the draw solution with the immersed system. This may be due to the thicker biofilm present onto the membrane surface with the immersed system, which further contributes to the removal of these nutrients as they permeate through. Overall, the nutrients content in the draw solution falls well below the limits considered for drinking water, which provides evidence of the good water quality with this process for both configurations.

Table 5.2 - *Concentrations of phosphates, ammonium, and nitrates in the draw solution after FO filtration and comparison with drinking water limits from regulators.*

Compound	Day	Concentration (µg/l)		Limits for drinking water (µg/l)
		External	Immersed	
Phosphates	1	0.27	0	None
	2	0.12	0.09	
	3	0	0.33	
	4	0	0	
	5	0	0	
	6	0	0	
	7	0	0	
Ammonium	1	5.48	4.16	500 [509]
	2	21.52	2.14	
	3	13.95	2.40	
	4	33.67	4.38	
	5	18.81	0	
	6	7.57	0	
	7	5.73	0	
Nitrates	1	5.67	2.05	50 000 [509]
	2	4.05	2.39	
	3	3.57	1.67	
	4	3.00	2.45	
	5	2.24	2.23	
	6	2.57	2.28	
	7	2.62	2.14	

5.4. Conclusions

Two different methods of FO integration with sewage wastewater treatment have been investigated in this study. The removal of nutrients, as well as the total production of biomass have been found greater with the immersed system due to the higher growth of microalgae, therefore reaching a higher concentration inside the reactor. However, this regular increase of concentration will eventually lead to a decline of both factors when the biomass concentration will be too high for the light to penetrate the medium and efficiently supply energy to the culture. This issue can be solved by increasing the wastewater flow rate, and therefore decreasing the hydraulic retention time in the reactor. However, by doing so, the efficiency of nutrient removal will ultimately be reduced, as well as the amount of biomass harvested. Concerning the performances of the FO filtration, the external system is demonstrated to be more efficient due to both the higher permeate water flux, and the easier cleaning of the membrane by simple flushing. Overall, we recommend the use of an external FO dewatering system, which allows a greater flexibility and a more sustainable operation.

General Conclusion

This study revealed key parameters related to fouling during the dewatering of microalgal biomass by forward osmosis, and gave a better understanding of the mechanisms involved. The impact of the draw solution has been shown and divalent cation-free solution have to be preferred for the reduction of fouling. Moreover, calcium-containing draw solutions have to be prohibited, as they drastically increases membrane fouling. This implied that seawater or brine may not be the best choice of draw solutions for the dewatering of microalgae biomass. Also, the choice of microalgae specie is also crucial in order to reduces fouling issues. Indeed, microalgae with a cell wall carbohydrate composition close to *Chlorella vulgaris*, without fructose and low amount of glucose, mannose and galactose have to be preferred.

This study also gave insights for the integration of forward osmosis within the continuous treatment of wastewater by microalgae. Indeed, many parameters can affect the performances of both the filtration and water treatment performances. The main finding was that an external integration of forward osmosis is demonstrated to be more efficient due to both the higher permeate water flux, and the easier cleaning of the membrane by simple flushing. Overall, we recommend the use of an external FO dewatering system, which allows a greater flexibility and a more sustainable operation.

In conclusion, forward osmosis can be successfully used for the pre-concentration of microalgal biomass. However, the choice of draw solution and microalgae specie is critical for the sustainability of the process. The performances and durability can be further improved through the improvement of forward osmosis membranes characteristics. Indeed, the concentration polarization phenomenon, as well as fouling, still holds the filtration performances back. These issues can be solved through further research on membrane fabrication/modification. Also, recent techniques, such as microfluidics, used for the separation of microalgae from their cultivation medium might compete with, if not outperform, forward osmosis. The future of forward osmosis for microalgae dewatering, but also for other applications, will mostly depend on the improvement of membranes performances.

References

1. Mata, T.M., A.A. Martins, and N.S. Caetano, *Microalgae for biodiesel production and other applications: A review.* Renewable and Sustainable Energy Reviews, 2010. **14**(1): p. 217-232.

2. Kirrolia, A., N.R. Bishnoi, and R. Singh, *Microalgae as a boon for sustainable energy production and its future research & development aspects.* Renewable and Sustainable Energy Reviews, 2013. **20**(0): p. 642-656.

3. Abdel-Raouf, N., A.A. Al-Homaidan, and I.B.M. Ibraheem, *Microalgae and wastewater treatment.* Saudi Journal of Biological Sciences, 2012. **19**(3): p. 257-275.

4. Cai, T., S.Y. Park, and Y. Li, *Nutrient recovery from wastewater streams by microalgae: Status and prospects.* Renewable and Sustainable Energy Reviews, 2013. **19**: p. 360-369.

5. Lesmana, S.O., et al., *Studies on potential applications of biomass for the separation of heavy metals from water and wastewater.* Biochemical Engineering Journal, 2009. **44**(1): p. 19-41.

6. Clarens, A.F., et al., *Environmental Life Cycle Comparison of Algae to Other Bioenergy Feedstocks.* Environmental Science & Technology, 2010. **44**(5): p. 1813-1819.

7. Pires, J.C.M., et al., *Carbon dioxide capture from flue gases using microalgae: Engineering aspects and biorefinery concept.* Renewable and Sustainable Energy Reviews, 2012. **16**(5): p. 3043-3053.

8. Lam, M.K., K.T. Lee, and A.R. Mohamed, *Current status and challenges on microalgae-based carbon capture.* International Journal of Greenhouse Gas Control, 2012. **10**: p. 456-469.

9. Greenwell, H.C., et al., *Placing microalgae on the biofuels priority list: a review of the technological challenges.* Journal of the Royal Society Interface, 2010. **7**(46): p. 703-726.

10. Amer, L., B. Adhikari, and J. Pellegrino, *Technoeconomic analysis of five microalgae-to-biofuels processes of varying complexity.* Bioresource Technology, 2011. **102**(20): p. 9350-9359.

11. Molina Grima, E., et al., *Recovery of microalgal biomass and metabolites: process options and economics.* Biotechnology Advances, 2003. **20**(7–8): p. 491-515.

12. Rawat, I., et al., *Dual role of microalgae: Phycoremediation of domestic wastewater and biomass production for sustainable biofuels production.* Applied Energy, 2011. **88**(10): p. 3411-3424.

13. Kim, J., et al., *Methods of downstream processing for the production of biodiesel from microalgae.* Biotechnology Advances, 2013. **31**(6): p. 862-876.

14. Brennan, L. and P. Owende, *Biofuels from microalgae—A review of technologies for production, processing, and extractions of biofuels and co-products.* Renewable and Sustainable Energy Reviews, 2010. **14**(2): p. 557-577.

15. Cath, T.Y., A.E. Childress, and M. Elimelech, *Forward osmosis: Principles, applications, and recent developments.* Journal of Membrane Science, 2006. **281**(1–2): p. 70-87.

16. Achilli, A., T.Y. Cath, and A.E. Childress, *Power generation with pressure retarded osmosis: An experimental and theoretical investigation.* Journal of Membrane Science, 2009. **343**(1–2): p. 42-52.

17. Ge, Q., M. Ling, and T.-S. Chung, *Draw solutions for forward osmosis processes: Developments, challenges, and prospects for the future.* Journal of Membrane Science, 2013. **442**: p. 225-237.

18. Achilli, A., et al., *The forward osmosis membrane bioreactor: A low fouling alternative to MBR processes.* Desalination, 2009. **239**(1): p. 10-21.

19. Cath, T.Y., et al., *A multi-barrier osmotic dilution process for simultaneous desalination and purification of impaired water.* Journal of Membrane Science, 2010. **362**(1-2): p. 417-426.

20. Valladares Linares, R., et al., *Rejection of micropollutants by clean and fouled forward osmosis membrane.* Water Research, 2011. **45**(20): p. 6737-6744.

21. Jin, X., et al., *Removal of boron and arsenic by forward osmosis membrane: Influence of membrane orientation and organic fouling.* Journal of Membrane Science, 2012. **389**: p. 182-187.

22. Parida, V. and H.Y. Ng, *Forward osmosis organic fouling: Effects of organic loading, calcium and membrane orientation.* Desalination, 2013. **312**(0): p. 88-98.

23. Mi, B. and M. Elimelech, *Organic fouling of forward osmosis membranes: Fouling reversibility and cleaning without chemical reagents.* Journal of Membrane Science, 2010. **348**(1-2): p. 337-345.

24. Boo, C., et al., *Colloidal fouling in forward osmosis: Role of reverse salt diffusion.* Journal of Membrane Science, 2012. **390-391**: p. 277-284.

25. Park, M., et al., *Modeling of colloidal fouling in forward osmosis membrane: Effects of reverse draw solution permeation.* Desalination, 2013. **314**: p. 115-123.

26. Zhao, S. and L. Zou, *Effects of working temperature on separation performance, membrane scaling and cleaning in forward osmosis desalination.* Desalination, 2011. **278**(1-3): p. 157-164.

27. Li, Z.-Y., et al., *Flux patterns and membrane fouling propensity during desalination of seawater by forward osmosis.* Water Research, 2012. **46**(1): p. 195-204.

28. Xie, M., et al., *Impact of humic acid fouling on membrane performance and transport of pharmaceutically active compounds in forward osmosis.* Water Research, 2013. **47**(13): p. 4567-4575.

29. Valladares Linares, R., et al., *NOM and TEP fouling of a forward osmosis (FO) membrane: Foulant identification and cleaning.* Journal of Membrane Science, 2012. **421–422**(0): p. 217-224.

30. Marlaire, R.D., *NASA envisions "clean energy" from algae grown in waste water.*

31. Buckwalter, P., et al., *Dewatering microalgae by forward osmosis.* Desalination, 2013. **312**: p. 19-22.

32. Zou, S., et al., *The role of physical and chemical parameters on forward osmosis membrane fouling during algae separation.* Journal of Membrane Science, 2011. **366**(1-2): p. 356-362.

33. Zou, S., et al., *Direct microscopic observation of forward osmosis membrane fouling by microalgae: Critical flux and the role of operational conditions.* Journal of Membrane Science, 2013. **436**: p. 174-185.

34. Zhen-Feng, S., et al., *Culture of Scenedesmus sp. LX1 in the modified effluent of a wastewater treatment plant of an electric factory by photo-membrane bioreactor.* Bioresource Technology, 2011. **102**(17): p. 7627-7632.

35. Honda, R., et al., *Carbon dioxide capture and nutrients removal utilizing treated sewage by concentrated microalgae cultivation in a membrane photobioreactor.* Bioresource Technology, 2012. **125**(0): p. 59-64.

36. Bilad, M.R., et al., *Coupled cultivation and pre-harvesting of microalgae in a membrane photobioreactor (MPBR).* Bioresource Technology, (0).

37. Prathima Devi, M., G. Venkata Subhash, and S. Venkata Mohan, *Heterotrophic cultivation of mixed microalgae for lipid accumulation and wastewater treatment during sequential growth and starvation phases: Effect of nutrient supplementation.* Renewable Energy, 2012. **43**: p. 276-283.

38. Beer, L.L., et al., *Engineering algae for biohydrogen and biofuel production.* Curr Opin Biotechnol, 2009. **20**(3): p. 264-71.

39. Mandalam, R.K. and B.O. Palsson, *Elemental balancing of biomass and medium composition enhances growth capacity in high-density Chlorella vulgaris cultures.* Biotechnol Bioeng, 1998. **59**(5): p. 605-11.

40. Bhola, V., et al., *Effects of parameters affecting biomass yield and thermal behaviour of Chlorella vulgaris.* J Biosci Bioeng, 2011. **111**(3): p. 377-382.

41. Lourenço, S.O., et al., *Distribution of intracellular nitrogen in marine microalgae: Calculation of new nitrogen-to-protein conversion factors.* European Journal of Phycology, 2004. **39**(1): p. 17-32.

42. Bhola, V., et al., *Effects of parameters affecting biomass yield and thermal behaviour of Chlorella vulgaris.* J Biosci Bioeng, 2011. **111**(3): p. 377-82.

43. Tam, N.F.Y. and Y.S. Wong, *Effect of ammonia concentrations on growth of Chlorella vulgaris and nitrogen removal from media.* Bioresour Technol, 1996. **57**(1): p. 45-50.

44. Dragone, G., et al., *Nutrient limitation as a strategy for increasing starch accumulation in microalgae.* Applied Energy, 2011. **88**(10): p. 3331-3335.

45. Lv, J.M., et al., *Enhanced lipid production of Chlorella vulgaris by adjustment of cultivation conditions.* Bioresour Technol, 2010. **101**(17): p. 6797-804.

46. Yang, J., et al., *Growth and lipid accumulation properties of a freshwater microalga, Chlorella ellipsoidea YJ1, in domestic secondary effluents.* Applied Energy, 2011. **88**(10): p. 3295-3299.

47. Richardson, B., et al., *Effects of nitrogen limitation on the growth and composition of unicellular algae in continuous culture.* Appl Microbiol, 1969. **18**(2): p. 245-50.

48. Chen, M., et al., *Effect of nutrients on growth and lipid accumulation in the green algae Dunaliella tertiolecta.* Bioresour Technol, 2011. **102**(2): p. 1649-55.

49. Young, E.B. and J. Beardall, *Modulation of photosynthesis and inorganic carbon acquisition in a marine microalga by nitrogen, iron, and light availability.* Canadian Journal of Botany, 2005. **83**(7): p. 917-928.

50. Osborne, B.A. and R.J. Geider, *Effect of nitrate-nitrogen limitation on photosynthesis of the diatom Phaeodactylum tricornutum Bohlin (Bacillariophyceae).* Plant, Cell & Environment, 1986. **9**(8): p. 617-625.

51. Küppers, U. and M. Weidner, *Seasonal variation of enzyme activities in Laminaria hyperborea.* Planta, 1980. **148**(3): p. 222-230.

52. Falkowski, P.G., A. Sukenik, and R. Herzig, *NITROGEN LIMITATION IN ISOCHRYSIS GALBANA (HAPTOPHYCEAE). II. RELATIVE ABUNDANCE OF CHLOROPLAST PROTEINS1.* Journal of Phycology, 1989. **25**(3): p. 471-478.

53. Prézelin, B.B., G. Samuelsson, and H.A. Matlick, *Photosystem II photoinhibition and altered kinetics of photosynthesis during nutrient-dependent high-light photoadaptation in Gonyaulax polyedra.* Marine Biology, 1986. **93**(1): p. 1-12.

54. Kolber, Z., J. Zehr, and P. Falkowski, *Effects of Growth Irradiance and Nitrogen Limitation on Photosynthetic Energy Conversion in Photosystem II.* Plant Physiol, 1988. **88**(3): p. 923-9.

55. Vanlerberghe, G.C., et al., *Relationship between NH(+)(4) Assimilation Rate and in Vivo Phosphoenolpyruvate Carboxylase Activity : Regulation of Anaplerotic Carbon Flow in the Green Alga Selenastrum minutum.* Plant Physiology, 1990. **94**(1): p. 284-290.

56. Turpin, D.H., *EFFECTS OF INORGANIC N AVAILABILITY ON ALGAL PHOTOSYNTHESIS AND CARBON METABOLISM.* Journal of Phycology, 1991. **27**(1): p. 14-20.

57. Moseley, J.L., C.W. Chang, and A.R. Grossman, *Genome-based approaches to understanding phosphorus deprivation responses and PSR1 control in Chlamydomonas reinhardtii.* Eukaryot Cell, 2006. **5**(1): p. 26-44.

58. Davey, M., et al., *Nutrient limitation of picophytoplankton photosynthesis and growth in the tropical North Atlantic.* Limnology and Oceanography, 2008. **53**(5): p. 1722-1733.

59. Bougaran, G., O. Bernard, and A. Sciandra, *Modeling continuous cultures of microalgae colimited by nitrogen and phosphorus.* J Theor Biol, 2010. **265**(3): p. 443-54.

60. Wykoff, D.D., et al., *The Regulation of Photosynthetic Electron Transport during Nutrient Deprivation in Chlamydomonas reinhardtii.* Plant Physiology, 1998. **117**(1): p. 129-139.

61. Peršić, V., et al., *Changes in N and P limitation induced by water level fluctuations in Nature Park Kopački Rit (Croatia): nutrient enrichment bioassay.* Aquatic Ecology, 2009. **43**(1): p. 27-36.

62.   Sun, Y. and C. Wang, *The optimal growth conditions for the biomass production of Isochrysis galbana and the effects that phosphorus, Zn2+, CO2, and light intensity have on the biochemical composition of Isochrysis galbana and the activity of extracellular CA.* Biotechnology and Bioprocess Engineering, 2009. **14**(2): p. 225-231.

63.   Kozlowska-Szerenos, B., I. Bialuk, and S. Maleszewski, *Enhancement of photosynthetic O2 evolution in Chlorella vulgaris under high light and increased CO2 concentration as a sign of acclimation to phosphate deficiency.* Plant Physiol Biochem, 2004. **42**(5): p. 403-9.

64.   Jacob, J. and D.W. Lawlor, *In vivo photosynthetic electron transport does not limit photosynthetic capacity in phosphate-deficient sunflower and maize leaves.* Plant, Cell & Environment, 1993. **16**(7): p. 785-795.

65.   Zer, H. and I. Ohad, *Light, redox state, thylakoid-protein phosphorylation and signaling gene expression.* Trends in Biochemical Sciences, 2003. **28**(9): p. 467-470.

66.   Quisel, J.D., D.D. Wykoff, and A.R. Grossman, *Biochemical characterization of the extracellular phosphatases produced by phosphorus-deprived Chlamydomonas reinhardtii.* Plant Physiol, 1996. **111**(3): p. 839-48.

67.   Spijkerman, E., *Phosphorus acquisition by Chlamydomonas acidophila under autotrophic and osmo-mixotrophic growth conditions.* Journal of Experimental Botany, 2007. **58**(15/16): p. 4195-4202.

68.   Davies, A.G. and J.A. Sleep, *The photosynthetic response of nutrient-depleted dilute cultures of Skeletonema costatum to pulses of ammonium and nitrate; the importance of phosphate.* Journal of Plankton Research, 1989. **11**(1): p. 141-164.

69.   Varela, D.E., V. Willers, and D.W. Crawford, *Effect of Zinc Availability on Growth, Morphology, and Nutrient Incorporation in a Coastal and an Oceanic Diatom(1).* J Phycol, 2011. **47**(2): p. 302-12.

70.   Rochaix, J., *Assembly, Function, and Dynamics of the Photosynthetic Machinery in Chlamydomonas reinhardtii.* Plant Physiology, 2001. **127**(4): p. 1394-1398.

71.   Terauchi, A.M., et al., *Trophic status of Chlamydomonas reinhardtii influences the impact of iron deficiency on photosynthesis.* Photosynth Res, 2010. **105**(1): p. 39-49.

72.   Hill, K.L., et al., *Regulated copper uptake in Chlamydomonas reinhardtii in response to copper availability.* Plant Physiol, 1996. **112**(2): p. 697-704.

73.   Glass, J.B., F. Wolfe-Simon, and A.D. Anbar, *Coevolution of metal availability and nitrogen assimilation in cyanobacteria and algae.* Geobiology, 2009. **7**(2): p. 100-23.

74.   Estevez, M.S., G. Malanga, and S. Puntarulo, *Iron-dependent oxidative stress in Chlorella vulgaris.* Plant Science, 2001. **161**(1): p. 9-17.

75.   Bajguz, A., *Suppression of Chlorella vulgaris growth by cadmium, lead, and copper stress and its restoration by endogenous brassinolide.* Arch Environ Contam Toxicol, 2011. **60**(3): p. 406-16.

76.   Moseley, J.L., et al., *Adaptation to Fe-deficiency requires remodeling of the photosynthetic apparatus.* The EMBO Journal, 2002. **21**(24): p. 6709-6720.

77.   Michel, K.P. and E.K. Pistorius, *Adaptation of the photosynthetic electron transport chain in cyanobacteria to iron deficiency: The function of IdiA and IsiA.* Physiol Plant, 2004. **120**(1): p. 36-50.

78.   Dubinsky, Z. and O. Schofield, *From the light to the darkness: thriving at the light extremes in the oceans.* Hydrobiologia, 2010. **639**(1): p. 153-171.

79.   Cornet, J.-F., *Calculation of optimal design and ideal productivities of volumetrically lightened photobioreactors using the constructal approach.* Chemical Engineering Science, 2010. **65**(2): p. 985-998.

80.   Carvalho, A.P., et al., *Light requirements in microalgal photobioreactors: an overview of biophotonic aspects.* Appl Microbiol Biotechnol, 2011. **89**(5): p. 1275-88.

81.   Subba Rao, D.V., Y. Pan, and F. Al-Yamani, *Growth and photosynthetic rates of Chlamydomonas plethora and Nitzschia frustula cultures isolated from Kuwait Bay, Arabian*

Gulf, and their potential as live algal food for tropical mariculture. Marine Ecology, 2005. **26**(1): p. 63-71.

82. Yeh, K.-L., J.-S. Chang, and W.-m. chen, *Effect of light supply and carbon source on cell growth and cellular composition of a newly isolated microalga Chlorella vulgaris ESP-31.* Engineering in Life Sciences, 2010. **10**(3): p. 201-208.

83. Voronova, E.N., et al., *Changes in the condition of photosynthetic apparatus of a diatom alga Thallassiosira weisflogii during photoadaptation and photodamage.* Russian Journal of Plant Physiology, 2009. **56**(6): p. 753-760.

84. Choudhury, N.K. and R.K. Behera, *Photoinhibition of Photosynthesis: Role of Carotenoids in Photoprotection of Chloroplast Constituents.* Photosynthetica, 2001. **39**(4): p. 481-488.

85. Peers, G., et al., *An ancient light-harvesting protein is critical for the regulation of algal photosynthesis.* Nature, 2009. **462**(7272): p. 518-521.

86. Kang, C.D., et al., *Complementary limiting factors of astaxanthin synthesis during photoautotrophic induction of Haematococcus pluvialis: C/N ratio and light intensity.* Appl Microbiol Biotechnol, 2007. **74**(5): p. 987-94.

87. Wu, Y., K. Gao, and U. Riebesell, *CO_2-induced seawater acidification affects physiological performance of the marine diatom Phaeodactylum tricornutum.* Biogeosciences, 2010. **7**(9): p. 2915-2923.

88. Hill, W.R. and S.E. Fanta, *Phosphorus and light colimit periphyton growth at subsaturating irradiances.* Freshwater Biology, 2008. **53**(2): p. 215-225.

89. Soletto, D., et al., *Effects of carbon dioxide feeding rate and light intensity on the fed-batch pulse-feeding cultivation of Spirulina platensis in helical photobioreactor.* Biochemical Engineering Journal, 2008. **39**(2): p. 369-375.

90. Westerhoff, P., et al., *Growth parameters of microalgae tolerant to high levels of carbon dioxide in batch and continuous-flow photobioreactors.* Environ Technol, 2010. **31**(5): p. 523-32.

91. Baker, J.W., et al., *GROWTH AND TOXICITY OF PRYMNESIUM PARVUM (HAPTOPHYTA) AS A FUNCTION OF SALINITY, LIGHT, AND TEMPERATURE1.* Journal of Phycology, 2007. **43**(2): p. 219-227.

92. Henley, W.J., et al., *Photoacclimation and photoinhibition in Ulva rotundata as influenced by nitrogen availability.* Planta, 1991. **184**(2): p. 235-43.

93. Yun, Y.-S. and J.M. Park, *Development of gas recycling photobioreactor system for microalgal carbon dioxide fixation.* Korean Journal of Chemical Engineering, 1997. **14**(4): p. 297-300.

94. Li, D., et al., *Effect of Iron Stress, Light Stress, and Nitrogen Source on Physiological Aspects of Marine Red Tide Alga.* Journal of Plant Nutrition, 2004. **27**(1): p. 29-41.

95. Dickman, E.M., M.J. Vanni, and M.J. Horgan, *Interactive effects of light and nutrients on phytoplankton stoichiometry.* Oecologia, 2006. **149**(4): p. 676-689.

96. Zucchi, M.R. and O. Necchi, *Effects of temperature, irradiance and photoperiod on growth and pigment content in some freshwater red algae in culture.* Phycological Research, 2001. **49**(2): p. 103-114.

97. Jacob-Lopes, E., et al., *Development of operational strategies to remove carbon dioxide in photobioreactors.* Chemical Engineering Journal, 2009. **153**(1–3): p. 120-126.

98. Vesk, M. and S.W. Jeffrey, *EFFECT OF BLUE-GREEN LIGHT ON PHOTOSYNTHETIC PIGMENTS AND CHLOROPLAST STRUCTURE IN UNICELLULAR MARINE ALGAE FROM SIX CLASSES1.* Journal of Phycology, 1977. **13**(3): p. 280-288.

99. Mercado, J.M., et al., *Blue light effect on growth, light absorption characteristics and photosynthesis of five benthic diatom strains.* Aquatic Botany, 2004. **78**(3): p. 265-277.

100. Wang, C.-Y., C.-C. Fu, and Y.-C. Liu, *Effects of using light-emitting diodes on the cultivation of Spirulina platensis.* Biochemical Engineering Journal, 2007. **37**(1): p. 21-25.

101. Qiang, H., Y. Zarmi, and A. Richmond, *Combined effects of light intensity, light-path and culture density on output rate of Spirulina platensis (Cyanobacteria).* European Journal of Phycology, 1998. **33**(2): p. 165-171.

102. Zijffers, J.W., et al., *Maximum photosynthetic yield of green microalgae in photobioreactors.* Mar Biotechnol, 2010. **12**(6): p. 708-18.

103. Giordano, M., J. Beardall, and J.A. Raven, *CO2 concentrating mechanisms in algae: mechanisms, environmental modulation, and evolution.* Annu Rev Plant Biol, 2005. **56**: p. 99-131.

104. and, A.K. and L. Reinhold, *CO2 CONCENTRATING MECHANISMS IN PHOTOSYNTHETIC MICROORGANISMS.* Annual Review of Plant Physiology and Plant Molecular Biology, 1999. **50**(1): p. 539-570.

105. Miyachi, S., I. Iwasaki, and Y. Shiraiwa, *Historical perspective on microalgal and cyanobacterial acclimation to low- and extremely high-CO2 conditions.* Photosynth Res, 2003. **77**(2): p. 139-153.

106. Sakai, N., et al., *Chlorella strains from hot springs tolerant to high temperature and high CO2.* Energy Conversion and Management, 1995. **36**(6–9): p. 693-696.

107. Murakami, M., et al., *The biological CO2 fixation using Chlorella sp. with high capability in fixing CO2*, in *Studies in Surface Science and Catalysis*, M.A.K.I.S.Y. T. Inui and T. Yamaguchi, Editors. 1998, Elsevier. p. 315-320.

108. Tang, D., et al., *CO2 biofixation and fatty acid composition of Scenedesmus obliquus and Chlorella pyrenoidosa in response to different CO2 levels.* Bioresour Technol, 2011. **102**(3): p. 3071-6.

109. Hanagata, N., et al., *Tolerance of microalgae to high CO2 and high temperature.* Phytochemistry, 1992. **31**(10): p. 3345-3348.

110. Kurano, N., et al., *Fixation and utilization of carbon dioxide by microalgal photosynthesis.* Energy Conversion and Management, 1995. **36**(6–9): p. 689-692.

111. Iwasaki, I., et al., *Effect of extremely high-CO2 stress on energy distribution between photosystem I and photosystem II in a 'high-CO2' tolerant green alga, Chlorococcum littorale and the intolerant green alga Stichococcus bacillaris.* Journal of Photochemistry and Photobiology B: Biology, 1998. **44**(3): p. 184-190.

112. Satoh, A., et al., *Regulation of energy balance in photosystems in response to changes in CO2 concentrations and light intensities during growth in extremely-high-CO2-tolerant green microalgae.* Plant Cell Physiol, 2002. **43**(4): p. 440-51.

113. Pesheva, I., et al., *Changes in Photosynthetic Characteristics Induced by Transferring Air-Grown Cells of Chlorococcum littorale to High-CO2 Conditions.* Plant and Cell Physiology, 1994. **35**(3): p. 379-387.

114. Sasaki, T., et al., *Development of Vacuoles and Vacuolar H+-ATPase Activity under Extremely High CO2 Conditions in Chlorococcum littorale Cells.* Plant Biology, 1999. **1**(1): p. 68-75.

115. Ugwu, C.U., H. Aoyagi, and H. Uchiyama, *Photobioreactors for mass cultivation of algae.* Bioresour Technol, 2008. **99**(10): p. 4021-8.

116. Contreras, A., et al., *Interaction between CO2-mass transfer, light availability, and hydrodynamic stress in the growth of phaeodactylum tricornutum in a concentric tube airlift photobioreactor.* Biotechnol Bioeng, 1998. **60**(3): p. 317-25.

117. Kantarci, N., F. Borak, and K.O. Ulgen, *Bubble column reactors.* Process Biochemistry, 2005. **40**(7): p. 2263-2283.

118. Necchi, O. and M.R. Zucchi, *Photosynthetic performance of freshwater Rhodophyta in response to temperature, irradiance, pH and diurnal rhythm.* Phycological Research, 2001. **49**(4): p. 305-318.

119. Olaizola, M., *Microalgal removal of CO2 from flue gases: Changes in medium pH and flue gas composition do not appear to affect the photochemical yield of microalgal cultures.* Biotechnology and Bioprocess Engineering, 2003. **8**(6): p. 360-367.

120. Gerloff-Elias, A., E. Spijkerman, and T. PrÖSchold, *Effect of external pH on the growth, photosynthesis and photosynthetic electron transport of Chlamydomonas acidophila Negoro, isolated from an extremely acidic lake (pH 2.6).* Plant, Cell & Environment, 2005. **28**(10): p. 1218-1229.

121. Bartual, A. and J.A. Gálvez, *Growth and Biochemical Composition of the Diatom Phaeodactylum tricornutum at Different pH and Inorganic Carbon Levels under Saturating and Subsaturating Light Regimes*, in *Botanica Marina*2002. p. 491.

122. Stojkovic, J.B.a.S., *Microalgae under global environmental change: Implications for growth and productivity, populations and trophic flow.* ScienceAsia, 2006. **32**(1513-1874): p. 1-10.

123. Converti, A., et al., *Effect of temperature and nitrogen concentration on the growth and lipid content of Nannochloropsis oculata and Chlorella vulgaris for biodiesel production.* Chemical Engineering and Processing: Process Intensification, 2009. **48**(6): p. 1146-1151.

124. Sanchez, J.F., et al., *Biomass and lutein productivity of Scenedesmus almeriensis: influence of irradiance, dilution rate and temperature.* Appl Microbiol Biotechnol, 2008. **79**(5): p. 719-29.

125. Sushchik, N.N., et al., *A Temperature Dependence of the Intra- and Extracellular Fatty-Acid Composition of Green Algae and Cyanobacterium.* Russian Journal of Plant Physiology, 2003. **50**(3): p. 374-380.

126. Jiang, H. and K. Gao, *EFFECTS OF LOWERING TEMPERATURE DURING CULTURE ON THE PRODUCTION OF POLYUNSATURATED FATTY ACIDS IN THE MARINE DIATOM PHAEODACTYLUM TRICORNUTUM (BACILLARIOPHYCEAE)1.* Journal of Phycology, 2004. **40**(4): p. 651-654.

127. Huner, N.P.A., G. Öquist, and F. Sarhan, *Energy balance and acclimation to light and cold.* Trends in Plant Science, 1998. **3**(6): p. 224-230.

128. Gao, K., et al., *Combined Effects of Ultraviolet Radiation and Temperature on Morphology, Photosynthesis, and DNA of Arthrospira (Spirulina) Platensis (Cyanophyta)(1).* J Phycol, 2008. **44**(3): p. 777-86.

129. Beardall, J., S. Stojkovic, and S. Larsen, *Living in a high CO2 world: impacts of global climate change on marine phytoplankton.* Plant Ecology & Diversity, 2009. **2**(2): p. 191-205.

130. Radmann, E.M., C.O. Reinehr, and J.A.V. Costa, *Optimization of the repeated batch cultivation of microalga Spirulina platensis in open raceway ponds.* Aquaculture, 2007. **265**(1–4): p. 118-126.

131. Norsker, N.-H., et al., *Microalgal production — A close look at the economics.* Biotechnol Adv, 2011. **29**(1): p. 24-27.

132. Singh, J. and S. Gu, *Commercialization potential of microalgae for biofuels production.* Renewable and Sustainable Energy Reviews, 2010. **14**(9): p. 2596-2610.

133. Chisti, Y., *Biodiesel from microalgae.* Biotechnol Adv, 2007. **25**(3): p. 294-306.

134. Borowitzka, M.A., *Commercial production of microalgae: ponds, tanks, tubes and fermenters.* J Biotechnol, 1999. **70**(1–3): p. 313-321.

135. Zeng, X., et al., *Microalgae bioengineering: From CO2 fixation to biofuel production.* Renewable and Sustainable Energy Reviews, 2011. **15**(6): p. 3252-3260.

136. Jorquera, O., et al., *Comparative energy life-cycle analyses of microalgal biomass production in open ponds and photobioreactors.* Bioresour Technol, 2010. **101**(4): p. 1406-1413.

137. Cooney, M.J., G. Young, and R. Pate, *Bio-oil from photosynthetic microalgae: Case study.* Bioresour Technol, 2011. **102**(1): p. 166-177.

138. Amaro, H.M., A.C. Guedes, and F.X. Malcata, *Advances and perspectives in using microalgae to produce biodiesel.* Applied Energy, 2011. **88**(10): p. 3402-3410.

139. Amin, S., *Review on biofuel oil and gas production processes from microalgae.* Energy Conversion and Management, 2009. **50**(7): p. 1834-1840.

140. Davis, R., A. Aden, and P.T. Pienkos, *Techno-economic analysis of autotrophic microalgae for fuel production.* Applied Energy, 2011. **88**(10): p. 3524-3531.

141.   *Wageningen University & Research, Photobioreactor.* Available from: https://www.wur.nl/en/newsarticle/Sustainable-algae-cultivation-making-headway.htm.

142.   *Explore Biotech.* Available from: https://explorebiotech.com/everything-need-know-algal-biotechnology/.

143.   Garbisu, C., et al., *Inorganic nitrogen and phosphate removal from water by free-living and polyvinyl-immobilized Phormidium laminosum in batch and continuous-flow bioreactors.* Enzyme and Microbial Technology, 1994. **16**(5): p. 395-401.

144.   Rai, L.C., J.P. Gaur, and H.D. Kumar, *Phycology and heavy-metal pollution.* Biological Reviews of the Cambridge Philosophical Society, 1981. **56**(2): p. 99-151.

145.   D.G. Redalje, E.O.D., J. De la Noüe, P. Mayzaud, A.H. Nonomura, R.C. Cassin, *Algae as ideal waste removers: biochemical pathways.* M.E. Huntley (Ed.), Biotreatment of Agricultural Wastewater, Press, Boca, Raton, CRC (1989), pp. 91–110.

146.   J. De la Noüe, D.P., *Tertiary treatment of urban wastewater by chitosan-immobilized Phormidium sp.* Algal Biotechnology, Elsevier Applied Science, New Yourk (1988), pp. 159–168.

147.   J.D., M.A.O.R.C.E.L.D.C., *Standardization in wastewater biomass growth.* Igiene Moderna 94(1): 24-32

1990.

148.   Wong, P.K. and K.Y. Chan, *Growth and value of Chlorella salina grown on highly saline sewage effluent.* Agriculture, Ecosystems & Environment, 1990. **30**(3): p. 235-250.

149.   Renaud, S.M., D.L. Parry, and L.-V. Thinh, *Microalgae for use in tropical aquaculture I: Gross chemical and fatty acid composition of twelve species of microalgae from the Northern Territory, Australia.* Journal of Applied Phycology, 1994. **6**(3): p. 337-345.

150.   Palmer, C.M., *A COMPOSITE RATING OF ALGAE TOLERATING ORGANIC POLLUTION2.* Journal of Phycology, 1969. **5**(1): p. 78-82.

151.   Lavoie, A. and J. de la Noüe, *Hyperconcentrated cultures of Scenedesmus obliquus.* Water Res, 1985. **19**(11): p. 1437-1442.

152.   Pouliot, Y., P. Talbot, and J. De la Noue, *Biotreatment of swine manure by the production of Spirulina biomass.* Entropie Paris, 1986. **22**(130-131): p. 73-77.

153.   Phang, S.-M. and O. Kim-Chong, *Algal biomass production in digested palm oil mill effluent.* Biological Wastes, 1988. **25**(3): p. 177-191.

154.   Ibraheem, I.B.M., 1998. Utilization of certain algae in the treatment of wastewater. Ph.D. Thesis, Fac. of Sci. Al-Azhar Univ., Cairo, Egypt, pp. 197.

155.   Kaplan, D., Christiaen, D., Arad, S., *Binding of heavy metals by algal polysaccharides.* In: Stadler, T., Mollion, J., Verdus, M.C., Karamanos, Y., Morvan, H., Christiaen, D. (Eds.), Algal Biotechnology, Elsevier Applied Science, London, pp. 179–187., 1988.

156.   Tam, N.F.Y. and Y.S. Wong, *Wastewater nutrient removal by Chlorella pyrenoidosa and Scenedesmus sp.* Environmental Pollution, 1989. **58**(1): p. 19-34.

157.   Alam, F., S. Mobin, and H. Chowdhury, *Third Generation Biofuel from Algae.* Procedia Engineering, 2015. **105**: p. 763-768.

158.   de Vries, S.C., et al., *Resource use efficiency and environmental performance of nine major biofuel crops, processed by first-generation conversion techniques.* Biomass and Bioenergy, 2010. **34**(5): p. 588-601.

159.   Sims, R.E.H., et al., *An overview of second generation biofuel technologies.* Bioresour Technol, 2010. **101**(6): p. 1570-1580.

160.   Banse, M., et al., *Impact of EU biofuel policies on world agricultural production and land use.* Biomass and Bioenergy, 2011. **35**(6): p. 2385-2390.

161.   Secchi, S., et al., *Land use change in a biofuels hotspot: The case of Iowa, USA.* Biomass and Bioenergy, 2011. **35**(6): p. 2391-2400.

162.   Ozkan, A., et al., *Reduction of water and energy requirement of algae cultivation using an algae biofilm photobioreactor.* Bioresour Technol, 2012. **114**: p. 542-548.

163. Harun, R., et al., *Exploring alkaline pre-treatment of microalgal biomass for bioethanol production.* Applied Energy, 2011. **88**(10): p. 3464-3467.

164. Suali, E. and R. Sarbatly, *Conversion of microalgae to biofuel.* Renewable and Sustainable Energy Reviews, 2012. **16**(6): p. 4316-4342.

165. Milledge, J.J. and S. Heaven, *A review of the harvesting of micro-algae for biofuel production.* Reviews in Environmental Science and Bio/Technology, 2012. **12**(2): p. 165-178.

166. Leite, G.B., A.E. Abdelaziz, and P.C. Hallenbeck, *Algal biofuels: challenges and opportunities.* Bioresour Technol, 2013. **145**: p. 134-41.

167. Sawayama, S., T. Minowa, and S.Y. Yokoyama, *Possibility of renewable energy production and CO2 mitigation by thermochemical liquefaction of microalgae.* Biomass and Bioenergy, 1999. **17**(1): p. 33-39.

168. Dote, Y., et al., *Recovery of liquid fuel from hydrocarbon-rich microalgae by thermochemical liquefaction.* Fuel, 1994. **73**(12): p. 1855-1857.

169. Rodolfi, L., et al., *Microalgae for oil: Strain selection, induction of lipid synthesis and outdoor mass cultivation in a low-cost photobioreactor.* Biotechnology and Bioengineering, 2009. **102**(1): p. 100-112.

170. Gouveia, L. and A.C. Oliveira, *Microalgae as a raw material for biofuels production.* Journal of Industrial Microbiology & Biotechnology, 2009. **36**(2): p. 269-274.

171. Peng, W., et al., *Pyrolytic characteristics of microalgae as renewable energy source determined by thermogravimetric analysis.* Bioresour Technol, 2001. **80**(1): p. 1-7.

172. Damiani, M.C., et al., *Lipid analysis in Haematococcus pluvialis to assess its potential use as a biodiesel feedstock.* Bioresour Technol, 2010. **101**(11): p. 3801-3807.

173. Fjerbaek, L., K.V. Christensen, and B. Norddahl, *A review of the current state of biodiesel production using enzymatic transesterification.* Biotechnol Bioeng, 2009. **102**(5): p. 1298-315.

174. Branyikova, I., et al., *Microalgae--novel highly efficient starch producers.* Biotechnol Bioeng, 2011. **108**(4): p. 766-76.

175. Liu, Z.Y., G.C. Wang, and B.C. Zhou, *Effect of iron on growth and lipid accumulation in Chlorella vulgaris.* Bioresour Technol, 2008. **99**(11): p. 4717-22.

176. Mohan, D., C.U. Pittman, and P.H. Steele, *Pyrolysis of Wood/Biomass for Bio-oil: A Critical Review.* Energy & Fuels, 2006. **20**(3): p. 848-889.

177. Shuping, Z., et al., *Production and characterization of bio-oil from hydrothermal liquefaction of microalgae Dunaliella tertiolecta cake.* Energy, 2010. **35**(12): p. 5406-5411.

178. Ross, A.B., et al., *Hydrothermal processing of microalgae using alkali and organic acids.* Fuel, 2010. **89**(9): p. 2234-2243.

179. Yang, C., et al., *Bio-oil from hydro-liquefaction of Dunaliella salina over Ni/REHY catalyst.* Bioresour Technol, 2011. **102**(6): p. 4580-4.

180. Schimming, V., et al., *Evidence by 15N CPMAS and 15N-13C REDOR NMR for fixation of atmospheric CO2 by amino groups of biopolymers in the solid state [1].* Journal of the American Chemical Society, 1999. **121**(20): p. 4892-4893.

181. Sugimoto, H., T. Kimura, and S. Inoue, *Photoresponsive molecular switch to control chemical fixation of CO2 [10].* Journal of the American Chemical Society, 1999. **121**(10): p. 2325-2326.

182. Lin, C.C., W.T. Liu, and C.S. Tan, *Removal of carbon dioxide by absorption in a rotating packed bed.* Industrial and Engineering Chemistry Research, 2003. **42**(11): p. 2381-2386.

183. Wang, B., et al., *CO2 bio-mitigation using microalgae.* Appl Microbiol Biotechnol, 2008. **79**(5): p. 707-718.

184. Sydney, E.B., et al., *Potential carbon dioxide fixation by industrially important microalgae.* Bioresour Technol, 2010. **101**(15): p. 5892-5896.

185. Sawayama, S., et al., *CO2 fixation and oil production through microalga.* Energy Conversion and Management, 1995. **36**(6–9): p. 729-731.

186. Apt, K.E. and P.W. Behrens, *Commercial developments in microalgal biotechnology.* Journal of Phycology, 1999. **35**(2): p. 215-226.

187. Jeong, M.L., J.M. Gillis, and J.Y. Hwang, *Carbon Dioxide Mitigation by Microalgal Photosynthesis.* Bulletin of the Korean Chemical Society, 2003. **24**(12): p. 1763-1766.

188. Hirata, S., et al., *Carbon dioxide fixation in batch culture of Chlorella sp. using a photobioreactor with a sunlight-cellection device.* Journal of Fermentation and Bioengineering, 1996. **81**(5): p. 470-472.

189. Kajiwara, S., et al., *Design of the bioreactor for carbon dioxide fixation by Synechococcus PCC7942.* Energy Conversion and Management, 1997. **38, Supplement**: p. S529-S532.

190. Yun, Y.S., et al., *Carbon dioxide fixation by algal cultivation using wastewater nutrients.* Journal of Chemical Technology and Biotechnology, 1997. **69**(4): p. 451-455.

191. Ota, M., et al., *Fatty acid production from a highly CO2 tolerant alga, Chlorocuccum littorale, in the presence of inorganic carbon and nitrate.* Bioresour Technol, 2009. **100**(21): p. 5237-5242.

192. de Morais, M.G. and J.A.V. Costa, *Isolation and selection of microalgae from coal fired thermoelectric power plant for biofixation of carbon dioxide.* Energy Conversion and Management, 2007. **48**(7): p. 2169-2173.

193. de Morais, M.G. and J.A. Costa, *Carbon dioxide fixation by Chlorella kessleri, C. vulgaris, Scenedesmus obliquus and Spirulina sp. cultivated in flasks and vertical tubular photobioreactors.* Biotechnol Lett, 2007. **29**(9): p. 1349-52.

194. Xu, L., et al., *Microalgal bioreactors: Challenges and opportunities.* Engineering in Life Sciences, 2009. **9**(3): p. 178-189.

195. Acién Fernández, F.G., et al., *Airlift-driven external-loop tubular photobioreactors for outdoor production of microalgae: assessment of design and performance.* Chemical Engineering Science, 2001. **56**(8): p. 2721-2732.

196. Bosma, R., et al., *Prediction of volumetric productivity of an outdoor photobioreactor.* Biotechnol Bioeng, 2007. **97**(5): p. 1108-20.

197. Meiser, A., U. Schmid-Staiger, and W. Trösch, *Optimization of eicosapentaenoic acid production byPhaeodactylum tricornutumin the flat panel airlift (FPA) reactor.* Journal of Applied Phycology, 2004. **16**(3): p. 215-225.

198. Chini Zittelli, G., et al., *Productivity and photosynthetic efficiency of outdoor cultures of Tetraselmis suecica in annular columns.* Aquaculture, 2006. **261**(3): p. 932-943.

199. Nedbal, L., et al., *A photobioreactor system for precision cultivation of photoautotrophic microorganisms and for high-content analysis of suspension dynamics.* Biotechnol Bioeng, 2008. **100**(5): p. 902-10.

200. *Microalgae Production from Power Plant Flue Gas Environmental Implications on a Life Cycle Basis*, 2001, United States. Dept. of Energy ;: Washington, D.C. :.

201. Maeda, K., et al., *CO2 fixation from the flue gas on coal-fired thermal power plant by microalgae.* Energy Conversion and Management, 1995. **36**(6–9): p. 717-720.

202. Zeiler, K.G., et al., *The use of microalgae for assimilation and utilization of carbon dioxide from fossil fuel-fired power plant flue gas.* Energy Conversion and Management, 1995. **36**(6–9): p. 707-712.

203. Farooq, U., et al., *Biosorption of heavy metal ions using wheat based biosorbents – A review of the recent literature.* Bioresour Technol, 2010. **101**(14): p. 5043-5053.

204. Volesky, B., *Biosorption and me.* Water Res, 2007. **41**(18): p. 4017-4029.

205. Mallick, N., *Biotechnological potential of immobilized algae for wastewater N, P and metal removal: A review.* Biometals, 2002. **15**(4): p. 377-390.

206. Volesky, B., *Advances in biosorption of metals: Selection of biomass types.* FEMS Microbiology Reviews, 1994. **14**(4): p. 291-302.

207. de-Bashan, L.E. and Y. Bashan, *Immobilized microalgae for removing pollutants: review of practical aspects.* Bioresour Technol, 2010. **101**(6): p. 1611-27.

208. Moreno-Garrido, I., *Microalgae immobilization: Current techniques and uses.* Bioresour Technol, 2008. **99**(10): p. 3949-3964.

209. Monteiro, C.M., P.M.L. Castro, and F.X. Malcata, *Cadmium Removal by Two Strains of Desmodesmus pleiomorphus Cells.* Water, Air, and Soil Pollution, 2010. **208**(1): p. 17-27.

210. Zhou, J.L., P.L. Huang, and R.G. Lin, *Sorption and desorption of Cu and Cd by macroalgae and microalgae.* Environmental Pollution, 1998. **101**(1): p. 67-75.

211. Akhtar, N., J. Iqbal, and M. Iqbal, *Removal and recovery of nickel(II) from aqueous solution by loofa sponge-immobilized biomass of Chlorella sorokiniana: characterization studies.* Journal of Hazardous Materials, 2004. **108**(1–2): p. 85-94.

212. Wilkinson, S.C., K.H. Goulding, and P.K. Robinson, *Mercury removal by immobilized algae in batch culture systems.* Journal of Applied Phycology, 1990. **2**(3): p. 223-230.

213. Cañizares-Villanueva, R.O., F. Martínez-Jerónimo, and F. Espinosa-Chávez, *Acute toxicity to Daphnia magna of effluents containing Cd, Zn, and a mixture Cd-Zn, after metal removal by Chlorella vulgaris.* Environmental Toxicology, 2000. **15**(3): p. 160-164.

214. Garnham, G.W., G.A. Codd, and G.M. Gadd, *Accumulation of cobalt, zinc and manganese by the estuarine green microalga Chlorella salina immobilized in alginate microbeads.* Environ Sci Technol, 1992. **26**(9): p. 1764-1770.

215. Avery, S.V., G.A. Codd, and G.M. Gadd, *Salt-stimulation of caesium accumulation in the euryhaline green microalga Chlorella salina: potential relevance to the development of a biological Cs-removal process.* Microbiology, 1993. **139**(9): p. 2239-2244.

216. Travieso, L., et al., *Heavy Metal Removal by Microalgae.* Bulletin of Environmental Contamination and Toxicology, 1999. **62**(2): p. 144-151.

217. Wilde, E.W. and J.R. Benemann, *Bioremoval of heavy metals by the use of microalgae.* Biotechnol Adv, 1993. **11**(4): p. 781-812.

218. Trevan, M., *Micro-algal biotechnology Edited by M. A. Borowitzka and L. J. Borowitzka, Cambridge University Press, Cambridge, 1988. pp. 477, price £45.00. ISBN 0-521-323495.* Journal of Chemical Technology & Biotechnology, 1990. **47**(2): p. 181-182.

219. Spolaore, P., et al., *Commercial applications of microalgae.* J Biosci Bioeng, 2006. **101**(2): p. 87-96.

220. Becker, W., *Microalgae in Human and Animal Nutrition*, in *Handbook of Microalgal Culture*. 2007, Blackwell Publishing Ltd. p. 312-351.

221. Patel, A., et al., *Purification and characterization of C-Phycocyanin from cyanobacterial species of marine and freshwater habitat.* Protein Expression and Purification, 2005. **40**(2): p. 248-255.

222. Vadiraja, B.B., N.W. Gaikwad, and K.M. Madyastha, *Hepatoprotective Effect of C-Phycocyanin: Protection for Carbon Tetrachloride andR-(+)-Pulegone-Mediated Hepatotoxicty in Rats.* Biochemical and Biophysical Research Communications, 1998. **249**(2): p. 428-431.

223. Sekar, S. and M. Chandramohan, *Phycobiliproteins as a commodity: trends in applied research, patents and commercialization.* Journal of Applied Phycology, 2008. **20**(2): p. 113-136.

224. Chrismadha, T. and M.A. Borowitzka, *Effect of cell density and irradiance on growth, proximate composition and eicosapentaenoic acid production ofPhaeodactylum tricornutum grown in a tubular photobioreactor.* Journal of Applied Phycology, 1994. **6**(1): p. 67-74.

225. Luiten, E.E.M., et al., *Realizing the promises of marine biotechnology.* Biomolecular Engineering, 2003. **20**(4–6): p. 429-439.

226. Doughman, S.D., S. Krupanidhi, and C.B. Sanjeevi, *Omega-3 fatty acids for nutrition and medicine: considering microalgae oil as a vegetarian source of EPA and DHA.* Curr Diabetes Rev, 2007. **3**(3): p. 198-203.

227. Beach, E.S., et al., *Preferential technological and life cycle environmental performance of chitosan flocculation for harvesting of the green algae Neochloris oleoabundans.* Bioresour Technol, 2012. **121**: p. 445-9.

228. Sander, K. and G.S. Murthy, *Life cycle analysis of algae biodiesel.* The International Journal of Life Cycle Assessment, 2010. **15**(7): p. 704-714.

229. Salim, S., M.H. Vermue, and R.H. Wijffels, *Ratio between autoflocculating and target microalgae affects the energy-efficient harvesting by bio-flocculation.* Bioresour Technol, 2012. **118**: p. 49-55.

230. Bilad, M.R., et al., *Harvesting microalgal biomass using submerged microfiltration membranes.* Bioresour Technol, 2012. **111**: p. 343-52.

231. *Flottweg SE*. Available from: https://www.flottweg.com/applications/edible-fats-and-oils-biofuels/algae/.

232. Zhang, J. and B. Hu, *A novel method to harvest microalgae via co-culture of filamentous fungi to form cell pellets.* Bioresour Technol, 2012. **114**: p. 529-35.

233. Papazi, A., P. Makridis, and P. Divanach, *Harvesting Chlorella minutissima using cell coagulants.* Journal of Applied Phycology, 2010. **22**(3): p. 349-355.

234. Mojaat, M., et al., *Optimal selection of organic solvents for biocompatible extraction of beta-carotene from Dunaliella salina.* J Biotechnol, 2008. **133**(4): p. 433-41.

235. Perreault, F., et al., *Effect of aluminum on cellular division and photosynthetic electron transport in Euglena gracilis and Chlamydomonas acidophila.* Environ Toxicol Chem, 2010. **29**(4): p. 887-92.

236. Banerjee, C., et al., *Study of polyacrylamide grafted starch based algal flocculation towards applications in algal biomass harvesting.* Int J Biol Macromol, 2012. **51**(4): p. 456-61.

237. Farooq, W., et al., *Efficient microalgae harvesting by organo-building blocks of nanoclays.* Green Chemistry, 2013. **15**(3): p. 749-755.

238. Lee, Y.C., et al., *Harvesting of oleaginous Chlorella sp. by organoclays.* Bioresour Technol, 2013. **132**: p. 440-5.

239. Sukenik, A., D. Bilanovic, and G. Shelef, *Flocculation of microalgae in brackish and sea waters.* Biomass, 1988. **15**(3): p. 187-199.

240. Bilanovic, D., G. Shelef, and A. Sukenik, *Flocculation of microalgae with cationic polymers — Effects of medium salinity.* Biomass, 1988. **17**(1): p. 65-76.

241. Abd-El-Haleem, D.A., et al., *Isolation and characterization of extracellular bioflocculants produced by bacteria isolated from Qatari ecosystems.* Pol J Microbiol, 2008. **57**(3): p. 231-9.

242. Kim, D.G., et al., *Harvest of Scenedesmus sp. with bioflocculant and reuse of culture medium for subsequent high-density cultures.* Bioresour Technol, 2011. **102**(3): p. 3163-8.

243. Lee, A.K., D.M. Lewis, and P.J. Ashman, *Microbial flocculation, a potentially low-cost harvesting technique for marine microalgae for the production of biodiesel.* Journal of Applied Phycology, 2009. **21**(5): p. 559-567.

244. Vandamme, D., et al., *Flocculation of Chlorella vulgaris induced by high pH: role of magnesium and calcium and practical implications.* Bioresour Technol, 2012. **105**: p. 114-9.

245. Lee, et al., *Effects of harvesting method and growth stage on the flocculation of the green alga Botryococcus braunii.* Letters in Applied Microbiology, 1998. **27**(1): p. 14-18.

246. Wu, Z., et al., *Evaluation of flocculation induced by pH increase for harvesting microalgae and reuse of flocculated medium.* Bioresour Technol, 2012. **110**: p. 496-502.

247. Hanotu, J., H.C.H. Bandulasena, and W.B. Zimmerman, *Microflotation performance for algal separation.* Biotechnology and Bioengineering, 2012. **109**(7): p. 1663-1673.

248. Henderson, R.K., S.A. Parsons, and B. Jefferson, *The impact of differing cell and algogenic organic matter (AOM) characteristics on the coagulation and flotation of algae.* Water Res, 2010. **44**(12): p. 3617-24.

249. Zimmerman, W.B., V. Tesař, and H.C.H. Bandulasena, *Towards energy efficient nanobubble generation with fluidic oscillation.* Current Opinion in Colloid & Interface Science, 2011. **16**(4): p. 350-356.

250. Cheng, Y.L., et al., *Harvesting of Scenedesmus obliquus FSP-3 using dispersed ozone flotation.* Bioresour Technol, 2011. **102**(1): p. 82-7.

251. Cheng, Y.-L., et al., *Dispersed ozone flotation of Chlorella vulgaris.* Bioresour Technol, 2010. **101**(23): p. 9092-9096.

252. Garg, S., et al., *Flotation of marine microalgae: effect of algal hydrophobicity.* Bioresour Technol, 2012. **121**: p. 471-4.

253. Ahmad, A.L., et al., *Crossflow microfiltration of microalgae biomass for biofuel production.* Desalination, 2012. **302**: p. 65-70.

254. Zhang, X., et al., *Harvesting algal biomass for biofuels using ultrafiltration membranes.* Bioresour Technol, 2010. **101**(14): p. 5297-304.

255. Chen, X., C. Huang, and T. Liu, *Harvesting of microalgae Scenedesmus sp. using polyvinylidene fluoride microfiltration membrane.* Desalination and Water Treatment, 2012. **45**(1-3): p. 177-181.

256. Bhave, R., et al., *Membrane-Based Energy Efficient Dewatering of Microalgae in Biofuels Production and Recovery of Value Added Co-Products.* Environ Sci Technol, 2012. **46**(10): p. 5599-5606.

257. Rios, S.D., et al., *Dynamic Microfiltration in Microalgae Harvesting for Biodiesel Production.* Industrial & Engineering Chemistry Research, 2011. **50**(4): p. 2455-2460.

258. Frappart, M., et al., *Influence of hydrodynamics in tangential and dynamic ultrafiltration systems for microalgae separation.* Desalination, 2011. **265**(1-3): p. 279-283.

259. Rios, S.D., et al., *Antifouling microfiltration strategies to harvest microalgae for biofuel.* Bioresour Technol, 2012. **119**: p. 406-18.

260. NASA. *OMEGA Project.* Available from: https://www.nasa.gov/centers/ames/news/features/2012/omega_algae_feature.html.

261. Markou, G. and E. Nerantzis, *Microalgae for high-value compounds and biofuels production: a review with focus on cultivation under stress conditions.* Biotechnol Adv, 2013. **31**(8): p. 1532-42.

262. Barros, A.I., et al., *Harvesting techniques applied to microalgae: A review.* Renewable and Sustainable Energy Reviews, 2015. **41**: p. 1489-1500.

263. Cath, T., A. Childress, and M. Elimelech, *Forward osmosis: Principles, applications, and recent developments.* Journal of Membrane Science, 2006. **281**(1-2): p. 70-87.

264. Zhao, S., et al., *Recent developments in forward osmosis: Opportunities and challenges.* Journal of Membrane Science, 2012. **396**: p. 1-21.

265. *Available online: http://en.wikipedia.org/wiki/Osmotic_pressure.*

266. Kravath, R.E. and J.A. Davis, *Desalination of sea water by direct osmosis.* Desalination, 1975. **16**(2): p. 151-155.

267. Kessler, J.O. and C.D. Moody, *Drinking water from sea water by forward osmosis.* Desalination, 1976. **18**(3): p. 297-306.

268. Moody, C.D. and J.O. Kessler, *Forward osmosis extractors.* Desalination, 1976. **18**(3): p. 283-295.

269. McCutcheon, J.R., R.L. McGinnis, and M. Elimelech, *A novel ammonia—carbon dioxide forward (direct) osmosis desalination process.* Desalination, 2005. **174**(1): p. 1-11.

270. McCutcheon, J.R., R.L. McGinnis, and M. Elimelech, *Desalination by ammonia–carbon dioxide forward osmosis: Influence of draw and feed solution concentrations on process performance.* Journal of Membrane Science, 2006. **278**(1-2): p. 114-123.

271. McGinnis, R.L. and M. Elimelech, *Energy requirements of ammonia–carbon dioxide forward osmosis desalination.* Desalination, 2007. **207**(1-3): p. 370-382.

272. Khaydarov, R.A. and R.R. Khaydarov, *Solar powered direct osmosis desalination.* Desalination, 2007. **217**(1–3): p. 225-232.

273. TAN, et al., *A novel hybrid forward osmosis - nanofiltration (FO-NF) process for seawater desalination: Draw solution selection and system configuration.* Vol. 13. 2010, L'Aquila, ITALIE: Desalination Publications. 6.

274. Ling, M.M. and T.-S. Chung, *Desalination process using super hydrophilic nanoparticles via forward osmosis integrated with ultrafiltration regeneration.* Desalination, 2011. **278**(1-3): p. 194-202.

275. Zhao, S., L. Zou, and D. Mulcahy, *Brackish water desalination by a hybrid forward osmosis–nanofiltration system using divalent draw solute.* Desalination, 2012. **284**: p. 175-181.

276. Bamaga, O.A., et al., *Hybrid FO/RO desalination system: Preliminary assessment of osmotic energy recovery and designs of new FO membrane module configurations.* Desalination, 2011. **268**(1-3): p. 163-169.

277. BAMAGA, et al., *Application of forward osmosis in pretreatment of seawater for small reverse osmosis desalination units.* Vol. 5. 2009, L'Aquila, ITALIE: Desalination Publications. 9.

278. Yangali-Quintanilla, V., et al., *Indirect desalination of Red Sea water with forward osmosis and low pressure reverse osmosis for water reuse.* Desalination, 2011. **280**(1-3): p. 160-166.

279. *Oasys Water Inc.*; Available from: http://oasyswater.com/news-post/power-magazine-water-and-wastewater-treatment-technology-update/.

280. Klaysom, C., et al., *Forward and pressure retarded osmosis: Potential solutions for global challenges in energy and water supply.* Chemical Society Reviews, 2013. **42**(16): p. 6959-6989.

281. Coday, B.D., et al., *The sweet spot of forward osmosis: Treatment of produced water, drilling wastewater, and other complex and difficult liquid streams.* Desalination, 2014. **333**(1): p. 23-35.

282. Kim, E.-S., Y. Liu, and M. Gamal El-Din, *The effects of pretreatment on nanofiltration and reverse osmosis membrane filtration for desalination of oil sands process-affected water.* Separation and Purification Technology, 2011. **81**(3): p. 418-428.

283. Sutzkover-Gutman, I. and D. Hasson, *Feed water pretreatment for desalination plants.* Desalination, 2010. **264**(3): p. 289-296.

284. Cartinella, J.L., et al., *Removal of natural steroid hormones from wastewater using membrane contactor processes.* Environ Sci Technol, 2006. **40**(23): p. 7381-6.

285. Cath, T.Y., et al., *Membrane contactor processes for wastewater reclamation in space: Part I. Direct osmotic concentration as pretreatment for reverse osmosis.* Journal of Membrane Science, 2005. **257**(1–2): p. 85-98.

286. Holloway, R.W., et al., *Forward osmosis for concentration of anaerobic digester centrate.* Water Res, 2007. **41**(17): p. 4005-14.

287. Cornelissen, E., et al., *Membrane fouling and process performance of forward osmosis membranes on activated sludge.* Journal of Membrane Science, 2008. **319**(1-2): p. 158-168.

288. Cornelissen, E.R., et al., *The innovative osmotic membrane bioreactor (OMBR) for reuse of wastewater.* Water Sci Technol, 2011. **63**(8): p. 1557-65.

289. Xiao, D., et al., *Modeling salt accumulation in osmotic membrane bioreactors: Implications for FO membrane selection and system operation.* Journal of Membrane Science, 2011. **366**(1–2): p. 314-324.

290. Chen, L., et al., *Performance of a submerged anaerobic membrane bioreactor with forward osmosis membrane for low-strength wastewater treatment.* Water Res, 2014. **50**: p. 114-123.

291. Tang, M.K. and H.Y. Ng, *Impacts of different draw solutions on a novel anaerobic forward osmosis membrane bioreactor (AnFOMBR).* Water Sci Technol, 2014. **69**(10): p. 2036-42.

292. Gu, Y., et al., *Development of anaerobic osmotic membrane bioreactor for low-strength wastewater treatment at mesophilic condition.* Journal of Membrane Science, 2015. **490**: p. 197-208.

293. Gao, Y., et al., *Novel Approach To Characterizing the Growth of a Fouling Layer during Membrane Filtration via Optical Coherence Tomography.* Environ Sci Technol, 2014. **48**(24): p. 14273-14281.

294. Alturki, A., et al., *Performance of a novel osmotic membrane bioreactor (OMBR) system: Flux stability and removal of trace organics.* Bioresour Technol, 2012. **113**: p. 201-206.

295. Wang, X., et al., *Integration of micro-filtration into osmotic membrane bioreactors to prevent salinity build-up.* Bioresour Technol, 2014. **167**: p. 116-123.

296. Qiu, G., et al., *Direct and Complete Phosphorus Recovery from Municipal Wastewater Using a Hybrid Microfiltration-Forward Osmosis Membrane Bioreactor Process with Seawater Brine as Draw Solution.* Environ Sci Technol, 2015. **49**(10): p. 6156-6163.

297. Holloway, R.W., et al., *Removal of Trace Organic Chemicals and Performance of a Novel Hybrid Ultrafiltration-Osmotic Membrane Bioreactor.* Environ Sci Technol, 2014. **48**(18): p. 10859-10868.

298. Holloway, R.W., et al., *Long-term pilot scale investigation of novel hybrid ultrafiltration-osmotic membrane bioreactors.* Desalination, 2015. **363**: p. 64-74.

299. Wang, X., V.W.C. Chang, and C.Y. Tang, *Osmotic membrane bioreactor (OMBR) technology for wastewater treatment and reclamation: Advances, challenges, and prospects for the future.* Journal of Membrane Science, 2016. **504**: p. 113-132.

300. Dova, M.I., K.B. Petrotos, and H.N. Lazarides, *On the direct osmotic concentration of liquid foods. Part I: Impact of process parameters on process performance.* Journal of Food Engineering, 2007. **78**(2): p. 422-430.

301. Sant'Anna, V., L.D.F. Marczak, and I.C. Tessaro, *Membrane concentration of liquid foods by forward osmosis: Process and quality view.* Journal of Food Engineering, 2012. **111**(3): p. 483-489.

302. Petrotos, K.B., et al., *A description of a flat geometry direct osmotic concentrator to concentrate tomato juice at ambient temperature and low pressure.* Journal of Food Engineering, 2010. **97**(2): p. 235-242.

303. Jiao, B., A. Cassano, and E. Drioli, *Recent advances on membrane processes for the concentration of fruit juices: a review.* Journal of Food Engineering, 2004. **63**(3): p. 303-324.

304. Petrotos, K.B., P. Quantick, and H. Petropakis, *A study of the direct osmotic concentration of tomato juice in tubular membrane – module configuration. I. The effect of certain basic process parameters on the process performance.* Journal of Membrane Science, 1998. **150**(1): p. 99-110.

305. Changrue, V., et al., *Effect of osmotic dehydration on the dielectric properties of carrots and strawberries.* Journal of Food Engineering, 2008. **88**(2): p. 280-286.

306. Khoyi, M.R. and J. Hesari, *Osmotic dehydration kinetics of apricot using sucrose solution.* Journal of Food Engineering, 2007. **78**(4): p. 1355-1360.

307. Park, K.J., et al., *Osmotic dehydration kinetics of pear D'anjou (Pyrus communis L.).* Journal of Food Engineering, 2002. **52**(3): p. 293-298.

308. Eren, İ. and F. Kaymak-Ertekin, *Optimization of osmotic dehydration of potato using response surface methodology.* Journal of Food Engineering, 2007. **79**(1): p. 344-352.

309. Ozdemir, M., et al., *Optimization of osmotic dehydration of diced green peppers by response surface methodology.* LWT - Food Science and Technology, 2008. **41**(10): p. 2044-2050.

310. Uddin, M.B., P. Ainsworth, and Ş. İbanoğlu, *Evaluation of mass exchange during osmotic dehydration of carrots using response surface methodology.* Journal of Food Engineering, 2004. **65**(4): p. 473-477.

311. Babu, B.R., N.K. Rastogi, and K.S.M.S. Raghavarao, *Effect of process parameters on transmembrane flux during direct osmosis.* Journal of Membrane Science, 2006. **280**(1–2): p. 185-194.

312. Nayak, C.A., S.S. Valluri, and N.K. Rastogi, *Effect of high or low molecular weight of components of feed on transmembrane flux during forward osmosis.* Journal of Food Engineering, 2011. **106**(1): p. 48-52.

313. Aydiner, C., et al., *A novel implementation of water recovery from whey: "forward–reverse osmosis" integrated membrane system.* Desalination and Water Treatment, 2013. **51**(4-6): p. 786-799.

314. Garcia-Castello, E.M. and J.R. McCutcheon, *Dewatering press liquor derived from orange production by forward osmosis.* Journal of Membrane Science, 2011. **372**(1–2): p. 97-101.

315. Wrolstad, R.E., et al., *Composition and Sensory Characterization of Red Raspberry Juice Concentrated by Direct-Osmosis or Evaporation.* Journal of Food Science, 1993. **58**(3): p. 633-637.

316. Rodriguez-Saona, L.E., et al., *DEVELOPMENT AND PROCESS OPTIMIZATION OF RED RADISH CONCENTRATE EXTRACT AS POTENTIAL NATURAL RED COLORANT.* Journal of Food Processing and Preservation, 2001. **25**(3): p. 165-182.

317. Herron, J.R., et al., *Osmotic concentration apparatus and method for direct osmotic concentration of fruit juices*, 1994, Google Patents.

318. Sotthivirat, S., J.L. Haslam, and V.J. Stella, *Controlled porosity-osmotic pump pellets of a poorly water-soluble drug using sulfobutylether-beta-cyclodextrin, (SBE) 7M-beta-CD, as a solubilizing and osmotic agent.* J Pharm Sci, 2007. **96**(9): p. 2364-74.

319. Verma, R.K., S. Arora, and S. Garg, *Osmotic pumps in drug delivery.* Crit Rev Ther Drug Carrier Syst, 2004. **21**(6): p. 477-520.

320. Keraliya, R.A., et al., *Osmotic Drug Delivery System as a Part of Modified Release Dosage Form.* ISRN Pharmaceutics, 2012. **2012**: p. 528079.

321. Bhatt, P.P., *Osmotic drug delivery systems for poorly soluble drugs*, 2004, PharmaVentures Ltd.: Oxford, UK.

322. Yang, Q., K.Y. Wang, and T.-S. Chung, *A novel dual-layer forward osmosis membrane for protein enrichment and concentration.* Separation and Purification Technology, 2009. **69**(3): p. 269-274.

323. Loeb, S., *Production of energy from concentrated brines by pressure-retarded osmosis.* Journal of Membrane Science, 1976. **1**: p. 49-63.

324. Loeb, S., F. Van Hessen, and D. Shahaf, *Production of energy from concentrated brines by pressure-retarded osmosis.* Journal of Membrane Science, 1976. **1**: p. 249-269.

325. Veerman, J., et al., *Reverse electrodialysis: Performance of a stack with 50 cells on the mixing of sea and river water.* Journal of Membrane Science, 2009. **327**(1–2): p. 136-144.

326. WEINSTEIN, J.N. and F.B. LEITZ, *Electric Power from Differences in Salinity: The Dialytic Battery.* Science, 1976. **191**(4227): p. 557-559.

327. Wick, G.L. and W.R. Schmitt, *PROSPECTS FOR RENEWABLE ENERGY FROM THE SEA.* Marine Technology Society Journal, 1977. **11**(5-6): p. 16-21.

328. Yip, N.Y., et al., *Thin-Film Composite Pressure Retarded Osmosis Membranes for Sustainable Power Generation from Salinity Gradients.* Environmental Science & Technology, 2011. **45**(10): p. 4360-4369.

329. MCGINNIS, et al., *Global Challenges in Energy and Water Supply : The Promise of Engineered Osmosis*. Vol. 42. 2008, Washington, DC, ETATS-UNIS: American Chemical Society. 5.

330. *Waterworld Article. Available online: http://www.waterworld.com/articles/wwi/print/volume-28/issue-2/regional-spotlight-europe/norway-s-osmotic-power-a-salty.html (accessed on 14 April 2017).*

331. Schäfer, A.I., A.G. Fane, and T.D. Waite, *Nanofiltration : principles and applications*. 2005, Oxford: Elsevier.

332. Zhang, S., et al., *Well-constructed cellulose acetate membranes for forward osmosis: Minimized internal concentration polarization with an ultra-thin selective layer.* Journal of Membrane Science, 2010. **360**(1–2): p. 522-535.

333. Cano-Odena, A., et al., *Optimization of cellulose acetate nanofiltration membranes for micropollutant removal via genetic algorithms and high throughput experimentation.* Journal of Membrane Science, 2011. **366**(1–2): p. 25-32.

334. Wang, K.Y., R.C. Ong, and T.-S. Chung, *Double-Skinned Forward Osmosis Membranes for Reducing Internal Concentration Polarization within the Porous Sublayer.* Industrial & Engineering Chemistry Research, 2010. **49**(10): p. 4824-4831.

335. Herron, J., *Asymmetric forward osmosis membranes*, 2008, Google Patents.

336. Zhang, S., et al., *Molecular design of the cellulose ester-based forward osmosis membranes for desalination.* Chemical Engineering Science, 2011. **66**(9): p. 2008-2018.

337. Ong, R.C. and T.-S. Chung, *Fabrication and positron annihilation spectroscopy (PAS) characterization of cellulose triacetate membranes for forward osmosis.* Journal of Membrane Science, 2012. **394–395**: p. 230-240.

338. Aerts, P., et al., *The role of the nature of the casting substrate on the properties of membranes prepared via immersion precipitation.* Journal of Membrane Science, 2006. **283**(1–2): p. 320-327.

339. Yip, N.Y., et al., *Thin-Film Composite Pressure Retarded Osmosis Membranes for Sustainable Power Generation from Salinity Gradients.* Environ Sci Technol, 2011. **45**(10): p. 4360-4369.

340. Yip, N.Y., et al., *High Performance Thin-Film Composite Forward Osmosis Membrane.* Environ Sci Technol, 2010. **44**(10): p. 3812-3818.

341. Tiraferri, A., et al., *Relating performance of thin-film composite forward osmosis membranes to support layer formation and structure.* Journal of Membrane Science, 2011. **367**(1-2): p. 340-352.

342. Wei, X., et al., *A novel method of surface modification on thin-film-composite reverse osmosis membrane by grafting hydantoin derivative.* Journal of Membrane Science, 2010. **346**(1): p. 152-162.

343. Yu, Y., et al., *Nanoporous polyethersulfone (PES) membrane with enhanced flux applied in forward osmosis process.* Journal of Membrane Science, 2011. **375**(1–2): p. 63-68.

344. Ghosh, A.K. and E.M.V. Hoek, *Impacts of support membrane structure and chemistry on polyamide–polysulfone interfacial composite membranes.* Journal of Membrane Science, 2009. **336**(1–2): p. 140-148.

345. Song, X., Z. Liu, and D.D. Sun, *Nano Gives the Answer: Breaking the Bottleneck of Internal Concentration Polarization with a Nanofiber Composite Forward Osmosis Membrane for a High Water Production Rate.* Advanced Materials, 2011. **23**(29): p. 3256-3260.

346. Bui, N.-N., et al., *Electrospun nanofiber supported thin film composite membranes for engineered osmosis.* Journal of Membrane Science, 2011. **385–386**: p. 10-19.

347. Hoover, L.A., J.D. Schiffman, and M. Elimelech, *Nanofibers in thin-film composite membrane support layers: Enabling expanded application of forward and pressure retarded osmosis.* Desalination, 2013. **308**: p. 73-81.

348. McCutcheon, J.R. and M. Elimelech, *Influence of concentrative and dilutive internal concentration polarization on flux behavior in forward osmosis.* Journal of Membrane Science, 2006. **284**(1-2): p. 237-247.

349. Zydney, A.L., *Stagnant film model for concentration polarization in membrane systems.* Journal of Membrane Science, 1997. **130**(1–2): p. 275-281.

350. Sablani, S.S., et al., *Concentration polarization in ultrafiltration and reverse osmosis: a critical review.* Desalination, 2001. **141**(3): p. 269-289.

351. Thorsen, T., *Concentration polarisation by natural organic matter (NOM) in NF and UF.* Journal of Membrane Science, 2004. **233**(1–2): p. 79-91.

352. Kim, S. and E.M.V. Hoek, *Modeling concentration polarization in reverse osmosis processes.* Desalination, 2005. **186**(1–3): p. 111-128.

353. Song, L. and M. Elimelech, *Theory of concentration polarization in crossflow filtration.* Journal of the Chemical Society, Faraday Transactions, 1995. **91**(19): p. 3389-3398.

354. Elimelech, M. and S. Bhattacharjee, *A novel approach for modeling concentration polarization in crossflow membrane filtration based on the equivalence of osmotic pressure model and filtration theory.* Journal of Membrane Science, 1998. **145**(2): p. 223-241.

355. Mulder, M., *Basic Principles of Membrane Technology*. 1996: Kluwer Academic.

356. Mehta, G.D. and S. Loeb, *Performance of permasep B-9 and B-10 membranes in various osmotic regions and at high osmotic pressures.* Journal of Membrane Science, 1978. **4**(0): p. 335-349.

357. Mehta, G.D. and S. Loeb, *Internal polarization in the porous substructure of a semipermeable membrane under pressure-retarded osmosis.* Journal of Membrane Science, 1978. **4**(0): p. 261-265.

358. Gray, G.T., J.R. McCutcheon, and M. Elimelech, *Internal concentration polarization in forward osmosis: role of membrane orientation.* Desalination, 2006. **197**(1-3): p. 1-8.

359. Lee, K.L., R.W. Baker, and H.K. Lonsdale, *Membranes for power generation by pressure-retarded osmosis.* Journal of Membrane Science, 1981. **8**(2): p. 141-171.

360. Loeb, S., et al., *Effect of porous support fabric on osmosis through a Loeb-Sourirajan type asymmetric membrane.* Journal of Membrane Science, 1997. **129**(2): p. 243-249.

361. Achilli, A., T.Y. Cath, and A.E. Childress, *Selection of inorganic-based draw solutions for forward osmosis applications.* Journal of Membrane Science, 2010. **364**(1-2): p. 233-241.

362. Yong, J.S., W.A. Phillip, and M. Elimelech, *Coupled reverse draw solute permeation and water flux in forward osmosis with neutral draw solutes.* Journal of Membrane Science, 2012. **392-393**: p. 9-17.

363. Bamaga, O.A., A. Yokochi, and E.G. Beaudry, *Application of forward osmosis in pretreatment of seawater for small reverse osmosis desalination units.* Desalination and Water Treatment, 2009. **5**(1-3): p. 183-191.

364. Phuntsho, S., et al., *A novel low energy fertilizer driven forward osmosis desalination for direct fertigation: Evaluating the performance of fertilizer draw solutions.* Journal of Membrane Science, 2011. **375**(1-2): p. 172-181.

365. Ge, Q., et al., *Exploration of polyelectrolytes as draw solutes in forward osmosis processes.* Water Res, 2012. **46**(4): p. 1318-1326.

366. Phuntsho, S., et al., *Blended fertilizers as draw solutions for fertilizer-drawn forward osmosis desalination.* Environmental Science and Technology, 2012. **46**(8): p. 4567-4575.

367. Tan, C.H. and H.Y. Ng, *A novel hybrid forward osmosis - nanofiltration (FO-NF) process for seawater desalination: Draw solution selection and system configuration.* Desalination and Water Treatment, 2010. **13**(1-3): p. 356-361.

368. McCormick, P., et al., *Water, salt, and ethanol diffusion through membranes for water recovery by forward (direct) osmosis processes.* Journal of Membrane Science, 2008. **325**(1): p. 467-478.

369. Kim, T.-w., et al., *Systematic approach for draw solute selection and optimal system design for forward osmosis desalination.* Desalination, 2012. **284**: p. 253-260.

370. Lutchmiah, K., et al., *Forward osmosis for application in wastewater treatment: A review.* Water Res, 2014. **58**: p. 179-197.

371. Bowden, K.S., A. Achilli, and A.E. Childress, *Organic ionic salt draw solutions for osmotic membrane bioreactors.* Bioresour Technol, 2012. **122**: p. 207-216.

372. Ling, M.M., K.Y. Wang, and T.-S. Chung, *Highly Water-Soluble Magnetic Nanoparticles as Novel Draw Solutes in Forward Osmosis for Water Reuse.* Industrial & Engineering Chemistry Research, 2010. **49**(12): p. 5869-5876.

373. Neff, R.A., *Solvent extractor*, 1964, Google Patents.

374. Batchelder, G.W., *Process for the demineralization of water*, 1965, Google Patents.

375. Glew, D.N., *Process for liquid recovery and solution concentration*, 1965, Google Patents.

376. McGinnis, R.L., *Osmotic desalinization process*, 2002, Google Patents.

377. Ling, M.M. and T.-S. Chung, *Novel dual-stage FO system for sustainable protein enrichment using nanoparticles as intermediate draw solutes.* Journal of Membrane Science, 2011. **372**(1-2): p. 201-209.

378. Ling, M.M., T.-S. Chung, and X. Lu, *Facile synthesis of thermosensitive magnetic nanoparticles as "smart" draw solutes in forward osmosis.* Chemical Communications, 2011. **47**(38): p. 10788-10790.

379. Ge, Q., et al., *Hydrophilic Superparamagnetic Nanoparticles: Synthesis, Characterization, and Performance in Forward Osmosis Processes.* Industrial & Engineering Chemistry Research, 2011. **50**(1): p. 382-388.

380. Bai, H., Z. Liu, and D.D. Sun, *Highly water soluble and recovered dextran coated Fe3O4 magnetic nanoparticles for brackish water desalination.* Separation and Purification Technology, 2011. **81**(3): p. 392-399.

381. Ge, Q., et al., *Exploration of polyelectrolytes as draw solutes in forward osmosis processes.* Water Res, 2012. **46**(4): p. 1318-26.

382. Yen, S.K., et al., *Study of draw solutes using 2-methylimidazole-based compounds in forward osmosis.* Journal of Membrane Science, 2010. **364**(1-2): p. 242-252.

383. Ge, Q., et al., *Polyelectrolyte-Promoted Forward Osmosis–Membrane Distillation (FO–MD) Hybrid Process for Dye Wastewater Treatment.* Environ Sci Technol, 2012. **46**(11): p. 6236-6243.

384. Lee, S., et al., *Comparison of fouling behavior in forward osmosis (FO) and reverse osmosis (RO).* Journal of Membrane Science, 2010. **365**(1-2): p. 34-39.

385. Mi, B. and M. Elimelech, *Chemical and physical aspects of organic fouling of forward osmosis membranes.* Journal of Membrane Science, 2008. **320**(1-2): p. 292-302.

386. She, Q., et al., *Relating reverse and forward solute diffusion to membrane fouling in osmotically driven membrane processes.* Water Res, 2012. **46**(7): p. 2478-2486.

387. *Zena Membranes*. Available from: http://www.zena-membranes.cz/index.php/news.

388. *Wageningen University & Research, Membrane Fouling*. Available from: http://www.wur.nl/en/show/Isolation-and-characterization-of-microorganism-involved-in-membrane-biofouling-1.htm.

389. Buffle, J., et al., *A Generalized Description of Aquatic Colloidal Interactions: The Three-colloidal Component Approach.* Environ Sci Technol, 1998. **32**(19): p. 2887-2899.

390. Tang, C.Y., T.H. Chong, and A.G. Fane, *Colloidal interactions and fouling of NF and RO membranes: A review.* Adv Colloid Interface Sci, 2011. **164**(1–2): p. 126-143.

391. Vrijenhoek, E.M., S. Hong, and M. Elimelech, *Influence of membrane surface properties on initial rate of colloidal fouling of reverse osmosis and nanofiltration membranes.* Journal of Membrane Science, 2001. **188**(1): p. 115-128.

392. Tang, C.Y., Y.-N. Kwon, and J.O. Leckie, *The role of foulant–foulant electrostatic interaction on limiting flux for RO and NF membranes during humic acid fouling—Theoretical basis, experimental evidence, and AFM interaction force measurement.* Journal of Membrane Science, 2009. **326**(2): p. 526-532.

393. Hoek, E.M.V., S. Bhattacharjee, and M. Elimelech, *Effect of Membrane Surface Roughness on Colloid–Membrane DLVO Interactions.* Langmuir, 2003. **19**(11): p. 4836-4847.

394. Al-Juboori, R.A. and T. Yusaf, *Biofouling in RO system: Mechanisms, monitoring and controlling.* Desalination, 2012. **302**: p. 1-23.

395. Janjaroen, D., et al., *Roles of ionic strength and biofilm roughness on adhesion kinetics of Escherichia coli onto groundwater biofilm grown on PVC surfaces.* Water Res, 2013. **47**(7): p. 2531-42.

396. Brant, J.A. and A.E. Childress, *Assessing short-range membrane–colloid interactions using surface energetics.* Journal of Membrane Science, 2002. **203**(1–2): p. 257-273.

397. Sim, L.N., et al., *Investigations of the coupled effect of cake-enhanced osmotic pressure and colloidal fouling in RO using crossflow sampler-modified fouling index ultrafiltration.* Desalination, 2011. **273**(1): p. 184-196.

398. Sim, S.T.V., et al., *Colloidal metastability and membrane fouling – Effects of crossflow velocity, flux, salinity and colloid concentration.* Journal of Membrane Science, 2014. **469**: p. 174-187.

399. Chong, T.H., F.S. Wong, and A.G. Fane, *Implications of critical flux and cake enhanced osmotic pressure (CEOP) on colloidal fouling in reverse osmosis: Experimental observations.* Journal of Membrane Science, 2008. **314**(1–2): p. 101-111.

400. Motsa, M.M., B.B. Mamba, and A.R.D. Verliefde, *Combined colloidal and organic fouling of FO membranes: The influence of foulant–foulant interactions and ionic strength.* Journal of Membrane Science, 2015. **493**: p. 539-548.

401. Gu, Y., et al., *Organic fouling of thin-film composite polyamide and cellulose triacetate forward osmosis membranes by oppositely charged macromolecules.* Water Res, 2013. **47**(5): p. 1867-1874.

402. Zularisam, A.W., A.F. Ismail, and R. Salim, *Behaviours of natural organic matter in membrane filtration for surface water treatment — a review.* Desalination, 2006. **194**(1): p. 211-231.

403. Parida, V. and H.Y. Ng, *Forward osmosis organic fouling: Effects of organic loading, calcium and membrane orientation.* Desalination, 2013. **312**: p. 88-98.

404. Zou, L., et al., *Surface hydrophilic modification of RO membranes by plasma polymerization for low organic fouling.* Journal of Membrane Science, 2011. **369**(1–2): p. 420-428.

405. Miyoshi, T., et al., *Important fractions of organic matter causing fouling of seawater reverse osmosis (SWRO) membranes.* Desalination, 2016. **390**: p. 72-80.

406. Motsa, M.M., et al., *Organic fouling in forward osmosis membranes: The role of feed solution chemistry and membrane structural properties.* Journal of Membrane Science, 2014. **460**: p. 99-109.

407. She, Q., et al., *Membrane fouling in osmotically driven membrane processes: A review.* Journal of Membrane Science, 2016. **499**: p. 201-233.

408. Antony, A., et al., *Scale formation and control in high pressure membrane water treatment systems: A review.* Journal of Membrane Science, 2011. **383**(1–2): p. 1-16.

409. Zhang, M., et al., *Gypsum scaling in pressure retarded osmosis: Experiments, mechanisms and implications.* Water Res, 2014. **48**: p. 387-395.

410. Mi, B. and M. Elimelech, *Gypsum Scaling and Cleaning in Forward Osmosis: Measurements and Mechanisms.* Environ Sci Technol, 2010. **44**(6): p. 2022-2028.

411. Arkhangelsky, E., et al., *Effects of scaling and cleaning on the performance of forward osmosis hollow fiber membranes.* Journal of Membrane Science, 2012. **415–416**: p. 101-108.

412. Liu, Y., R. Xiong, and Y. Li, *Robust and Accurate Multiple-Camera Pose Estimation toward Robotic Applications.* International Journal of Advanced Robotic Systems, 2014. **11**(9): p. 153.

413. Phuntsho, S., et al., *Membrane scaling and flux decline during fertiliser-drawn forward osmosis desalination of brackish groundwater.* Water Res, 2014. **57**: p. 172-182.

414. Mi, B. and M. Elimelech, *Silica scaling and scaling reversibility in forward osmosis.* Desalination, 2013. **312**: p. 75-81.

415. Herzberg, M. and M. Elimelech, *Biofouling of reverse osmosis membranes: Role of biofilm-enhanced osmotic pressure.* Journal of Membrane Science, 2007. **295**(1–2): p. 11-20.

416. Flemming, H.-C., *Reverse osmosis membrane biofouling.* Experimental Thermal and Fluid Science, 1997. **14**(4): p. 382-391.

417. Baker, J.S. and L.Y. Dudley, *Biofouling in membrane systems — A review.* Desalination, 1998. **118**(1): p. 81-89.

418. Vrouwenvelder, J.S. and D. van der Kooij, *Diagnosis, prediction and prevention of biofouling of NF and RO membranes.* Desalination, 2001. **139**(1): p. 65-71.

419. Flemming, H.C. and J. Wingender, *The biofilm matrix.* Nat Rev Microbiol, 2010. **8**(9): p. 623-33.

420. Chong, T.H., F.S. Wong, and A.G. Fane, *The effect of imposed flux on biofouling in reverse osmosis: Role of concentration polarisation and biofilm enhanced osmotic pressure phenomena.* Journal of Membrane Science, 2008. **325**(2): p. 840-850.

421. Ivnitsky, H., et al., *Biofouling formation and modeling in nanofiltration membranes applied to wastewater treatment.* Journal of Membrane Science, 2010. **360**(1–2): p. 165-173.

422. Kwan, S.E., E. Bar-Zeev, and M. Elimelech, *Biofouling in forward osmosis and reverse osmosis: Measurements and mechanisms.* Journal of Membrane Science, 2015. **493**: p. 703-708.

423. Yoon, H., et al., *Biofouling occurrence process and its control in the forward osmosis.* Desalination, 2013. **325**: p. 30-36.

424. Valladares Linares, R., et al., *Impact of spacer thickness on biofouling in forward osmosis.* Water Res, 2014. **57**: p. 223-233.

425. Kim, C.-M., et al., *Effects of phosphate limitation in feed water on biofouling in forward osmosis (FO) process.* Desalination, 2014. **349**: p. 51-59.

426. Kumar, M., S.S. Adham, and W.R. Pearce, *Investigation of Seawater Reverse Osmosis Fouling and Its Relationship To Pretreatment Type.* Environ Sci Technol, 2006. **40**(6): p. 2037-2044.

427. Ginic-Markovic, M., et al., *Biofouling resistance of polysulfobetaine coated reverse osmosis membranes.* Desalination, 2015. **369**: p. 37-45.

428. Wang, J., et al., *Improving the water flux and bio-fouling resistance of reverse osmosis (RO) membrane through surface modification by zwitterionic polymer.* Journal of Membrane Science, 2015. **493**: p. 188-199.

429. Razzak, S.A., et al., *Integrated CO2 capture, wastewater treatment and biofuel production by microalgae culturing—A review.* Renewable and Sustainable Energy Reviews, 2013. **27**: p. 622-653.

430. Gudin, C. and C. Thepenier, *Bioconversion of solar energy into organic chemicals by microalgae.* Advances in biotechnological processes, 1986. **6** p. 73-110.

431. Chen, C.-Y., et al., *Cultivation, photobioreactor design and harvesting of microalgae for biodiesel production: A critical review.* Bioresource Technology, 2011. **102**(1): p. 71-81.

432. Petruševski, B., et al., *Tangential flow filtration: A method to concentrate freshwater algae.* Water Research, 1995. **29**(5): p. 1419-1424.

433. Rickman, M., J. Pellegrino, and R. Davis, *Fouling phenomena during membrane filtration of microalgae.* Journal of Membrane Science, 2012. **423-424**: p. 33-42.

434. Bilad, M.R., H.A. Arafat, and I.F.J. Vankelecom, *Membrane technology in microalgae cultivation and harvesting: A review.* Biotechnology Advances, 32 (2014) 1283-1300., 2014. **32**(7): p. 1283-1300.

435. Zhang, X., et al., *Processing municipal wastewaters by forward osmosis using CTA membrane.* Journal of Membrane Science, 2014. **468**: p. 269-275.

436. Petrotos, K.B. and H.N. Lazarides, *Osmotic concentration of liquid foods.* Journal of Food Engineering, 2001. **49**(2–3): p. 201-206.

437. Marlaire, R.D., *NASA envisions "clean energy" from algae grown in waste water.* http://www.nasa.gov/centers/ames/news/features/2009/clean_energy_042209.html, 2009.

438. Nguyen, N.C., et al., *Application of forward osmosis on dewatering of high nutrient sludge.* Bioresource Technology, 2013. **132**(0): p. 224-229.

439. Lundin, C., C.S.o.M.D.o.E. Science, and Engineering, *A Novel Hybrid Forward Osmosis Process for Drinking Water Augmentation Using Impaired Water and Saline Water Sources*. 2008: Colorado School of Mines.

440. Suwarno, S.R., et al., *The impact of flux and spacers on biofilm development on reverse osmosis membranes.* Journal of Membrane Science, 2012. **405–406**(0): p. 219-232.

441. Hodaifa, G., et al., *Biomass production of Scenedesmus obliquus from mixtures of urban and olive-oil mill wastewaters used as culture medium.* Applied Energy, 2013. **104**: p. 345-352.

442. Lúcia Helena Ribeiro Rodrigues, A.A., Maria Teresa Raya-Rodriguez and Nelson Ferreira Fontoura, *Algal density assessed by spectrophotometry: A calibration curve for the unicellular algae Pseudokirchneriella subcapitata.* Journal of Environmental Chemistry and Ecotoxicology, 2011. **3.8**: p. 225-228.

443. Chisti, Y., *Biodiesel from microalgae.* Biotechnology Advances, 2007. **25**(3): p. 294-306.

444. Arnal, J.M., et al., *Concentration of brines from RO desalination plants by natural evaporation.* Desalination, 2005. **182**(1-3): p. 435-439.

445. Tang, C.Y., et al., *Coupled effects of internal concentration polarization and fouling on flux behavior of forward osmosis membranes during humic acid filtration.* Journal of Membrane Science, 2010. **354**(1-2): p. 123-133.

446. Jin, X., et al., *Boric Acid Permeation in Forward Osmosis Membrane Processes: Modeling, Experiments, and Implications.* Environmental Science & Technology, 2011. **45**(6): p. 2323-2330.

447. Jin, X., et al., *Rejection of pharmaceuticals by forward osmosis membranes.* Journal of Hazardous Materials, 2012. **227–228**: p. 55-61.

448. Coday, B.D., et al., *Effects of Transmembrane Hydraulic Pressure on Performance of Forward Osmosis Membranes.* Environmental Science & Technology, 2013. **47**(5): p. 2386-2393.

449. Bensadoun, A. and D. Weinstein, *Assay of proteins in the presence of interfering materials.* Analytical Biochemistry, 1976. **70**(1): p. 241-250.

450. DuBois, M., et al., *Colorimetric Method for Determination of Sugars and Related Substances.* Analytical Chemistry, 1956. **28**(3): p. 350-356.

451. Ren, J. and J.R. McCutcheon, *A new commercial thin film composite membrane for forward osmosis.* Desalination, 343 (2014) 187-193, (0).

452. Nightingale, E.R., *Phenomenological Theory of Ion Solvation. Effective Radii of Hydrated Ions.* The Journal of Physical Chemistry, 1959. **63**(9): p. 1381-1387.

453. Schaep, J., et al., *Influence of ion size and charge in nanofiltration.* Separation and Purification Technology, 1998. **14**(1–3): p. 155-162.

454. Gu, Y., et al., *Organic fouling of thin-film composite polyamide and cellulose triacetate forward osmosis membranes by oppositely charged macromolecules.* Water Research, 2013. **47**(5): p. 1867-1874.

455. Gao, D.-W., et al., *Membrane fouling in an anaerobic membrane bioreactor: Differences in relative abundance of bacterial species in the membrane foulant layer and in suspension.* Journal of Membrane Science, 2010. **364**(1-2): p. 331-338.

456. Davis, T.A., et al., *Metal Selectivity of Sargassum spp. and Their Alginates in Relation to Their α-l-Guluronic Acid Content and Conformation.* Environmental Science & Technology, 2002. **37**(2): p. 261-267.

457. Jin, X., X. Huang, and E.M.V. Hoek, *Role of Specific Ion Interactions in Seawater RO Membrane Fouling by Alginic Acid.* Environmental Science & Technology, 2009. **43**(10): p. 3580-3587.

458. Jin, X., et al., *Effects of feed water temperature on separation performance and organic fouling of brackish water RO membranes.* Desalination, 2009. **239**(1–3): p. 346-359.

459. Takeda, H., *Taxonomical assignment of chlorococal algae from their cell wall composition.* The International Journal of Plant Biochemistry, 1993. **34**(4): p. 1053-1055.

460. Tajmir-Riahi, H.-A., *Sugar interaction with calcium ion. synthesis and vibrational spectra of crystalline β-d-fructose and its calcium halide adducts.* Journal of Inorganic Biochemistry, 1986. **27**(2): p. 123-131.

461. Fang, Y., et al., *Binding behavior of calcium to polyuronates: Comparison of pectin with alginate.* Carbohydrate Polymers, 2008. **72**(2): p. 334-341.

462. Rolland, F., B. Moore, and J. Sheen, *Sugar Sensing and Signaling in Plants.* The Plant Cell, 2002. **14**(suppl 1): p. 185-205.

463. Hetherington, A.M. and C. Brownlee, *The Generation Of Ca2+ Signals In Plants.* Annual Review of Plant Biology, 2004. **55**(1): p. 401-427.

464. Larronde-Larretche, M. and X. Jin, *Microalgae (Scenedesmus obliquus) dewatering using forward osmosis membrane: Influence of draw solution chemistry.* Algal Research, 2016. **15**: p. 1-8.

465. Bilad, M.R., H.A. Arafat, and I.F. Vankelecom, *Membrane technology in microalgae cultivation and harvesting: a review.* Biotechnol Adv, 2014. **32**(7): p. 1283-300.

466. Jin, X., X. Huang, and E.M.V. Hoek, *Role of Specific Ion Interactions in Seawater RO Membrane Fouling by Alginic Acid.* Environ Sci Technol, 2009. **43**(10): p. 3580-3587.

467.   Davis, T.A., et al., *Metal Selectivity of Sargassum spp. and Their Alginates in Relation to Their α-l-Guluronic Acid Content and Conformation.* Environ Sci Technol, 2003. **37**(2): p. 261-267.

468.   Tadros, T., *Interfacial forces in aqueous media, Carel J. van Oss, Marcel Dekker Inc., New York, 1994, viii + 440 pp., price US$165.00. ISBN 0 8247 9168 1.* Journal of Chemical Technology & Biotechnology, 1995. **64**(3): p. 311-311.

469.   Kim, S., et al., *Crossflow membrane filtration of interacting nanoparticle suspensions.* Journal of Membrane Science, 2006. **284**(1–2): p. 361-372.

470.   Kim, A.S. and E.M.V. Hoek, *Cake Structure in Dead-End Membrane Filtration: Monte Carlo Simulations.* Environmental Engineering Science, 2002. **19**(6): p. 373-386.

471.   Baerdemaeker, T.D., et al., *Benchmark study on algae harvesting with backwashable submerged flat panel membranes.* Bioresour Technol, 2013. **129**: p. 582-591.

472.   Wicaksana, F., et al., *Microfiltration of algae (Chlorella sorokiniana): Critical flux, fouling and transmission.* Journal of Membrane Science, 2012. **387–388**: p. 83-92.

473.   James, G.O., et al., *Fatty acid profiling of Chlamydomonas reinhardtii under nitrogen deprivation.* Bioresource Technology, 2011. **102**(3): p. 3343-3351.

474.   Ruiz-Marin, A., L.G. Mendoza-Espinosa, and T. Stephenson, *Growth and nutrient removal in free and immobilized green algae in batch and semi-continuous cultures treating real wastewater.* Bioresour Technol, 2010. **101**(1): p. 58-64.

475.   Kong, Q.X., et al., *Culture of microalgae Chlamydomonas reinhardtii in wastewater for biomass feedstock production.* Appl Biochem Biotechnol, 2010. **160**(1): p. 9-18.

476.   Fan, L.-H., et al., *Evaluation of a membrane-sparged helical tubular photobioreactor for carbon dioxide biofixation by Chlorella vulgaris.* Journal of Membrane Science, 2008. **325**(1): p. 336-345.

477.   Chen, C.Y., et al., *Biosorption of cadmium by CO(2)-fixing microalga Scenedesmus obliquus CNW-N.* Bioresour Technol, 2012. **105**: p. 74-80.

478.   Ren, J. and J.R. McCutcheon, *A new commercial thin film composite membrane for forward osmosis.* Desalination, 2014. **343**: p. 187-193.

479.   Kim, C., et al., *Boron transport in forward osmosis: Measurements, mechanisms, and comparison with reverse osmosis.* Journal of Membrane Science, 2012. **419–420**: p. 42-48.

480.   Hoek, E.M.V. and M. Elimelech, *Cake-Enhanced Concentration Polarization: A New Fouling Mechanism for Salt-Rejecting Membranes.* Environ Sci Technol, 2003. **37**(24): p. 5581-5588.

481.   Xie, M., et al., *Role of Reverse Divalent Cation Diffusion in Forward Osmosis Biofouling.* Environ Sci Technol, 2015. **49**(22): p. 13222-13229.

482.   De Baerdemaeker, T., et al., *Benchmark study on algae harvesting with backwashable submerged flat panel membranes.* Bioresour Technol, 2013. **129**: p. 582-91.

483.   Arabi, S. and G. Nakhla, *Impact of magnesium on membrane fouling in membrane bioreactors.* Separation and Purification Technology, 2009. **67**(3): p. 319-325.

484.   Lee, S. and M. Elimelech, *Relating Organic Fouling of Reverse Osmosis Membranes to Intermolecular Adhesion Forces.* Environ Sci Technol, 2006. **40**(3): p. 980-987.

485.   Petruševski, B., et al., *Tangential flow filtration: A method to concentrate freshwater algae.* Water Res, 1995. **29**(5): p. 1419-1424.

486.   de Kerchove, A.J. and M. Elimelech, *Calcium and Magnesium Cations Enhance the Adhesion of Motile and Nonmotile Pseudomonas aeruginosa on Alginate Films.* Langmuir, 2008. **24**(7): p. 3392-3399.

487.   Vandanjon, L., et al., *Effects of shear on two microalgae species. Contribution of pumps and valves in tangential flow filtration systems.* Biotechnol Bioeng, 1999. **63**(1): p. 1-9.

488.   Rolland, F., B. Moore, and J. Sheen, *Sugar sensing and signaling in plants.* Plant Cell, 2002. **14**(205): p. S185-205.

489.   Hetherington, A.M. and C. Brownlee, *The generation of Ca(2+) signals in plants.* Annu Rev Plant Biol, 2004. **55**: p. 401-27.

490. Templeton, D.W., et al., *Separation and quantification of microalgal carbohydrates.* Journal of Chromatography A, 2012. **1270**: p. 225-234.

491. Aspinall, G.O., *The Polysaccharides*. 2014: Elsevier Science.

492. Guo, J., Y. Lu, and R. Whiting, *Metal-Ion Interactions with Sugars. The Crystal Structure of CaCl2-Fructose Complex.* Bulletin of the Korean Chemical Society, 2012. **33**(6): p. 2028-2030.

493. Cioci, G., et al., *Structural basis of calcium and galactose recognition by the lectin PA-IL of Pseudomonas aeruginosa.* FEBS Letters, 2003. **555**(2): p. 297-301.

494. Jiang, K.-s. and G.A. Barber, *Polysaccharide from cell walls of Chlamydomonas reinhardtii.* Phytochemistry, 1975. **14**(11): p. 2459-2461.

495. Guo, S.-L., et al., *Characterization of flocculating agent from the self-flocculating microalga Scenedesmus obliquus AS-6-1 for efficient biomass harvest.* Bioresource Technology, 2013. **145**(0): p. 285-289.

496. Voigt, J., P. Münzner, and H.-P. Vogeler, *The cell-wall glycoproteins of Chlamydomonas reinhardtii: analysis of the in vitro translation products.* Plant Science, 1991. **75**(1): p. 129-142.

497. Cheng, Y.-S., et al., *The impact of cell wall carbohydrate composition on the chitosan flocculation of Chlorella.* Process Biochemistry, 2011. **46**(10): p. 1927-1933.

498. Kim, B., G. Gwak, and S. Hong, *Review on methodology for determining forward osmosis (FO) membrane characteristics: Water permeability (A), solute permeability (B), and structural parameter (S).* Desalination, 2017. **422**(Supplement C): p. 5-16.

499. Koutsou, C.P., S.G. Yiantsios, and A.J. Karabelas, *Direct numerical simulation of flow in spacer-filled channels: Effect of spacer geometrical characteristics.* Journal of Membrane Science, 2007. **291**(1-2): p. 53-69.

500. Koutsou, C.P., S.G. Yiantsios, and A.J. Karabelas, *A numerical and experimental study of mass transfer in spacer-filled channels: Effects of spacer geometrical characteristics and Schmidt number.* Journal of Membrane Science, 2009. **326**(1): p. 234-251.

501. Staverman, A.J., *The theory of measurement of osmotic pressure.* Recueil des Travaux Chimiques des Pays-Bas, 1951. **70**(4): p. 344-352.

502. She, Q., X. Jin, and C.Y. Tang, *Osmotic power production from salinity gradient resource by pressure retarded osmosis: Effects of operating conditions and reverse solute diffusion.* Journal of Membrane Science, 2012. **401–402**(0): p. 262-273.

503. Larronde-Larretche, M. and X. Jin, *Microalgal biomass dewatering using forward osmosis membrane: Influence of microalgae species and carbohydrates composition.* Algal Research, 2017. **23**: p. 12-19.

504. Praveen, P. and K.-C. Loh, *Nitrogen and phosphorus removal from tertiary wastewater in an osmotic membrane photobioreactor.* Bioresour Technol, 2016. **206**: p. 180-187.

505. Tiraferri, A. and M. Elimelech, *Direct quantification of negatively charged functional groups on membrane surfaces.* Journal of Membrane Science, 2012. **389**: p. 499-508.

506. Lee, S. and Y.C. Kim, *Calcium carbonate scaling by reverse draw solute diffusion in a forward osmosis membrane for shale gas wastewater treatment.* Journal of Membrane Science, 2017. **522**: p. 257-266.

507. Aiyuk, S. and W. Verstraete, *Sedimentological evolution in an UASB treating SYNTHES, a new representative synthetic sewage, at low loading rates.* Bioresour Technol, 2004. **93**(3): p. 269-278.

508. Luo, H., et al., *A review on the recovery methods of draw solutes in forward osmosis.* Journal of Water Process Engineering, 2014. **4**(Supplement C): p. 212-223.

509. *Council Directive 98/83/EC of 3 November 1998 on the quality of water intended for human consumption* Official Journal p. P. 0032 - 0054.

List of author's publications and conference presentations

Publications:

Tang, L., et al., *Imparting antimicrobial and anti-adhesive properties to polysulfone membranes through modification with silver nanoparticles and polyelectrolyte multilayers.* Journal of Colloid and Interface Science, 2015. **451**(Supplement C): p. 125-133.

Larronde-Larretche, M. and X. Jin, *Microalgae (Scenedesmus obliquus) dewatering using forward osmosis membrane: Influence of draw solution chemistry.* Algal Research, 2016. **15**: p. 1-8.

Larronde-Larretche, M. and X. Jin, *Microalgal biomass dewatering using forward osmosis membrane: Influence of microalgae species and carbohydrates composition.* Algal Research, 2017. **23**: p. 12-19.

Publications under review / preparation:

Larronde-Larretche, M. and X. Jin, *Integration of Forward Osmosis in the Treatment of Sewage by Chlorella vulgaris: Comparison between Internal and Immersed Systems.*

Conference presentations:

5th UK Algae Conference, Glasgow, UK, 2015, *Concentration of Microalgal Biomass by Forward Osmosis.*

9th International Membrane Science and Technology Conference (IMSTEC), Adelaide, Australia, 2016, *Toward a Better Understanding of the Fouling Mechanisms during Microalgae Dewatering by Forward Osmosis.*

8th International Water Association - Membrane Technology Conference (IWA-MTC), Singapore, 2017, *Integration of Forward Osmosis in the Treatment of Sewage by Chlorella vulgaris.*

Appendices

Appendix 1: Composition of Modified BG11 Medium

Component	Concentration (mg/L)
$NaNO_3$	1500
$MgSO_4 \cdot 7H_2O$	7
$K_2HPO_4 \cdot 3H_2O$	40
$CaCl_2 \cdot 2H_2O$	36
H_3BO_3	2.86
$MnCl_2 \cdot 4H_2O$	1.81
Na_2EDTA	1
$Na_2MoO_4 \cdot 7H_2O$	0.391
$ZnSO_4 \cdot 7H2O$	0.222
$CuSO_4 \cdot 5H2O$	0.079
$CoCl_2 \cdot 6H_2O$	0.05

Appendix 2: Calibration Curve - Determination of Biomass Concentration

The following example explains the method that has been applied for the determination of microalgae concentration from the optical density measured at 435nm. This example has been conducted with *S. obliquus*. The accurate concentration of microalgae biomass was measure from the, filtration and subsequent drying of a known volume of biomass.

Calibration curve - Absorbance vs OD - *S. obliquus*

$$y = 0.0414x^2 + 0.2302x$$
$$R^2 = 0.9999$$
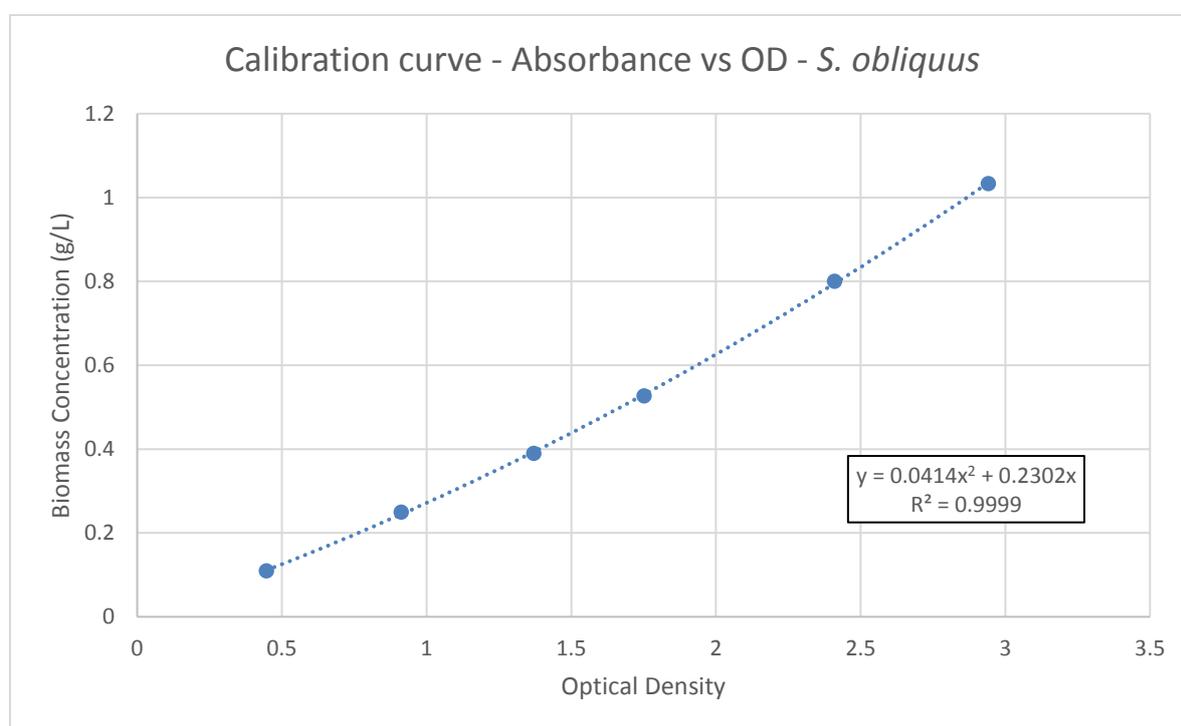
Appendix 3: Example of Determination of Pure Water Permeability

The following figure gives the method of determination of the pure water permeability of the CTA-ES membrane. Using a dead-end filtration cell, pure water is pressurized using compressed air. 5 experiments are conducted using 5 different pressures. The permeate was collected and the volume measured. The time necessary to collect this permeate was also measured. The water flux was calculated using the following equation:

$$Jw = \frac{V}{S_m \cdot t}$$

where Jw is the permeate flux (m³/m²/s), V is the volume of the permeate (m³), S_m is the membrane surface (m²), and t is the time of the experiment (s). The water flux can also be calculated from the following equation:

$$Jw = A \cdot \Delta P$$

where A is the pure water permeability (m.s⁻¹.Pa⁻¹), and ΔP is the hydraulic pressure applied across the membrane (Pa). Plotting the water flux as function of the hydraulic pressure difference and applying a linear regression gives the pure water permeability A as slope of the curve, as shown below. Using this method, for the CTA-ES membrane, the pure water coefficient of the membrane is determined to be 1.51×10^{-12} m.s⁻¹.Pa⁻¹.

177
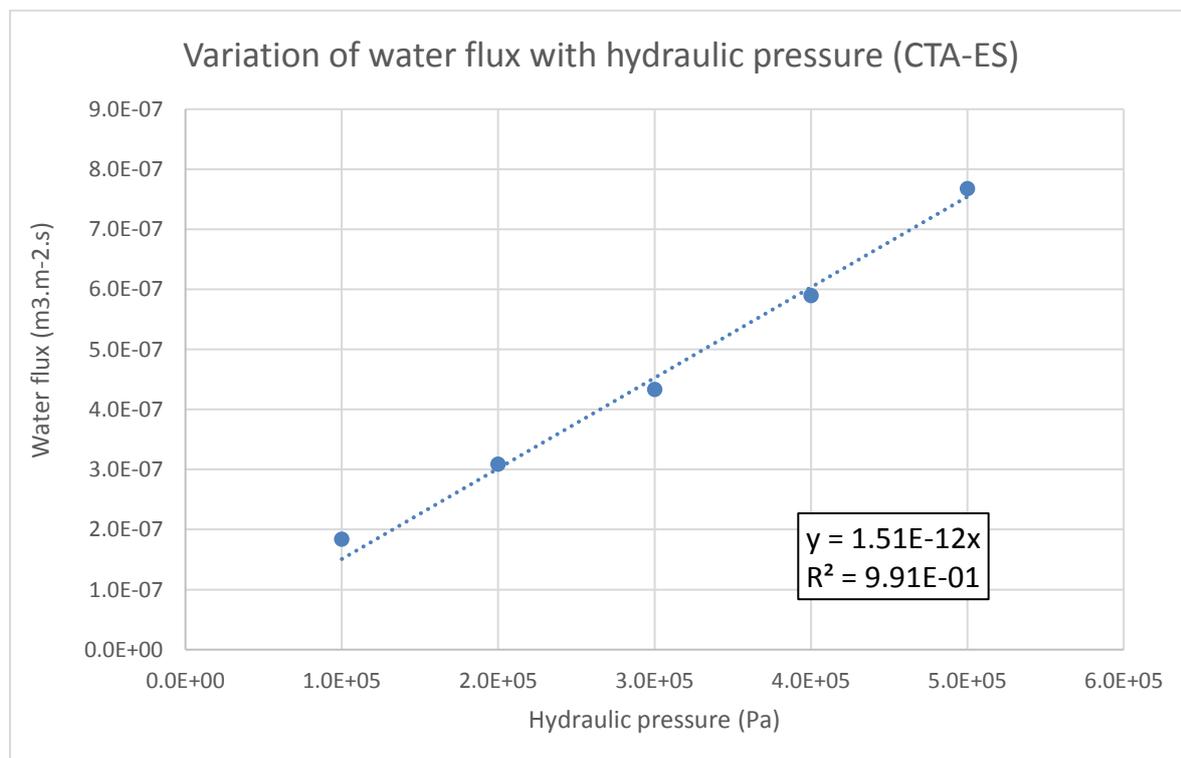
Appendix 4: Conceptual Illustration of Forward Osmosis (FO) Applied to Microalgae Dewatering
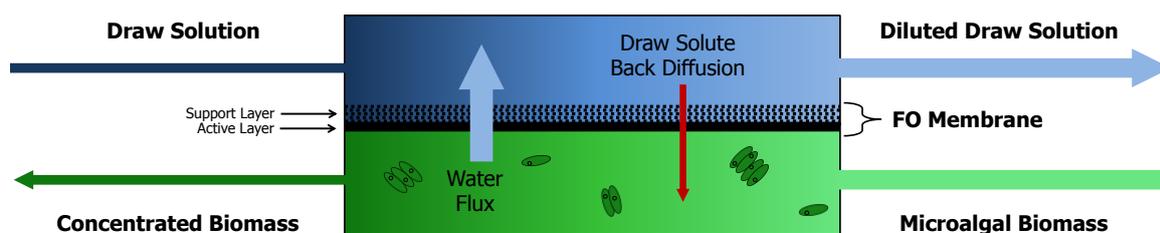

Conceptual illustration of microalgae dewatering by forward osmosis (FO) is depicted above. The orientation of membrane active layer facing algal biomass and support layer facing draw solution (DS) is applied in order to reduce membrane fouling propensity. DS (e.g., ocean water) with high osmotic pressure circulates on one side of the FO membrane, while the other side (the feed side) of the membrane is in contact with algal biomass suspension. It is the natural tendency for clean water to be "pumped" out of the algal suspension and pass into the DS due to the osmotic pressure difference across the membrane. All algal biomass are retained in the feed side due to the high retention nature of membrane. A concentration factor of 4-20 can be achieved, which will allow efficient algal biomass recovery in the following process. Back diffusion of solutes from DS to feed side also takes place. In this FO dewatering process, only a small amount of electricity is require for delivering DS and/or algal suspension ($0.01 - 0.06$ kWh/m^3).

Appendix 5: Example of Water Flux vs Concentration Factor Figures method and realization.

This example was conducted with the CTA-ES membrane with the AL-FS orientation, sea salts (70 g/L) as draw solution, and *S. obliquus* biomass as feed solution. As the duration of each experiment varied, it was necessary to process the data in a meaningful way by plotting the water flux as function of the concentration factor instead of the time. This allowed a better comparison of the water flux data for each experiment. During each experiment, the water flux was recorded by mass difference on the draw side every 2 min (Δm). The volume of permeate was calculated using the following equation:

$$V_{Permeate}(t) = \sum_{0}^{t} \Delta m(t)$$

where $V_{permeate}(t)$ is the volume of permeate at a precise time (L), and $\Delta m(t)$ is the mass difference between two weight measurements. The water flux is then displayed as function of the permeate volume as shown in the figure below. A polynomial regression is also fitted on the data obtained


Evolution of Water flux as function of the permeate volume

$y = -1.4019E\text{-}06x^2 + 4.7917E\text{-}04x + 5.9824E\text{+}00$
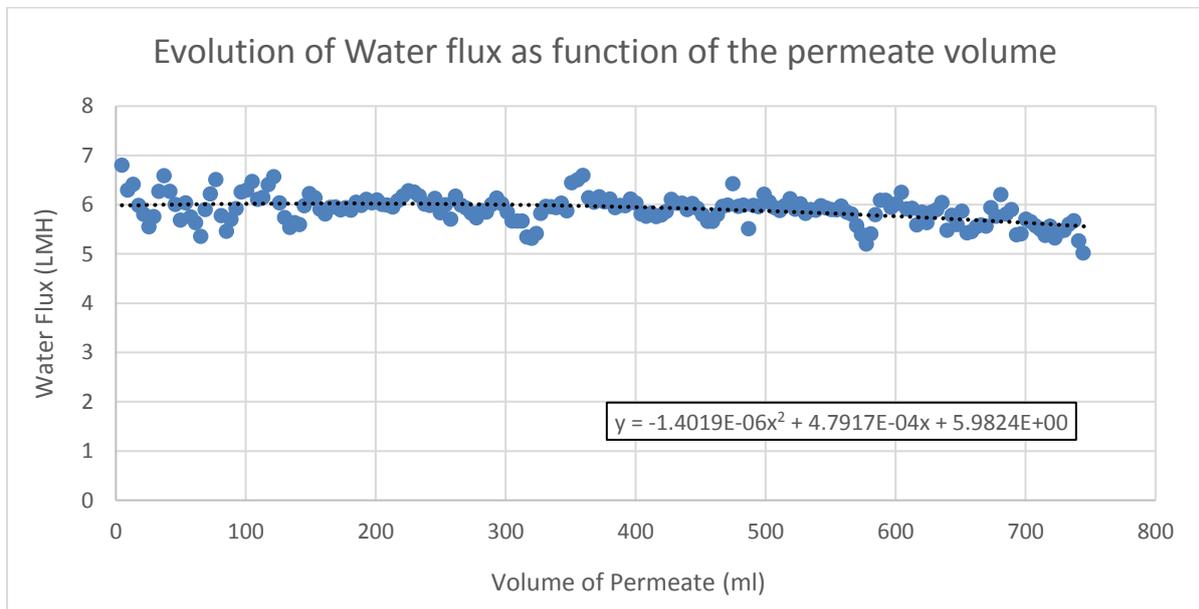
The concentration is defined as:
$$CF == \frac{V_{Feed}(i)}{V_{Feed}(i) - V_{permeate}}$$

which gives
$$V_{permeate} = V_{Feed}(i) - \frac{V_{Feed}(i)}{CF}$$

where CF is the concentration factor, $V_{Feed}(i)$ is the initial volume of the feed solution (L), and $V_{permeate}$ is the volume of permeate (L).

Then, the volume of permeate, noted "x" in the polynomial regression, is replaced by: $\left(V_{Feed}(i) - \frac{V_{Feed}(i)}{CF}\right)$. Finally, the water flux is calculated for concentration factors from 1 to 4 and shown in a figure as below.
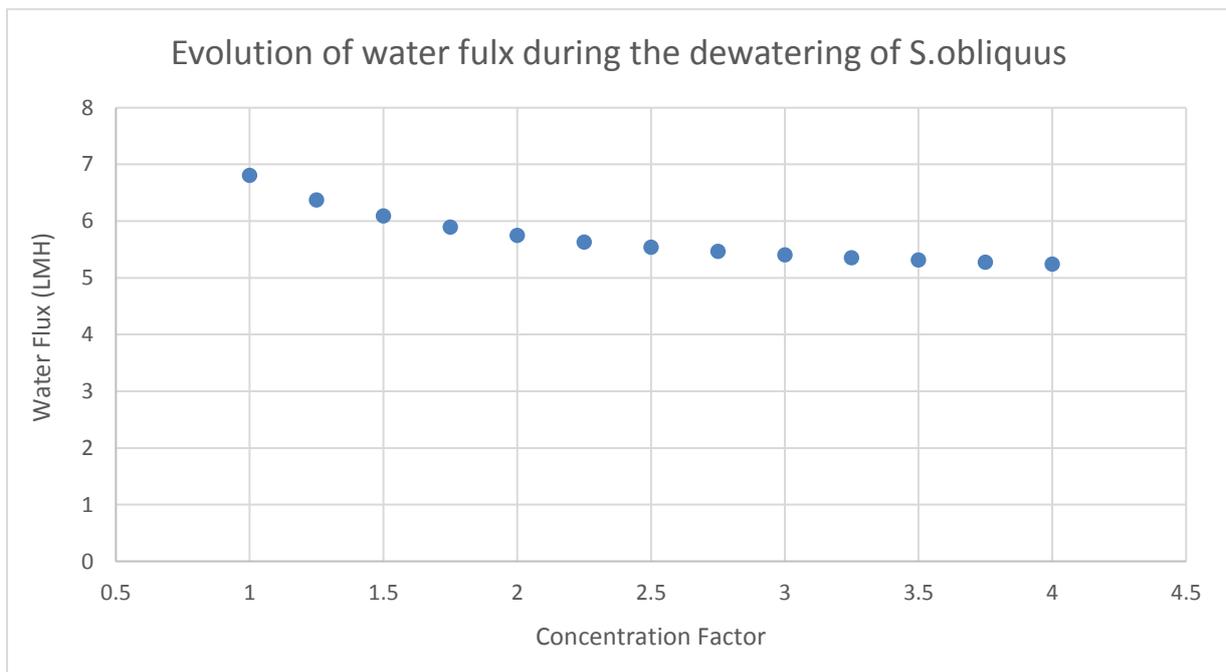
Appendix 6: Example of Determination of the Structural parameter

The following figure gives the method of determination of the selectivity coefficient of the CTA-ES membrane with NaCl as Draw solution. The crossflow FO filtration system presented on Figure 2.2 is used here for the determination of the structural parameter. The feed solution contains pure water whereas the draw solution contains NaCl. Four different NaCl concentrations are used for the determination of the structural parameter. Feed and Draw solutions are circulated at a velocity of 19.2 cm/s for 30 min. The NaCl concentration in the feed solution is measured at the end of the experiment and allowed to calculate the solute diffusion. The water flux is also measured by mass difference on the draw side. As the water flux can be defined as:

$$Jw = \left(\frac{1}{K}\right) \cdot \ln\left(\frac{A \cdot \pi_D + B}{A \cdot \pi_F + B + Jw}\right)$$

with $\quad K = \dfrac{l_{eff}}{D_{eff}} = \dfrac{\tau \cdot l / \varepsilon}{D} = \dfrac{S}{D}$

where, K is the resistance to solute diffusion (s/m), l_{eff} is the effective length (m), D_{eff} is the effective diffusion coefficient (m²/s), τ is the tortuosity, l is the length (m), D is the diffusion coefficient (m²/s), ε is the porosity, and S is the structural parameter (m^{-1}). Arranging the above equations lead to the following equation:

$$D \cdot \ln\left(\frac{A \cdot \pi_D + B}{A \cdot \pi_F + B + Jw}\right) = S \cdot Jw$$

Plotting $\;D \cdot \ln\left(\dfrac{A \cdot \pi_D + B}{A \cdot \pi_F + B + Jw}\right)$ as a function of Jw allows the determination of the structural parameter, S, given as the regression coefficient of the linear fitting curve. This is presented in the next figure. The same procedure is done with all membranes and solutes used in this study.

CTA-ES membrane S parameter determination with NaCl

$y = 5.46E\text{-}04x + 6.34E\text{-}10$
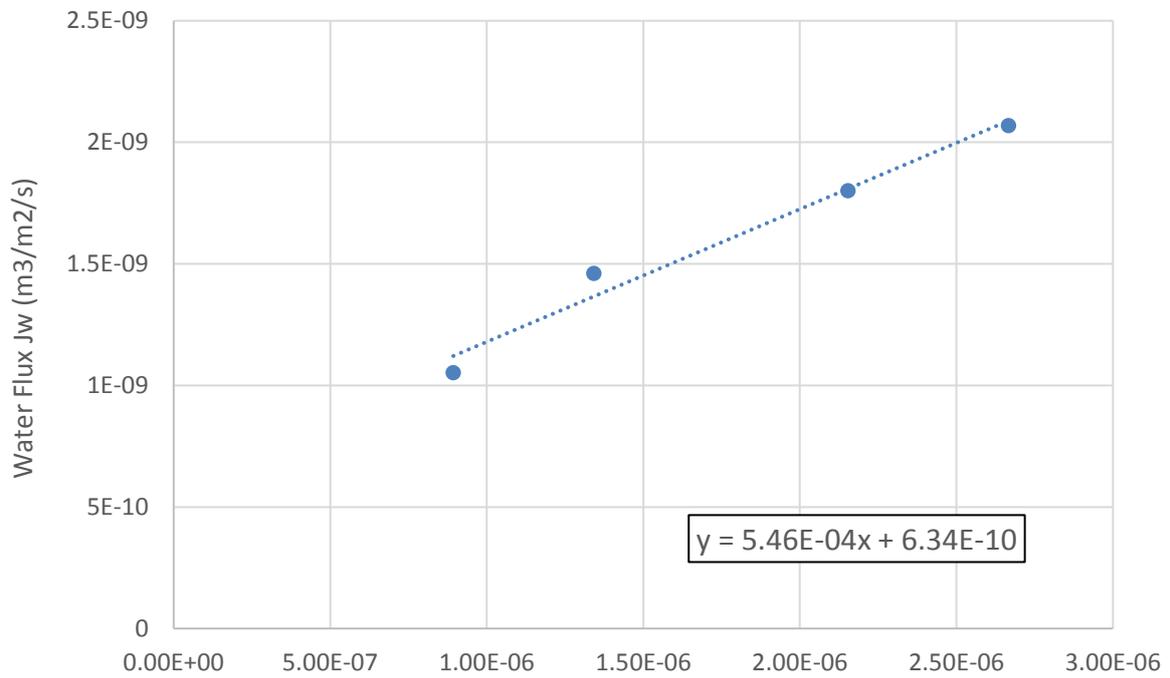
$$D \cdot \ln\left(\frac{A \cdot \pi_D + B}{A \cdot \pi_F + B + Jw}\right)$$

Appendix 7: Calibration curves: Conductivity vs Solute concentration

The following calibration curves were made in order to calculate the concentration of the draw solutions and assess the reverse solute diffusion through the membrane, from the measurement of conductivity. For each draw solute, the calibration was divided into three ranges of concentrations in order to increase the accuracy of the calculation of solute concentration.

NaCl low range
$y = -708.11x^2 + 130.21x$
$R^2 = 0.9999$

NaCl medium range
$y = -47.536x^2 + 119.48x$
$R^2 = 0.9999$

NaCl high range
$y = -9.0218x^2 + 91.64x$
$R^2 = 0.9991$

Sea salts low range
$y = -0.0725x^2 + 1.7918x$
$R^2 = 0.9994$

Sea salts medium range
$y = 1.557x + 0.1393$
$R^2 = 0.9973$

Sea salts high range
$y = -0.00256x^2 + 1.28716x + 1.07417$
$R^2 = 0.99984$
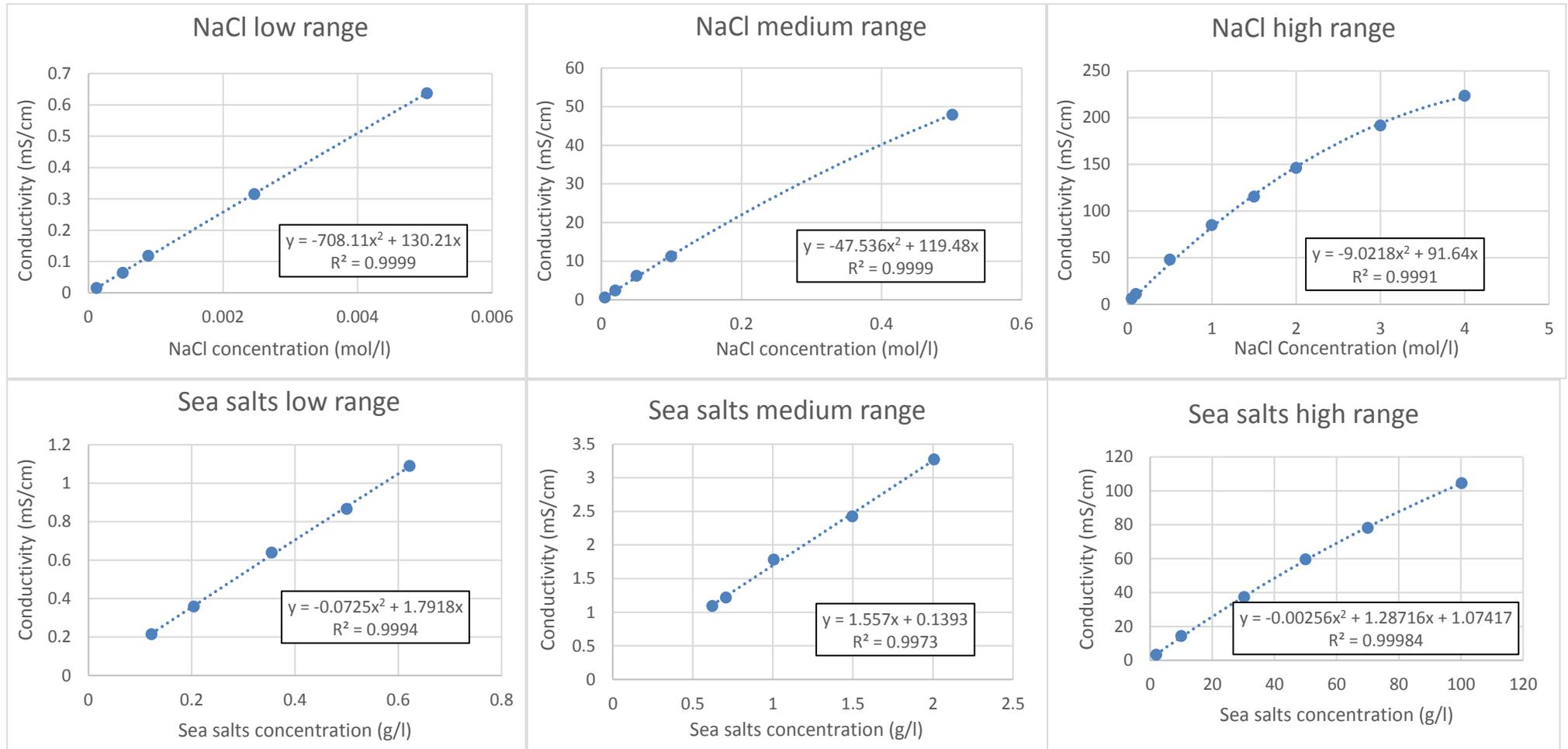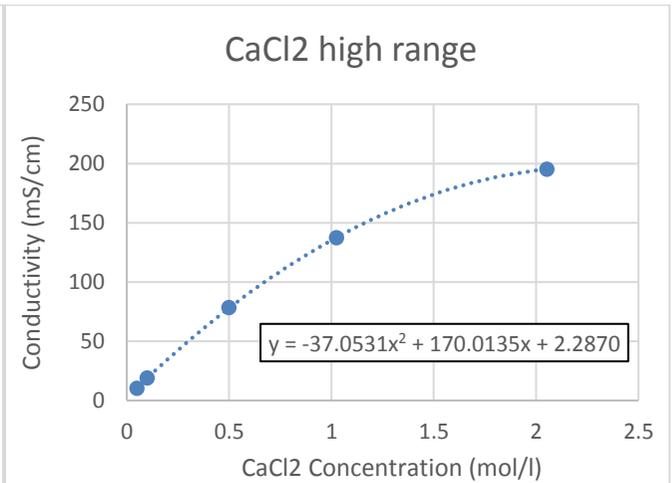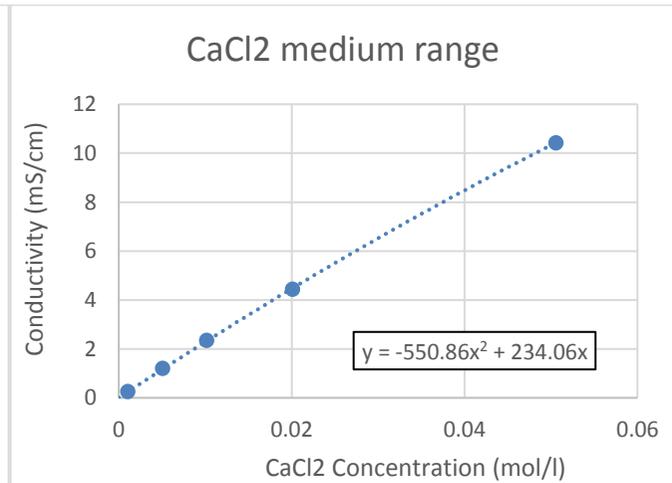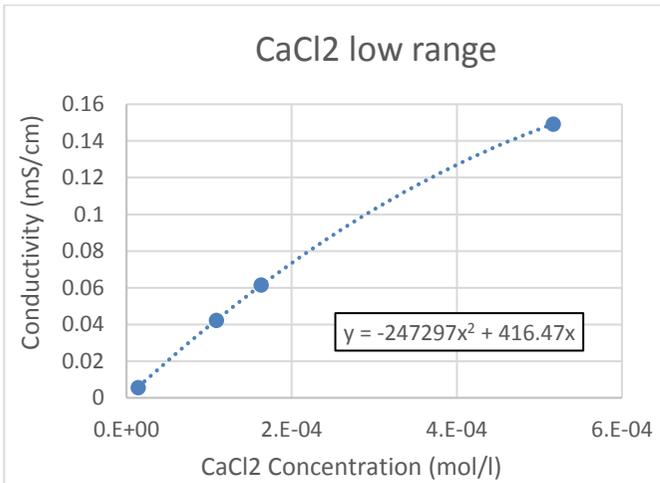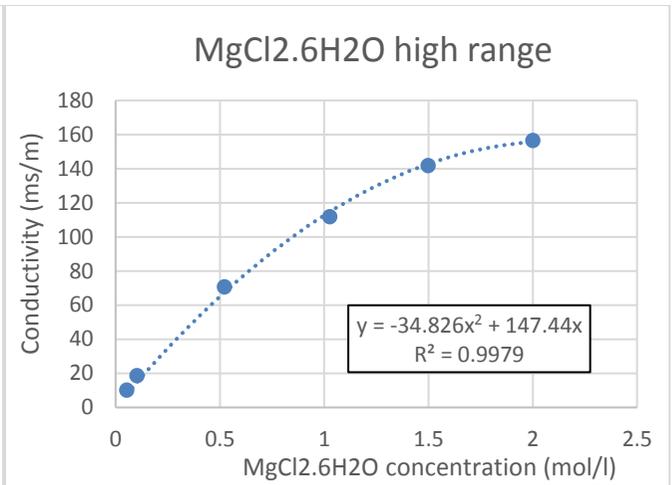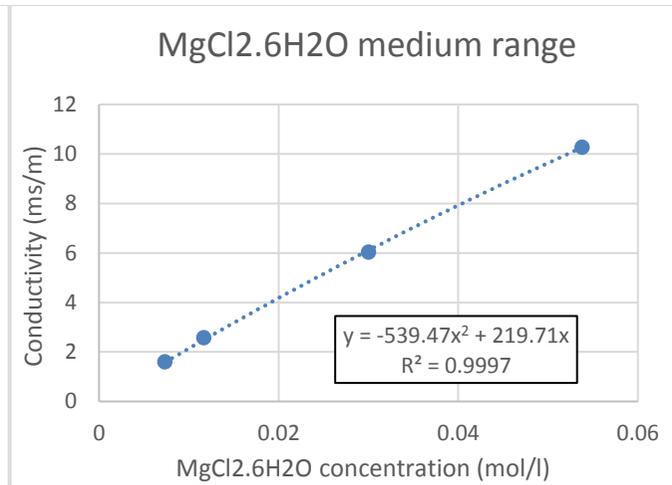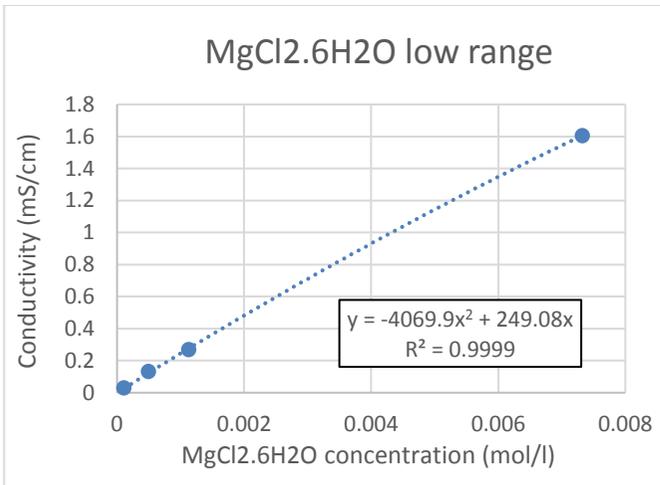
Appendix 8: Reproducibility Test

(a)

(b)
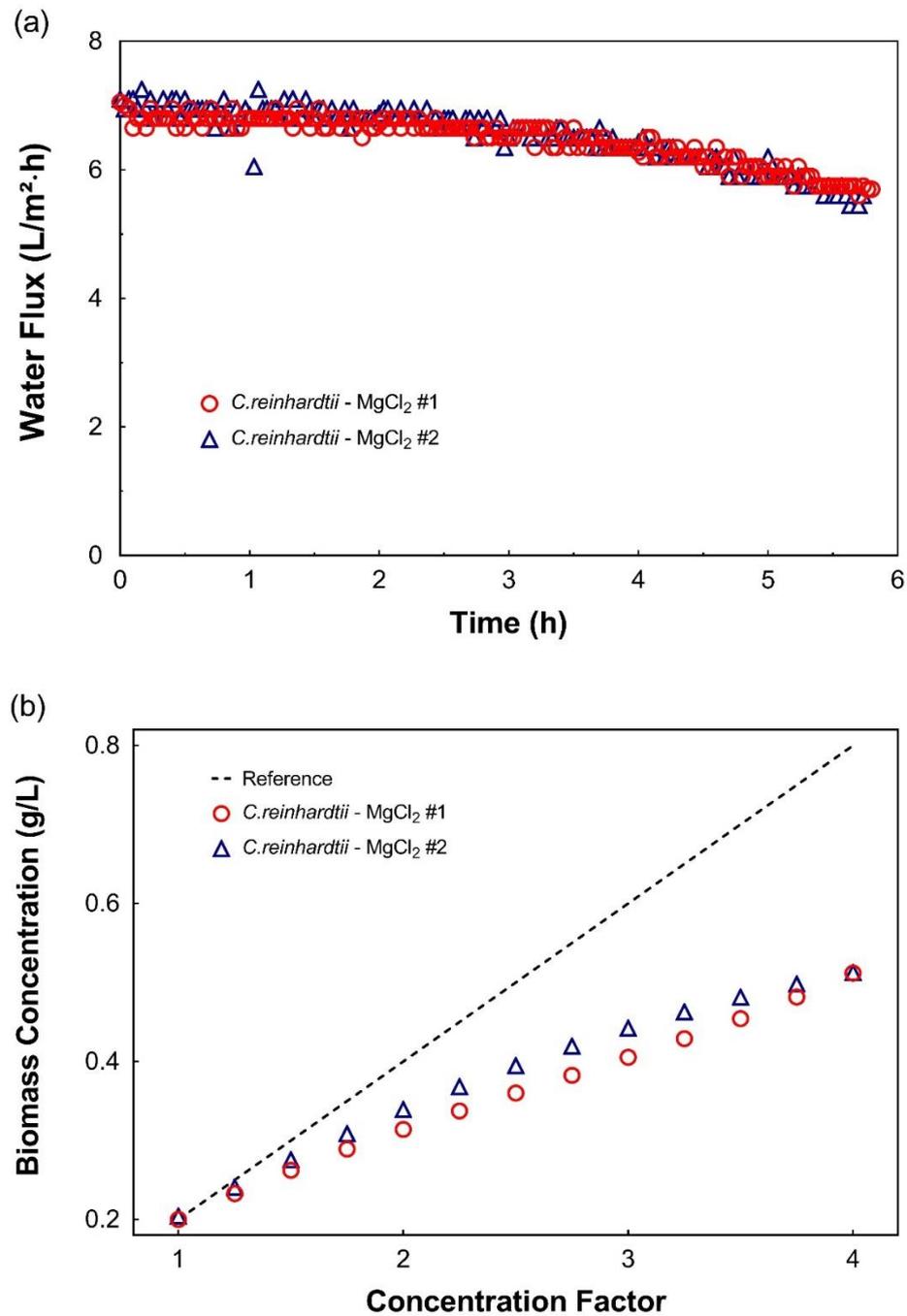
Reproducibility tests on water flux (a) and biomass concentration (b), during the dewatering of *Chlamydomonas reinhardtii* biomass with $MgCl_2$ as draw solution. The reference (black dash line) in (b) represents the theoretical biomass concentration in the feed tank according to the initial concentration and the concentration factor reached.